

NAG 1-639

IN-24-CR

392315

P-233

WASHINGTON UNIVERSITY  
SEVER INSTITUTE OF TECHNOLOGY

---

HIERARCHIC MODELS FOR LAMINATED PLATES

by

Ricardo Luis Actis

Prepared under the direction of Professor B. A. Szabó

---

A dissertation presented to the Sever Institute of  
Washington University in partial fulfillment  
of the requirements for the degree of

DOCTOR OF SCIENCE

December, 1991

Saint Louis, Missouri

(NASA-CR-187327) HIERARCHIC MODELS FOR  
LAMINATED PLATES Ph.D. Thesis (Washington  
Univ.) 233 p CSCL 110

N92-14121

Unclass

63/24 0054235

WASHINGTON UNIVERSITY  
SEVER INSTITUTE OF TECHNOLOGY

---

ABSTRACT

---

HIERARCHIC MODELS FOR LAMINATED PLATES

By Ricardo Luis Actis

---

ADVISOR: Professor Barna A. Szabó

---

December, 1991

Saint Louis, Missouri

---

Structural plates and shells are three-dimensional bodies, one dimension of which happens to be much smaller than the other two. Thus the quality of a plate or shell model must be judged on the basis of how well its exact solution approximates the corresponding three-dimensional problem. Of course, the exact solution depends not only on the choice of the model but also on the topology, material properties, loading and constraints. The desired degree of approximation depends on the analyst's goals in performing the analysis. For these reasons models have to be chosen adaptively. Hierarchic sequences of models make adaptive

selection of the model which is best suited for the purposes of a particular analysis possible.

The principles governing the formulation of hierarchic models for laminated plates are presented. The essential features of the hierarchic models described herein are: (a) The exact solutions corresponding to the hierarchic sequence of models converge to the exact solution of the corresponding problem of elasticity for a fixed laminate thickness, and (b) the exact solution of each model converges to the same limit as the exact solution of the corresponding problem of elasticity with respect to the laminate thickness approaching zero.

The formulation is based on one parameter ( $\beta$ ) which characterizes the hierarchic sequence of models, and a set of constants whose influence has been assessed by a numerical sensitivity study. The recommended selection of these constants results in the number of fields increasing by three for each increment in the power of  $\beta$ .

Numerical examples analyzed with the proposed sequence of models are included and good correlation with the reference solutions was found. Results were obtained for laminated strips (plates in cylindrical bending) and for square and rectangular plates with uniform loading and with homogeneous boundary conditions. Cross-ply and angle-ply laminates were evaluated and the results compared with those of MSC/PROBE.

Hierarchic models make the computation of any engineering data possible to an arbitrary level of precision within the framework of the theory of elasticity.

# Table of Contents

<b>1</b>	<b>Introduction</b>	<b>1</b>
1.1	The Finite Element Method in Two Dimensions . . . . .	4
1.2	Plate Models . . . . .	9
1.2.1	Shear-Deformation Models . . . . .	10
1.2.2	Discrete-Layer Models . . . . .	28
1.2.3	Hierarchic Models . . . . .	32
<b>2</b>	<b>Laminated Strip</b>	<b>34</b>
2.1	Hierarchic Models for Laminated Composites . . . . .	35
2.1.1	The Model Characterized by $\beta^0$ . . . . .	41
2.1.2	The Model Characterized by $\beta^1$ . . . . .	43
2.1.3	The Model Characterized by $\beta^2$ . . . . .	45
2.2	The Boundary Layer . . . . .	46
2.3	Boundary Conditions for Hierarchic Models . . . . .	48
2.4	The Limiting Case with Respect to $\beta \rightarrow 0$ . . . . .	50

2.4.1	The Model Characterized by $\beta^0$ . . . . .	50
2.4.2	The Model Characterized by $\beta^1$ . . . . .	52
2.4.3	The Model Characterized by $\beta^2$ . . . . .	55
2.4.4	Hierarchic Models Characterized by $\beta^0$ and $\beta^1$ . . . . .	56
<b>3</b>	<b>Solution of the Strip Model</b>	<b>59</b>
3.1	The Numerical Problem . . . . .	59
3.2	Examples . . . . .	65
3.2.1	Model Problem 1: The Infinite Strip . . . . .	65
3.2.2	Model problem 2: The Cantilever Beam . . . . .	80
3.3	Conclusions . . . . .	88
<b>4</b>	<b>Laminated Plates</b>	<b>90</b>
4.1	Models for Laminated Plates . . . . .	91
4.1.1	The Model Characterized by $\beta^0$ . . . . .	98
4.1.2	The Model Characterized by $\beta^1$ . . . . .	101
4.1.3	The Model Characterized by $\beta^2$ . . . . .	103
4.2	The Limiting Case with Respect to $\beta \rightarrow 0$ . . . . .	107
4.3	Sensitivity Study . . . . .	117
<b>5</b>	<b>Laminated Plate Examples</b>	<b>125</b>
5.1	Description of Example Problems . . . . .	127
5.2	Cross-ply Laminate . . . . .	133

5.2.1	Square Plate . . . . .	133
5.2.2	Rectangular Plate . . . . .	148
5.2.3	Other Cases of Cross-ply Laminates . . . . .	148
5.3	Angle-ply Laminate . . . . .	154
5.3.1	Square $-45/+45/-45$ Plate . . . . .	154
5.3.2	Square $-30/+30/-30$ Plate . . . . .	155
5.3.3	Rectangular $-45/+45/-45$ Plate . . . . .	157
5.3.4	Other Cases of Angle-ply Laminate . . . . .	160
5.4	Conclusions . . . . .	173
6	Summary and Conclusions	175
7	Acknowledgements	179
A	Laminated Strip: Expansion of the Equilibrium Equations up to the Third Power of $\beta$	180
B	Laminated strips: Computation of the Transverse Functions for a 3-ply Laminate	183
C	Laminated Strip: Lamina Stiffness Submatrices	188
D	Laminated Strip: The Load Vector	200
E	Laminated Strip: Computation of Engineering Quantities	204

## List of Tables

4.1	Values of the Coefficients $\lambda_i$ in [in-lb] for Four Stacking Sequences .	115
4.2	Sensitivity Study- $\beta^2$ Model. Simply supported 90/0/90 square plate ( $a/h = 4$ ). Influence of $m, n, s, t$ . . . . .	120
5.1	Estimated Relative Error in Energy Norm (%) at $p = 8$ . . . . .	132
5.2	Normalized Stresses and Displacements for a Simply Supported 90/0/90 Square Plate ( $b/a = 1$ ) . . . . .	135
5.3	Normalized Stresses and Displacements for a Simply Supported 90/0/90 Rectangular Plate ( $b/a = 3$ ) . . . . .	149
5.4	Normalized Stresses and Displacements for a Simply Supported $-45/+$ $45/-45$ Square Plate ( $b/a = 1$ ) . . . . .	156
5.5	Normalized Stresses and Displacements for a Simply Supported $-30/+$ $30/-30$ Square Plate ( $b/a = 1$ ) . . . . .	158
5.6	Normalized Stresses and Displacements for a Simply Supported $-45/+$ $45/-45$ Rectangular Plate ( $b/a = 3$ ) . . . . .	159

## List of Figures

2.1	Infinite strip. Notation. . . . .	36
3.1	Model problem 1: Notation for the case of three layers. . . . .	65
3.2	Model problem 1: Central deflection for the three-layer laminate. . .	71
3.3	Model problem 1: Central deflection for the five-layer laminate. . .	71
3.4	Model problem 1: Central deflection for the three-layer laminate. For the outer layers: $(E_1 - E_2^2/E_3)/E_1 = 0.7$ . . . . .	72
3.5	Model problem 1: Central deflection for the three-layer laminate. Comparison of $\beta^0$ vs. $\beta^n$ , $(n = 1, 2, 3)$ . . . . .	72
3.6	Model problem 1: The function $\bar{u}_x(0, y)$ for $L/h = 20$ . Three-layer laminate. . . . .	73
3.7	Model problem 1: The function $\bar{u}_x(0, y)$ for $L/h = 10$ . Three-layer laminate. . . . .	73
3.8	Model problem 1: The function $\bar{u}_x(0, y)$ for $L/h = 4$ . Three-layer laminate. . . . .	74



3.9 Model problem 1: The function $\bar{u}_x(0, y)$ for $L/h = 4$ . Five-layer laminate. . . . .	74
3.10 Model problem 1: The function $\bar{\sigma}_x(\ell/2, y)$ for $L/h = 10$ . Three-layer laminate. . . . .	75
3.11 Model problem 1: The function $\bar{\sigma}_x(\ell/2, y)$ for $L/h = 4$ . Three-layer laminate. . . . .	75
3.12 Model problem 1: The function $\bar{\sigma}_x(\ell/2, y)$ for $L/h = 4$ . Five-layer laminate. . . . .	76
3.13 Model problem 1: The function $\bar{\tau}_{xy}(0, y)$ . Direct computation for $L/h = 10$ . Three-layer laminate. . . . .	76
3.14 Model problem 1: The function $\bar{\tau}_{xy}(0, y)$ . Direct computation for $L/h = 4$ . Three-layer laminate. . . . .	77
3.15 Model problem 1: The function $\bar{\tau}_{xy}(0, y)$ . Direct computation for $L/h = 4$ . Five-layer laminate. . . . .	77
3.16 Model problem 1: The function $\bar{\tau}_{xy}(0, y)$ computed by integration of the equilibrium equation for $L/h = 10$ . Three-layer laminate. . . . .	78
3.17 Model problem 1: The function $\bar{\tau}_{xy}(0, y)$ computed by integration of equilibrium equation for $L/h = 4$ . Three-layer laminate. . . . .	78
3.18 Model problem 1: The function $\bar{\sigma}_y(\ell/2, y)$ for $L/h = 4$ . Three-layer laminate. . . . .	79
3.19 Model problem 2: Notation. . . . .	81

3.20	Model problem 2: Finite element mesh for the reference solution. . .	81
3.21	Model problem 2: End deflection. . . . .	83
3.22	Model problem 2: The function $\bar{\sigma}_x(0, y)$ . . . . .	83
3.23	Model problem 2: The function $\bar{\tau}_{xy}(0, y)$ . . . . .	84
3.24	Model problem 2: The function $\bar{\sigma}_x(h/3, y)$ . . . . .	84
3.25	Model problem 2: The function $\bar{\tau}_{xy}(h/6, y)$ . Direct computation. . .	85
3.26	Model problem 2: The function $\bar{\tau}_{xy}(h/6, y)$ computed by integration of the equilibrium equation. . . . .	85
3.27	Model problem 2: The function $\bar{\tau}_{xy}(h, y)$ . Direct computation. . . .	86
3.28	Model problem 2: The function $\bar{\tau}_{xy}(h, y)$ computed by integration of the equilibrium equation. . . . .	86
3.29	Model problem 2: The function $\bar{\sigma}_y(\ell, y)$ . . . . .	87
3.30	Model problem 2: The function $\bar{\sigma}_y(0.997\ell, y)$ . . . . .	87
4.1	Cross-ply square plate. Influence of $m, n, s$ on the strain energy of the solution. . . . .	121
4.2	Cross-ply rectangular plate. Influence of $m, n, s$ on the strain energy of the solution. . . . .	121
4.3	Cross-ply square and rectangular plate. Influence of $m, n, s$ on the strain energy of the solution. . . . .	122
4.4	Angle-ply square and rectangular plate. Influence of $m, n, s$ on the strain energy of the solution. . . . .	122

4.5	Cross-ply square plate. Influence of $m, n, s, t$ on the strain energy of the solution. . . . .	123
4.6	Cross-ply rectangular plate. Influence of $m, n, s, t$ on the strain energy of the solution. . . . .	123
4.7	Angle-ply square and rectangular plate. Influence of $m, n, s, t$ on the strain energy of the solution. . . . .	124
4.8	Cross-ply square plate. Influence of $m, n, s, t$ on the strain energy of the solution. . . . .	124
5.1	Model problems: Notation. . . . .	128
5.2	Simply supported orthotropic (90/0/90) square plate: The function $U_z(a/2, a/2, 0)$ . . . . .	136
5.3	Simply supported orthotropic (90/0/90) square plate: The function $\bar{u}_x(0, a/2, z)$ for $a/h = 4$ . . . . .	139
5.4	Simply supported orthotropic (90/0/90) square plate: The function $\bar{u}_x(0, a/2, z)$ for $a/h = 10$ . . . . .	139
5.5	Simply supported orthotropic (90/0/90) square plate: The function $\bar{u}_y(a/2, 0, z)$ for $a/h = 4$ . . . . .	140
5.6	Simply supported orthotropic (90/0/90) square plate: The function $\bar{u}_y(a/2, 0, z)$ for $a/h = 10$ . . . . .	140
5.7	Simply supported orthotropic (90/0/90) square plate: The function $\bar{\sigma}_x(a/2, a/2, z)$ for $a/h = 4$ . . . . .	141

5.8	Simply supported orthotropic (90/0/90) square plate: The function $\bar{\sigma}_x(a/2, a/2, z)$ for $a/h = 10$ . . . . .	141
5.9	Simply supported orthotropic (90/0/90) square plate: The function $\bar{\sigma}_y(a/2, a/2, z)$ for $a/h = 4$ . . . . .	142
5.10	Simply supported orthotropic (90/0/90) square plate: The function $\bar{\sigma}_y(a/2, a/2, z)$ for $a/h = 10$ . . . . .	142
5.11	Simply supported orthotropic (90/0/90) square plate: The function $\bar{\tau}_{zx}(0, a/2, z)$ for $a/h = 4$ . . . . .	143
5.12	Simply supported orthotropic (90/0/90) square plate: The function $\bar{\tau}_{zx}(0, a/2, z)$ for $a/h = 10$ . . . . .	143
5.13	Simply supported orthotropic (90/0/90) square plate: The function $\bar{\tau}_{yz}(a/2, 0, z)$ for $a/h = 4$ . . . . .	144
5.14	Simply supported orthotropic (90/0/90) square plate: The function $\bar{\tau}_{yz}(a/2, 0, z)$ for $a/h = 10$ . . . . .	144
5.15	Simply supported orthotropic (90/0/90) square plate: The function $\bar{\sigma}_z(a/2, a/2, z)$ for $a/h = 4$ . . . . .	145
5.16	Simply supported orthotropic (90/0/90) square plate: Finite element mesh for the reference solution ( $a/h = 10$ ). . . . .	145
5.17	Simply supported orthotropic (90/0/90) square plate: Deformed configuration ( $a/h = 10$ ). . . . .	146

5.18 Simply supported orthotropic (90/0/90) square plate: Estimated relative error in energy norm for $a/h = 4$ . . . . .	147
5.19 Simply supported orthotropic (90/0/90) square plate: Estimated relative error in energy norm for $a/h = 10$ . . . . .	147
5.20 Simply supported orthotropic (90/0/90) rectangular plate: The function $\bar{\sigma}_x(a/2, b/2, z)$ for $a/h = 4$ . . . . .	151
5.21 Simply supported orthotropic (90/0/90) rectangular plate: The function $\bar{\sigma}_y(a/2, b/2, z)$ for $a/h = 4$ . . . . .	151
5.22 Simply supported orthotropic (90/0/90) rectangular plate: The function $\bar{\tau}_{zx}(0, b/2, z)$ for $a/h = 4$ . . . . .	152
5.23 Simply supported orthotropic (90/0/90) rectangular plate: The function $\bar{\tau}_{yz}(a/2, 0, z)$ for $a/h = 4$ . . . . .	152
5.24 Orthotropic (90/0/90) square plate, one side clamped. Influence of number of layers in $U_z(a/2, a, 0)$ . . . . .	153
5.25 Three-ply square plate. Two sides simply supported: The function $U_z(a/2, a/2, 0)$ . . . . .	153
5.26 Five-ply square plate. Two sides simply supported: The function $U_z(a/2, a/2, 0)$ . . . . .	161
5.27 Simply supported angle-ply $(-45/+45/-45)$ square plate: The function $U_z(a/2, a/2, 0)$ . . . . .	161

5.28 Simply supported angle-ply $(-45/ + 45/ - 45)$ square plate: The function $\bar{u}_x(0, a/2, z)$ for $a/h = 4$ . . . . .	162
5.29 Simply supported angle-ply $(-45/ + 45/ - 45)$ square plate: The function $\bar{u}_y(0, a/2, z)$ for $a/h = 4$ . . . . .	162
5.30 Simply supported angle-ply $(-45/ + 45/ - 45)$ square plate: The function $\bar{\sigma}_x(a/2, a/2, z)$ for $a/h = 4$ . . . . .	163
5.31 Simply supported angle-ply $(-45/ + 45/ - 45)$ square plate: The function $\bar{\tau}_{xy}(a/2, a/2, z)$ for $a/h = 4$ . . . . .	163
5.32 Simply supported angle-ply $(-45/ + 45/ - 45)$ square plate: The function $\bar{\tau}_{zx}(0, a/2, z)$ for $a/h = 4$ . . . . .	164
5.33 Simply supported angle-ply $(-45/ + 45/ - 45)$ square plate: The function $\bar{\sigma}_z(a/2, a/2, z)$ for $a/h = 4$ . . . . .	164
5.34 Simply supported angle-ply $(-45/ + 45/ - 45)$ square plate. Esti- mated relative error in energy norm for $a/h = 4$ . . . . .	165
5.35 Simply supported angle-ply $(-45/ + 45/ - 45)$ square plate. Esti- mated relative error in energy norm for $a/h = 10$ . . . . .	165
5.36 Simply supported angle-ply $(-30/ + 30/ - 30)$ square plate: The function $U_z(a/2, a/2, 0)$ . . . . .	166
5.37 Simply supported angle-ply $(-30/ + 30/ - 30)$ square plate: The function $\bar{u}_x(0, a/2, z)$ for $a/h = 4$ . . . . .	166

5.38 Simply supported angle-ply ( $-30^\circ / +30^\circ - 30^\circ$ ) square plate: The function $\bar{\sigma}_x(a/2, a/2, z)$ for $a/h = 4$ . . . . .	167
5.39 Simply supported angle-ply ( $-30^\circ / +30^\circ - 30^\circ$ ) square plate: The function $\bar{\sigma}_y(a/2, a/2, z)$ for $a/h = 4$ . . . . .	167
5.40 Simply supported angle-ply ( $-30^\circ / +30^\circ - 30^\circ$ ) square plate: The function $\bar{\sigma}_z(a/2, a/2, z)$ for $a/h = 4$ . . . . .	168
5.41 Simply supported angle-ply ( $-30^\circ / +30^\circ - 30^\circ$ ) square plate: The function $\bar{\tau}_{xz}(0, a/2, z)$ for $a/h = 4$ . . . . .	168
5.42 Simply supported angle-ply ( $-30^\circ / +30^\circ - 30^\circ$ ) square plate: The function $\bar{\tau}_{yz}(a/2, 0, z)$ for $a/h = 4$ . . . . .	169
5.43 Simply supported angle-ply ( $-30^\circ / +30^\circ - 30^\circ$ ) square plate: The function $\bar{\tau}_{xy}(a/2, 0, z)$ for $a/h = 4$ . . . . .	169
5.44 Simply supported angle-ply ( $-45^\circ / +45^\circ - 45^\circ$ ) rectangular plate: The function $U_z(a/2, a/2, 0)$ . . . . .	170
5.45 Simply supported angle-ply ( $-45^\circ / +45^\circ - 45^\circ$ ) rectangular plate: The function $\bar{\sigma}_x(a/2, b/2, z)$ for $a/h = 4$ . . . . .	170
5.46 Simply supported angle-ply ( $-45^\circ / +45^\circ - 45^\circ$ ) rectangular plate: The function $\bar{\sigma}_y(a/2, b/2, z)$ for $a/h = 4$ . . . . .	171
5.47 Simply supported angle-ply ( $-45^\circ / +45^\circ - 45^\circ$ ) rectangular plate: The function $\bar{\tau}_{xz}(0, b/2, z)$ for $a/h = 4$ . . . . .	171

5.48 Simply supported $-45/+45/-45$ rectangular plate: The function $\bar{\tau}_{yz}(a/2, 0, z)$ for $a/h = 4$ . . . . .	172
5.49 Square plate. Influence of fiber orientation on a three-ply laminate: The function $U_z(a/2, a/2, 0)$ . . . . .	172
B.1 Three-ply laminate. Notation. . . . .	183
C.1 Laminated Strip. Notation . . . . .	189
D.1 Three-ply problem. Notation. . . . .	200



# Chapter 1

## Introduction

The use of fiber-reinforced composite materials in structural applications has stimulated considerable research activity in the study of the mechanical behavior of laminated plates and shells.

Structural plates and shells are three-dimensional bodies, one dimension of which happens to be much smaller than the other two. Thus the quality of a plate or shell model must be judged on the basis of how well its exact solution approximates the corresponding three-dimensional problem. Of course, the exact solution depends not only on the choice of the model but also on the topology, material properties, loading and constraints. The desired degree of approximation depends on the analyst's goals in performing the analysis. For these reasons models have to be chosen adaptively.

There are two types of information which are of substantial engineering interest in the analysis of laminated plates:

1. The structural response (i.e. load-deflection relationships, shear forces, bending moments, etc.) is characterized by the fact that laminated composites typically have very large bending modulus to shear modulus ratios.
2. The strength response (e.g. the conditions under which delamination occurs, crack propagation problems, etc.) is characterized by the facts that at the laminar interfaces the normal and shear stresses are continuous, hence the shear strains are discontinuous, and stress singularities occur at external boundaries.

Initially, the research efforts were focussed on the development of analysis tools to predict the structural response of the laminates. Soon it was realized that the classical plate model, extensively used for homogeneous isotropic materials, led to considerable error when applied to laminated plates. The reason: *the classical plate model fails to account for shear deformation effects*, which are of critical importance when the materials have very large elastic modulus to shear modulus ratios.

Three-dimensional models are suitable for investigating the strength response of laminated media, but they are computationally demanding and not feasible for practical problems. The alternative was to develop two-dimensional models that could give reasonable results. Of course what is 'reasonable' depends on the goals of the computation. First-order and higher-order shear-deformation models were developed to account for the effects of transverse shear strains. The terminology used in connection with high-order models refers to the level of truncation of terms

in a power series expansion for the displacements, rather than to the order of the final system of differential equations. The first-order models are simple but only adequate in predicting the gross response characteristics of the laminate for large length-to-thickness ratios. They give poor approximation for thick plates and near boundaries. Higher-order models are more cumbersome, but give more accurate results than first-order models. The main limitation of these models is that they do not allow for discontinuities in the slopes of the deflections at the interfaces of laminae as predicted by the three-dimensional elasticity solution.

The discrete-layer models were derived to overcome the limitation of shear-deformation models. They are based on assuming a displacement field which allows piecewise linear variation of the in-plane displacements. They give better results than shear-deformation models, and yield more accurate interlaminar stress distribution, even for very thick laminates. In general the number of differential equations depend on the number of layers in the laminate, making them impractical for large problems.

The approach developed herein combines the advantages of both, the shear-deformation models and the discrete-layer models. It allows for discontinuities in the slopes of the deflections at interfaces, and the number of degrees of freedom do not depend on the number of layers in the laminate. Unlike any other model, it also allows the construction of a sequence of models to satisfy the equilibrium equations to the desired degree of accuracy. In the limit it converges to the fully

three-dimensional solution. Depending on the goals of computation, the analyst can select the model that best fits the goals. Choosing progressively higher models, the computational effort increases, but of course the accuracy in the results is improved. If only structural response is required, a low-order model is generally sufficient.

Hierarchic sequences of models make adaptive selection of the model which is best suited for the purposes of a particular analysis possible. The advantages of the proposed models became apparent when comparing the results obtained from its implementation with those of the exact three-dimensional solution.

### 1.1 The Finite Element Method in Two Dimensions

The various plate theories (models) differ in the way the transverse variation of the displacement components is represented. The transverse variation of displacement components and the number of fields are decided a priori. The problem is to find the solution for the in-plane components of the displacement field. The finite element method is used to find the solution of the resulting two-dimensional problem. The following notation will be used: The solution domain is denoted by  $\Omega$  and its boundary by  $\Gamma$ . An arbitrary displacement vector function defined on  $\Omega$  is denoted by  $\vec{u}$ , its cartesian components by  $u_x$ ,  $u_y$ ,  $u_z$ . The strain energy of  $\vec{u}$  is denoted by  $\mathcal{U}(\vec{u})$ , the energy norm of  $\vec{u}$ , by  $\|\vec{u}\|_{E(\Omega)}$  and the set of functions on  $\Omega$  which satisfy the condition  $\mathcal{U}(\vec{u}) < \infty$  is denoted by  $E(\Omega)$ . The potential energy of  $\vec{u}$

is denoted by  $\Pi(\vec{u})$ . A subset of  $E(\Omega)$  characterized by the finite element mesh  $\Delta$  and the polynomial degree of elements  $p$ , is denoted by  $S_p(\Delta)$ . The subset of  $S_p(\Delta)$  which satisfies the prescribed kinematic boundary conditions is denoted by  $\tilde{S}_p(\Delta)$ . The subset of  $\tilde{S}_p(\Delta)$  which vanishes on those boundaries where essential boundary conditions are prescribed is denoted by  $\tilde{S}_p^{(0)}(\Delta)$  and the number of degrees of freedom, the dimension of  $\tilde{S}_p^{(0)}(\Delta)$ , by  $N_p$ . The exact solution is denoted by  $\vec{u}_{EX}$  and the finite element solution is denoted by  $\vec{u}_{FE}$ .

Numerous variational principles can be employed for formulating the governing equations of an elasticity problem. For example, the principle of minimum potential energy, the principle of minimum complementary potential energy, and the Hellinger-Reissner principle are commonly used. However the most generally used formulation is based upon the total potential energy of the elastic body which can be written as:

$$\Pi(\vec{u}) = \mathcal{U}(\vec{u}) - \mathcal{F}(\vec{u}) \quad (1.1)$$

where  $\mathcal{F}(\vec{u})$  is the potential of the applied loads. Minimization of  $\Pi$  on a space of admissible functions leads to a satisfaction of the equilibrium conditions. In the finite element method a finite dimensional space  $S_p(\Delta) \subset E(\Omega)$  is constructed and  $\Pi$  is minimized on  $S_p(\Delta)$ . The resulting system of linear equations is represented by

$$[K] \{a\} = \{r\} \quad (1.2)$$

where  $[K]$  is the stiffness matrix,  $\{a\}$  is the set of coefficients which characterize the finite element solution and  $\{r\}$  is the load vector which represents the applied loads.

In this study the displacement formulation of the finite element method is employed in two dimensions. Proper selection of  $S_p(\Delta)$  is important because the performance of the numerical solution procedure depends on it. Most commonly  $S_p(\Delta)$  is constructed by one of the following approaches:

1. In the h-version the errors of approximation are controlled by mesh refinement, that is the size of the largest element, usually denoted by  $h_{\max}$  is chosen small enough so that the errors of discretization are sufficiently small. The mathematical basis for this is the limit process:

$$\lim_{h_{\max} \rightarrow 0} \|\vec{u}_{EX} - \vec{u}_{FE}\|_{E(\Omega)} = 0. \quad (1.3)$$

2. In the p-version the errors of approximation are controlled by increasing the polynomial degree of elements, that is the mesh is fixed and the lowest polynomial degree assigned to elements in the mesh, denoted by  $p_{\min}$ , is chosen large enough so that the errors of discretization are sufficiently small. The mathematical basis for this is the limit process:

$$\lim_{p_{\min} \rightarrow \infty} \|\vec{u}_{EX} - \vec{u}_{FE}\|_{E(\Omega)} = 0. \quad (1.4)$$

3. In the hp-version the errors of approximation are controlled by mesh refinement and increase of the polynomial degree of elements. Therefore the h- and p-versions are special cases of the hp-version.

Orderly sequences of discretization by mesh refinement, increase of the polynomial degree of elements, or a combination of both, are respectively called h-, p- and hp-extensions. The term extension refers to the progressive increase of the number of degrees of freedom in these processes.

The decision of whether the h-, p- or the hp-version should be used in a specific case depends on the nature of the exact solution  $\vec{u}_{EX}$ . Further information related to the subject may be found in [1].

Finite element models are comprised of three principal parts: Idealization, discretization and extraction:

1. **Idealization.** Idealization consists of the selection of the appropriate theory and the generalized formulation. Examples of theories are the linear theory of elasticity in two or three dimensions, engineering theories of beams, plates, shells and large displacement-small strain theory. Examples of generalized formulations are: the principle of minimum potential energy and the Hellinger-Reissner principle. Idealization, together with the input data, completely determine the exact solution  $\vec{u}_{EX}$ .
2. **Discretization.** Discretization creates a family of functions  $S_p(\Delta)$ . In solving stress analysis problems, users of finite element codes control the space

$S_p(\Delta)$  and thereby the error of approximation. In solving design problems, users control both  $\vec{u}_{EX}$  and  $S_p(\Delta)$ .

3. **Extraction.** Extraction refers to the procedures used for the computation of engineering data from the finite element solution. Computation of engineering data involves the computation of functionals such as stresses and stress intensity factors. We denote the functionals of interest by  $\Phi_i(\vec{u}_{FE})$  ( $i = 1, 2, \dots, n$ ). These functionals provide the information on which engineering decisions are based. It is important therefore that the errors in approximating these functionals be acceptably small in the sense that they will not significantly influence engineering decisions. In general we would like to have:

$$|\Phi_i(\vec{u}_{EX}) - \Phi_i(\vec{u}_{FE})| \leq \tau_i |\Phi_i(\vec{u}_{EX})| \quad (1.5)$$

where  $\tau_i$  is the relative error tolerance chosen by the analyst.

The analysis is completed when the computed data pass acceptance criteria set by the analyst. When the data do not pass the acceptance test then the discretization is modified, using information generated in the previous cycle of analysis and a new finite element solution is obtained.



## 1.2 Plate Models

In an increasing number of engineering applications, especially in the aerospace, marine and automobile industries, the use of structural components made of laminated composite materials has shown a great potential. The most attractive properties of the composite materials are the high strength and stiffness to weight ratios and their excellent fatigue strength, which is combined with ease of fabrication and resistance to corrosion.

Shear deformation effects are of critical importance in the analysis of laminated composite plates and shells. For thick laminated forms, or in the presence of local discontinuities, such as holes, reinforcements, etc., and at the boundaries, the transverse components of stress and strain have a strong influence on its strength. At the boundaries, "*boundary layer effects*" occur that is, the stress distribution is substantially different from the stress distribution in the interior.

Because the solution of the fully three-dimensional problem is computationally expensive, and not feasible for practical problems, several two-dimensional linear approximations have been developed. Most of the available methods of analysis for multilayered anisotropic plates and shells are extensions of the methods originally developed for homogeneous isotropic plates and shells, and are based on the principle of virtual work in conjunction with an assumed displacement field.

Many laminated plate models have been proposed over the years with various degrees of success. In the following sections, a review of the most important approaches will be presented. For each the review includes:

- (a) Description and assumptions;
- (b) Displacement field;
- (c) Stress-strain law;
- (d) Method for obtaining the governing equations;
- (e) Advantages and disadvantages.

The notation used is consistent with the one used to present the proposed model in Chapter 2 for the laminated strip.

Many writers refer to alternative representations of plates and shells as theories. Thus, in the literature one encounters references to membrane theory, Kirchhoff theory, Reissner-Mindlin theory, etc. It is better and more descriptive to use the word ‘model’ however, since one wishes to model the mechanical response by mathematical means of various solid objects, one dimension of which happens to be much smaller than the other two.

### 1.2.1 Shear-Deformation Models

Most high-order models for laminated plates are extensions of the classical plate model to account for the effect of the transverse components of strain in the plate.

The classical Kirchhoff plate model, extensively used in the analysis of thin isotropic plates, will lead to considerable errors when applied to laminated plates. Since the transverse shear moduli of modern composite materials are very low as compared with the in-plane moduli, the transverse shear deformation becomes significant, and cannot be neglected as in the case of homogeneous isotropic materials. The classical plate model underestimates deflections and overestimates natural frequencies. For plates with length to thickness ratio of 10, for instance, the classical plate model predicts natural frequencies 25% higher than those predicted by shear-deformation models [2].

In this group of models, there are two main categories: The first-order shear-deformation models, and the higher-order models. First-order models generally provide reasonable good results for the structural response of the plate. However they fail to accurately predict the through thickness stresses at discontinuities. Higher-order models are more accurate than the first-order models, but also more cumbersome and computationally demanding.

Shear deformation models do not account for continuity of the normal and shear stress components acting on laminar interfaces. Laminates are represented as homogeneous, orthotropic materials, with the material properties selected so as to account for the average axial, shear and bending stiffness of the laminates.

In the evaluation of first-order plate models, the middle surface of the plate is assumed to lie in the  $x - y$  plane. The two-dimensional domain occupied by the

middle surface is denoted by  $\Omega$  and the the boundary of  $\Omega$  is denoted by  $\Gamma$ . The thickness of the plate is denoted by  $h$  and the side surface of the plate is denoted by  $S$ , that is:  $S = \Gamma \times (-h/2, +h/2)$ .

The displacement field is assumed to be of the form:

$$u_x = u_{x|0}(x, y) + u_{x|1}(x, y)z \quad (1.6)$$

$$u_y = u_{y|0}(x, y) + u_{y|1}(x, y)z \quad (1.7)$$

$$u_z = u_{z|0}(x, y) \quad (1.8)$$

where  $u_{x|0}(x, y)$ ,  $u_{x|1}(x, y)$ ,  $u_{y|0}(x, y)$ , etc. are functions to be determined.

The strain-displacement relations of the small displacement-small strain theory are used:

$$\epsilon_x = \frac{\partial u_x}{\partial x} = \frac{\partial u_{x|0}}{\partial x} + \frac{\partial u_{x|1}}{\partial x}z \quad (1.9)$$

$$\epsilon_y = \frac{\partial u_y}{\partial y} = \frac{\partial u_{y|0}}{\partial y} + \frac{\partial u_{y|1}}{\partial y}z \quad (1.10)$$

$$\epsilon_z = \frac{\partial u_z}{\partial z} = \frac{\partial u_{z|0}}{\partial z} = 0 \quad (1.11)$$

$$\gamma_{xy} = \frac{\partial u_x}{\partial y} + \frac{\partial u_y}{\partial x} = \frac{\partial u_{x|0}}{\partial y} + \frac{\partial u_{y|0}}{\partial x} + z \left( \frac{\partial u_{x|1}}{\partial y} + \frac{\partial u_{y|1}}{\partial x} \right) \quad (1.12)$$

$$\gamma_{xz} = \frac{\partial u_x}{\partial z} + \frac{\partial u_z}{\partial x} = u_{x|1} + \frac{\partial u_{z|0}}{\partial x} \quad (1.13)$$

$$\gamma_{yz} = \frac{\partial u_y}{\partial z} + \frac{\partial u_z}{\partial y} = u_{y|1} + \frac{\partial u_{z|0}}{\partial y} \quad (1.14)$$

These models are, essentially, extensions of the classical plate model, which is discussed first.

### 1.2.1.1 The Classical Plate Model

The discussion of the classical plate model will follow the general outline of [1], and it will elaborate on isotropic plates. The extension to laminated plates will be included in the evaluation of the higher-order models.

(a) The classical plate model (CPM), also known as the Kirchhoff-Love model assumes that “Normals to the middle surface of the plate prior to deformation remains straight lines and normal after deformation”. This is equivalent to consider negligible the transverse shear strains, i.e.  $\gamma_{xz} = \gamma_{yz} = 0$  in (1.13)-(1.14).

(b) Under these conditions the assumed displacement field reduces to:

$$u_{x|1} = -\frac{\partial u_{z|0}}{\partial x} \quad (1.15)$$

$$u_{y|1} = -\frac{\partial u_{z|0}}{\partial y} . \quad (1.16)$$

Assuming transverse loading only,  $u_{x|0} = u_{y|0} = 0$ , and denoting  $u_{z|0}$  as  $w$ :

$$u_{x|1} = -\frac{\partial w}{\partial x} \quad (1.17)$$

$$u_{y|1} = -\frac{\partial w}{\partial y} \quad (1.18)$$

then (1.6)-(1.8) can be written as:

$$u_x = -\frac{\partial w}{\partial x} z \quad (1.19)$$

$$u_y = -\frac{\partial w}{\partial y} z \quad (1.20)$$

$$u_z = w(x, y). \quad (1.21)$$

(c) The stress-strain relations of linear elasticity, with the assumption that the stress  $\sigma_z$  is negligible in comparison with  $\sigma_x$  and  $\sigma_y$ , are:

$$\sigma_x = \frac{E}{1-\nu^2} (\epsilon_x + \nu\epsilon_y), \quad \sigma_y = \frac{E}{1-\nu^2} (\nu\epsilon_x + \epsilon_y) \quad (1.22)$$

$$\tau_{xy} = G\gamma_{xy}, \quad \tau_{xz} = G\gamma_{xz}, \quad \tau_{yz} = G\gamma_{yz} \quad (1.23)$$

where  $E$  is the modulus of elasticity,  $\nu$  is the Poisson's ratio, and  $G \stackrel{\text{def}}{=} E/2(1+\nu)$  is the shear modulus.

In the analysis of plates not the stresses but the stress resultants are of primary interest. The stress resultants are the *membrane forces*:

$$F_x \stackrel{\text{def}}{=} \int_{-h/2}^{+h/2} \sigma_x dz, \quad F_y \stackrel{\text{def}}{=} \int_{-h/2}^{+h/2} \sigma_y dz, \quad F_{xy} = F_{yx} \stackrel{\text{def}}{=} \int_{-h/2}^{+h/2} \tau_{xy} dz \quad (1.24)$$

the *shear forces*:

$$Q_x \stackrel{\text{def}}{=} - \int_{-h/2}^{+h/2} \tau_{xz} dz, \quad Q_y \stackrel{\text{def}}{=} - \int_{-h/2}^{+h/2} \tau_{yz} dz \quad (1.25)$$

and the *moments*:

$$M_x \stackrel{\text{def}}{=} - \int_{-h/2}^{+h/2} \sigma_x z dz, \quad M_y \stackrel{\text{def}}{=} - \int_{-h/2}^{+h/2} \sigma_y z dz \quad (1.26)$$

$$M_{xy} = -M_{yx} \stackrel{\text{def}}{=} - \int_{-h/2}^{+h/2} \tau_{xy} z dz. \quad (1.27)$$

$M_x$ ,  $M_y$  are called *bending moments*;  $M_{xy}$  is called *twisting moment*. From the strain-displacement relations (1.9)-(1.14), the stress-strain relations (1.22)-(1.23) and the stress resultants (1.24)-(1.27) we have:

$$F_x = \frac{Eh}{(1-\nu^2)} \left( \frac{\partial u_{x|0}}{\partial x} + \nu \frac{\partial u_{y|0}}{\partial y} \right) \quad (1.28)$$

$$F_y = \frac{E h}{(1 - \nu^2)} \left( \nu \frac{\partial u_{x|0}}{\partial x} + \frac{\partial u_{y|0}}{\partial y} \right) \quad (1.29)$$

$$F_{xy} = G h \left( \frac{\partial u_{x|0}}{\partial y} + \frac{\partial u_{y|0}}{\partial x} \right) \quad (1.30)$$

$$Q_x = -G h \left( u_{x|1} + \frac{\partial u_{z|0}}{\partial x} \right) \quad (1.31)$$

$$Q_y = -G h \left( u_{y|1} + \frac{\partial u_{z|0}}{\partial y} \right) \quad (1.32)$$

$$M_x = -\frac{E h^3}{12(1 - \nu^2)} \left( \frac{\partial u_{x|1}}{\partial x} + \nu \frac{\partial u_{y|1}}{\partial y} \right) \quad (1.33)$$

$$M_y = -\frac{E h^3}{12(1 - \nu^2)} \left( \nu \frac{\partial u_{x|1}}{\partial x} + \frac{\partial u_{y|1}}{\partial y} \right) \quad (1.34)$$

$$M_{xy} = -\frac{G h^3}{12} \left( \frac{\partial u_{x|1}}{\partial y} + \frac{\partial u_{y|1}}{\partial x} \right) \quad (1.35)$$

From the consideration of equilibrium of a plate element of size  $\Delta x \times \Delta y$ , we have

$F_{xy} = F_{yx}$  and:

$$\frac{\partial F_x}{\partial x} + \frac{\partial F_{xy}}{\partial y} = 0 \quad (1.36)$$

$$\frac{\partial F_{yx}}{\partial x} + \frac{\partial F_y}{\partial y} = 0 \quad (1.37)$$

$$\frac{\partial Q_x}{\partial x} + \frac{\partial Q_y}{\partial y} = q(x, y) \quad (1.38)$$

$$\frac{\partial M_x}{\partial x} + \frac{\partial M_{xy}}{\partial y} - Q_x = 0 \quad (1.39)$$

$$\frac{\partial M_{xy}}{\partial x} + \frac{\partial M_y}{\partial y} - Q_y = 0. \quad (1.40)$$

where  $q(x, y)$  is the transverse load over the surface of the plate.

(d) The governing equations are obtained using the principle of virtual work. The virtual work formulation is obtained by multiplying (1.36)-(1.40) by test functions

$v_{x|0}$ ,  $v_{y|0}$ ,  $v_{z|0}$ ,  $v_{x|1}$  and  $v_{y|1}$ , summing and integrating over domain  $\Omega$ . Upon integration by parts the following equation is obtained:

$$\begin{aligned}
& \iint_{\Omega} \left[ F_x \frac{\partial v_{x|0}}{\partial x} + F_{xy} \left( \frac{\partial v_{x|0}}{\partial y} + \frac{\partial v_{y|0}}{\partial x} \right) + F_y \frac{\partial v_{y|0}}{\partial y} \right] dx dy - \\
& \iint_{\Omega} \left( Q_x \frac{\partial v_{z|0}}{\partial x} + Q_y \frac{\partial v_{z|0}}{\partial y} \right) dx dy + \\
& \iint_{\Omega} \left( -M_x \frac{\partial v_{x|1}}{\partial x} - M_{xy} \frac{\partial v_{x|1}}{\partial y} - Q_x v_{x|1} \right) dx dy + \\
& \iint_{\Omega} \left( -M_{xy} \frac{\partial v_{y|1}}{\partial x} - M_y \frac{\partial v_{y|1}}{\partial y} - Q_y v_{y|1} \right) dx dy \\
& = \iint_{\Omega} q v_{z|0} dx dy + \oint (F_n v_{n|0} + F_t v_{t|0}) dt - \\
& \oint Q_n v_{z|0} dt - \oint (M_n v_{n|1} + M_{nt} v_{t|1}) dt
\end{aligned} \tag{1.41}$$

where  $v_{n|0}$ ,  $v_{t|0}$  are the normal and tangential components of the vector  $\{v_{x|0} \ v_{y|0}\}$  with respect to the boundary.

To obtain the standard form of the principle of virtual work  $\mathcal{B}(u, v) = \mathcal{F}(v)$ , the expressions (1.28)-(1.35) are substituted for  $F_x$ ,  $F_y$ ,  $Q_x$ ,  $Q_y$ ,  $M_x$ ,  $M_y$ ,  $M_{xy}$  in (1.41). In  $\mathcal{B}(u, v)$ ,  $u$  now represents the trial functions  $u_{x|0}$ ,  $u_{y|0}$ ,  $u_{z|0}$ ,  $u_{x|1}$ ,  $u_{y|1}$ , and  $v$  represents the test functions  $v_{x|0}$ ,  $v_{y|0}$ ,  $v_{z|0}$ ,  $v_{x|1}$ ,  $v_{y|1}$ . The trial and test functions and their derivatives are square integrable so that all integrals are properly defined. Substituting (1.19)-(1.21) into (1.41), the terms containing  $Q_x$ ,  $Q_y$  cancel and the following relationship is obtained:

$$\begin{aligned}
D \iint_{\Omega} & \left[ \left( \frac{\partial^2 w}{\partial x^2} + \nu \frac{\partial^2 w}{\partial y^2} \right) \frac{\partial^2 v}{\partial x^2} + 2(1 - \nu) \frac{\partial^2 w}{\partial x \partial y} \frac{\partial^2 v}{\partial x \partial y} + \left( \nu \frac{\partial^2 w}{\partial x^2} + \frac{\partial^2 w}{\partial y^2} \right) \frac{\partial^2 v}{\partial y^2} \right] dx dy \\
& = \iint_{\Omega} q v dx dy + \oint M_n \frac{\partial v}{\partial n} dt - \oint V_n v dt
\end{aligned} \tag{1.42}$$



where:  $V_n \stackrel{\text{def}}{=} Q_n + \partial M_{nt}/\partial t$ , and

$$D \stackrel{\text{def}}{=} \frac{Eh^3}{12(1-\nu^2)} \quad (1.43)$$

is the plate constant. The integrals are well defined if  $w$  and  $v$  have square integrable second derivatives. Defining:

$$\begin{aligned} \mathcal{B}(w, v) \stackrel{\text{def}}{=} D \iint_{\Omega} & \left[ \frac{\partial^2 w}{\partial x^2} \frac{\partial^2 v}{\partial x^2} + \nu \left( \frac{\partial^2 w}{\partial x^2} \frac{\partial^2 v}{\partial y^2} + \frac{\partial^2 w}{\partial y^2} \frac{\partial^2 v}{\partial x^2} \right) \right. \\ & \left. + \frac{\partial^2 w}{\partial y^2} \frac{\partial^2 v}{\partial y^2} + 2(1-\nu) \frac{\partial^2 w}{\partial x \partial y} \frac{\partial^2 v}{\partial x \partial y} \right] dx dy \end{aligned} \quad (1.44)$$

and

$$\mathcal{F}(v) \stackrel{\text{def}}{=} \iint_{\Omega} q v dx dy + \oint M_n \frac{\partial v}{\partial n} dt - \oint V_n v dt. \quad (1.45)$$

The set of functions for which  $\mathcal{B}(u, u) < \infty$  is denoted by  $E(\Omega)$ . The statement of the principle of virtual work depends on the boundary conditions. When tractions are prescribed on the entire boundary then the principle of virtual work is stated as follows: "Find  $w \in E(\Omega)$  such that  $\mathcal{B}(w, v) = \mathcal{F}(v)$  for all  $v \in E(\Omega)$ ".

On the boundary of the plate either  $w$  or  $V_n$  and either  $\partial w/\partial n$  or  $M_n$  are given. The restrictions on  $w$  and  $\partial w/\partial n$  are the kinematic boundary conditions. Commonly used boundary conditions are: Fixed:  $w = \partial w/\partial n = 0$ ; free:  $M_n = V_n = 0$ ; simply supported:  $w = 0, M_n = 0$ ; symmetry:  $\partial w/\partial n = V_n = 0$ ; antisymmetry: same as simple support. Note that in the case of simple support  $w = 0$  on  $\Gamma$  hence  $\partial w/\partial t = 0$  also and therefore  $u_t = 0$  on  $S$ . Thus both tangential displacement components are zero on  $S$ .

(e) As observed earlier, the classical plate model represents well the overall behavior of isotropic plates in the interior regions for “large” length-to-thickness ratios. It leads to considerable error near the boundaries and when analyzing laminated plates because it fails in accounting for shear deformation effects.

#### 1.2.1.2 First-Order Shear-Deformation Models

(a) The simplest of all the laminated plate models which are an improvement over the CPM is the Reissner-Mindlin type model, which incorporates the effect of shear deformation [3]-[4]. The introduction of shear deformation into a laminated plate model was first accomplished by Stavsky [5], for isotropic layers with the same Poisson ratios. Whitney and Pagano [6] investigated the application to laminated plates consisting of an arbitrary number of bonded anisotropic layers, each having one plane of material symmetry parallel to the central plane of the plate. They found the deflections of the plate to be dependent upon the selection of the shear correction factor, and that the stress distribution did not improve for low span-to-depth ratios over that given by the CPM.

(b) In the Reissner-Mindlin model the assumed mode of deformation is represented by the displacement components (1.6)-(1.8), and is described as follows: “A *plane section normal to the middle surface of the plate before deformation is assumed to remain plane but not necessarily normal to it after deformation.*”. Assuming

$u_{x|0} = u_{y|0} = 0$  and defining  $\beta_x = -u_{x|1}$ ,  $\beta_y = -u_{y|1}$  and  $w = u_{z|0}$ :

$$u_x = -\beta_x(x, y)z, \quad u_y = -\beta_y(x, y)z, \quad u_z = w(x, y) \quad (1.46)$$

The physical interpretation of  $\beta_x$  and  $\beta_y$  is rotation.

(c) Again, the stress-strain relations of linear elasticity, with the assumption that the stress  $\sigma_z$  is negligible in comparison with  $\sigma_x$  and  $\sigma_y$ , is used for each layer.

$$\begin{Bmatrix} \sigma_x \\ \sigma_y \\ \tau_{xy} \end{Bmatrix} = \begin{bmatrix} Q_{11} & Q_{12} & Q_{16} \\ Q_{12} & Q_{22} & Q_{26} \\ Q_{16} & Q_{26} & Q_{66} \end{bmatrix} \begin{Bmatrix} \epsilon_x \\ \epsilon_y \\ \gamma_{xy} \end{Bmatrix} \quad (1.47)$$

$$\begin{Bmatrix} \tau_{yz} \\ \tau_{xz} \end{Bmatrix} = \begin{bmatrix} Q_{44} & Q_{45} \\ Q_{45} & Q_{55} \end{bmatrix} \begin{Bmatrix} \gamma_{yz} \\ \gamma_{xz} \end{Bmatrix} \quad (1.48)$$

where  $Q_{ij}$  are the coefficients of the material stiffness matrix in the laminate coordinate system. Shear correction factors are used for the transverse shear resultants as discussed later. The definition of the stress resultants is the same as in (1.24)-(1.27).

(d) The displacement field (1.46) predicts a uniform shear across the laminae, which is incorrect. This prompted the introduction of a shear correction factor into the shear stress resultant. The derivation of the principle of virtual work is based on (1.41) and (1.31)-(1.35), however (1.31)-(1.35) are modified as follows for the case of cross-ply laminates:

$$M_x = - \left( D_{11} \frac{\partial u_{x|1}}{\partial x} + D_{12} \frac{\partial u_{y|1}}{\partial y} \right) \equiv \left( D_{11} \frac{\partial \beta_x}{\partial x} + D_{12} \frac{\partial \beta_y}{\partial y} \right) \quad (1.49)$$

$$M_y = - \left( D_{12} \frac{\partial u_{x|1}}{\partial x} + D_{22} \frac{\partial u_{y|1}}{\partial y} \right) \equiv \left( D_{12} \frac{\partial \beta_x}{\partial x} + D_{22} \frac{\partial \beta_y}{\partial y} \right) \quad (1.50)$$

$$M_{xy} = -D_{66} \left( \frac{\partial u_{x|1}}{\partial y} + \frac{\partial u_{y|1}}{\partial x} \right) \equiv D_{66} \left( \frac{\partial \beta_x}{\partial y} + \frac{\partial \beta_y}{\partial x} \right) \quad (1.51)$$

$$Q_x = -\kappa G_1 \left( u_{x|1} + \frac{\partial u_{z|0}}{\partial x} \right) \equiv -\kappa G_1 \left( -\beta_x + \frac{\partial w}{\partial x} \right) \quad (1.52)$$

$$Q_y = -\kappa G_2 \left( u_{y|1} + \frac{\partial u_{z|0}}{\partial y} \right) \equiv -\kappa G_2 \left( -\beta_y + \frac{\partial w}{\partial y} \right) \quad (1.53)$$

where the  $\kappa$  is the shear correction factor and:

$$G_1 = \int_{-h/2}^{+h/2} Q_{55} dz, \quad G_2 = \int_{-h/2}^{+h/2} Q_{44} dz$$

$$D_{ij} = \int_{-h/2}^{+h/2} Q_{ij} z^2 dz, \quad i, j = 1, 2, 6.$$

Various values have been proposed for  $\kappa$ . For isotropic plates for example, Reissner [7] proposed the value of  $5/6$ . In [3] Mindlin considered the propagation of elastic waves in isotropic plates and concluded that  $\kappa$  depends on Poisson's ratio, and it "ranges almost linearly from 0.76 for  $\nu = 0$  to 0.91 for  $\nu = 1/2$ ". In practice very often the value  $\kappa = 5/6$  is used, independently of Poisson's ratio. Modification of the shear modulus by a shear correction factor  $\kappa$  is a modelling decision commonly justified by the argument that the assumed linear variation of  $u_x$ ,  $u_y$  with respect to  $z$  leads to a plate model which is overly stiff in shear. Similar range of values can be used for laminated plates depending on the material properties [6].

On substituting (1.49)-(1.53) into (1.41) we have:

$$\mathcal{B}(\beta_x, \beta_y, w; \varphi_x, \varphi_y, v) = \mathcal{F}(\varphi_x, \varphi_y, v) \quad (1.54)$$

where:

$$\mathcal{B}(\beta_x, \beta_y, w; \varphi_x, \varphi_y, v) \stackrel{\text{def}}{=} \iint_{\Omega} \left[ D_{11} \frac{\partial \beta_x}{\partial x} \frac{\partial \varphi_x}{\partial x} + D_{12} \left( \frac{\partial \beta_x}{\partial x} \frac{\partial \varphi_y}{\partial y} + \frac{\partial \beta_y}{\partial y} \frac{\partial \varphi_x}{\partial x} \right) + \right.$$

$$\begin{aligned}
& D_{22} \frac{\partial \beta_y}{\partial y} \frac{\partial \varphi_y}{\partial y} + D_{66} \left( \frac{\partial \beta_x}{\partial y} + \frac{\partial \beta_y}{\partial x} \right) \left( \frac{\partial \varphi_x}{\partial y} + \frac{\partial \varphi_y}{\partial x} \right) \Big] dx dy \\
& + \kappa \iint_{\Omega} \left[ G_1 \left( \frac{\partial w}{\partial x} - \beta_x \right) \left( \frac{\partial v}{\partial x} - \varphi_x \right) + \right. \\
& \quad \left. G_2 \left( \frac{\partial w}{\partial y} - \beta_y \right) \left( \frac{\partial v}{\partial y} - \varphi_y \right) \right] dx dy \tag{1.55}
\end{aligned}$$

$$\mathcal{F}(\varphi_x, \varphi_y, v) \stackrel{\text{def}}{=} \iint_{\Omega} q v dx dy + \oint_{\Gamma} \left( M_n \varphi_n + M_{nt} \varphi_t - Q_n v \right) ds \tag{1.56}$$

where  $v$ ,  $\varphi_x$ ,  $\varphi_y$  are the test functions.

The commonly used boundary conditions are:

- Fixed:  $\beta_n = \beta_t = w = 0$ .
- Free:  $M_n = M_{nt} = Q_n = 0$ .
- Simply supported:
  1. Soft simple support:  $w = 0$ ,  $M_n = M_{nt} = 0$ .
  2. Hard simple support:  $w = 0$ ,  $\beta_t = 0$ ,  $M_n = 0$ .
- Symmetric:  $\beta_n = 0$ ,  $M_{nt} = 0$ ,  $Q_n = 0$ .
- Antisymmetric: Same as hard simple support.

Observe that in the Reissner-Mindlin model simple support can be defined in two different ways, whereas in the Kirchhoff model only one definition is possible. In the Kirchhoff model simple support means hard simple support.

(e) Despite the increased generality of the shear-deformation model, the flexural stress distribution show little improvement over those of the classical laminated

plate model. Higher order terms are needed in the power series expansion of the assumed displacement field to properly model the behavior of the laminates.

The performance of the first-order shear-deformation model is dependent on the factors used to adjust the transverse shear stiffness. Several approaches have been proposed for calculating the composite shear correction factors for different laminates. Most of these approaches are based on matching certain gross response characteristics, as predicted by the first-order model, with the corresponding characteristics of the three-dimensional elasticity model [8]. The proposed correction factors are functions of the lamination parameters only. They do not account for the influence of the loading conditions in the distribution of the transverse shear strains in the thickness direction. As an attempt to incorporate the actual distribution of the transverse shear strains in the thickness direction, in calculating the transverse shear stiffness, a predictor-corrector approach has been proposed by Noor [9] which is outlined in the following paragraph.

The predictor phase consists of using a first-order shear-deformation model to calculate the initial estimates for the gross response characteristics of the laminate (vibration frequencies, average through-the-thickness displacement, etc.) as well as the in-plane strains and stresses in the thickness direction. An initial set of composite correction factors are required in this phase. Then, the three-dimensional equilibrium equations and the constitutive relations are used to compute the transverse stresses and strains as well as the transverse shear strain energy distribution in

the thickness direction. The correction phase consists of calculating the composite shear correction factors by matching the integral of the transverse shear strain energy in the thickness direction with that obtained with the first-order model. These composite correction factors are then used to adjust the transverse shear stiffness of the laminate to obtain better estimates for the gross response characteristics, as well as for the distributions of displacements and in-plane stresses in the thickness direction. The predictor-corrector approach appears to be effective for the determination of the global and detailed response characteristics of multilayered cylinders [10], [11].

#### 1.2.1.3 Higher-Order Shear-Deformation Models

To overcome the limitations of the first-order shear-deformation model, higher-order models that involve higher order derivatives of the transverse displacements were developed. These models proved to be more accurate but also more cumbersome and demanding on computational resources. A significant amount of research has been conducted in this field. For example, Whitney and Sun [12] included one additional term in each component of the displacement field given by (1.6)-(1.8) and derived the governing equations from Hamilton's principle. Lo, Christensen and Wu [13] included one additional term per field as compared with [12] and derived the governing equations using the principle of stationary potential energy. This model does not require the use of shear correction factors. The same displacement field was used by Chomkwah and Avula [14] but they derive the governing equations based

on the minimization of the total potential energy and using the Lagrange multiplier technique to constraint the displacement functions to satisfy the stress boundary conditions. Reddy [15] and Reddy and Liu [16] proposed a similar displacement field as in [13] and also imposed a parabolic variation of the transverse shear strains through the thickness to satisfy the zero tangential stress on the surface of the plate. The principle of virtual displacements was used to derive the equilibrium equations. The equilibrium requirements are not satisfied at the interfaces. Several survey papers can be found in the literature of laminated composites (see for instance [10], [11], [17]).

The model presented by Reddy [15] was selected as representative of the higher-order shear-deformation models to be evaluated in what follows.

(a) This model accounts not only for transverse shear strains, but also for a parabolic variation of the transverse shear strains through the thickness, and consequently, there is no need for using shear correction factors.

(b) the proposed displacement field is given by:

$$u_x = u_{x|0}(x, y) + u_{x|1}(x, y)z + u_{x|2}(x, y)z^2 + u_{x|3}(x, y)z^3 \quad (1.57)$$

$$u_y = u_{y|0}(x, y) + u_{y|1}(x, y)z + u_{y|2}(x, y)z^2 + u_{y|3}(x, y)z^3 \quad (1.58)$$

$$u_z = u_{z|0}(x, y) = w(x, y) \quad (1.59)$$

where  $u_{x|0}$ ,  $u_{x|1}$ ,  $u_{y|0}$ , etc. are independent functions. The functions  $u_{x|2}$ ,  $u_{x|3}$ ,  $u_{y|2}$  and  $u_{y|3}$  are determined using the condition that the transverse shear stresses  $\tau_{xz}$  and  $\tau_{yz}$  vanish on the top and bottom surfaces of the plate. For laminated plates of



orthotropic materials, these conditions are equivalent to forcing the corresponding shear strains to be zero. From the conditions  $\gamma_{xz}(z = \pm h/2) = \gamma_{yz}(z = \pm h/2) = 0$ , the following relations are obtained:

$$u_{x|2} = u_{y|2} = 0 \quad (1.60)$$

$$u_{x|3} = -\frac{4}{3h^2} \left( u_{x|1} + \frac{\partial w}{\partial x} \right) \quad (1.61)$$

$$u_{y|3} = -\frac{4}{3h^2} \left( u_{y|1} + \frac{\partial w}{\partial y} \right) \quad (1.62)$$

and the displacement field for Reddy's model thus becomes

$$u_x = u_{x|0} + z \left[ u_{x|1} - \frac{4}{3} \left( \frac{z}{h} \right)^2 \left( u_{x|1} + \frac{\partial w}{\partial x} \right) \right] \quad (1.63)$$

$$u_y = u_{y|0} + z \left[ u_{y|1} - \frac{4}{3} \left( \frac{z}{h} \right)^2 \left( u_{y|1} + \frac{\partial w}{\partial y} \right) \right] \quad (1.64)$$

$$u_z = w(x, y) \quad (1.65)$$

(c) The constitutive equations incorporate the assumption that each layer possesses a plane of elastic symmetry parallel to the x-y plane. The constitutive equations for a layer are written in terms of the plane-stress-reduced elastic constants in the material axes of the layers. After transformation, the lamina constitutive equations are expressed in terms of stresses and strains in the global coordinates as follows:

$$\begin{Bmatrix} \sigma_x \\ \sigma_y \\ \tau_{xy} \end{Bmatrix} = \begin{bmatrix} Q_{11} & Q_{12} & Q_{16} \\ Q_{12} & Q_{22} & Q_{26} \\ Q_{16} & Q_{26} & Q_{66} \end{bmatrix} \begin{Bmatrix} \epsilon_x \\ \epsilon_y \\ \gamma_{xy} \end{Bmatrix} \quad (1.66)$$

$$\begin{Bmatrix} \tau_{yz} \\ \tau_{xz} \end{Bmatrix} = \begin{bmatrix} Q_{44} & Q_{45} \\ Q_{45} & Q_{55} \end{bmatrix} \begin{Bmatrix} \gamma_{yz} \\ \gamma_{xz} \end{Bmatrix} \quad (1.67)$$

The stress resultants are defined as in (1.24)-(1.27), but because of the additional terms in the displacement field selected, five extra resultants need to be defined. These are:

$$R_x \stackrel{\text{def}}{=} \int_{-h/2}^{+h/2} z^2 \tau_{xz} dz, \quad R_y \stackrel{\text{def}}{=} \int_{-h/2}^{+h/2} z^2 \tau_{yz} dz \quad (1.68)$$

$$P_x \stackrel{\text{def}}{=} \int_{-h/2}^{+h/2} z^3 \sigma_x dz, \quad P_y \stackrel{\text{def}}{=} \int_{-h/2}^{+h/2} z^3 \sigma_y dz, \quad P_{xy} \stackrel{\text{def}}{=} \int_{-h/2}^{+h/2} z^3 \tau_{xy} dz \quad (1.69)$$

(d) As established before, the equilibrium equations are obtained using the principle of virtual displacements, i.e.,

$$\begin{aligned} \int_{-h/2}^{+h/2} \iint_{\Omega} (\sigma_x \delta \epsilon_x + \sigma_y \delta \epsilon_y + \tau_{xy} \delta \gamma_{xy} + \tau_{xz} \delta \gamma_{xz} + \tau_{yz} \delta \gamma_{yz}) dy dx dz \\ + \iint_{\Omega} q \delta w dx dy = 0 \end{aligned} \quad (1.70)$$

where the integration is performed over the entire domain of the plate. Introducing strain relations similar to (1.9)-(1.14) and the stress resultants mentioned above,

(1.70) can be written as:

$$\begin{aligned} \iint_{\Omega} \left\{ F_x \frac{\partial \delta u_{x|0}}{\partial x} + M_x \frac{\partial \delta u_{x|1}}{\partial x} + P_x \left[ -\frac{4}{3h^2} \left( \frac{\partial \delta u_{x|1}}{\partial x} + \frac{\partial^2 \delta w}{\partial x^2} \right) \right] + F_y \frac{\partial \delta u_{y|0}}{\partial y} \right. \\ + M_y \frac{\partial \delta u_{y|1}}{\partial y} + P_y \left[ -\frac{4}{3h^2} \left( \frac{\partial \delta u_{y|1}}{\partial y} + \frac{\partial^2 \delta w}{\partial y^2} \right) \right] + F_{xy} \left( \frac{\partial \delta u_{x|0}}{\partial y} + \frac{\partial \delta u_{y|0}}{\partial x} \right) \\ + M_{xz} \left( \frac{\partial \delta u_{x|1}}{\partial y} + \frac{\partial \delta u_{y|1}}{\partial x} \right) + P_{xy} \left[ -\frac{4}{3h^2} \left( \frac{\partial \delta u_{x|1}}{\partial y} + \frac{\partial \delta u_{y|1}}{\partial x} + 2 \frac{\partial^2 \delta w}{\partial x \partial y} \right) \right] \\ + Q_y \left( \delta u_{y|1} + \frac{\partial \delta w}{\partial y} \right) + Q_x \left( \delta u_{x|1} + \frac{\partial \delta w}{\partial x} \right) + R_y \left[ -\frac{4}{h^2} \left( \delta u_{y|1} + \frac{\partial \delta w}{\partial y} \right) \right] \\ \left. + R_x \left[ -\frac{4}{h^2} \left( \delta u_{x|1} + \frac{\partial \delta w}{\partial x} \right) \right] q \delta w \right\} dx dy = 0. \end{aligned} \quad (1.71)$$

Integrating by parts and collecting the coefficients of  $\delta u_{x|0}$ ,  $\delta u_{y|0}$ ,  $\delta w$ ,  $\delta u_{x|1}$ , and  $\delta u_{y|1}$ , five equilibrium equations are obtained in terms of the stress resultants.

$$\frac{\partial F_x}{\partial x} + \frac{\partial F_{xy}}{\partial y} = 0 \quad (1.72)$$

$$\frac{\partial F_{xy}}{\partial x} + \frac{\partial F_y}{\partial y} = 0 \quad (1.73)$$

$$\frac{\partial Q_x}{\partial x} + \frac{\partial Q_y}{\partial y} + q - \frac{4}{h^2} \left( \frac{\partial R_x}{\partial x} + \frac{\partial R_y}{\partial y} \right) + \frac{4}{3h^2} \left( \frac{\partial^2 P_x}{\partial x^2} + 2 \frac{\partial^2 P_{xy}}{\partial x \partial y} + \frac{\partial^2 P_y}{\partial y^2} \right) = 0 \quad (1.74)$$

$$\frac{\partial M_x}{\partial x} + \frac{\partial M_{xy}}{\partial y} - Q_x + \frac{4}{h^2} R_x - \frac{4}{3h^2} \left( \frac{\partial P_x}{\partial x} + \frac{\partial P_{xy}}{\partial y} \right) = 0 \quad (1.75)$$

$$\frac{\partial M_{xy}}{\partial x} + \frac{\partial M_y}{\partial y} - Q_y + \frac{4}{h^2} R_y - \frac{4}{3h^2} \left( \frac{\partial P_{xy}}{\partial x} + \frac{\partial P_y}{\partial y} \right) = 0 \quad (1.76)$$

Finally, the stress resultants are related to the strain components and further to the generalized displacements, and the solution can be obtained after application of the boundary conditions.

Reddy's model requires a total of six boundary conditions per edge. These include  $u_{0|n}$  or  $F_n$ ,  $u_{0|ns}$  or  $F_{ns}$ ,  $w$  or  $Q_n$ ,  $\partial w / \partial n$  or  $P_n$ ,  $u_{1|n}$  or  $M_n$ ,  $u_{1|ns}$  or  $M_{ns}$ .

(e) Reddy applied the above model to obtain exact results for simply supported, symmetric cross-ply rectangular plates. These results were compared with the three-dimensional elasticity solutions of Pagano [18] and with those obtained using the first-order shear-deformation model of Reddy and Chao [19]. It was shown that the higher-order model gives stresses that are greatly improved over those given by first-order shear-deformation model. However the shear stresses obtained were found to be on the low side of the values given by the three-dimensional solution. This error may be due to the fact that continuity of stresses across the interfaces was not imposed.

### 1.2.2 Discrete-Layer Models

All laminated plate models discussed above, assume that the displacements vary through the thickness of the laminate according to a single expression, not allowing for possible discontinuities in the derivatives of the displacements at the interfaces of adjoining laminae. In the discrete-layer models the displacement field is expressed as piecewise linear functions in the thickness direction. Some of the work in this line is briefly described in the following paragraphs.

Srinivas [20] considered an arbitrary number of layers, and described the displacement field as continuous and piecewise-smooth functions (smooth within each layer). No shear correction factors were introduced, but the number of fields equations and edge boundary conditions depended on the number of layers.

Di Sciuva [21] proposed a displacement field which allows piecewise linear variation of the  $u_x$  and  $u_y$  displacements, and constant value of the  $u_z$  displacement component. The assumed displacement field also allows the contact conditions at the interfaces to be satisfied, thus reducing the number of displacements parameters to five. This model does not require the use of shear correction factors, and the governing equations are obtained using a variational principle. The normal stress in the thickness direction is neglected, and as a consequence, local effects, such as *boundary layer effects*, geometric discontinuities, etc., are beyond the capabilities of the model. A multilayered anisotropic flat plate element was developed by Di Sciuva [22] by making use of this formulation. The finite element is a rectangle

with 32 degrees of freedom which include extension, bending and transverse shear deformation. Numerical tests carried out by Di Scuva on two sample problems show that the element is very efficient in predicting gross response of thin and thick laminated plate under static loading.

Toledano and Murakami [23] developed a model for arbitrary laminate configurations based upon Reissner's [24] new mixed variational principle for displacements and transverse stresses. They assumed a piecewise-linear in-plane displacement distribution to guarantee continuity of interlaminar stresses. Transverse displacements are taken to be constant throughout the entire thickness of the plate. Therefore, shear strains are constant within each layer, but differ from layer to layer. The transverse stresses are assumed to be quadratic functions of the local thickness coordinate across each layer. The application of Reissner's new principle results in automatically yielding the appropriate shear correction factors for the transverse shear constitutive equations. Numerical results were obtained for symmetric, anti-symmetric, and arbitrary laminates in cylindrical bending and were compared with the exact three-dimensional elasticity solutions. A good agreement was observed between the two sets of results. The main shortcoming of this model is that the number of field equations and boundary conditions depend upon the number of layers.

Bhaskar and Varadant [25] also proposed a model using a piecewise displacement distribution for symmetric laminates subjected to antisymmetric loading. For the

$u_x$  and  $u_y$  displacement components they selected unknown functions of the in-plane coordinates, multiplied by pre-defined polynomials of degree three in the transverse direction and multiplied by the Heaviside Unit Step Function and summing over the plate interfaces. The variation of  $u_z$  is assumed to be quadratic in  $z$ , and the same for all layers. The assumed displacement field satisfies the displacement compatibility at interfaces and the zero shear condition on the free surfaces of the plate. Stress continuities at interfaces are also enforced to solve for the functions of the in-plane coordinates. The principle of minimum total potential is used to derive the governing equations. The total number of independent variables is four. The model was compared with the exact three-dimensional elasticity solution of a laminated strip under cylindrical bending for large ( $L/h = 50$ ) to medium ( $L/h = 12.5$ ) length-to-thickness ratios. The agreement between the two sets of results is very good.

Barbero and Reddy [26] developed a model allowing for piecewise approximation of the displacements through individual laminae. For the  $u_x$  and  $u_y$  displacement components they assume one function which depends on the in-plane coordinates  $x$  and  $y$ , and represent the displacement of the reference plane of the laminate, and other set of functions depending on  $x, y$  and  $z$ , which vanish in the reference plane. These later functions are expressed as a linear combination of undetermined functions of  $(x, y)$  and known functions of  $z$ . The number of these later functions depending on the number of layers. Transverse displacements are taken to be

constant throughout the entire thickness of the plate. The proposed displacement field has the form:

$$u_x(x, y, z) = u_x(x, y) + U_x(x, y, z) \quad (1.77)$$

$$u_y(x, y, z) = u_y(x, y) + U_y(x, y, z) \quad (1.78)$$

$$u_z(x, y, z) = u_z(x, y) = w(x, y) \quad (1.79)$$

where  $u_x(x, y)$ ,  $u_y(x, y)$ ,  $u_z(x, y)$  are the displacement of a point  $(x, y, 0)$  on the reference plane of the laminate, and  $U_x$  and  $U_y$  are functions which vanish on the reference plane:

$$U_x(x, y, 0) = U_y(x, y, 0) = 0 \quad (1.80)$$

The functions  $U_x$  and  $U_y$  are expressed as:

$$U_x(x, y, z) = \sum_{j=1}^n U_x^j(x, y) \phi_j(z) \quad (1.81)$$

$$U_y(x, y, z) = \sum_{j=1}^n U_y^j(x, y) \phi_j(z) \quad (1.82)$$

where  $\phi_j$  are any continuous functions that satisfy the condition:

$$\phi_j(0) = 0, \quad j = 1, 2, \dots, n. \quad (1.83)$$

In a finite element approximation,  $\phi_j$  denote the global basis functions.

The equilibrium equations are derived using the principle of virtual displacements, rendering a set of  $(2n + 1)$  differential equations,  $n$  being the number of layers through the thickness. The same number of boundary conditions need to be specified. The application of this model to a two-layer cross-ply plate strip in

cylindrical bending and to a rectangular plate of three orthotropic layers show excellent agreement with the corresponding three-dimensional elasticity solutions. The model gives accurate interlaminar stress distributions, even for very thick ( $L/h = 4$ ) plates. The main shortcoming of this model is that the number of equations and boundary conditions depend on the number of layers in the laminate.

### 1.2.3 Hierarchic Models

The first rigorous proof of the relation between the three-dimensional solution and the plate model was given by Morgenstern [27] in 1959. The construction of hierarchic models for homogeneous isotropic plates and shells was discussed by Szabó and Sahrman in [28]. Additional discussion and examples are available in [29], [1], [30], [31]. In this work the principles governing the derivation of a hierarchic sequence of models for laminated composites are presented. Once again, the exact solution corresponding to each particular model is viewed as an approximation to the problem of elasticity in which the elastic body is comprised of orthotropic laminae. The basis for approximation is the degree to which the equilibrium equations of the problem of elasticity are satisfied. Hierarchic sequences of models make adaptive selection of the model which is best suited for the purposes of a particular analysis possible.

The essential features of the hierarchic models are as follows:

1. The exact solutions corresponding to the hierarchic sequence of models converge to the exact solution of the corresponding problem of elasticity for a



fixed laminate thickness,

$$\lim_{i \rightarrow \infty} \|u_{EX}^{(3D)} - u_{EX}^{(HM|i)}\|_{E(\Omega)} = 0$$

where  $i$  represents the  $i$ th model of the hierarchic sequence and  $\|\cdot\|_{E(\Omega)}$  is the energy norm.

2. The exact solution of each model converges to the same limit as the exact solution of the corresponding problem of elasticity with respect to the laminate thickness ( $h$ ) approaching zero.

$$\lim_{h \rightarrow 0} \frac{\|u_{EX}^{(HM|i)} - u_{EX}^{(3D)}\|_{E(\Omega)}}{\|u_{EX}^{(3D)}\|_{E(\Omega)}} = 0, \quad i = 1, 2, \dots$$

3. When  $u_{EX}^{(3D)}$  is smooth:

$$\frac{\|u_{EX}^{(3D)} - u_{EX}^{(HM|i)}\|_{E(\Omega)}}{\|u_{EX}^{(HM|i)}\|_{E(\Omega)}} \approx C h^{\alpha_i}$$

where  $C$  is a constant, independent of  $i$ ;  $\alpha_i$  is a constant which depends on  $i$ , and  $\alpha_{i+1} > \alpha_i$ .

These requirements are important because, typically, the solution of the problem of elasticity in the interior regions of the domain can be approximated well by the lowest in the hierarchic sequence of models but near the boundaries higher models are needed.

In order to focus on the essentials, the derivation for the case of laminated strips is presented first (Chapter 2), and the more general case is presented in Chapter 4.

## Chapter 2

### Laminated Strip

As mentioned earlier, hierarchic models for homogeneous isotropic plates and shells were discussed by Szabó and Sahrman in [1]. The hierarchic models proposed in [1] satisfied the requirements 1 and 3 indicated in Chapter 1, but satisfied requirement 2 only in the case of zero Poisson's ratio. The modifications needed to satisfy condition 2 were clarified later by Babuška and Li [2]. Additional discussion and examples are available in [3], [4]. In this Chapter the principles governing the derivation of a hierarchic sequence of models for laminated strips are presented. Once again, the exact solution corresponding to each particular model is viewed as an approximation to the problem of linear elasticity in which the elastic body comprises orthotropic laminae. The basis for approximation is the degree to which the equilibrium equations of the problem of elasticity are satisfied.

In order to focus on the essentials, the derivation presented herein is for the case of laminated strips only. Since plane-strain conditions are considered, this problem

represents a particular case of the three-dimensional elasticity problem. The more general case will be presented in Chapter 4.

## 2.1 Hierarchic Models for Laminated Composites

Consider the infinite strip shown in Fig. 2.1, consisting of three or more laminae which are symmetrically arranged with respect to the middle plane. The following assumptions are made with respect to the the load:

1. The load  $q(x)$  is antisymmetric with respect to the middle surface.
2. The load  $q(x) = 0$  for  $|x| \geq L/2$ ,  $L$  is some fixed number.
3. The equilibrium equations are satisfied:

$$\int_{-\infty}^{+\infty} q(x) dx = 0 \quad \int_{-\infty}^{+\infty} q(x)x dx = 0. \quad (2.1)$$

Assumptions (2) and (3) are introduced so that boundary conditions do not have to be considered. Boundary conditions will be discussed separately. We will be interested in the limiting process  $h/L \rightarrow 0$ . Observe that fixing  $L$  and letting  $h \rightarrow 0$  is equivalent to fixing  $h$  and letting  $L \rightarrow \infty$ .

Let  $u_x(x, y)$ ,  $u_y(x, y)$  denote the displacement field for the infinite strip under the normal load  $q(x)$ , satisfying the equilibrium equations (with zero body forces):

$$\frac{\partial \sigma_x}{\partial x} + \frac{\partial \tau_{xy}}{\partial y} = 0 \quad (2.2)$$

$$\frac{\partial \tau_{xy}}{\partial x} + \frac{\partial \sigma_y}{\partial y} = 0 \quad (2.3)$$

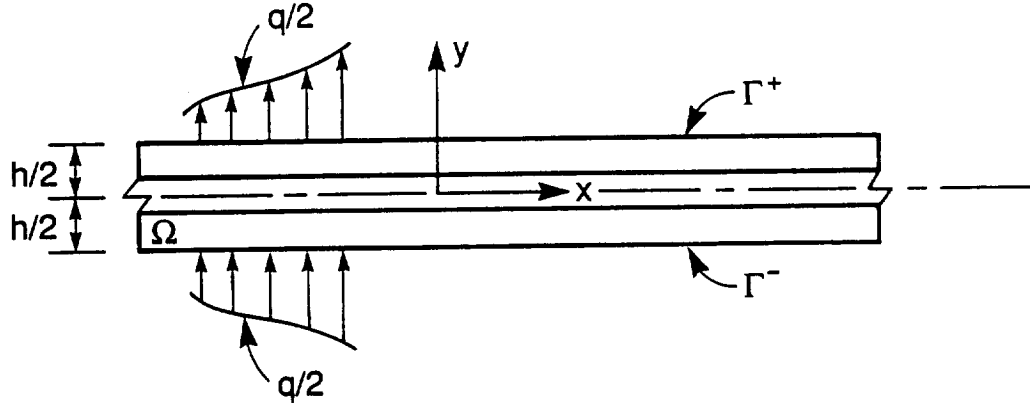


Figure 2.1: Infinite strip. Notation.

and with boundary conditions:

$$\sigma_y(x, \pm h/2) = \frac{1}{2} q(x) \quad (2.4)$$

$$\tau_{xy}(x, \pm h/2) = 0. \quad (2.5)$$

The stress-strain relations of two-dimensional elasticity are used:

$$\begin{aligned} \sigma_x &= E_1 \epsilon_x + E_2 \epsilon_y + E_4 \gamma_{xy} \\ \sigma_y &= E_2 \epsilon_x + E_3 \epsilon_y + E_5 \gamma_{xy} \\ \tau_{xy} &= E_4 \epsilon_x + E_5 \epsilon_y + E_6 \gamma_{xy} \end{aligned} \quad (2.6)$$

where the  $E_i$  are only function of  $y$ , and the strains are related to the displacements (small-strain, small-deformation theory) by:

$$\begin{aligned} \epsilon_x &= \frac{\partial u_x}{\partial x} \\ \epsilon_y &= \frac{\partial u_y}{\partial y} \\ \gamma_{xy} &= \frac{\partial u_x}{\partial y} + \frac{\partial u_y}{\partial x}. \end{aligned} \quad (2.7)$$

We now consider a partial Fourier transformation of the problem described by (2.2)-(2.5). For any integrable function  $q(x)$ , we can write the Fourier transform as:

$$Q(\beta) = \int_{-\infty}^{+\infty} q(x) e^{-i\beta x} dx \quad (2.8)$$

therefore, conditions (2.1) are represented by:

$$Q(0) = 0, \quad \left. \frac{dQ(\beta)}{d\beta} \right|_{\beta=0} = 0. \quad (2.9)$$

From (2.8) we find that:

$$Q'(\beta) = i\beta Q(\beta) \quad (2.10)$$

that is, the derivatives become multiplications by  $i\beta$  in the Fourier transformed variables. The partial Fourier transformations of  $u_x$ ,  $u_y$  are denoted by:

$$\phi(\beta, y) = \int_{-\infty}^{+\infty} u_x(x, y) e^{-i\beta x} dx \quad (2.11)$$

$$\psi(\beta, y) = \int_{-\infty}^{+\infty} u_y(x, y) e^{-i\beta x} dx. \quad (2.12)$$

Therefore, the strains in the transformed variables are obtained using (2.7) and (2.11), (2.12):

$$\hat{\epsilon}_x = i\beta \phi(\beta, y) \quad (2.13)$$

$$\hat{\epsilon}_y = \psi'(\beta, y) \quad (2.14)$$

$$\hat{\gamma}_{xy} = \phi'(\beta, y) + i\beta \psi(\beta, y) \quad (2.15)$$

where the primes represent differentiation with respect to  $y$ . Substituting (2.13)-(2.15) into (2.6), and considering the case  $E_4 = E_5 = 0$  (which is the case for

orthotropic materials when the material axes are parallel with the  $x - y$  axes), the equilibrium equations (2.2), (2.3) can be written as:

$$-\beta^2 E_1 \phi + i \beta E_2 \psi' + (E_6 \phi')' + i \beta (E_6 \psi)' = 0 \quad (2.16)$$

$$-\beta^2 E_6 \psi + i \beta (E_2 \phi)' + (E_3 \psi')' + i \beta E_6 \phi' = 0 \quad (2.17)$$

which are the Fourier transformed forms of equations (2.2), (2.3). Further, (2.4) and (2.5) become:

$$i \beta E_2(h/2) \phi(\beta, h/2) + E_3(h/2) \psi'(\beta, h/2) = \frac{1}{2} Q(\beta) \quad (2.18)$$

$$E_6(h/2) \phi'(\beta, h/2) + i \beta E_6(h/2) \psi(\beta, h/2) = 0. \quad (2.19)$$

Note that for any fixed  $\beta$ , (2.16)-(2.19) is a parameter-dependent boundary value problem on  $(-h/2, +h/2)$ , with parameter  $\beta$ . Solving (2.16)-(2.19), the displacement components  $u_x$ ,  $u_y$  are obtained as the inverse Fourier transform of  $\phi(\beta, y)$ ,  $\psi(\beta, y)$ .

Formally, (2.16) and (2.17) can be alternatively obtained by assuming the displacement field to be of the form:

$$u_x = \phi(\beta, y) e^{i\beta x} \quad (2.20)$$

$$u_y = \psi(\beta, y) e^{i\beta x} \quad (2.21)$$

where  $u_x$ ,  $u_y$  are complex functions, and both the real and imaginary parts represent admissible displacements. In such a case, using (2.6) and (2.7) into (2.2) (2.3), the following equilibrium equations are obtained:

$$e^{i\beta x} \{-\beta^2 E_1 \phi + i \beta E_2 \psi' + (E_6 \phi')' + i \beta (E_6 \psi)'\} = 0 \quad (2.22)$$

$$e^{i\beta x} \{-\beta^2 E_6 \psi + i\beta(E_2 \phi)' + (E_3 \psi')' + i\beta E_6 \phi'\} = 0. \quad (2.23)$$

These equations must hold for any choice of  $x$ . Therefore, they are formally identical to (2.16), (2.17).

The displacement field minimizes the potential energy functional

$$\Pi(u) = \frac{1}{2} \mathcal{B}(u, u) - \mathcal{F}(u) \quad (2.24)$$

over the subspace  $E^n(\Omega)$ :

$$E^n(\Omega) = \left\{ \vec{u} \left| u_x = \sum_{j=0}^{n_1} u_{x|j} \phi_j(y), u_y = \sum_{j=0}^{n_2} u_{y|j} \psi_j(y) \right. \right\} \quad (2.25)$$

where  $\phi_j, \psi_j$  are given functions. If we denote the exact solution of the model of order  $n$  by  $\vec{u}_{EX}^n$ , we select the functions  $\phi_j, \psi_j$  such that the modeling error:

$$\frac{\|\vec{u}_{EX} - \vec{u}_{EX}^n\|_{E^n(\Omega)}}{\|\vec{u}_{EX}^n\|_{E^n(\Omega)}} \leq C(n) h^{\alpha_n} \quad (2.26)$$

i.e., the relative difference between the model of order  $n$  (different  $n_i$  for  $u_x$  and  $u_y$  are possible) and the exact solution in energy norm, is such that  $\alpha_n$  is not larger for any other set of functions  $\phi_j, \psi_j$ . The optimal functions are those which maximize the rate of convergence ( $\alpha_n$ ) of the model of order  $n$ .

It has been shown in reference [5] that the functions  $\phi(\beta, y), \psi(\beta, y)$  admit an expansion about  $\beta = 0$  with coefficients which are certain functions of  $y$ , and that the  $\phi_j, \psi_j$  in (2.25) must be these coefficient functions to maximize  $\alpha_n$ . It is also shown in [5], that it is not necessary to use the boundary conditions (2.18), (2.19), only the homogeneous equations (2.16) and (2.17) are needed to obtain these functions.

The functions  $\phi(\beta, y)$  and  $\psi(\beta, y)$  are complex functions of the form:

$$\phi(\beta, y) = \phi_a(\beta, y) + i \phi_b(\beta, y) \quad (2.27)$$

$$\psi(\beta, y) = \psi_a(\beta, y) + i \psi_b(\beta, y) \quad (2.28)$$

where  $\phi_a$ ,  $\phi_b$  are antisymmetric real functions, and  $\psi_a$  and  $\psi_b$  are symmetric real functions with respect to the middle surface of the strip, i.e. the x-axis. Expanding  $\phi(\beta, y)$ ,  $\psi(\beta, y)$  into a power series with respect to  $\beta$ :

$$\phi(\beta, y) = [\phi_{a0}(y) + i \phi_{b0}(y)] + \beta[\phi_{a1}(y) + i \phi_{b1}(y)] + \beta^2[\phi_{a2}(y) + i \phi_{b2}(y)] + \dots \quad (2.29)$$

$$\psi(\beta, y) = [\psi_{a0}(y) + i \psi_{b0}(y)] + \beta[\psi_{a1}(y) + i \psi_{b1}(y)] + \beta^2[\psi_{a2}(y) + i \psi_{b2}(y)] + \dots \quad (2.30)$$

On substituting (2.29) and (2.30) into the equilibrium equations (2.16) and (2.17) and separating into real and imaginary parts we have:

The real part of (2.16) is:

$$\begin{aligned} (E_6 \phi'_{a0})' &+ \beta[(E_6 \phi'_{a1})' - (E_6 \psi'_{b0})' - E_2 \psi'_{b0}] + \\ &+ \beta^2[(E_6 \phi'_{a2})' - (E_6 \psi'_{b1})' - E_2 \psi'_{b1} - E_1 \phi_{a0}] + \\ &+ \beta^3[(E_6 \phi'_{a3})' - (E_6 \psi'_{b2})' - E_2 \psi'_{b2} - E_1 \phi_{a1}] + \dots = 0. \end{aligned} \quad (2.31)$$

The imaginary part of (2.16) is:

$$\begin{aligned} (E_6 \phi'_{b0})' &+ \beta[(E_6 \phi'_{b1})' + (E_6 \psi'_{a0})' + E_2 \psi'_{a0}] + \\ &+ \beta^2[(E_6 \phi'_{b2})' + (E_6 \psi'_{a1})' + E_2 \psi'_{a1} - E_1 \phi_{b0}] + \\ &+ \beta^3[(E_6 \phi'_{b3})' + (E_6 \psi'_{a2})' + E_2 \psi'_{a2} - E_1 \phi_{b1}] + \dots = 0. \end{aligned} \quad (2.32)$$



The real part of (2.17) is:

$$\begin{aligned}
& (E_3\psi'_{a0})' + \beta[(E_3\psi'_{a1})' - E_6\phi'_{b0} - (E_2\phi'_{b0})'] + \\
& + \beta^2[(E_3\psi'_{a2})' - (E_2\phi'_{b1})' - E_6\phi'_{b1} - E_6\psi_{a0}] + \\
& + \beta^3[(E_3\psi'_{a3})' - (E_2\phi'_{b2})' - E_6\phi'_{b2} - E_6\psi_{a1}] + \dots = 0. \quad (2.33)
\end{aligned}$$

The imaginary part of (2.17) is:

$$\begin{aligned}
& (E_3\psi'_{b0})' + \beta[(E_3\psi'_{b1})' + E_6\phi'_{a0} + (E_2\phi'_{a0})'] + \\
& + \beta^2[(E_3\psi'_{b2})' + (E_2\phi'_{a1})' + E_6\phi'_{a1} - E_6\psi_{b0}] + \\
& + \beta^3[(E_3\psi'_{b3})' + (E_2\phi'_{a2})' + E_6\phi'_{a2} - E_6\psi_{b1}] + \dots = 0. \quad (2.34)
\end{aligned}$$

These equations hold for any choice of  $\beta$ . In many practical problems the material properties are symmetric functions of  $y$ , for example, as noted earlier, the strip may comprise laminae which are symmetrically arranged with respect to the  $x$ -axis. For the sake of simplicity only the symmetric case is considered in the following.

### 2.1.1 The Model Characterized by $\beta^0$

Setting  $\beta = 0$  in equations (2.31) to (2.34) we have:

$$(E_6\phi'_{a0})' = 0, \quad (E_6\phi'_{b0})' = 0 \quad (2.35)$$

$$(E_3\psi'_{a0})' = 0, \quad (E_3\psi'_{b0})' = 0. \quad (2.36)$$

Knowing that  $\phi_{a0}(y)$  and  $\phi_{b0}(y)$  are antisymmetric and  $\psi_{a0}(y)$  and  $\psi_{b0}(y)$  are symmetric, and integrating, we have:

$$\phi_{a0}(y) = a_0 F_0(y), \quad \phi_{b0}(y) = b_0 F_0(y) \quad (2.37)$$

$$\psi_{a0} = c_0, \quad \psi_{b0} = d_0 \quad (2.38)$$

where

$$F_0(y) \stackrel{\text{def}}{=} \int_0^y \frac{1}{E_6(t)} dt. \quad (2.39)$$

Referring to (2.25) the case  $\beta = 0$  yields:

$$u_x(x, y) = u_{x|1}(x) F_0(y) \quad (2.40)$$

$$u_y(x, y) = u_{y|0}(x). \quad (2.41)$$

The real and imaginary parts are not linearly independent, hence both lead to the same functional form. One possible choice for  $u_{x|1}$ ,  $u_{y|0}$  are constants. For instance:

$$u_x = a_0 F_0(y) \quad (2.42)$$

$$u_y = c_0 \quad (2.43)$$

and the strain terms corresponding to these displacement components are  $\epsilon_x = 0$ ,  $\epsilon_y = 0$ ,  $\gamma_{xy} = a_0 F'_0$  where, as before, the prime represents differentiation with respect to  $y$ . This corresponds to constant shear stress, specifically:  $\tau_{xy} = a_0$ . Observe that this displacement field can represent rigid body displacement but cannot represent rigid body rotation. When  $E_6(y) = E_6$  is constant then this model is capable of representing rigid body displacement and rotation. This is because the displacement components

$$u_x = C_1 + C_3 y \quad (2.44)$$

$$u_y = C_2 - C_3 x, \quad (2.45)$$

where  $C_1, C_2, C_3$  are arbitrary constants, are represented by the model. Nevertheless, the model represented by (2.40), (2.41) is not a member of the hierarchic sequence of models because it does not satisfy the requirement that the exact solution of each member of the hierarchy must converge to the same limit as the the exact solution of the corresponding problem of elasticity with respect to  $h \rightarrow 0$ . This point will be discussed in greater detail in Section 2.4.1.

### 2.1.2 The Model Characterized by $\beta^1$

To find the mode of deformation for the model which satisfies the equilibrium equations up to the first power of  $\beta$ , we differentiate equations (2.31) to (2.34) with respect to  $\beta$  and let  $\beta = 0$ . In this case the following equations are obtained:

$$(E_6 \phi'_{a1})' - (E_6 \psi_{b0})' - E_2 \psi'_{b0} = 0 \quad (2.46)$$

$$(E_6 \phi'_{b1})' + (E_6 \psi_{a0})' + E_2 \psi'_{a0} = 0 \quad (2.47)$$

$$(E_3 \psi'_{a1})' - E_6 \phi'_{b0} - (E_2 \phi_{b0})' = 0 \quad (2.48)$$

$$(E_3 \psi'_{b1})' + E_6 \phi'_{a0} + (E_2 \phi_{a0})' = 0. \quad (2.49)$$

Using (2.38), (2.46) can be written as:

$$[E_6(\phi'_{a1} - \psi_{b0})]' = 0. \quad (2.50)$$

Solving for  $\phi_{a1}(y)$  and using the fact that  $\phi_{a1}(y)$  is antisymmetric:

$$E_6(\phi'_{a1} - \psi_{b0}) = a_1 \quad (2.51)$$

$$\phi'_{a1} = \frac{a_1}{E_6} + d_0 \quad (2.52)$$

$$\phi_{a1}(y) = a_1 \int_0^y \frac{1}{E_6(t)} dt + d_0 y \quad (2.53)$$

$$\phi_{a1}(y) = a_1 F_0(y) + d_0 y. \quad (2.54)$$

From (2.47), using (2.38):

$$[E_6(\phi'_{b1} + \psi_{a0})]' = 0 \quad (2.55)$$

$$E_6(\phi'_{b1} + \psi_{a0}) = b_1 \quad (2.56)$$

$$\phi'_{b1} = \frac{b_1}{E_6} - c_0 \quad (2.57)$$

$$\phi_{b1}(y) = b_1 F_0(y) - c_0 y. \quad (2.58)$$

From (2.48), using (2.37):

$$(E_3 \psi'_{a1})' = b_0 + (E_2 \phi_{b0})'. \quad (2.59)$$

Integrating once:

$$E_3 \psi'_{a1} = b_0 y + b_0 E_2 F_0(y) + f_1 \quad (2.60)$$

and solving for  $\psi_{a1}$ :

$$\psi_{a1}(y) = b_0 \int_0^y \frac{t}{E_3(t)} dt + b_0 \int_0^y \frac{E_2(t)}{E_3(t)} F_0(t) dt + f_1 \int_0^y \frac{1}{E_3(t)} dt + c_1. \quad (2.61)$$

Since the third term is antisymmetric,  $f_1 = 0$ . Then,

$$\psi_{a1}(y) = b_0 F_1(y) + c_1. \quad (2.62)$$

Similarly, integrating (2.49) twice:

$$\psi_{b1}(y) = -a_0 F_1(y) + d_1 \quad (2.63)$$

where

$$F_1(y) \stackrel{\text{def}}{=} \int_0^y \frac{t}{E_3(t)} dt + \int_0^y \frac{E_2(t)}{E_3(t)} F_0(t) dt. \quad (2.64)$$

The displacement field in this case is given by:

$$u_x(x, y) = u_{x|1}(x) F_0(y) + u_{x|2}(x) y \quad (2.65)$$

$$u_y(x, y) = u_{y|0}(x) + u_{y|2}(x) F_1(y). \quad (2.66)$$

Further discussion of this model is deferred to Section 2.4.2.

### 2.1.3 The Model Characterized by $\beta^2$

To find the mode of deformation corresponding to the model which satisfies the equilibrium equations up to the second power of  $\beta$ , we differentiate equations (2.31) to (2.34) with respect to  $\beta$  twice and let  $\beta = 0$ . The following equations are obtained:

$$(E_6 \phi'_{a2})' - (E_6 \psi_{b1})' - E_2 \psi'_{b1} - E_1 \phi_{a0} = 0 \quad (2.67)$$

$$(E_6 \phi'_{b2})' + (E_6 \psi_{a1})' + E_2 \psi'_{a1} - E_1 \phi_{b0} = 0 \quad (2.68)$$

$$(E_3 \psi'_{a2})' - (E_2 \phi_{b1})' - E_6 \phi'_{b1} - E_6 \psi_{a0} = 0 \quad (2.69)$$

$$(E_3 \psi'_{b2})' + (E_2 \phi_{a1})' + E_6 \phi'_{a1} - E_6 \psi_{b0} = 0. \quad (2.70)$$

Upon integrating, the following results are obtained:

$$\phi_{a2}(y) = a_0 F_2(y) + d_1 y + a_2 F_0(y) \quad (2.71)$$

$$\phi_{b2}(y) = b_0 F_2(y) - c_1 y + b_2 F_0(y) \quad (2.72)$$

and

$$\psi_{a2}(y) = b_1 F_1(y) - c_0 F_3(y) + c_2 \quad (2.73)$$

$$\psi_{b2}(y) = -a_1 F_1(y) - d_0 F_3(y) + d_2 \quad (2.74)$$

where:

$$F_2(y) \stackrel{\text{def}}{=} \int_0^y \left\{ \frac{1}{E_6(t)} \int_0^t \left[ E_1(t) F_0(t) - \frac{E_2(t)}{E_3(t)} t - \frac{E_2^2(t)}{E_3(t)} F_0(t) \right] dt - F_1(t) \right\} dt \quad (2.75)$$

and

$$F_3(y) \stackrel{\text{def}}{=} \int_0^y \frac{E_2(t)}{E_3(t)} t dt. \quad (2.76)$$

Therefore the displacement field can be written in the form:

$$u_x(x, y) = u_{x|1}(x) F_0(y) + u_{x|2}(x) y + u_{x|3}(x) F_2(y) \quad (2.77)$$

$$u_y(x, y) = u_{y|0}(x) + u_{y|2}(x) F_1(y) + u_{y|3}(x) F_3(y). \quad (2.78)$$

This mode of deformation satisfies both the real and imaginary parts of the equilibrium equations up to the second power of  $\beta$ . By continuing this process, the equilibrium equations can be satisfied to an arbitrary power of  $\beta$ . For additional details, see Appendices A and B.

## 2.2 The Boundary Layer

The foregoing analysis was concerned with an infinite strip and therefore the boundary conditions did not have to be considered. Terms which can be neglected for an infinite strip can be very significant near the boundary of a strip of finite size,

however. Therefore, in the neighborhood of boundaries, the exact solutions of low-order models can differ very substantially from one another and from the limiting case, i.e., the exact solution of the problem of elasticity. This sensitivity of exact solutions corresponding to various models in the small neighborhood of the boundary is called the *boundary layer effect* or *edge effect*.

Boundary layer effects are important from the point of view of engineering analysis because often the goal is to determine moments and shear forces at the boundary where the solution is model-dependent. An analysis of boundary layer effects for the Reissner-Mindlin plates is available in [6]. In the case of laminated plates the problem is even more complicated, due to the singularities caused by the material interfaces. To account for boundary layer effects, it should be possible to expand the laminate model near the boundary: The power of  $\beta$  near the boundary should be larger than the one used in the interior regions of the laminate. The answers to the questions: How much larger it needs to be, and what power of  $\beta$  is large enough far from the boundaries, are problem-dependent and can be found, in general, at the end of an adaptive process only.

Hierarchic models provide a framework for adaptive control: Let us rewrite (2.77), (2.78) in the following form:

$$u_x(x, y) = u_{x|1}(x)f_1(y) + u_{x|2}(x)f_2(y) + u_{x|3}(x)f_3(y) + \cdots \quad (2.79)$$

$$u_y(x, y) = u_{y|0}(x) + u_{y|2}(x)g_2(y) + u_{y|3}(x)g_3(y) + \cdots \quad (2.80)$$

where  $f_1(y) = F_0(y)$  and  $f_2(y) = \alpha_1 f_1(y) + \alpha_2 y$  with  $\alpha_1, \alpha_2$  selected such that  $f_2(y)$  is orthogonal to  $f_1(y)$ :

$$\int_{-h/2}^{+h/2} f_1(y) f_2(y) dy = 0. \quad (2.81)$$

Similarly,  $f_3(y) = \alpha_1 f_1(y) + \alpha_2 f_2(y) + \alpha_3 F_2(y)$  with  $\alpha_1, \alpha_2, \alpha_3$  selected such that  $f_3(y)$  is orthogonal to  $f_1(y)$  and  $f_2(y)$ , etc. In this way on the  $k$ th element ( $x_k < x < x_{k+1}$ ) we expect:

$$\int_{x_k}^{x_{k+1}} u_{x|i}^2 dx \rightarrow 0 \quad (2.82)$$

as  $i \rightarrow \infty$  very fast on those elements where the solution of the problem of elasticity is smooth and slowly where it is not smooth. Adaptive selection of models is based on making measures, such as this, very nearly equal over the entire solution domain.

### 2.3 Boundary Conditions for Hierarchic Models

The main motivation for using hierarchic models is to make adaptive control over errors of idealization possible. The sequence of exact solutions corresponding to a hierarchic sequence of models converges to the exact solution of the model based on the theory of elasticity. Since the exact solution depends on the boundary conditions, proper interpretation of the boundary conditions is important. In engineering analyses the choice of boundary conditions is usually a modelling decision, i.e., a convenient simplification of some possibly complicated physical conditions. In using hierarchic models the choice of boundary conditions must be such that the



solution of the problem of elasticity exists. Also, since the choice of boundary conditions affects the smoothness of the exact solution, hence the degree of difficulty encountered in controlling the errors of discretization, if modeling considerations allow alternative choices then the interpretation leading to the smoother solution is preferable.

Consider, for example, the problem of enforcing the boundary condition which allows no transverse displacement but allows rotation of the laminated strip at (say)  $x = \ell$ . In the terminology of structural analysis this is called simple support. There are several possible interpretations. One possible interpretation is:  $u_x(\ell, y)$  is unrestricted and:

$$u_{y|0}(\ell) = u_{y|2}(\ell) = u_{y|3}(\ell) = \cdots = 0 \quad (2.83)$$

i.e., the transverse displacement of every point of the strip is zero at  $x = \ell$ . Another possible interpretation is:  $u_x(\ell, y)$  is unrestricted and:

$$\int_{-h/2}^{+h/2} u_y(\ell, y) dy = 0 \quad (2.84)$$

i.e., only the average displacement in the  $y$ -direction is set to zero.

Certain interpretations of simple support are ruled out by the condition that the corresponding problem of elasticity would not have a solution. Thus the condition  $u_{y|0}(\ell) = 0$ , with  $u_{y|i}(\ell)$  ( $i = 2, 3, \dots$ ) are unrestricted, is generally not admissible because this would correspond to a point support. Point supports are permissible as constraints against rigid body displacements and rotations only.

Analogous considerations apply to other types of boundary conditions. For further discussion we refer to [3].

## 2.4 The Limiting Case with Respect to $\beta \rightarrow 0$

One of the requirements for the hierarchic models is that the exact solution of each model must converge to the same limit as the exact solution of the fully three-dimensional model when the laminate thickness approaches zero.

In the following Section it is shown that the exact solutions of the models corresponding to  $\beta^0$  and  $\beta^1$  differ from the exact solution of models corresponding to  $\beta^n$  with  $n \geq 2$ , when  $\beta \rightarrow 0$  unless some coefficients of the material stiffness matrix are modified. Guidelines are established for modifying the material coefficients such that the requirement represented by the equation:

$$\lim_{h \rightarrow 0} \frac{\|u_{EX}^{(HM|i)} - u_{EX}^{(3D)}\|_{E(\Omega)}}{\|u_{EX}^{(3D)}\|_{E(\Omega)}} = 0, \quad i = 1, 2, \dots \quad (2.85)$$

is satisfied. This is a generalization of the rationale used in the construction of the Reissner-Mindlin model for isotropic strips outlined in [3].

### 2.4.1 The Model Characterized by $\beta^0$

The exact solution minimizes the potential energy with respect to all functions  $u_{x|1}$ ,  $u_{y|0}$  for which the strain energy is finite:

$$\begin{aligned} \Pi = \frac{1}{2} \int_{-\infty}^{+\infty} \int_{-h/2}^{+h/2} \left[ E_1 (u'_{x|1})^2 (F_0)^2 + E_6 (u_{x|1} F'_0 + u'_{y|0})^2 \right] dy dx - \\ \int_{-\infty}^{+\infty} q u_{y|0} dx \end{aligned} \quad (2.86)$$

where the prime on  $u_{x|1}$ ,  $u_{y|0}$  represents differentiation with respect to  $x$  and the prime on  $F_0$  represents differentiation with respect to  $y$ . We denote:

$$C_1 = \int_{-h/2}^{+h/2} E_1 (F_0)^2 dy; \quad C_2 = \int_{-h/2}^{+h/2} E_6 (F_0')^2 dy \quad (2.87)$$

$$C_3 = \int_{-h/2}^{+h/2} E_6 F_0' dy; \quad C_4 = \int_{-h/2}^{+h/2} E_6 dy. \quad (2.88)$$

Observe that, given the definition of  $F_0$  in (2.39),  $C_1$  is of the order  $h^3$ ;  $C_2$ ,  $C_3$  and  $C_4$  are of order  $h$ . Therefore these constants can be written in the following form:

$$C_1 = h^3 K_1, \quad C_2 = h K_2, \quad C_3 = h K_3, \quad C_4 = h K_4. \quad (2.89)$$

The first variation of  $\Pi$  with respect to  $u_{x|1}$  is:

$$\delta \Pi(u_{x|1}) = \int_{-\infty}^{+\infty} \left( h^3 K_1 u'_{x|1} \delta u'_{x|1} + h K_2 u_{x|1} \delta u_{x|1} + h K_3 u'_{y|0} \delta u_{x|1} \right) dx \quad (2.90)$$

and the corresponding Euler equation is:

$$- h^3 K_1 u''_{x|1} + h K_2 u_{x|1} + h K_3 u'_{y|0} = 0. \quad (2.91)$$

Similarly, the Euler equation corresponding to the first variation of  $\Pi$  with respect to  $u_{y|0}$  is:

$$- h K_4 u''_{y|0} - h K_3 u'_{x|1} = q. \quad (2.92)$$

If we now apply Fourier transform to (2.91) and (2.92), the following expressions are obtained:

$$\begin{bmatrix} h^3 K_1 \xi^2 + h K_2 & i \xi h K_3 \\ -i \xi h K_3 & h K_4 \xi^2 \end{bmatrix} \begin{Bmatrix} U_{x|1} \\ U_{y|0} \end{Bmatrix} = \begin{Bmatrix} 0 \\ Q \end{Bmatrix} \quad (2.93)$$

where  $U_{x|1}(\xi)$  (resp.  $U_{y|0}(\xi)$ ) is the Fourier transform of  $u_{x|1}$  (resp.  $u_{y|0}$ ) and  $Q(\xi)$  is the Fourier transform of  $q(x)$ . Solving (2.93) for  $U_{x|1}$  and  $U_{y|0}$ :

$$D(\xi) U_{x|1} = B(\xi) Q; \quad D(\xi) U_{y|0} = C(\xi) Q \quad (2.94)$$

where:

$$D(\xi) = \xi^2 h^2 (K_2 K_4 - K_3^2) + \xi^4 h^4 K_1 K_4 \quad (2.95)$$

$$B(\xi) = -i \xi h K_3 \quad (2.96)$$

$$C(\xi) = h K_2 + \xi^2 h^3 K_1. \quad (2.97)$$

On dividing the first of (2.94) by  $-i \xi h K_3$  and the second by  $h K_2$  the following expressions are obtained:

$$\left[ i \xi h \left( \frac{K_2 K_4}{K_3} - K_3 \right) + i \xi^3 h^3 \frac{K_1 K_4}{K_3} \right] U_{x|1} = Q \quad (2.98)$$

$$\left[ \xi^2 h \left( K_4 - \frac{K_3^2}{K_2} \right) + \xi^4 h^3 \frac{K_1 K_4}{K_2} \right] U_{y|0} = \left( 1 + \xi^2 h^2 \frac{K_1}{K_2} \right) Q. \quad (2.99)$$

On performing the inverse Fourier transform, we have:

$$\left( \frac{K_2 K_4}{K_3} - K_3 \right) h u'_{x|1} - \frac{K_1 K_4}{K_3} h^3 u'''_{x|1} = q \quad (2.100)$$

$$\frac{K_1 K_4}{K_2} h^3 u^{IV}_{y|0} - \left( K_4 - \frac{K_3^2}{K_2} \right) h u''_{y|0} = q - h^2 \frac{K_1}{K_2} q''. \quad (2.101)$$

The significance of (2.100) and (2.101) is that the exact solution satisfies these equations hence these equations characterize the model corresponding to  $\beta^0$ .

#### 2.4.2 The Model Characterized by $\beta^1$

In this case taking the the displacement field given by (2.65) and (2.66), the potential energy functional is determined in the same way as for the  $\beta^0$  case. Taking the

first variation of  $\Pi$  with respect to each one of the displacement field components  $u_{x|1}$ ,  $u_{x|2}$ ,  $u_{y|0}$  and  $u_{y|2}$ , and applying the Fourier transform to the resulting Euler equations, the following expressions are obtained:

$$\begin{bmatrix} h^3 K_1 \xi^2 + h K_2 & i \xi h K_3 & h^3 K_5 \xi^2 + h K_3 & i h^3 \xi (K_{11} - K_6) \\ -i \xi h K_3 & h K_4 \xi^2 & -i h \xi K_4 & h^3 \xi^2 K_{12} \\ h^3 K_5 \xi^2 + h K_3 & i \xi h K_4 & h^3 K_8 \xi^2 + h K_4 & i h^3 \xi (K_{12} - K_7) \\ -i h^3 \xi (K_{11} - K_6) & h^3 \xi^2 K_{12} & -i h^3 \xi (K_{12} - K_7) & h^5 \xi^2 K_{10} + h^3 K_9 \end{bmatrix} \begin{Bmatrix} U_{x|1} \\ U_{y|0} \\ U_{x|2} \\ U_{y|2} \end{Bmatrix} = \begin{Bmatrix} 0 \\ Q \\ 0 \\ Q h^2 G_1 \end{Bmatrix} \quad (2.102)$$

where:

$$C_5 = h^3 K_5 = \int_{-h/2}^{+h/2} E_1 y (F_0) dy \quad (2.103)$$

$$C_6 = h^3 K_6 = \int_{-h/2}^{+h/2} E_2 (F_0) F_1' dy \quad (2.104)$$

$$C_7 = h^3 K_7 = \int_{-h/2}^{+h/2} E_2 y F_1' dy \quad (2.105)$$

$$C_8 = h^3 K_8 = \int_{-h/2}^{+h/2} E_1 y^2 dy \quad (2.106)$$

$$C_9 = h^3 K_9 = \int_{-h/2}^{+h/2} E_3 (F_1')^2 dy \quad (2.107)$$

$$C_{10} = h^5 K_{10} = \int_{-h/2}^{+h/2} E_6 (F_1)^2 dy \quad (2.108)$$

$$C_{11} = h^3 K_{11} = \int_{-h/2}^{+h/2} E_6 (F_0') F_1 dy \quad (2.109)$$

$$C_{12} = h^3 K_{12} = \int_{-h/2}^{+h/2} E_6 F_1 dy \quad (2.110)$$

$$F_1(h/2) = h^2 G_1. \quad (2.111)$$

Solving (2.102) for  $U_{x|2}$  and  $U_{y|0}$ :

$$D(\xi) U_{x|2} = B(\xi) Q; \quad D(\xi) U_{y|0} = C(\xi) Q \quad (2.112)$$

where:

$$D(\xi) = \xi^8 h^{12} D_1 + \xi^6 h^{10} D_2 + \xi^4 h^8 D_3 \quad (2.113)$$

$$B(\xi) = i\xi h^5 B_1 + i\xi^3 h^7 (B_2 + B_3 G_1) + i\xi^5 h^9 (B_4 + B_5 G_1) \quad (2.114)$$

$$C(\xi) = h^5 L_1 + \xi^2 h^7 (L_2 + L_3 G_1) + \xi^4 h^9 (L_4 + L_5 G_1) + \xi^6 h^{11} (L_6 + L_7 G_1). \quad (2.115)$$

Assuming that the solution is sufficiently smooth, and letting  $h \rightarrow 0$  for  $\xi \neq 0$  we can neglect higher order terms in the above expressions:

$$D(\xi) = \xi^4 h^8 D_3, \quad B(\xi) = i\xi h^5 B_1, \quad C(\xi) = h^5 L_1 \quad (2.116)$$

where:

$$D_3 = (K_7^2 - K_8 K_9) (K_2 K_4 - K_3^2) \quad (2.117)$$

$$B_1 = K_9 (K_2 K_4 - K_3^2) \quad (2.118)$$

$$L_1 = -K_9 (K_2 K_4 - K_3^2). \quad (2.119)$$

On substituting into (2.112), and performing the inverse Fourier transform, the following equations are obtained:

$$\left( \frac{K_7^2}{K_9} - K_8 \right) h^3 u_{x|2}''' = q \quad (2.120)$$

$$- \left( \frac{K_7^2}{K_9} - K_8 \right) h^3 u_{y|0}^{IV} = q \quad (2.121)$$

and similarly for the other two equations:

$$\frac{(K_7^2 - K_8 K_9) (K_2 K_4 - K_3^2)}{\Delta K} h u_{x|1}' = q \quad (2.122)$$

$$- \left( K_7 - \frac{K_8 K_9}{K_7} \right) h^3 u_{y|2}'' = q \quad (2.123)$$

where  $\Delta K = K_7(K_4 K_{11} + K_3 K_7 - K_4 K_6 - K_3 K_{12}) + K_9(K_4 K_5 - K_3 K_8)$ . Since  $q(x)$  satisfies the equilibrium equations on  $|x| \leq L/2$  and  $q(x) = 0$  for  $|x| > L/2$ ,

on integrating (2.122) it is clear that  $u_{x|1} = 0$  for  $|x| > L/2$ . The same is true for  $u_{y|2}$ :

$$\begin{aligned} u_{y|2}(x) &= -\frac{1}{(K_7 - K_8 K_9/K_7) h^3} \int_{-L/2}^x \int_{-L/2}^t q(s) ds dt \\ &= -\frac{1}{(K_7 - K_8 K_9/K_7) h^3} \int_{-L/2}^x q(t) (x - t) dt. \end{aligned} \quad (2.124)$$

For the integral identity used in (2.124) see, for example, eq. (10), p. 225 in [7]. In fact, since the strain energy is bounded, all functions  $u_{x|i}$  and  $u_{y|i}$  ( $i = 0, 1, \dots$ ) have to decay as  $|x| \rightarrow \infty$ , with the exception of  $u_{x|2}$  and  $u_{y|0}$ , which contain the rigid body displacement and rotation terms. Therefore the  $u_{x|2}$  and  $u_{y|0}$  are the dominant functions. Observe that these are the two functions which appear in the model characterized by  $\beta^0$ , see equations (2.100), (2.101).

### 2.4.3 The Model Characterized by $\beta^2$

When the equilibrium equations are satisfied up to the second power of  $\beta$ , the displacement field is given by (2.77) and (2.78). Note that  $F_1(y)$  and  $F_3(y)$  are both of order  $h^2$ . This is the first model for which the expressions representing the mode of deformation (see equations (2.77) and (2.78)) contain the complete set of coefficients up to the second power of  $h$ . The Euler equations for the dominant functions  $u_{x|2}$  and  $u_{y|0}$  are as follows:

$$(K_{20} - K_8) h^3 u_{x|2}''' = q \quad (2.125)$$

$$-(K_{20} - K_8) h^3 u_{y|0}^{IV} = q \quad (2.126)$$

where:

$$K_{20} = \frac{1}{h^3} \int_{-h/2}^{+h/2} E_3 (F_3')^2 dy \quad (2.127)$$

and thus, using (2.106);

$$K_{20} - K_8 = \frac{1}{h^3} \int_{-h/2}^{+h/2} \left( \frac{E_2^2}{E_3} - E_1 \right) y^2 dy. \quad (2.128)$$

The procedure for obtaining these equations is the same as the procedure used in Sections 2.4.1 and 2.4.2 but the details are omitted here.

#### 2.4.4 Hierarchic Models Characterized by $\beta^0$ and $\beta^1$

On comparing equations (2.120), (2.121) with (2.125), (2.126) it is clear that the model characterized by  $\beta^1$  does not converge to the same limit as the  $\beta^2$  model with respect to  $h \rightarrow 0$ . The reason for this is that the model characterized by  $\beta^1$  does not contain the complete set of coefficients in  $h^2$  for the  $u_y$  expansion. In order to satisfy the requirement represented by equation (2.85), it is necessary to substitute  $K_{20}$  for  $K_7^2/K_9$  in (2.120) and (2.121). Thus, through the simple device of modifying coefficients which represent material properties, the hierarchic sequence of models is extended “downward”: Solving for only four unknown functions of a single variable (i.e.,  $u_{x|1}(x)$ ,  $u_{x|2}(x)$ ,  $u_{y|0}(x)$ ,  $u_{y|2}(x)$ ) the same limiting solution is obtained with respect to the  $h \rightarrow 0$  as if the problem of elasticity had been solved.

On comparing equations (2.100) and (2.101) with (2.125) and (2.126), it is seen that, for the model characterized by  $\beta^0$  to converge to the same limit as the model



characterized by  $\beta^2$  it is necessary to have:

$$\left(\frac{K_2 K_4}{K_3} - K_3\right) = 0, \quad \frac{K_1 K_4}{K_3} = -(K_{20} - K_8) \quad (2.129)$$

and

$$K_4 - \frac{K_3^2}{K_2} = 0, \quad \frac{K_1 K_4}{K_2} = -(K_{20} - K_8). \quad (2.130)$$

The condition  $K_2 K_4 / K_3 - K_3 = 0$  (which is the same as the first of (2.130)) is satisfied if  $E_6(y)$  is replaced by a constant value. From the point of view of the limiting solution with respect to  $h \rightarrow 0$  it is immaterial which constant value is used since the essential coefficient,  $(K_{20} - K_8)$ , is independent of  $E_6$ , (see equation (2.128)). For finite values of  $h$ , on the other hand, it is important to use some "reasonable" replacement for  $E_6$ . For example, we may replace  $E_6$  by its average value  $\tilde{E}_6$ , defined as:

$$\tilde{E}_6 \stackrel{\text{def}}{=} \frac{2}{h} \int_0^{+h/2} E_6 dy. \quad (2.131)$$

Another possibility is to select the replacement for  $E_6(y)$  such that the function  $F_0(y)$  defined by (2.39) will be unchanged at  $y = h/2$ :

$$F_0(h/2) = \int_0^{+h/2} \frac{1}{E_6(y)} dy = \frac{h}{2 \hat{E}_6} \quad (2.132)$$

and thus we may replace  $E_6(y)$  by the harmonic average, denoted by  $\hat{E}_6$ :

$$\hat{E}_6 \stackrel{\text{def}}{=} \left( \frac{2}{h} \int_0^{+h/2} \frac{1}{E_6(y)} dy \right)^{-1}. \quad (2.133)$$

The harmonic average is less than or equal to the average. Therefore, using  $\hat{E}_6$  instead of  $\tilde{E}_6$  has the effect that the shear stiffness is generally smaller, which is

analogous to introducing a shear correction factor, less than or equal to unity, in the Reissner-Mindlin model for isotropic plates.

Observe that when  $E_6(y)$  is replaced by a constant value, which is one of the requirements for the model to be a member of the hierarchy, then  $F_0(y)$  and  $y$  are not linearly independent, and we can write  $F_0 = y$  instead of (2.39), hence from (2.87) to (2.89):

$$\frac{K_1 K_4}{K_2} = \frac{K_1 K_4}{K_3} = \frac{1}{h^3} \int_{-h/2}^{+h/2} E_1 y^2 dy \quad (2.134)$$

and therefore conditions (2.129) and (2.130) are satisfied when the material constant  $E_1$  is replaced by  $(E_1 - E_2^2/E_3)$  for each lamina. That is, the correct limiting case can be obtained for the simplest model, i.e., the model corresponding to  $\beta^0$ , through modification of the material properties.

That these modifications provide the correct limiting case for laminated strips is demonstrated by numerical examples in next Chapter.

## Chapter 3

### Solution of the Strip Model

This Chapter is devoted to the numerical verification of the models developed in Chapter 2 for the laminated strip. First, a description of the finite element implementation is discussed. The dimensional reduction accomplished by proper selection of the transverse functions made it possible to uncouple the  $x$  and  $y$  parts of the fields. Therefore the numerical solution requires only to solve a one-dimensional problem. Second, examples are presented in which the ability of the hierarchic sequence of models is demonstrated.

#### 3.1 The Numerical Problem

In this Section the numerical problem for the computation of functions  $u_{x|1}(x)$ ,  $u_{x|2}(x), \dots, u_{y|0}(x), u_{y|2}(x), \dots$  for the hierarchic sequence of models is formulated. The formulation is based on the p-version of the finite element method. Consider

the strain energy per unit width associated with the  $k$ th element of the laminate of length  $\ell_k$ .

$$\mathcal{U}_k = \frac{1}{2} \int_0^{\ell_k} \left( \sum_{n=1}^m \int_{y_n}^{y_{n+1}} (\sigma_x \epsilon_x + \sigma_y \epsilon_y + \tau_{xy} \gamma_{xy}) dy \right) dx \quad (3.1)$$

where  $m$  is the number of layers in the  $k$ th element.

The functions  $u_{x|i}$  and  $u_{y|i}$  in (2.77), (2.78) are written in terms of the basis functions as follows:

$$u_{x|i} = \sum_{j=1}^{p+1} a_j^{(i)} N_j(\xi) \quad (3.2)$$

$$u_{y|i} = \sum_{j=1}^{p+1} b_j^{(i)} N_j(\xi) \quad (3.3)$$

where  $a_j^{(i)}$  and  $b_j^{(i)}$  are constants,  $p$  is the polynomial degree of the  $x$ -direction expansion, and  $N_j(\xi)$  are basis functions for the  $(p+1)$ -dimensional space  $S^p$ . By definition,  $S^p$  is the space of polynomials of degree  $p$  on the standard element  $\Omega_{st} \stackrel{\text{def}}{=} \{\xi \mid -1 \leq \xi \leq +1\}$ . Specifically, the following basis functions are used for  $S^p$ :

$$N_1(\xi) = \frac{1-\xi}{2}, \quad N_2(\xi) = \frac{1+\xi}{2}, \quad N_i(\xi) = \phi_{i-1}(\xi), \quad i = 3, 4, \dots, p+1 \quad (3.4)$$

where  $\phi_j(\xi)$  is defined in terms of the Legendre polynomials  $P_{j-1}$

$$\phi_j(\xi) = \sqrt{\frac{2j-1}{2}} \int_{-1}^{\xi} P_{j-1}(t) dt, \quad j = 2, 3, \dots \quad (3.5)$$

For details we refer to [1]. The  $k$ th element is mapped onto the standard element by the transformation:

$$x = \frac{1-\xi}{2} x_k + \frac{1+\xi}{2} x_{k+1} \quad (3.6)$$

from which:

$$dx = \frac{x_{k+1} - x_k}{2} d\xi = \frac{\ell_k}{2} d\xi \quad (3.7)$$

where  $\ell_k \stackrel{\text{def}}{=} x_{k+1} - x_k$ . Using equations (2.7) and (3.2), (3.3) and the condition that the equilibrium equations are satisfied up to the second power of  $\beta$ , we have:

$$\begin{Bmatrix} \epsilon_x \\ \epsilon_y \\ \gamma_{xy} \end{Bmatrix} = \begin{bmatrix} \frac{2y}{\ell_k} [N'] & 0 & \frac{2}{\ell_k} F_0 [N'] & 0 & \frac{2}{\ell_k} F_2 [N'] & 0 \\ 0 & 0 & 0 & F_1' [N] & 0 & F_3' [N] \\ [N] & \frac{2}{\ell_k} [N'] & F_0' [N] & \frac{2}{\ell_k} F_1 [N'] & F_2' [N] & \frac{2}{\ell_k} F_3 [N'] \end{bmatrix} \begin{Bmatrix} \{a^{(1)}\} \\ \{b^{(1)}\} \\ \{a^{(2)}\} \\ \{b^{(2)}\} \\ \{a^{(3)}\} \\ \{b^{(3)}\} \end{Bmatrix} \quad (3.8)$$

or, in short hand;

$$\{\epsilon\} = [Q] \{a\}. \quad (3.9)$$

The strain energy for the  $n$ th lamina of the  $k$ th element is:

$$\mathcal{U}_{n|k} = \frac{1}{2} [a] \int_0^{\ell_k} \int_{y_n}^{y_{n+1}} ([Q])^T [E]^{(n|k)} [Q] dy dx \{a\} \quad (3.10)$$

or, in matrix form:

$$\mathcal{U}_n = \frac{1}{2} [a] [K]^{(n|k)} \{a\} \quad (3.11)$$

where  $[E]^{(n|k)}$  is the material stiffness matrix for lamina  $n$  of the  $k$ th element, and is given by:

$$[E]^{(n|k)} = \begin{bmatrix} E_1^{(n|k)} & E_2^{(n|k)} & E_4^{(n|k)} \\ E_2^{(n|k)} & E_3^{(n|k)} & E_5^{(n|k)} \\ E_4^{(n|k)} & E_5^{(n|k)} & E_6^{(n|k)} \end{bmatrix} \quad (3.12)$$

and  $[K]^{(n|k)}$  is the stiffness matrix for lamina  $n$  given by:

$$[K]^{(n|k)} = \begin{bmatrix} K_{11} & K_{12} & K_{13} & K_{14} & K_{15} & K_{16} \\ & K_{22} & K_{23} & K_{24} & K_{25} & K_{26} \\ & & K_{33} & K_{34} & K_{35} & K_{36} \\ & \text{sym.} & & K_{44} & K_{45} & K_{46} \\ & & & & K_{55} & K_{56} \\ & & & & & K_{66} \end{bmatrix} \quad (3.13)$$

The first submatrix of (3.13) is computed as follows:

$$\begin{aligned} [K_{11}] &= E_1^{(n|k)} \frac{\ell_k}{2} \int_{-1}^{+1} \int_{y_n}^{y_{n+1}} \left( \frac{2y}{\ell_k} \right)^2 \{N'\} [N'] dy d\xi \\ &+ E_4^{(n|k)} \frac{\ell_k}{2} \int_{-1}^{+1} \int_{y_n}^{y_{n+1}} \frac{2y}{\ell_k} \{N'\} [N] dy d\xi \\ &+ E_4^{(n|k)} \frac{\ell_k}{2} \int_{-1}^{+1} \int_{y_n}^{y_{n+1}} \frac{2y}{\ell_k} \{N\} [N'] dy d\xi \\ &+ E_6^{(n|k)} \frac{\ell_k}{2} \int_{-1}^{+1} \int_{y_n}^{y_{n+1}} \{N\} [N] dy d\xi \end{aligned} \quad (3.14)$$

Evaluating the integrals in the  $y$ -direction, and defining:

$$K_{ij}^{(st)} = \int_{-1}^{+1} N'_j N'_i d\xi, \quad (3.15)$$

$$M_{ij}^{(st)} = \int_{-1}^{+1} N_i N_j d\xi, \quad (3.16)$$

$$L_{ij}^{(st)} = \int_{-1}^{+1} N'_i N_j d\xi, \quad (3.17)$$

we can write  $[K_{11}]$  in the following way:

$$\begin{aligned} [K_{11}] &= \frac{2}{3\ell_k} E_1^{(n|k)} (y_{n+1}^3 - y_n^3) [K_{st}] + \frac{1}{2} E_4^{(n|k)} (y_{n+1}^2 - y_n^2) ([L_{st}] + [L_{st}]^T) \\ &+ \frac{1}{2} E_6^{(n|k)} \ell_k h_n [M_{st}]. \end{aligned} \quad (3.18)$$

The other submatrices in (3.13) are defined similarly (see Appendix C). The size of each submatrix is  $(p+1)(p+1)$ . The number of submatrices depends on the number of terms in the expansion of the displacement field. For example, for  $\beta^2$  there are 21 independent submatrices. Finally, the stiffness matrix of the  $k$ th element of the laminate is the sum of the stiffness matrices of each lamina in that element. Thus:

$$[K]^{(k)} = \sum_{n=1}^m [K]^{(n|k)} \quad k = 1, 2, \dots, M \quad (3.19)$$

where  $M$  is the number of elements in the mesh. The strain energy of the  $k$ th element can be written in matrix form as:

$$\mathcal{U}_k(\vec{u}) = \frac{1}{2} [a] [K]^{(k)} \{a\} \quad (3.20)$$

where  $[a]$  is the vector of the unknown coefficients of  $u_{x|i}$ ,  $u_{y|i}$ .

Writing the displacement components in the form (2.79), (2.80) and orthogonalizing the functions which represents the transverse variation of the displacement components, as in (2.81), serves to reduce the condition number of the stiffness matrices.

The potential energy functional  $\Pi(\vec{u})$  is defined as follows:

$$\Pi(\vec{u}) = \mathcal{U}(\vec{u}) - \mathcal{F}(\vec{u}) \quad (3.21)$$

where  $\mathcal{U}(\vec{u}) = \sum_{k=1}^M \mathcal{U}_k(\vec{u})$  is the strain energy of the laminate,  $\mathcal{F}(\vec{u})$  is the potential of the external loads, and  $\vec{u}$  are the displacement functions expressed in terms of the unknown coefficients  $a_j$ ,  $b_j$ , as indicated in (3.2) and (3.3). The functions  $u_{x|i}$ ,  $u_{y|i}$

which minimize the potential energy of the system are found by setting

$$\frac{\partial \Pi(\vec{u})}{\partial a_j} = 0. \quad (3.22)$$

The potential of the external loads per unit width of the laminate can be written as:

$$\mathcal{F}(\vec{u}) = \int_{\Gamma} (T_x u_x + T_y u_y) dx \quad (3.23)$$

where  $T_x$  and  $T_y$  are the tractions applied to the outer surfaces of the laminate in the x- and y-directions respectively. Considering the case of antisymmetric loading,  $T_x = 0$ , and using the mapping (3.6), we can write:

$$\mathcal{F}(\vec{u}) = \int_0^\ell T_y u_y dx \quad (3.24)$$

$$\mathcal{F}(\vec{u}) = \frac{\ell}{2} \int_{-1}^{+1} \frac{q_x(\xi)}{2} u_y(\xi, h/2) d\xi + \frac{\ell}{2} \int_{-1}^{+1} \frac{q_x(\xi)}{2} u_y(\xi, -h/2) d\xi. \quad (3.25)$$

Using the expansion (2.77), (2.78) and the mapping (3.6), the potential of the external forces can be written in matrix form as follows:

$$\mathcal{F}(\vec{u}) = [a] \{R\} \quad (3.26)$$

where  $\{R\}$  is the load vector (see Appendix D for details). Substituting (3.20) and (3.26) into (3.21):

$$\Pi(\vec{u}) = \frac{1}{2} [a] [K] \{a\} - [a] \{R\} \quad (3.27)$$

and, after applying the conditions (3.22), we get:

$$[K] \{a\} - \{R\} = 0 \quad (3.28)$$

which is the system of simultaneous linear equations from which the coefficients of the unknown functions  $u_{x|i}$  and  $u_{y|i}$  are computed.



## 3.2 Examples

Two representative model problems are discussed in the following. For the first model problem the solution is smooth. For the second model problem stress singularities occur at the boundaries.

### 3.2.1 Model Problem 1: The Infinite Strip

Consider an infinite strip composed of perfectly bonded orthotropic layers, symmetrically distributed with respect to the middle plane, i.e. the  $x$ -axis (Fig. 3.1). Two cases will be discussed in the following, in one case the number of layers is 3 in the other the number of layers is 5.

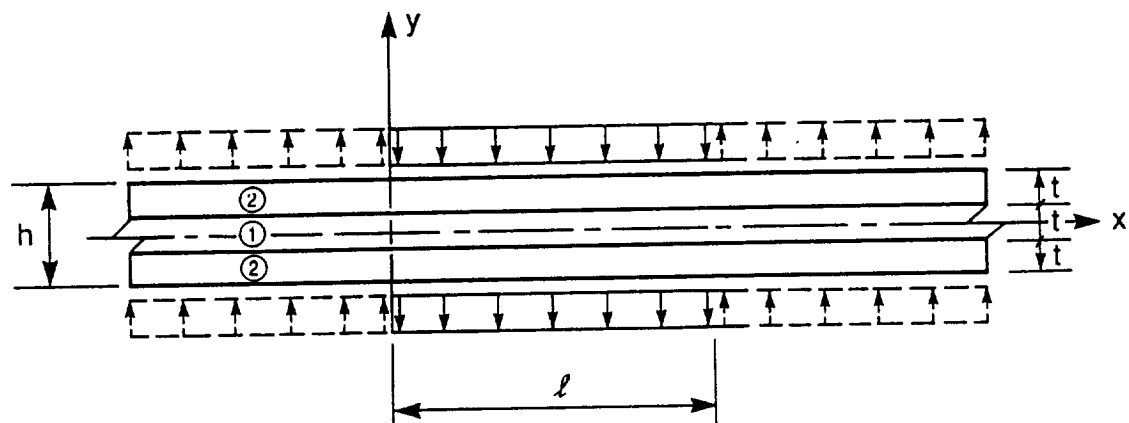


Figure 3.1: Model problem 1: Notation for the case of three layers.

The body is assumed to be in state of plane strain with respect to the  $xy$  plane. Antisymmetry conditions are imposed at  $x = 0$  and symmetry conditions are imposed at  $x = \ell/2$ . These boundary conditions are equivalent to a simply supported finite strip of length  $\ell$ , which is symmetrically loaded (with respect to  $x$ ) about  $x = \ell/2$ . Uniform load is applied as a normal traction to the top and bottom surfaces of the strip. All layers in the laminate are of equal thickness  $t$ , and are of a square symmetric unidirectional fibrous composite material possessing the following stiffness properties, which simulate a high-modulus graphite/epoxy composite:

$$E_L = 25.0 \times 10^6 \text{ psi} \quad E_T = 1.0 \times 10^6 \text{ psi}$$

$$G_{LT} = 0.5 \times 10^6 \text{ psi} \quad G_{TT} = 0.2 \times 10^6 \text{ psi}$$

$$\nu_{LT} = \nu_{TT} = 0.25$$

where  $L$  indicates the direction parallel to the fibers,  $T$  is the transverse direction, and  $\nu_{LT}$  is the Poisson ratio (i.e.,  $\nu_{LT} = -\epsilon_{TT}/\epsilon_{LL}$ , where  $\epsilon_{TT}$ ,  $\epsilon_{LL}$  are, respectively, the normal strains in the directions  $T$  and  $L$ ). These material properties were selected from reference [18].

For the three-layer laminate the  $L$ -direction coincides with the  $x$ -direction in the two outer layers, while the  $T$  is parallel to the  $x$ -direction in the central layer. For the five-layer laminate the  $L$ -direction coincides with the  $x$ -direction in the central and in the two outer layers, while the  $T$  is parallel to the  $x$ -direction in the other two layers. This arrangement of laminae is designated as 0/90/0/90/0.

The functions of main interest for this problem are the longitudinal and transverse stresses ( $\sigma_x$  and  $\sigma_y$ ) at  $x = \ell/2$ , the shear stress  $\tau_{xy}$  at  $x = 0$ , the deflection  $u_y$  at  $x = \ell/2$ , and the horizontal displacement  $u_x$  at  $x = 0$ .

In order to establish a reference solution which can be regarded as being sufficiently close to the exact solution of the problem of elasticity, the problem was solved using the finite element program MSC/PROBE<sup>1</sup> and an experimental program in which the algorithm described in Chapter 2 is implemented. In the reference solution obtained with MSC/PROBE each layer was discretized as a two-dimensional plane strain element with orthotropic material properties. Three or five finite elements were used and the solution was obtained for  $p$  ranging from 1 through 8. For all  $L/h$  ratios the estimated relative error in energy norm was below 1% at  $p = 8$ . The solution corresponding to  $p = 8$  will be used as the basis for comparison. The solutions corresponding to the proposed hierarchic models were obtained using only one laminated element. The polynomial degree was varied from 1 through 8 and the equilibrium equations were satisfied up to powers of  $\beta$  ranging from 0 to 3.

The model that satisfies the equilibrium equations up to the zeroth power of  $\beta$  was modified as indicated in Section 2.4.4. The transverse shear modulus of each

---

<sup>1</sup>MSC/PROBE: User's Manual, The MacNeal-Schwendler Corporation, 1600 S. Brentwood Blvd., Suite 840, St. Louis, Missouri 63144.

layer was made equal to the harmonic average  $\hat{E}_6$ . In the case of three layers:

$$\hat{E}_6 = 3 \left( \frac{1}{E_6^{(1)}} + \frac{2}{E_6^{(2)}} \right)^{-1} \quad (3.29)$$

and  $E_1$  for each layer was substituted for by  $(E_1 - E_2^2/E_3)$ . We will denote the modified model characterized by  $\beta^0$  with  $\beta_m^0$ , to differentiate from those cases where the unmodified  $\beta^0$  results are presented.

The model characterized by  $\beta^1$  was also modified according to the description in Section 2.4.4, and will be denoted as  $\beta^1$  since no results are presented for the unmodified case.

The following normalized quantities are defined to present the results:

$$\bar{\sigma}_x \stackrel{\text{def}}{=} \frac{\sigma_x(\ell/2, y)}{q}, \quad \bar{\sigma}_y \stackrel{\text{def}}{=} \frac{\sigma_y(\ell/2, y)}{q}, \quad \bar{\tau}_{xy} \stackrel{\text{def}}{=} \frac{\tau_{xy}(0, y)}{q} \quad (3.30)$$

$$\bar{u}_x \stackrel{\text{def}}{=} \frac{E_T u_x(0, y)}{q t} \quad (3.31)$$

$$U_y \stackrel{\text{def}}{=} \frac{100 E_T h^3 u_y(\ell/2, 0)}{q \ell^4} \quad (3.32)$$

where  $q$  is the applied traction and  $t$  is the thickness of each lamina.

The non-dimensional vertical deflection  $U_y$  of the beam is plotted against the  $L/h$  ratio in Fig. 3.2 for the three-layer laminate, and in Fig. 3.3 for the five-layer laminate.

It is seen that for large  $L/h$  ratios all models yield similar results. As  $L/h$  decreases, the  $\beta^0$  model underestimates the deflection while the  $\beta^1$  model is very close to the exact solution. For  $\beta^2$  and  $\beta^3$  the results are virtually identical with those of MSC/PROBE for the entire range of  $L/h$  values. The ratio between

$(E_1 - E_2^2/E_3)$  and  $E_1$  is only 0.99 for the top and bottom layers and 0.94 for the central layer, so that the influence of the modification of the material properties in the values of the deflection is almost negligible for all  $L/h$  ratios. To emphasize the influence of the material properties in the results for the  $\beta^0$  model, Fig. 3.4 shows the central deflection of the three-layer laminate for different material properties, selected such that the ratio  $(E_1 - E_2^2/E_3)/E_1 = 0.7$  for the outer layers, while  $E_6$  was made constant and equal to the harmonic average (see equation (3.29)). It is seen that the solution corresponding to the  $\beta^0$  model converges to a different limit than the other models as  $L/h \rightarrow \infty$  when the adjustment of the material properties is not performed. Finally, Fig. 3.5 indicates that if  $E_6$  is not modified at all, the  $\beta^0$  model converges to zero as  $L/h \rightarrow 0$ .

The results shown in Fig. 3.6 indicate that for large  $L/h$ , the solution of  $\beta_m^0$ , which is equivalent to the first-order shear-deformation model, gives a good representation of the actual displacement variation. As  $L/h$  becomes smaller, the effect of transverse shear becomes increasingly important and the linear approximation shows a significant deviation from the reference solution. The  $\beta^1$  solution gives much better results, even for very small  $L/h$  ratios. For  $\beta^2$  and  $\beta^3$  the improvement is even greater, especially for small  $L/h$  ratios. See Figures 3.7 and 3.8 for the three-layer laminate and Fig. 3.9 for the five-layer problem.

The same situation is true for the longitudinal stress  $\sigma_x$ , as shown in Figures 3.10 and 3.11 for the three layer problem and in Fig. 3.12 for the five-layer laminate.

The shear stress distribution was obtained directly from the solution vector using equation (2.6), and also by integrating the equilibrium equation (2.2) and imposing the stress free condition at the top and bottom surfaces. The direct calculation gives good results only for high powers of  $\beta$ , regardless of the  $L/h$  ratio (see Figures 3.13, 3.14 and 3.15), while integration of the equilibrium equations yields very close approximation for low powers of  $\beta$  when  $L/h$  is large and for high powers of  $\beta$  when  $L/h$  is small (see figures 3.16 and 3.17). Appendix E includes a detailed description for the calculation of engineering quantities from the finite element solution.

Finally, Fig. 3.18 shows the non-dimensional transverse stress distribution  $\bar{\sigma}_y$  for  $L/h = 4$  that was computed from the solution vector using equation (2.6). It is seen that the solution for  $\beta^2$  and  $\beta^3$  give accurate results, especially at the interface between layers. The original material properties were used in computing the stresses for the cases  $\beta_m^0$  and  $\beta^1$ .

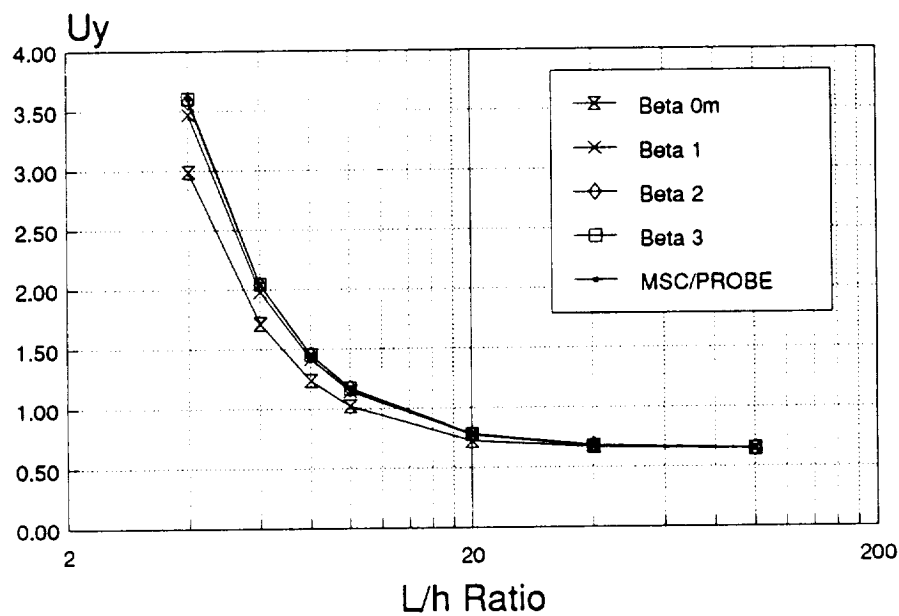


Figure 3.2: Model problem 1: Central deflection for the three-layer laminate.

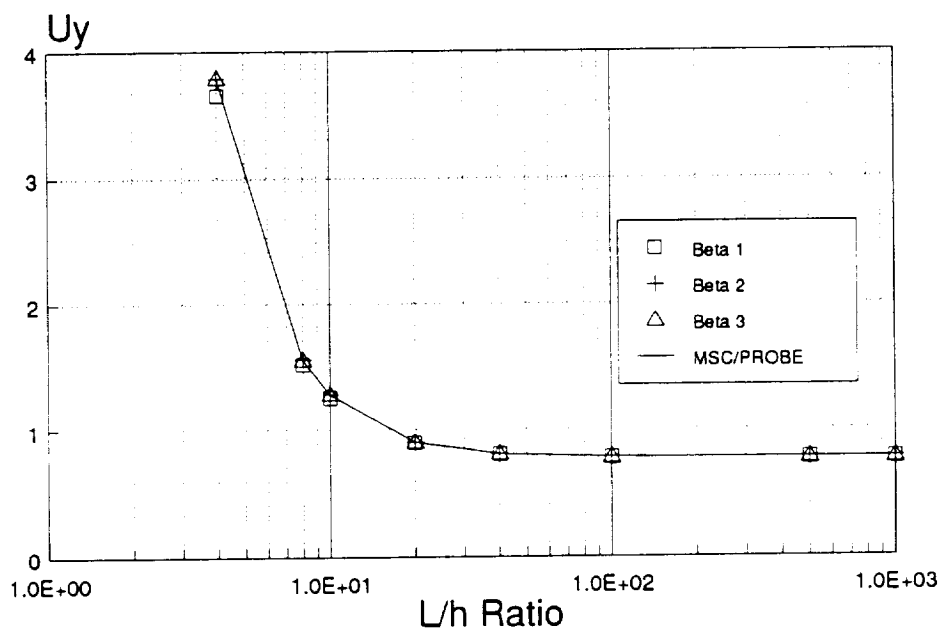


Figure 3.3: Model problem 1: Central deflection for the five-layer laminate.

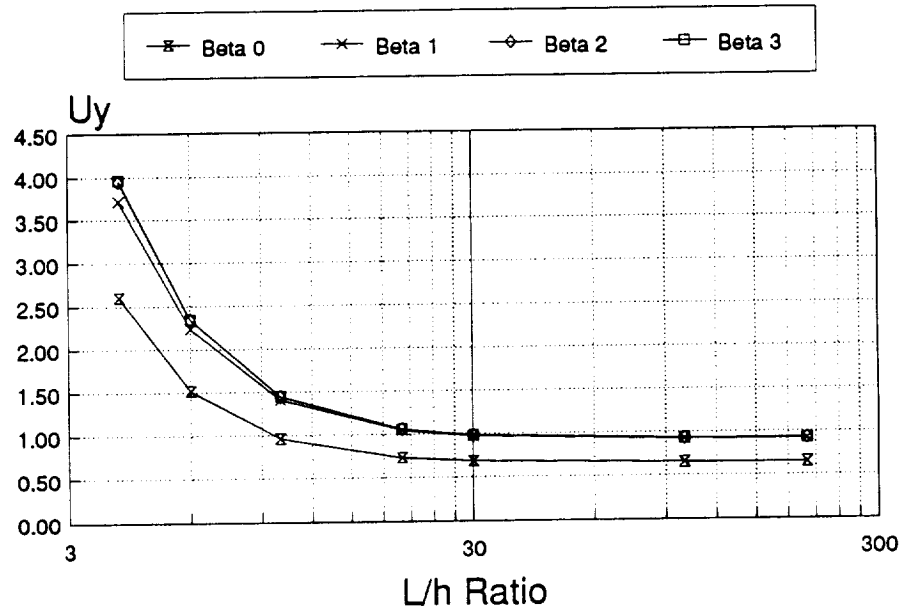


Figure 3.4: Model problem 1: Central deflection for the three-layer laminate. For the outer layers:  $(E_1 - E_2^2/E_3)/E_1 = 0.7$ .

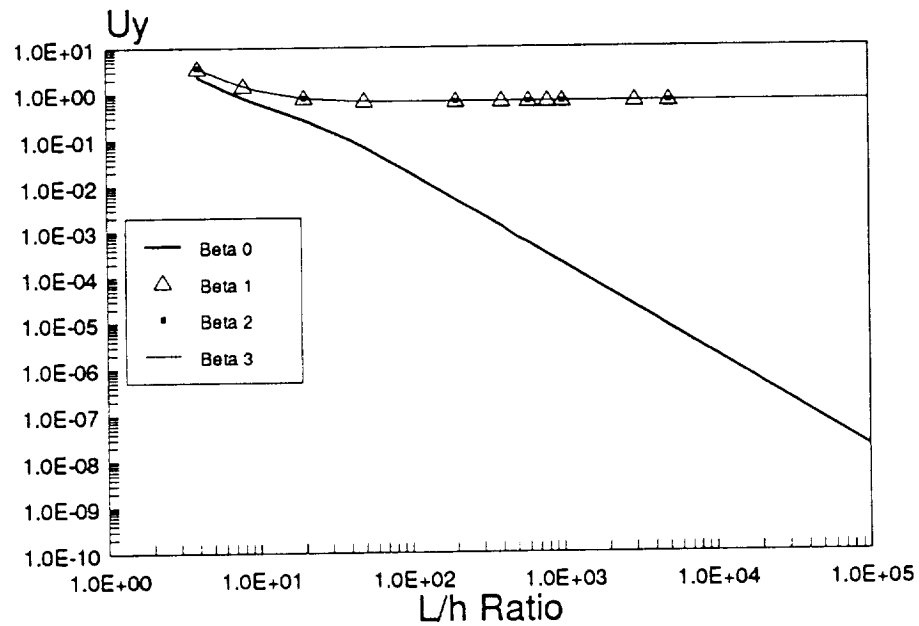
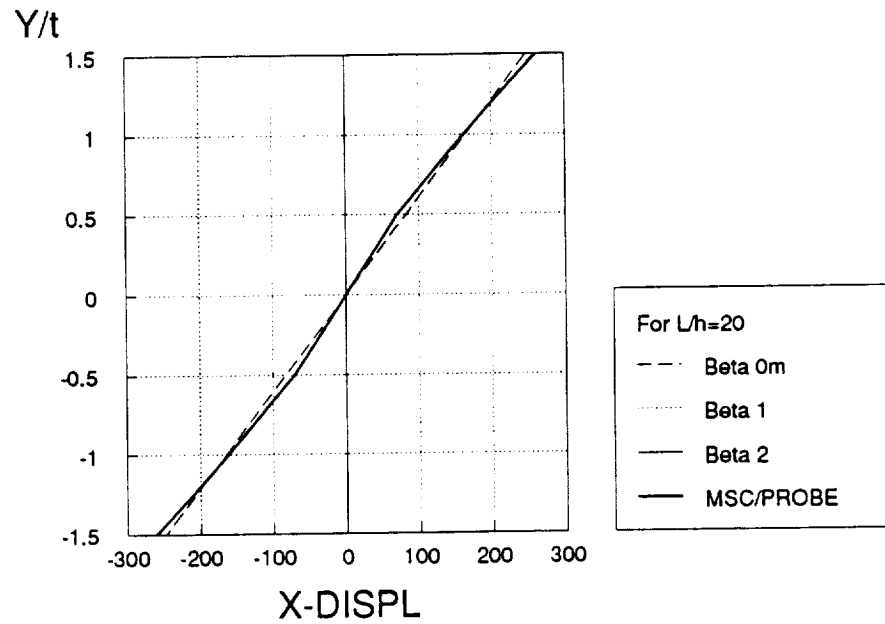
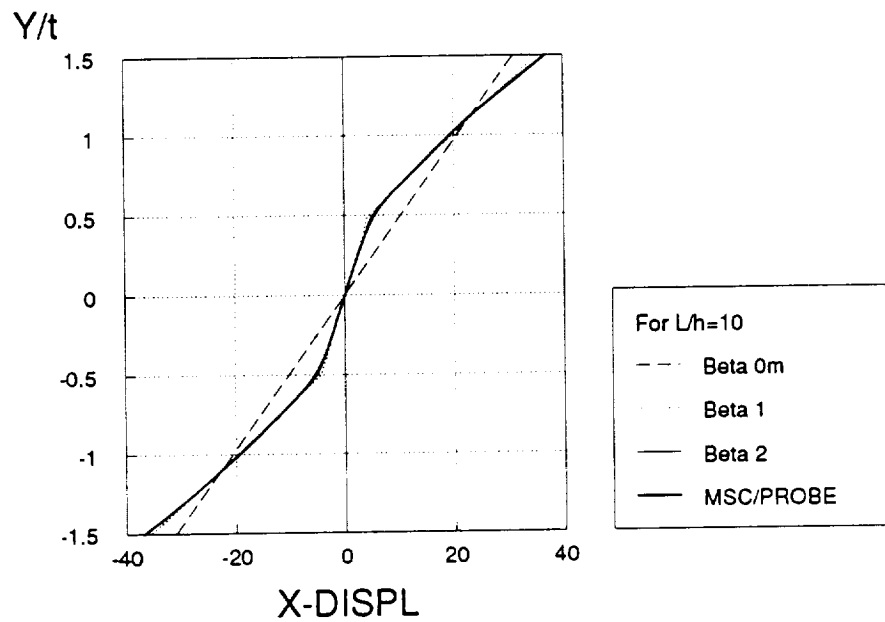


Figure 3.5: Model problem 1: Central deflection for the three-layer laminate. Comparison of  $\beta^0$  vs.  $\beta^n$ , ( $n = 1, 2, 3$ ).





**Figure 3.6:** Model problem 1: The function  $\bar{u}_x(0, y)$  for  $L/h = 20$ . Three-layer laminate.



**Figure 3.7:** Model problem 1: The function  $\bar{u}_x(0, y)$  for  $L/h = 10$ . Three-layer laminate.

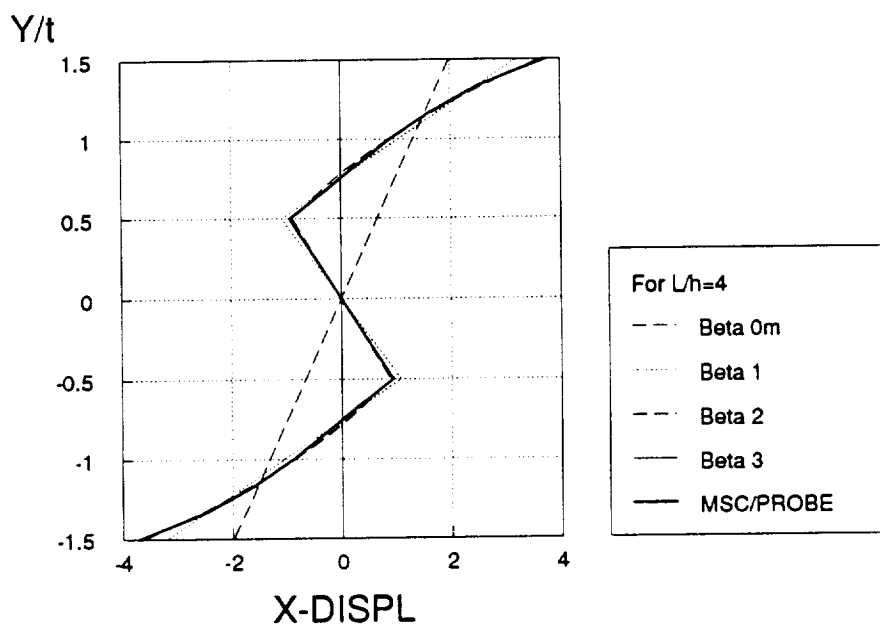


**Figure 3.8:** Model problem 1: The function  $\bar{u}_x(0, y)$  for  $L/h = 4$ . Three-layer laminate.

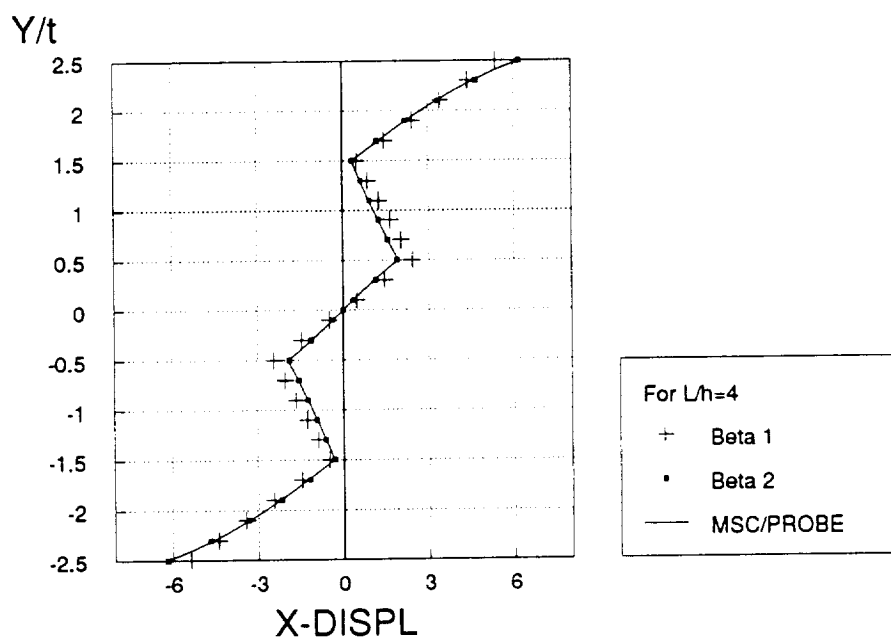


**Figure 3.9:** Model problem 1: The function  $\bar{u}_x(0, y)$  for  $L/h = 4$ . Five-layer laminate.

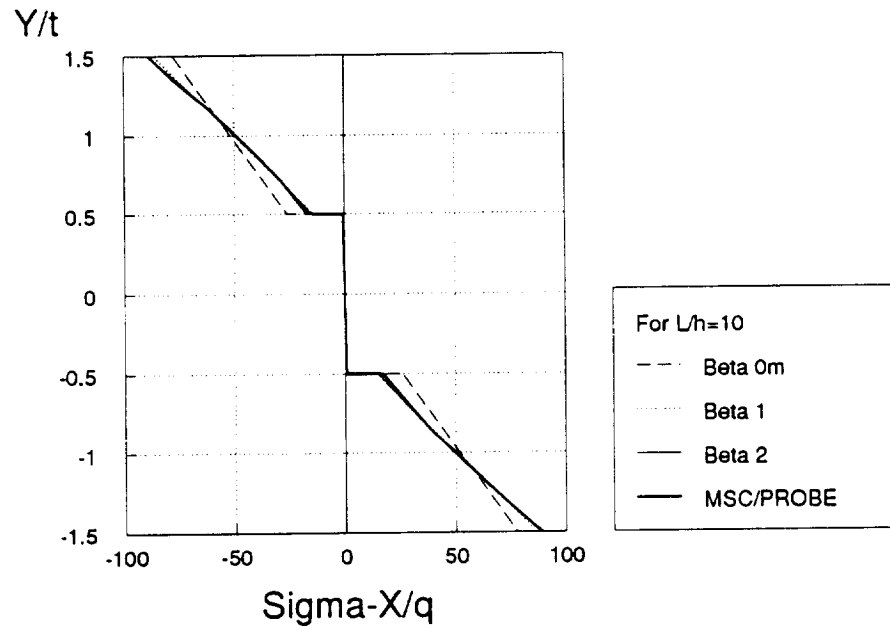


Figure 3.10: Model problem 1: The function  $\bar{\sigma}_x(\ell/2, y)$  for  $L/h = 10$ . Three-layer laminate.

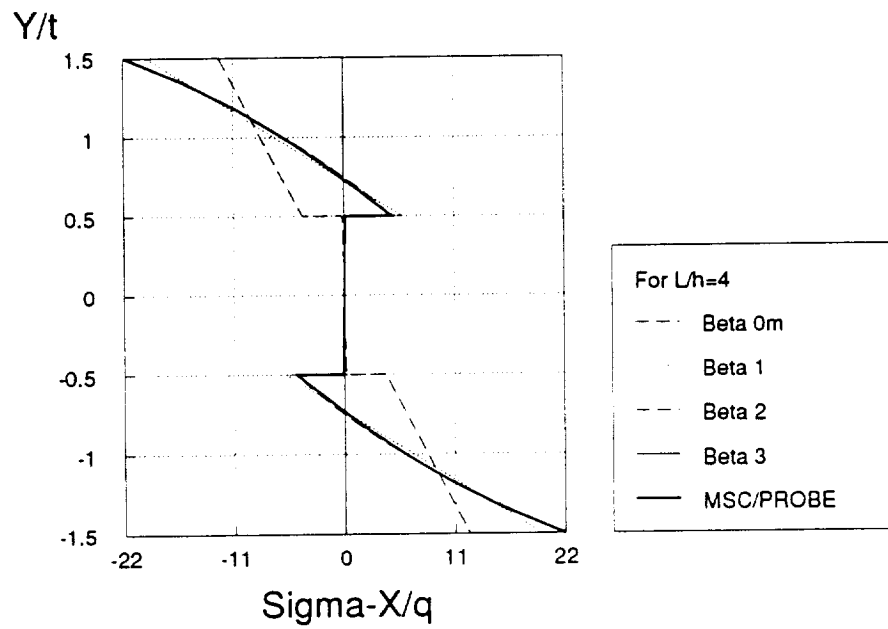


Figure 3.11: Model problem 1: The function  $\bar{\sigma}_x(\ell/2, y)$  for  $L/h = 4$ . Three-layer laminate.

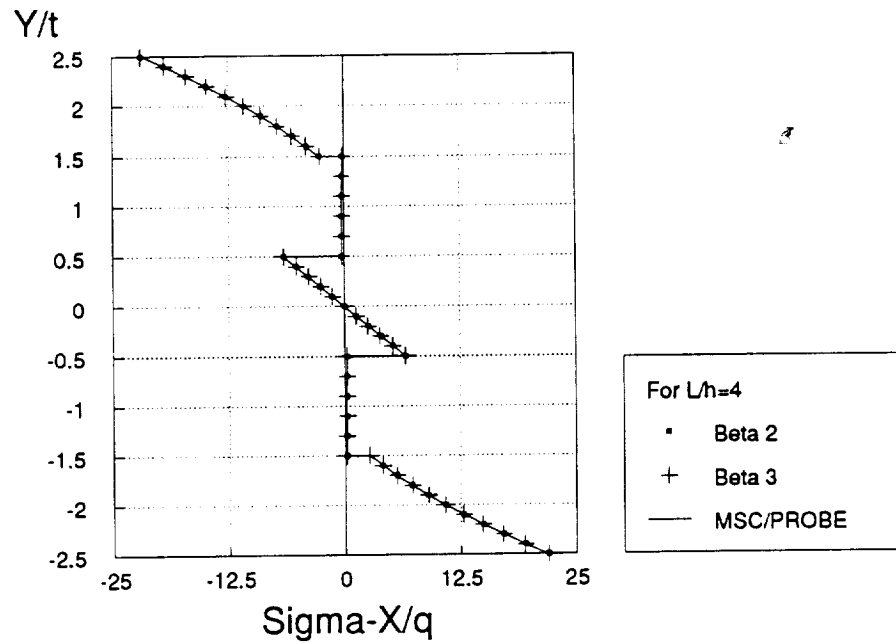


Figure 3.12: Model problem 1: The function  $\bar{\sigma}_x(\ell/2, y)$  for  $L/h = 4$ . Five-layer laminate.

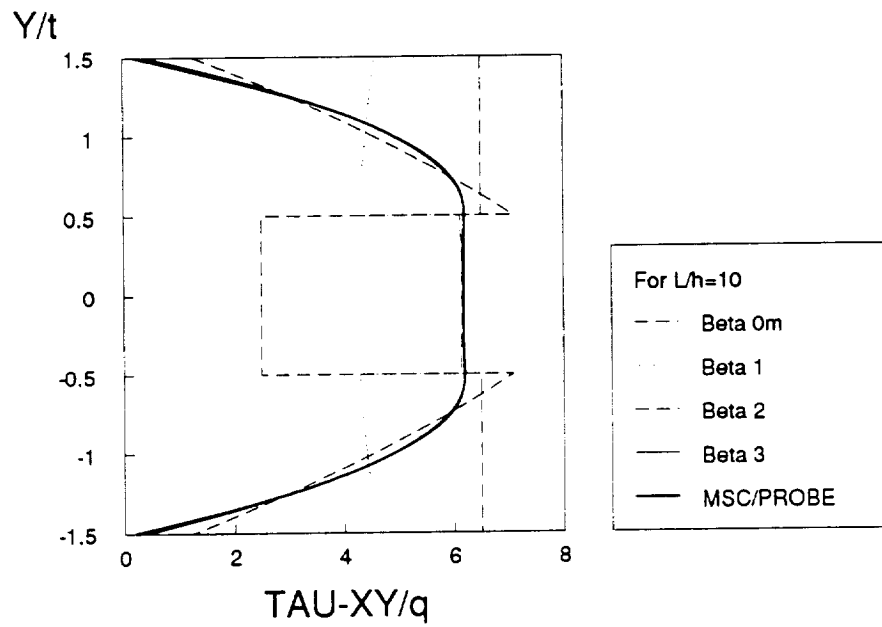
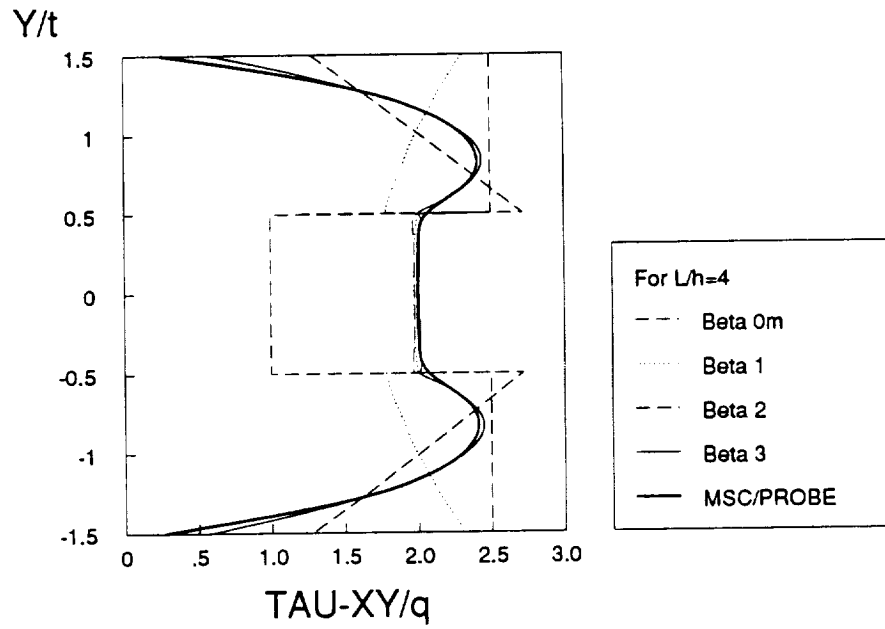
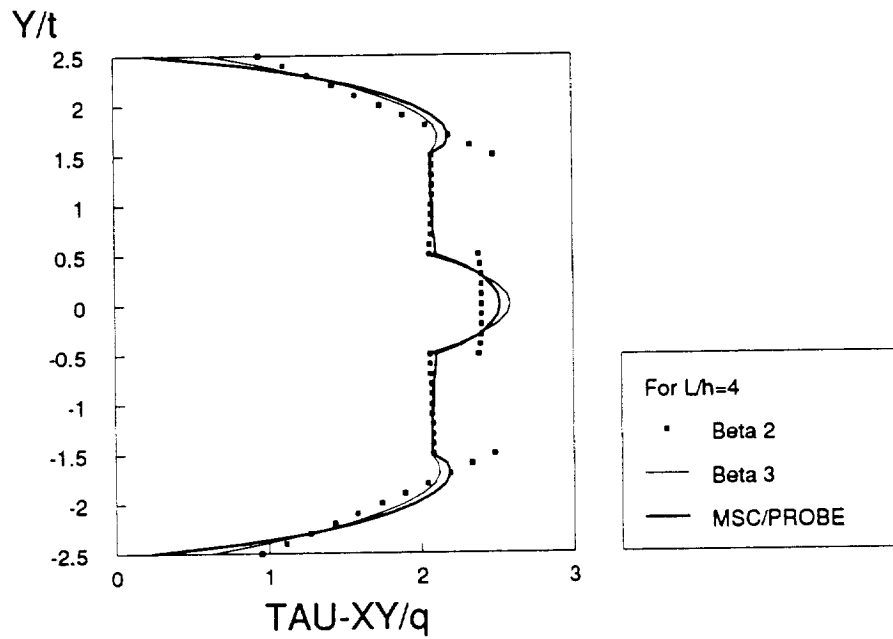


Figure 3.13: Model problem 1: The function  $\bar{\tau}_{xy}(0, y)$ . Direct computation for  $L/h = 10$ . Three-layer laminate.



**Figure 3.14:** Model problem 1: The function  $\bar{\tau}_{xy}(0, y)$ . Direct computation for  $L/h = 4$ . Three-layer laminate.



**Figure 3.15:** Model problem 1: The function  $\bar{\tau}_{xy}(0, y)$ . Direct computation for  $L/h = 4$ . Five-layer laminate.

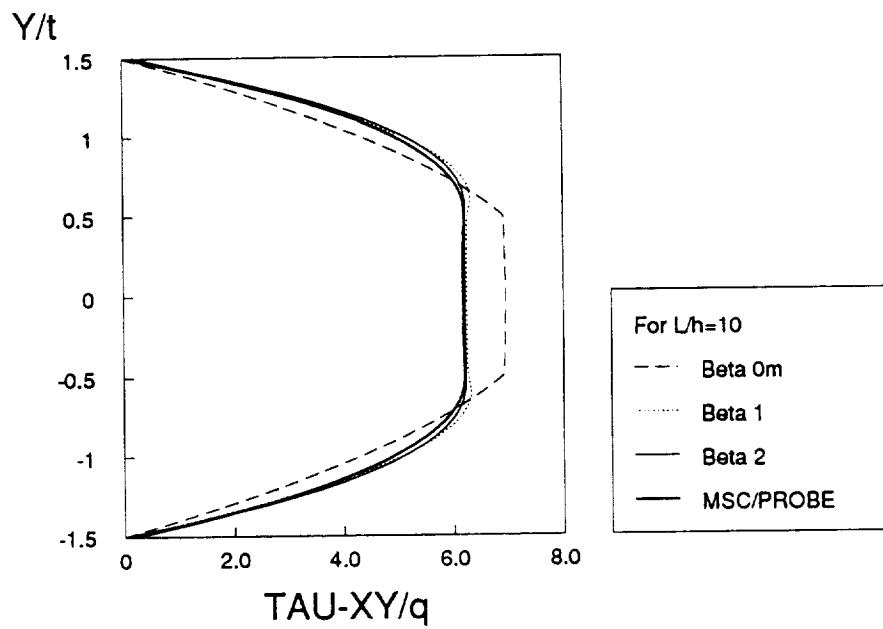


**Figure 3.16:** Model problem 1: The function  $\bar{\tau}_{xy}(0, y)$  computed by integration of the equilibrium equation for  $L/h = 10$ . Three-layer laminate.

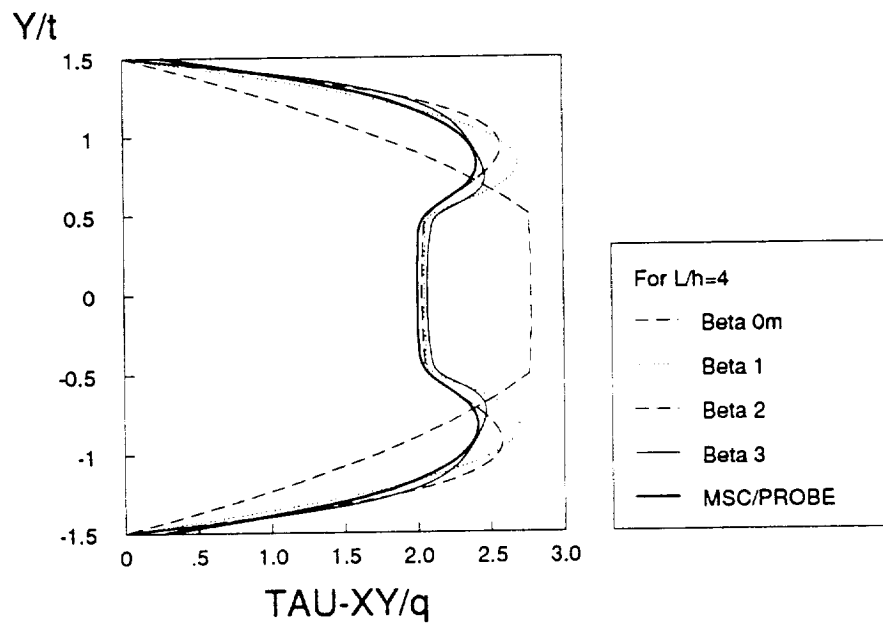


**Figure 3.17:** Model problem 1: The function  $\bar{\tau}_{xy}(0, y)$  computed by integration of the equilibrium equation for  $L/h = 4$ . Three-layer laminate.

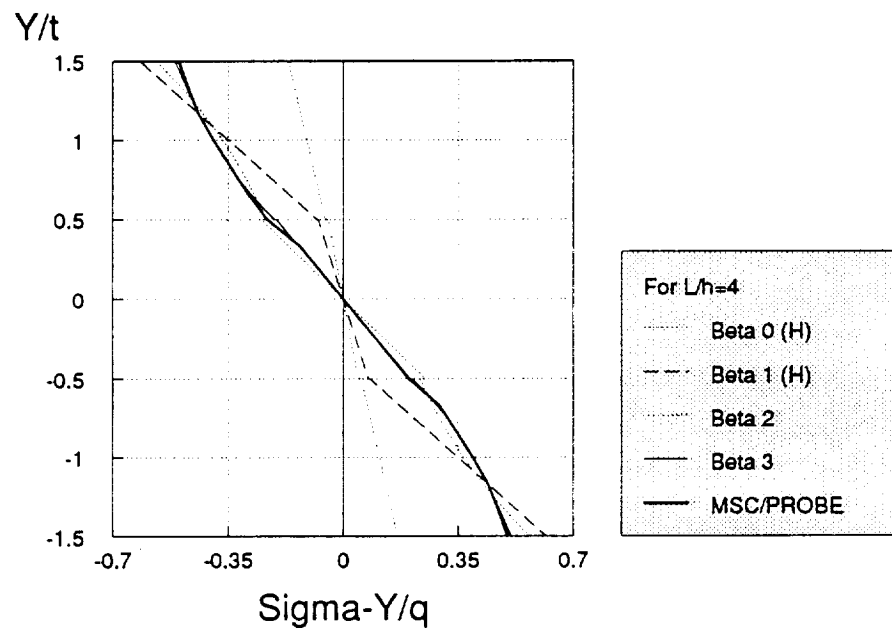


**Figure 3.18:** Model problem 1: The function  $\bar{\sigma}_y(\ell/2, y)$  for  $L/h = 4$ . Three-layer laminate.

### 3.2.2 Model problem 2: The Cantilever Beam

The laminated strip of the previous example is considered again but with different boundary conditions. At  $x = 0$ , both the horizontal and vertical displacements are set to zero (clamped edge), while the end  $x = \ell$  is free (Fig. 3.19). At  $x = 0$  singularities occur at the top and bottom surfaces, and boundary layer effects are dominant near the clamped edge. At  $x = \ell$  singularities occur at the interfaces. Of interest is the performance of the hierarchic model near the clamped edge and at the free edge.

The reference solution for this problem was again obtained using MSC/PROBE. The finite element mesh, shown in Fig. 3.20, consisted of 30 elements. The mesh was graded in geometric progression towards the singular points. At  $p = 8$  the estimated relative error in energy norm was less than 0.5%. At  $p = 8$  the total number of degrees of freedom is 1,783. Changing the location of the clamped edge, the same mesh was used to evaluate the singularities at the free edge.

The solution with the hierarchic model was obtained using only one element for the polynomial degree varying from 1 to 8, and the power of  $\beta$  from 0 to 3.

Fig. 3.21 shows the end deflection of the beam as a function of the degrees of freedom for  $L/h = 10$ . The solution for  $\beta_m^0$  differs by 9.7% from the solution by MSC/ PROBE, but for  $\beta^1$  the difference is only 1.22%.

Normal and shear stress distributions were computed at different locations along the beam. At  $x = 0$  the exact values of  $\sigma_x$  and  $\tau_{xy}$  are infinity at the top and



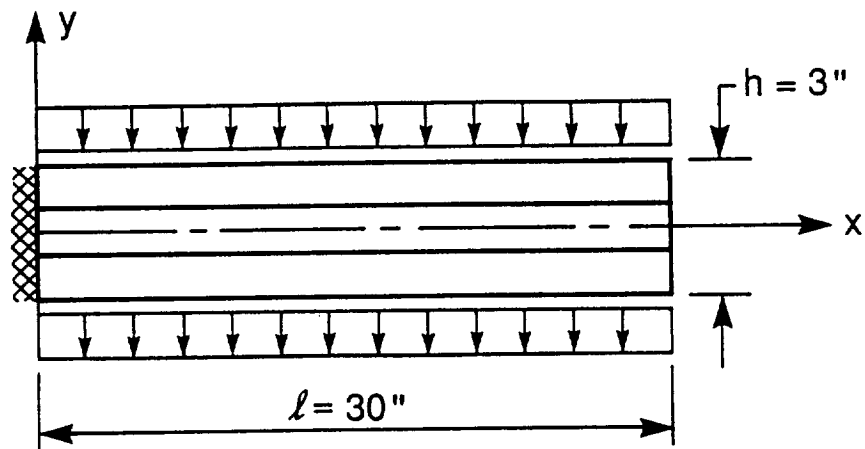


Figure 3.19: Model problem 2: Notation.

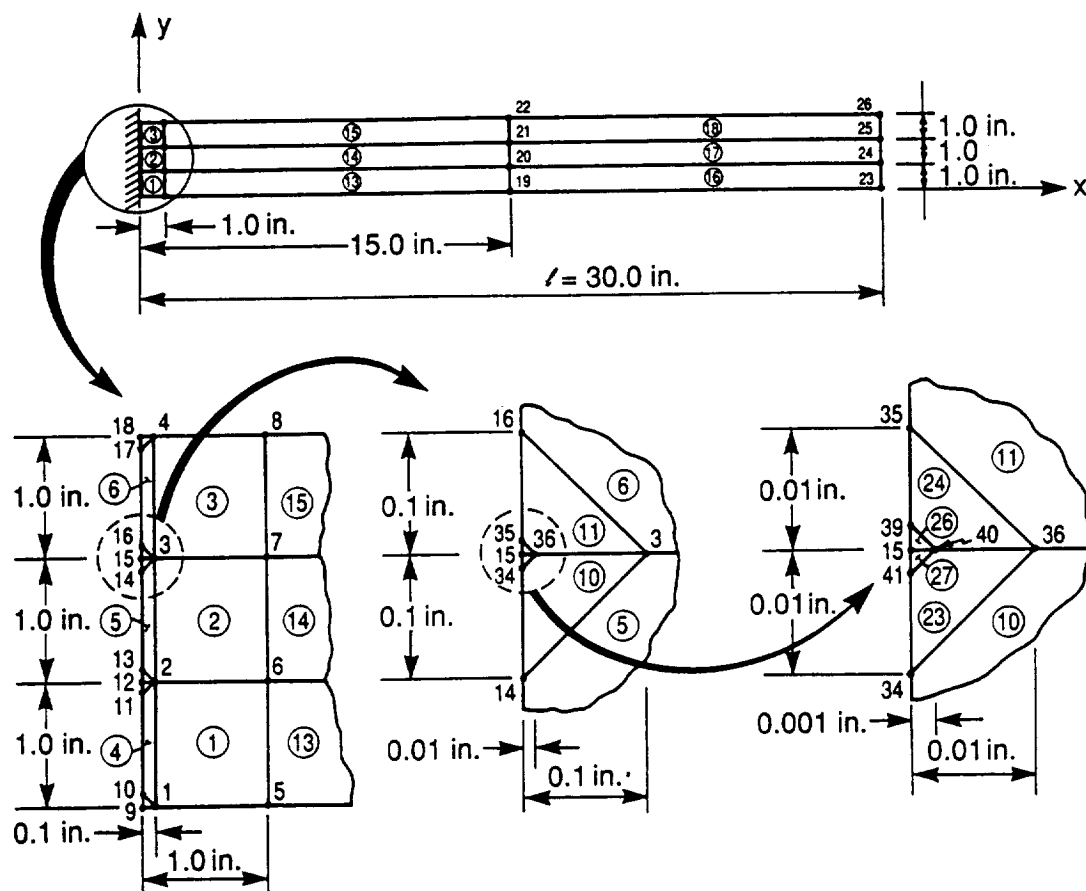


Figure 3.20: Model problem 2: Finite element mesh for the reference solution.

bottom surfaces. There are no singularities at the laminar interfaces. The solutions obtained by means of the proposed hierarchic models exhibited good convergence characteristics in terms of the normal and shear stresses at this Section, with the exception of the neighborhoods of the stress singularities at  $x/h = 0$ ,  $y/t = \pm 1.5$ . The results are shown in Figures 3.22 and 3.23.

At  $x = h/3$ , i.e., at only one lamina thickness away from the singularity, the normal stress distribution is in excellent agreement with that of MSC/PROBE for all powers of  $\beta$  larger than zero (see Fig. 3.24).

The shear stress distribution requires higher powers of  $\beta$  to approach the reference solution. At  $x = h/6$  (half the thickness of one layer) the solution corresponding to  $\beta^3$  gives accurate results for both methods (direct computation and integration of the equilibrium equations) as shown in Figures 3.25 and 3.26.

At  $x = h$  the shear stress computed directly from the solution vector is accurate only when the equilibrium equations are satisfied up to the third power of  $\beta$ . When they are computed through integration of the equilibrium equations, the results are accurate for all powers of  $\beta$  equal or greater than one (see Figures 3.27 and 3.28).

At the free end ( $x = \ell$ ), large stress gradients occur at the laminar interfaces. Figure 3.29 shows the normal stress  $\sigma_y$  at  $x = \ell$ , while Figure 3.30 show the stress distribution at a very short distance from the free edge ( $x = 0.997 \ell$ ). Note that the performance of the hierarchic sequence very close to the free end is very satisfactory.

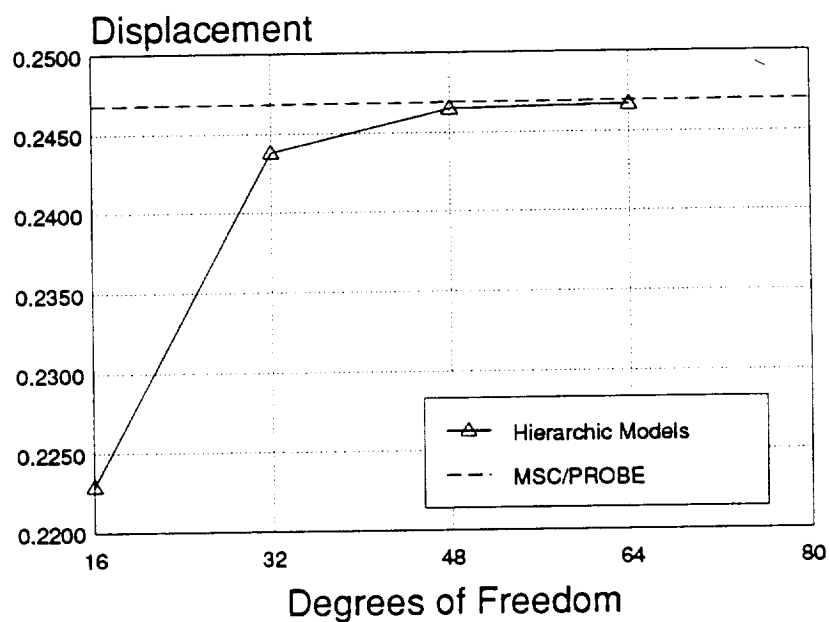


Figure 3.21: Model problem 2: End deflection.

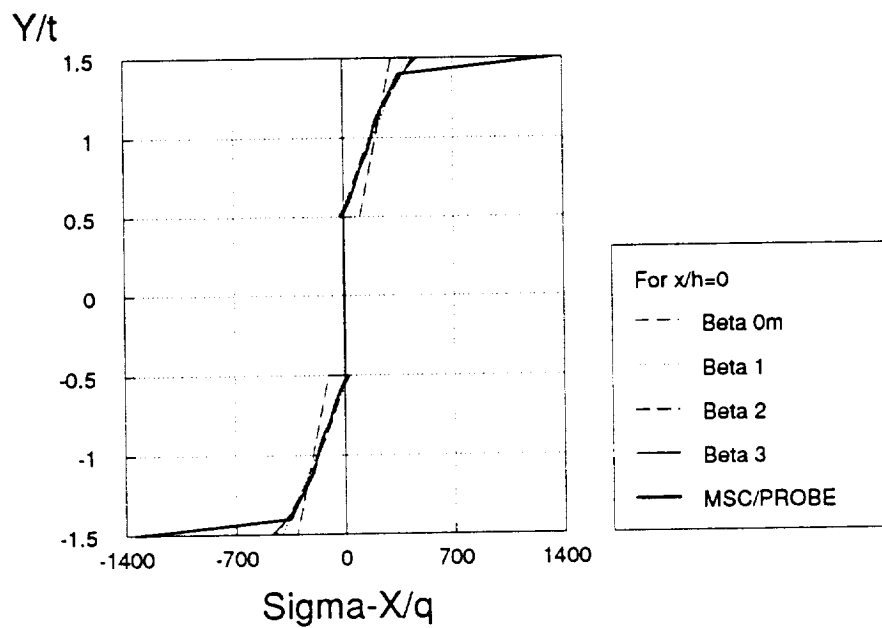


Figure 3.22: Model problem 2: The function  $\bar{\sigma}_x(0, y)$ .

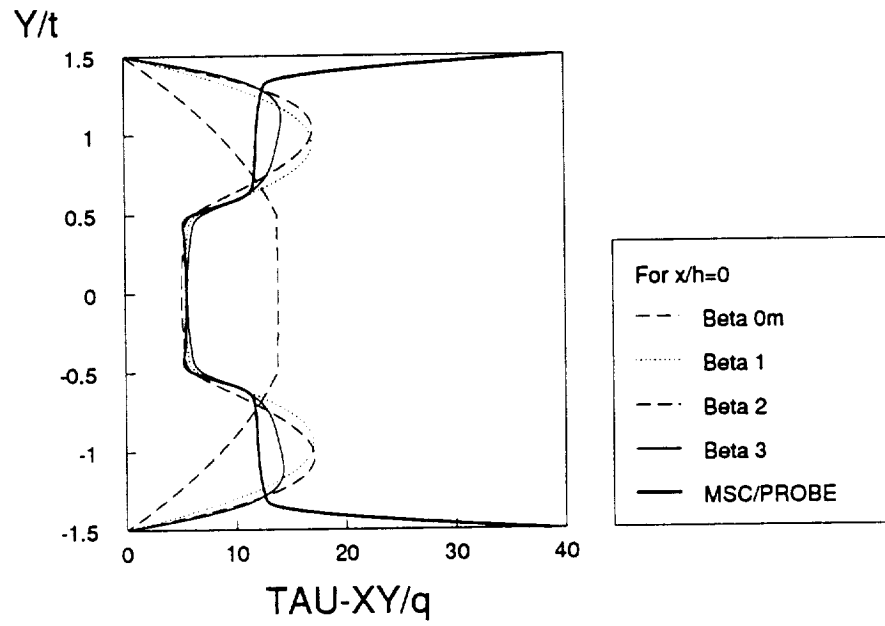


Figure 3.23: Model problem 2: The function  $\bar{\tau}_{xy}(0, y)$ .

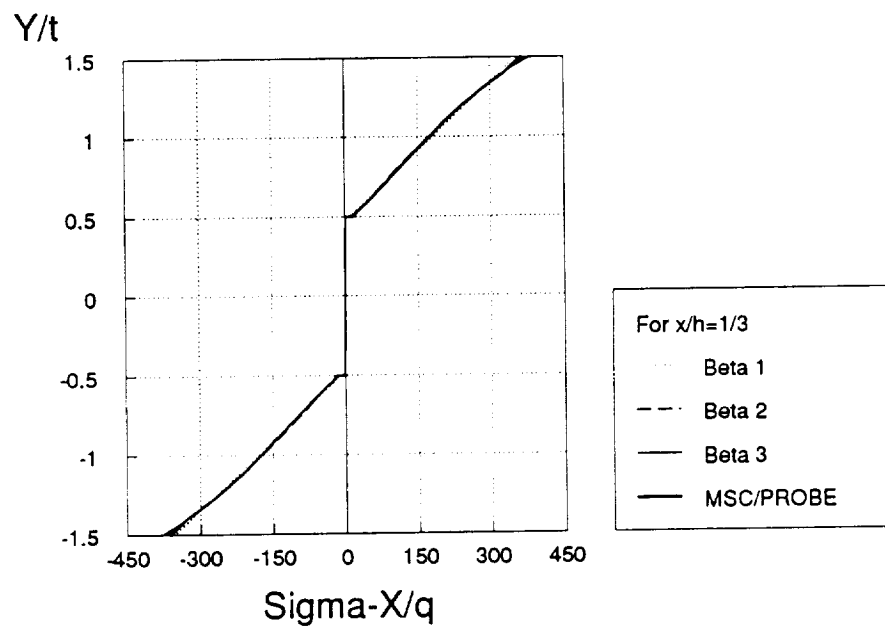
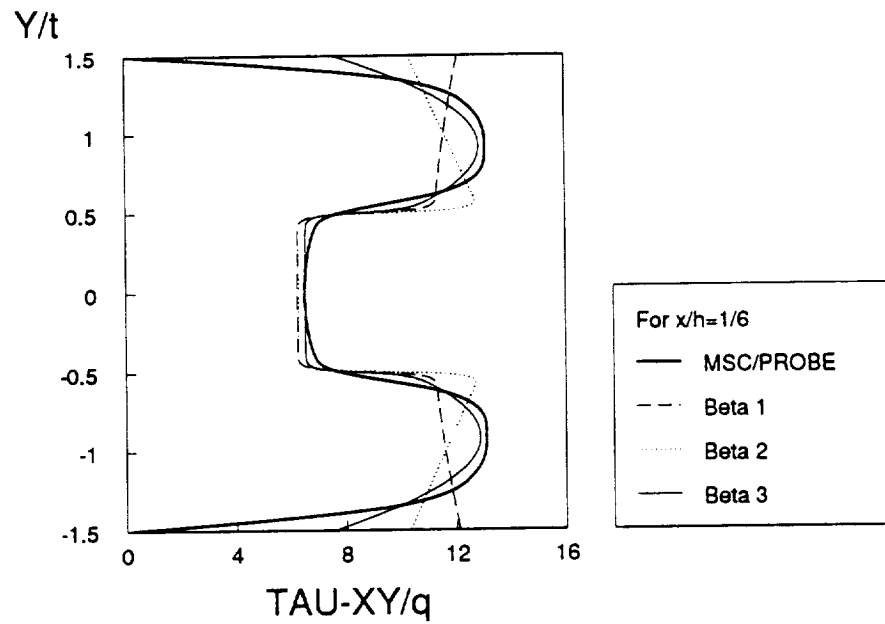
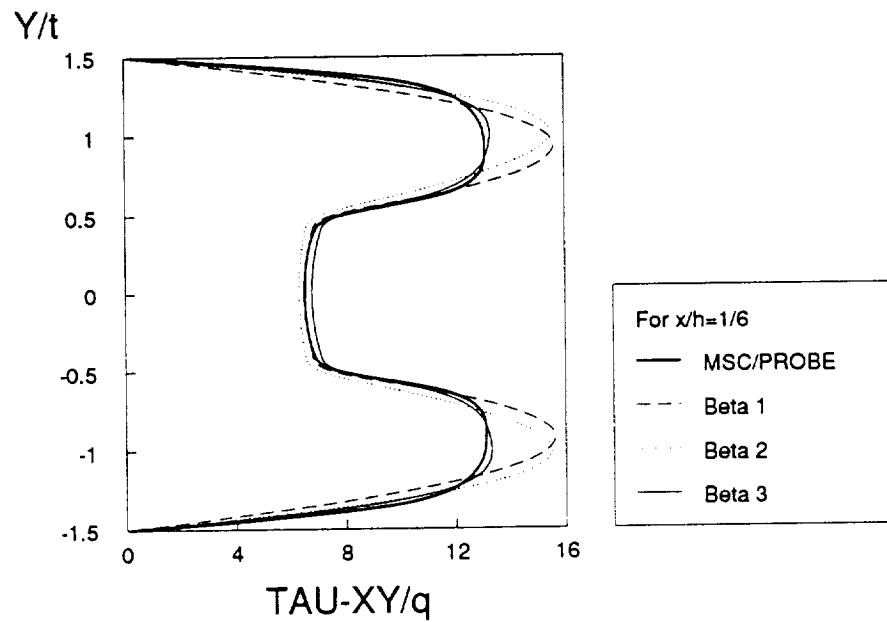


Figure 3.24: Model problem 2: The function  $\bar{\sigma}_x(h/3, y)$ .



**Figure 3.25:** Model problem 2: The function  $\bar{\tau}_{xy}(h/6, y)$ . Direct computation.



**Figure 3.26:** Model problem 2: The function  $\bar{\tau}_{xy}(h/6, y)$  computed by integration of the equilibrium equation.

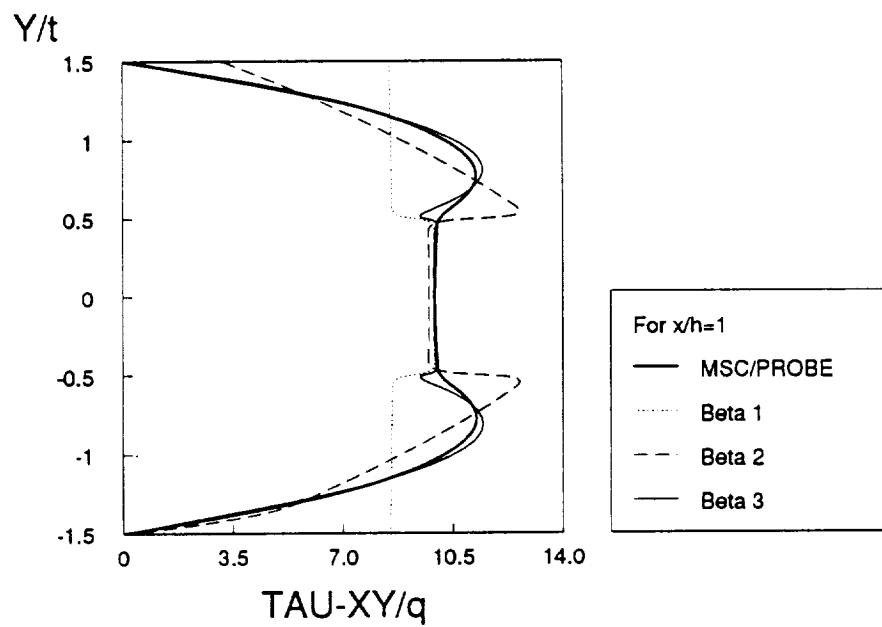


Figure 3.27: Model problem 2: The function  $\bar{\tau}_{xy}(h, y)$ . Direct computation.

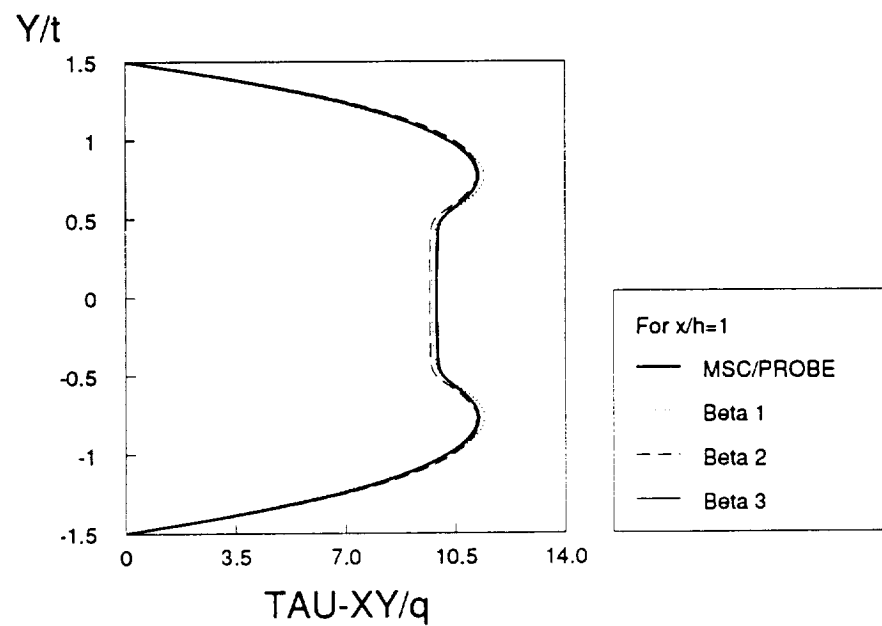


Figure 3.28: Model problem 2: The function  $\bar{\tau}_{xy}(h, y)$  computed by integration of the equilibrium equation.

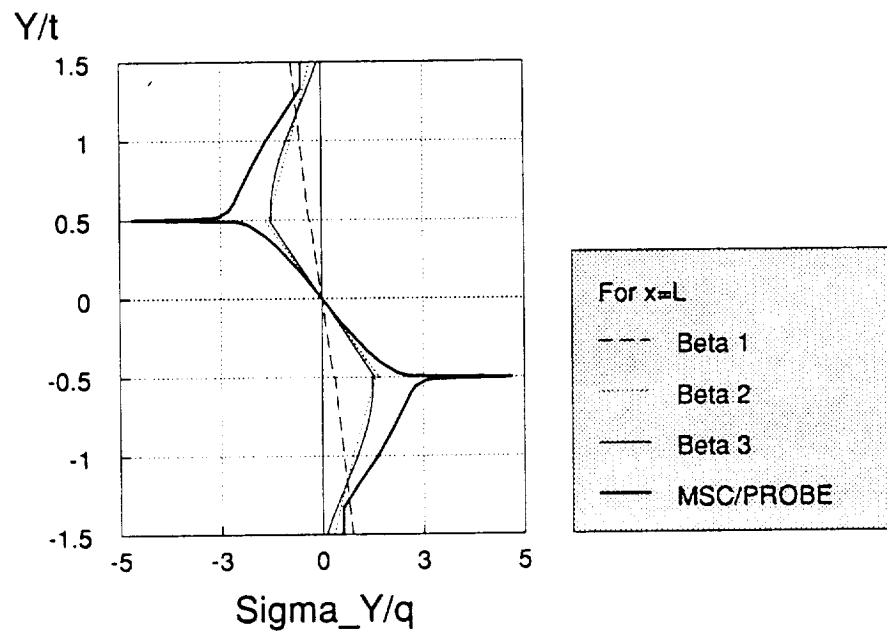


Figure 3.29: Model problem 2: The function  $\bar{\sigma}_y(\ell, y)$ .

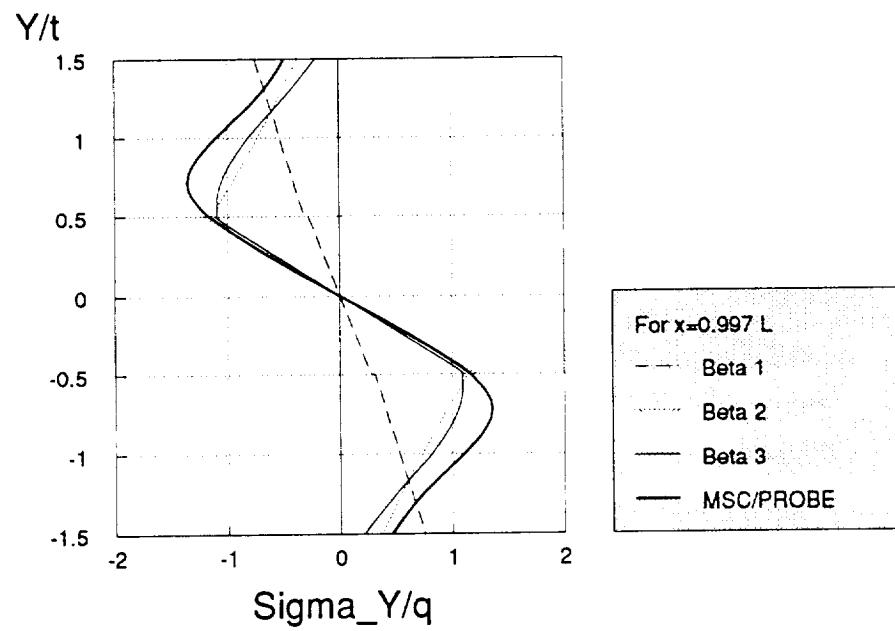


Figure 3.30: Model problem 2: The function  $\bar{\sigma}_y(0.997 \ell, y)$ .

### 3.3 Conclusions

- The derivation of a hierarchic sequence of models for laminated strips was outlined and their performance was demonstrated on the basis of the degree to which the equilibrium equations are satisfied. The powers of the parameter  $\beta$ , representing the degree to which the equilibrium equations are satisfied, have been used to identify members of the hierarchic sequence.
- The proper choice of a model from the hierarchic sequence for a particular application is problem dependent, that is, depends on the exact solution of the corresponding three-dimensional problem, the goals of computation, the degree of precision required, and the method by which the data of interest are computed. In general, the solution of the problem of elasticity in the smooth interior regions is very close to the solution corresponding to the lowest member of the hierarchy, whereas the solution near the boundaries is more complicated and thus requires the use of higher models.
- In the interest of computational efficiency, the hierarchic sequence of models has been extended downward to include the models characterized by  $\beta^0$  and  $\beta^1$ . This requires a modification of material properties, which is analogous to the generally accepted modification of material properties used in the Reissner-Mindlin model for homogeneous isotropic plates. In fact, the model characterized by  $\beta^0$  is the Reissner-Mindlin model, generalized for laminated composites, when the modified material properties are used. In the special



case, when the shear modulus is independent of  $y$ , the hierarchic model is the Reissner-Mindlin model. The shear correction factor can be assigned arbitrarily since the requirements set for hierarchic models are satisfied independently of the shear correction factor.

- The hierarchic framework described in Chapter 2 for laminated strips, and illustrated by examples in this Chapter, allows the development of reliable predictive capabilities for the structural and strength responses of structural components made of laminated composites. The more general case of laminated plates is addressed in the two following chapters.

## Chapter 4

### Laminated Plates

This Chapter describes the formulation of hierarchic models for laminated plates. As in the case of the laminated strip, this formulation is based on one parameter ( $\beta$ ) which characterizes the hierarchic sequence of models, and a set of constants whose influence have been assessed by a numerical sensitivity study. This approach has been adopted in order to limit the rate of increase of fields such that the number of fields added per model is always three.

The analysis is restricted to mid-plane symmetric laminated plates, i.e., when there is a lamina above the geometrical mid-plane at the same distance from the mid-plane and having identical orientation and properties for each lamina below the mid-plane. For such a symmetrical stacking sequence there is no coupling between membrane and bending terms. However, the normal stress-twist curvature coupling terms increase the complexity of the analysis by a significant measure when compared with the laminated strip evaluated in the previous chapters.

Numerical examples analyzed with the proposed sequence of models show good correlation with the reference solutions. Results were obtained for square and rectangular plates with uniform loading and with homogeneous boundary conditions. Cross-ply and angle-ply laminates were evaluated and the results compared with those of MSC/PROBE.

#### 4.1 Models for Laminated Plates

Consider an infinite flat plate of constant thickness  $h$  composed of thin layers of orthotropic elastic material perfectly bonded together. Each layer (lamina) possesses a plane of elastic symmetry parallel to the  $x - y$  plane. The laminae are symmetrically arranged with respect to the middle surface of the plate (i.e., the  $x - y$  plane). The load  $q(x, y)$  is antisymmetric with respect to the middle plane, and  $q(x, y) = 0$  for  $|x| \geq a$ ,  $|y| \geq b$ , with  $a$  and  $b$  some fixed numbers. Let  $\alpha = 1/a$  and  $\gamma = 1/b$ , and further let:

$$\beta = \min(\alpha, \gamma) \quad (4.1)$$

Based on the arguments outlined in Section 2.1, we write the displacement field in the following form:

$$\mathcal{U}_x(x, y, z) = \phi(\beta, z) e^{i\beta(mx+y)} \quad (4.2)$$

$$\mathcal{U}_y(x, y, z) = \psi(\beta, z) e^{i\beta(mx+y)} \quad (4.3)$$

$$\mathcal{U}_z(x, y, z) = \rho(\beta, z) e^{i\beta(mx+y)} \quad (4.4)$$

where  $\mathcal{U}_x, \mathcal{U}_y, \mathcal{U}_z$ , are complex functions, and both the real and imaginary parts represent admissible displacements, and  $\phi, \psi, \rho$  are the partial Fourier transformations of the displacement components  $u_x, u_y, u_z$ :

$$\phi(\beta, z) = \phi_a(\beta, z) + i \phi_b(\beta, z) \quad (4.5)$$

$$\psi(\beta, z) = \psi_a(\beta, z) + i \psi_b(\beta, z) \quad (4.6)$$

$$\rho(\beta, z) = \rho_a(\beta, z) + i \rho_b(\beta, z) \quad (4.7)$$

where  $\phi_a, \phi_b, \psi_a, \psi_b$  are antisymmetric real functions, and  $\rho_a$  and  $\rho_b$  are symmetric real functions with respect to the middle surface of the plate (laminate). The parameter  $m$  is included to assess the influence of the  $x$ - and  $y$ -directions in the solution corresponding to the transverse (or  $z$ ) direction.

The strain components in the transformed variables corresponding to the displacement field given by (4.2), (4.3) and (4.4) are:

$$\hat{\epsilon}_x = \frac{\partial \mathcal{U}_x}{\partial x} = i \beta m \phi e^{i \beta (mx+y)} \quad (4.8)$$

$$\hat{\epsilon}_y = \frac{\partial \mathcal{U}_y}{\partial y} = i \beta \psi e^{i \beta (mx+y)} \quad (4.9)$$

$$\hat{\epsilon}_z = \frac{\partial \mathcal{U}_z}{\partial z} = \rho' e^{i \beta (mx+y)} \quad (4.10)$$

$$\hat{\gamma}_{xy} = \frac{\partial \mathcal{U}_x}{\partial y} + \frac{\partial \mathcal{U}_y}{\partial x} = i \beta (\phi + m \psi) e^{i \beta (mx+y)} \quad (4.11)$$

$$\hat{\gamma}_{xz} = \frac{\partial \mathcal{U}_x}{\partial z} + \frac{\partial \mathcal{U}_z}{\partial x} = (\phi' + i \beta m \rho) e^{i \beta (mx+y)} \quad (4.12)$$

$$\hat{\gamma}_{yz} = \frac{\partial \mathcal{U}_y}{\partial z} + \frac{\partial \mathcal{U}_z}{\partial y} = (\psi' + i \beta \rho) e^{i \beta (mx+y)} \quad (4.13)$$

where the primes represent differentiation with respect to  $z$ .

Let  $\bar{x}$ ,  $\bar{y}$  be the material (lamina) coordinates for any layer rotated an angle  $\theta$  with respect to the global (laminate) coordinate system  $(x, y, z)$  about the  $z$ -axis. The stresses and strains in the rotated system can be written in terms of the global quantities as:

$$\{\bar{\sigma}\} = [T] \{\sigma\}, \quad \{\bar{\epsilon}\} = [T] \{\epsilon\} \quad (4.14)$$

and the stress-strain relations for each lamina in the local system are:

$$\{\bar{\sigma}\} = [C] \{\bar{\epsilon}\} \quad (4.15)$$

where  $[C]$  is the lamina material stiffness matrix in the lamina coordinate system  $(\bar{x}, \bar{y}, z)$  which contains only nine nonzero terms because there are three mutually perpendicular planes of elastic symmetry:

$$[C] = \begin{bmatrix} C_{11} & C_{12} & C_{13} & 0 & 0 & 0 \\ & C_{22} & C_{23} & 0 & 0 & 0 \\ & & C_{33} & 0 & 0 & 0 \\ \text{sym.} & & & C_{44} & 0 & 0 \\ & & & & C_{55} & 0 \\ & & & & & C_{66} \end{bmatrix} \quad (4.16)$$

and  $[T]$  is the transformation matrix:

$$[T] = \begin{bmatrix} m^2 & n^2 & 0 & 0 & 0 & 2mn \\ n^2 & m^2 & 0 & 0 & 0 & -2mn \\ 0 & 0 & 1 & 0 & 0 & 0 \\ 0 & 0 & 0 & m & -n & 0 \\ 0 & 0 & 0 & n & m & 0 \\ -mn & mn & 0 & 0 & 0 & m^2 - n^2 \end{bmatrix} \quad (4.17)$$

where  $m = \cos \theta$ ,  $n = \sin \theta$ . Combining (4.14) and (4.15) the stress-strain relations in the laminate coordinate system for any layer can be written as:

$$\{\sigma\} = [T]^{-1} [C] [T] \{\epsilon\}. \quad (4.18)$$

Defining

$$[Q] = [T]^{-1} [C] [T] \quad (4.19)$$

as the transformed lamina material matrix, equation (4.18) can be written as:

$$\begin{Bmatrix} \sigma_x \\ \sigma_y \\ \sigma_z \\ \tau_{yz} \\ \tau_{xz} \\ \tau_{xy} \end{Bmatrix} = \begin{bmatrix} Q_{11} & Q_{12} & Q_{13} & 0 & 0 & Q_{16} \\ & Q_{22} & Q_{23} & 0 & 0 & Q_{26} \\ & & Q_{33} & 0 & 0 & Q_{36} \\ & \text{sym.} & & Q_{44} & Q_{45} & 0 \\ & & & & Q_{55} & 0 \\ & & & & & Q_{66} \end{bmatrix} \begin{Bmatrix} \epsilon_x \\ \epsilon_y \\ \epsilon_z \\ \gamma_{yz} \\ \gamma_{xz} \\ \gamma_{xy} \end{Bmatrix}. \quad (4.20)$$

Note that  $[Q]$  has thirteen stiffness constants in the global system because there is only one plane of elastic symmetry (the one perpendicular to the  $z$ -axis).

The equilibrium equations with zero body force components are given by:

$$\frac{\partial \sigma_x}{\partial x} + \frac{\partial \tau_{xy}}{\partial y} + \frac{\partial \tau_{zx}}{\partial z} = 0 \quad (4.21)$$

$$\frac{\partial \tau_{xy}}{\partial x} + \frac{\partial \sigma_y}{\partial y} + \frac{\partial \tau_{yz}}{\partial z} = 0 \quad (4.22)$$

$$\frac{\partial \tau_{zx}}{\partial x} + \frac{\partial \tau_{yz}}{\partial y} + \frac{\partial \sigma_z}{\partial z} = 0. \quad (4.23)$$

Substituting equations (4.8) to (4.13) and (4.20) into (4.21) to (4.23) the following Fourier transformed form of the equilibrium equations are obtained:

$$\begin{aligned} & \{-\beta^2[(m^2 Q_{11} + 2m Q_{16} + Q_{66})\phi + (m^2 Q_{16} + m(Q_{12} + Q_{66}) + Q_{26})\psi] + \\ & i\beta[(m Q_{13} + Q_{36})\rho' + (Q_{45}\rho)' + (m Q_{55}\rho)'] + \\ & (Q_{45}\psi' + Q_{55}\phi')'\}e^{i\beta(mx+y)} = 0 \end{aligned} \quad (4.24)$$

$$\begin{aligned} & \{-\beta^2[(m^2 Q_{16} + m(Q_{12} + Q_{66}) + Q_{26})\phi + (Q_{22} + 2m Q_{26} + m^2 Q_{66})\psi] + \\ & i\beta[(Q_{23} + m Q_{36})\rho' + (Q_{44}\rho)' + (m Q_{45}\rho)'] + \\ & (Q_{44}\psi' + Q_{45}\phi')'\}e^{i\beta(mx+y)} = 0 \end{aligned} \quad (4.25)$$

$$\begin{aligned} & \{-\beta^2[(Q_{44} + 2m Q_{45} + m^2 Q_{55})\rho] + \\ & i\beta[(Q_{44} + m Q_{45})\psi' + (Q_{45} + m Q_{55})\phi' + ((m Q_{13} + Q_{36})\phi)' + \\ & ((Q_{23} + m Q_{36})\psi)'] + (Q_{33}\rho')'\}e^{i\beta(mx+y)} = 0. \end{aligned} \quad (4.26)$$

Expanding  $\phi(\beta, z)$ ,  $\psi(\beta, z)$  and  $\rho(\beta, z)$  into a power series with respect to  $\beta$ :

$$\phi(\beta, z) = [\phi_{a0}(z) + i\phi_{b0}(z)] + \beta[\phi_{a1}(z) + i\phi_{b1}(z)] + \beta^2[\phi_{a2}(z) + i\phi_{b2}(z)] + \dots \quad (4.27)$$

$$\psi(\beta, z) = [\psi_{a0}(z) + i\psi_{b0}(z)] + \beta[\psi_{a1}(z) + i\psi_{b1}(z)] + \beta^2[\psi_{a2}(z) + i\psi_{b2}(z)] + \dots \quad (4.28)$$

$$\rho(\beta, z) = [\rho_{a0}(z) + i\rho_{b0}(z)] + \beta[\rho_{a1}(z) + i\rho_{b1}(z)] + \beta^2[\rho_{a2}(z) + i\rho_{b2}(z)] + \dots \quad (4.29)$$

On substituting (4.27), (4.28), (4.29) into the equilibrium equations (4.24), (4.25), (4.26) and separating into real and imaginary parts we have:

The real part of (4.24):

$$\begin{aligned}
& (Q_{45}\psi'_{a0} + Q_{55}\phi'_{a0})' + \beta[(Q_{45}\psi'_{a1} + Q_{55}\phi'_{a1})' - (mQ_{13} + Q_{36})\rho'_{b0} - \\
& \quad ((Q_{45} + mQ_{55})\rho_{b0})'] + \\
& + \beta^2[(Q_{45}\psi'_{a2} + Q_{55}\phi'_{a2})' - (mQ_{13} + Q_{36})\rho'_{b1} - \\
& \quad ((Q_{45} + mQ_{55})\rho_{b1})' - (m^2Q_{11} + 2mQ_{16} + Q_{66})\phi_{a0} - \\
& \quad (m^2Q_{16} + m(Q_{12} + Q_{66}) + Q_{26})\psi_{a0}] + \dots = 0 \quad (4.30)
\end{aligned}$$

The real part of (4.25):

$$\begin{aligned}
& (Q_{44}\psi'_{a0} + Q_{45}\phi'_{a0})' + \beta[(Q_{44}\psi'_{a1} + Q_{45}\phi'_{a1})' - (Q_{23} + mQ_{36})\rho'_{b0} - \\
& \quad ((Q_{44} + mQ_{45})\rho_{b0})'] + \\
& + \beta^2[(Q_{44}\psi'_{a2} + Q_{45}\phi'_{a2})' - (Q_{23} + mQ_{36})\rho'_{b1} - \\
& \quad ((Q_{44} + mQ_{45})\rho_{b1})' - (m^2Q_{16} + m(Q_{12} + Q_{66}) + \\
& \quad Q_{26})\phi_{a0} - (Q_{22} + 2mQ_{26} + m^2Q_{66})\psi_{a0}] + \dots = 0 \quad (4.31)
\end{aligned}$$

The real part of (4.26):

$$\begin{aligned}
& (Q_{33}\rho'_{a0})' + \beta[(Q_{33}\rho'_{a1})' - (Q_{44} + mQ_{45})\psi'_{b0} - (Q_{45} + mQ_{55})\phi'_{b0} - \\
& \quad ((mQ_{13} + Q_{36})\phi_{b0})' - ((Q_{23} + mQ_{36})\psi_{b0})'] + \\
& + \beta^2[(Q_{33}\rho'_{a2})' - (Q_{44} + mQ_{45})\psi'_{b1} - (Q_{45} + mQ_{55})\phi'_{b1} -
\end{aligned}$$



$$\begin{aligned}
& ((m Q_{13} + Q_{36})\phi_{b1})' - ((Q_{23} + m Q_{36})\psi_{b1})' - \\
& (Q_{44} + 2 m Q_{45} + m^2 Q_{55})\rho_{a0}] + \dots = 0.
\end{aligned} \tag{4.32}$$

The imaginary part of (4.24):

$$\begin{aligned}
& (Q_{45}\psi'_{b0} + Q_{55}\phi'_{b0})' + \beta[(Q_{45}\psi'_{b1} + Q_{55}\phi'_{b1})' + (m Q_{13} + Q_{36})\rho'_{a0} + \\
& ((Q_{45} + m Q_{55})\rho_{a0})'] + \\
& + \beta^2[(Q_{45}\psi'_{b2} + Q_{55}\phi'_{b2})' + (m Q_{13} + Q_{36})\rho'_{a1} + \\
& ((Q_{45} + m Q_{55})\rho_{a1})' - (m^2 Q_{11} + 2 m Q_{16} + Q_{66})\phi_{b0} - \\
& (m^2 Q_{16} + m(Q_{12} + Q_{66}) + Q_{26})\psi_{b0}] + \dots = 0 \tag{4.33}
\end{aligned}$$

The imaginary part of (4.25):

$$\begin{aligned}
& (Q_{44}\psi'_{b0} + Q_{45}\phi'_{b0})' + \beta[(Q_{44}\psi'_{b1} + Q_{45}\phi'_{b1})' + (Q_{23} + m Q_{36})\rho'_{a0} + \\
& ((Q_{44} + m Q_{45})\rho_{a0})'] + \\
& + \beta^2[(Q_{44}\psi'_{b2} + Q_{45}\phi'_{b2})' + (Q_{23} + m Q_{36})\rho'_{a1} + \\
& ((Q_{44} + m Q_{45})\rho_{a1})' - (m^2 Q_{16} + m(Q_{12} + Q_{66}) \\
& + Q_{26})\phi_{b0} - (Q_{22} + 2 m Q_{26} + m^2 Q_{66})\psi_{b0}] + \dots = 0 \\
\end{aligned} \tag{4.34}$$

The imaginary part of (4.26):

$$\begin{aligned}
& (Q_{33}\rho'_{b0})' + \beta[(Q_{33}\rho'_{b1})' + (Q_{44} + m Q_{45})\psi'_{a0} + (Q_{45} + m Q_{55})\phi'_{a0} + \\
& ((m Q_{13} + Q_{36})\phi_{a0})' + ((Q_{23} + m Q_{36})\psi_{a0})'] +
\end{aligned}$$

$$\begin{aligned}
& + \beta^2 [(Q_{33}\rho'_{b2})' + (Q_{44} + m Q_{45})\psi'_{a1} + (Q_{45} + m Q_{55})\phi'_{a1} + \\
& ((m Q_{13} + Q_{36})\phi_{a1})' + ((Q_{23} + m Q_{36})\psi_{a1})' - \\
& (Q_{44} + 2 m Q_{45} + m^2 Q_{55})\rho_{b0}] + \dots = 0.
\end{aligned} \tag{4.35}$$

These equations hold for any choice of  $\beta$ . Solving for each power of  $\beta$  we obtain the transverse shape functions as described in the following Sections.

#### 4.1.1 The Model Characterized by $\beta^0$

Setting  $\beta = 0$  in equations (4.30) to (4.35) we have for the real parts of the equilibrium equations:

$$(Q_{45}\psi'_{a0} + Q_{55}\phi'_{a0})' = 0 \tag{4.36}$$

$$(Q_{44}\psi'_{a0} + Q_{45}\phi'_{a0})' = 0 \tag{4.37}$$

$$(Q_{33}\rho'_{a0})' = 0. \tag{4.38}$$

The solution of the above system requires six arbitrary constants. Knowing that  $\phi_{a0}(z)$ ,  $\psi_{a0}(z)$  are antisymmetric and  $\rho_{a0}(z)$  is symmetric, the number of arbitrary constants reduces to three. Integrating, we have:

$$\phi_{a0}(z) = a_0 \int_0^z \frac{Q_{44}}{Q_{44}Q_{55} - Q_{45}^2} dz - b_0 \int_0^z \frac{Q_{45}}{Q_{44}Q_{55} - Q_{45}^2} dz \tag{4.39}$$

$$\psi_{a0}(z) = b_0 \int_0^z \frac{Q_{55}}{Q_{44}Q_{55} - Q_{45}^2} dz - a_0 \int_0^z \frac{Q_{45}}{Q_{44}Q_{55} - Q_{45}^2} dz \tag{4.40}$$

$$\rho_{a0}(z) = c_0 \tag{4.41}$$

which can be written as:

$$\phi_{a0}(z) = a_0 F_A(z) + b_0 K_A(z) \tag{4.42}$$

$$\psi_{a0}(z) = b_0 G_A(z) + a_0 K_A(z) \quad (4.43)$$

$$\rho_{a0}(z) = c_0. \quad (4.44)$$

Similarly, solving the imaginary part of the equilibrium equations, we get:

$$\phi_{a0}(z) = d_0 F_A(z) + e_0 K_A(z) \quad (4.45)$$

$$\psi_{a0}(z) = e_0 G_A(z) + d_0 K_A(z) \quad (4.46)$$

$$\rho_{a0}(z) = f_0 \quad (4.47)$$

where

$$F_A(z) = \int_0^z \frac{Q_{44}}{Q_{44}Q_{55} - Q_{45}^2} dz \quad (4.48)$$

$$G_A(z) = \int_0^z \frac{Q_{55}}{Q_{44}Q_{55} - Q_{45}^2} dz \quad (4.49)$$

$$K_A(z) = - \int_0^z \frac{Q_{45}}{Q_{44}Q_{55} - Q_{45}^2} dz. \quad (4.50)$$

The real and imaginary parts are not linearly independent, hence both lead to the same functional form. The mode of deformation corresponding to  $\beta = 0$  can therefore be written in the following form:

$$u_x(x, y, z) = \hat{u}_1(x, y) F_A(z) + \hat{u}_2(x, y) K_A(z) \quad (4.51)$$

$$u_y(x, y, z) = \hat{u}_3(x, y) G_A(z) + \hat{u}_4(x, y) K_A(z) \quad (4.52)$$

$$u_z(x, y, z) = \hat{u}_5(x, y). \quad (4.53)$$

This mode of deformation contains five fields,  $\hat{u}_1(x, y)$ ,  $\hat{u}_2(x, y)$ ,  $\dots$ ,  $\hat{u}_5(x, y)$ , which are all real. To reduce the number of fields we impose additional constraints to

reflect the correlation existing between the integration constants  $a_0$ ,  $b_0$  or  $d_0$ ,  $e_0$  in (4.42), (4.43) and (4.45), (4.46). That is:

$$\hat{u}_2(x, y) = n \hat{u}_1(x, y), \quad \hat{u}_3(x, y) = n \hat{u}_4(x, y) \quad (4.54)$$

where  $n$  is an arbitrary constant. The displacement field (4.51)-(4.53), can be now written in the following way:

$$u_x(x, y, z) = \hat{u}_1(x, y) [F_A(z) + n K_A(z)] \quad (4.55)$$

$$u_y(x, y, z) = \hat{u}_4(x, y) [n G_A(z) + K_A(z)] \quad (4.56)$$

$$u_z(x, y, z) = \hat{u}_5(x, y) \quad (4.57)$$

which can be rewritten as:

$$u_x(x, y, z) = u_1(x, y) F_0(z, n) \quad (4.58)$$

$$u_y(x, y, z) = u_2(x, y) G_0(z, n) \quad (4.59)$$

$$u_z(x, y, z) = u_3(x, y) \quad (4.60)$$

where

$$F_0(z, n) = F_A(z) + n K_A(z) = \int_0^z \frac{Q_{44} - n Q_{45}}{Q_{44} Q_{55} - Q_{45}^2} dz \quad (4.61)$$

$$G_0(z, n) = n G_A(z) + K_A(z) = \int_0^z \frac{n Q_{55} - Q_{45}}{Q_{44} Q_{55} - Q_{45}^2} dz. \quad (4.62)$$

Note that this model does not depend on the value of the constant  $m$ ; only depends on the constant  $n$ . The influence of these and other constants in the solution of laminated plates is addressed in the next Section.

When  $Q_{44}$ ,  $Q_{45}$ ,  $Q_{55}$  are constant through the thickness, this model is capable of representing rigid body displacement and rotation. A similar situation was realized for the  $\beta^0$  laminated strip model in Section 2.1.1. Unless the material properties are modified as discussed later, this model does not satisfies the condition of converging to the same limit as the problem of elasticity as  $h \rightarrow 0$ .

#### 4.1.2 The Model Characterized by $\beta^1$

To find the mode of deformation for the model which satisfies the equilibrium equations up to the first power of  $\beta$ , we differentiate (4.30) to (4.35) with respect to  $\beta$  and let  $\beta = 0$ . In this case we have for the real parts:

$$(Q_{45}\psi'_{a1} + Q_{55}\phi'_{a1})' - (mQ_{13} + Q_{36})\rho'_{b0} - ((Q_{45} + mQ_{55})\rho_{b0})' = 0 \quad (4.63)$$

$$(Q_{44}\psi'_{a1} + Q_{45}\phi'_{a1})' - (Q_{23} + mQ_{36})\rho'_{b0} - ((Q_{44} + mQ_{45})\rho_{b0})' = 0 \quad (4.64)$$

$$\begin{aligned} (Q_{33}\rho'_{a1})' - (Q_{44} + mQ_{45})\psi'_{b0} - (Q_{45} + mQ_{55})\phi'_{b0} - \\ ((mQ_{13} + Q_{36})\phi_{b0})' - ((Q_{23} + mQ_{36})\psi_{b0})' = 0. \end{aligned} \quad (4.65)$$

Upon integration, we have:

$$\phi_{a1}(z) = a_1 F_A(z) + b_1 K_A(z) + m z \quad (4.66)$$

$$\psi_{a1}(z) = b_1 G_A(z) + a_1 K_A(z) + z \quad (4.67)$$

$$\rho_{a1}(z) = c_1 + d_0 H_A(z, m) + e_0 H_B(z, m). \quad (4.68)$$

Similarly, solving the imaginary part of the equilibrium equations, we get:

$$\phi_{b1}(z) = d_1 F_A(z) + e_1 K_A(z) - m z \quad (4.69)$$

$$\psi_{b1}(z) = e_1 G_A(z) + d_1 K_A(z) - z \quad (4.70)$$

$$\rho_{b1}(z) = -f_1 - a_0 H_A(z, m) - b_0 H_B(z, m) \quad (4.71)$$

where  $F_A(z)$ ,  $G_A(z)$ ,  $K_A(z)$  are defined in (4.48), (4.49), (4.50) and  $H_A(z, m)$ ,  $H_B(z, m)$  are given by:

$$H_A(z, m) = \int_0^z \frac{m z + (m Q_{13} + Q_{36}) F_A(z) + (Q_{23} + m Q_{36}) K_A(z)}{Q_{33}} dz \quad (4.72)$$

$$H_B(z, m) = \int_0^z \frac{z + (m Q_{13} + Q_{36}) K_A(z) + (Q_{23} + m Q_{36}) G_A(z)}{Q_{33}} dz. \quad (4.73)$$

The mode of deformation corresponding to the  $\beta^1$  model can be written in the following form:

$$u_x(x, y, z) = \hat{u}_1(x, y) F_A(z) + \hat{u}_2(x, y) K_A(z) + \hat{u}_3(x, y) z \quad (4.74)$$

$$u_y(x, y, z) = \hat{u}_4(x, y) G_A(z) + \hat{u}_5(x, y) K_A(z) + \hat{u}_6(x, y) z \quad (4.75)$$

$$u_z(x, y, z) = \hat{u}_7(x, y) + \hat{u}_8(x, y) H_A(z, m) + \hat{u}_9(x, y) H_B(z, m). \quad (4.76)$$

This mode of deformation now contains nine fields,  $\hat{u}_1(x, y)$ ,  $\hat{u}_2(x, y)$ ,  $\dots$ ,  $\hat{u}_9(x, y)$ .

Again, to reduce the number of fields we impose additional constraints as in the case of the  $\beta^0$  model:

$$\hat{u}_2(x, y) = n \hat{u}_1(x, y), \quad \hat{u}_4(x, y) = n \hat{u}_5(x, y), \quad \hat{u}_9(x, y) = s \hat{u}_8(x, y) \quad (4.77)$$

where  $n, s$  are arbitrary constants. The displacement field (4.74)-(4.76), can now be written in the following way:

$$u_x(x, y, z) = \hat{u}_1(x, y) [F_A(z) + n K_A(z)] + \hat{u}_3(x, y) z \quad (4.78)$$

$$u_y(x, y, z) = \hat{u}_5(x, y) [n G_A(z) + K_A(z)] + \hat{u}_6(x, y) z \quad (4.79)$$

$$u_z(x, y, z) = \hat{u}_7(x, y) + \hat{u}_8(x, y) [H_A(z, m) + s H_B(z, m)] \quad (4.80)$$

which can be rewritten as:

$$u_x(x, y, z) = u_1(x, y) F_0(z, n) + u_4(x, y) z \quad (4.81)$$

$$u_y(x, y, z) = u_2(x, y) G_0(z, n) + u_5(x, y) z \quad (4.82)$$

$$u_z(x, y, z) = u_3(x, y) + u_6(x, y) H_0(z, m, s) \quad (4.83)$$

where  $F_0(z, n)$ ,  $G_0(z, n)$  are defined in (4.61), (4.62), and  $H_0(z, m, s)$  is given by:

$$\begin{aligned} H_0(z, m, s) &= H_A(z, m) + s H_B(z, m) \\ &= \int_0^z \frac{(m+s)z + (mQ_{13} + Q_{36})F_0(z, s) + (Q_{23} + mQ_{36})G_0(z, s)}{Q_{33}} dz. \end{aligned} \quad (4.84)$$

This mode of deformation, which satisfies the equilibrium equations up the first power of  $\beta$ , depends on three parameters  $m, n, s$ , and has a total of nine fields (three more fields than the  $\beta^0$  model).

#### 4.1.3 The Model Characterized by $\beta^2$

To find the mode of deformation for the model which satisfies the equilibrium equations up to the second power of  $\beta$ , we differentiate (4.30) to (4.35) twice with respect to  $\beta$  and let  $\beta = 0$ . Upon integration of the resulting differential equations,

we have for the real part:

$$\phi_{a2}(z) = c_1 F_A(z) + c_2 K_A(z) + m z + a_0 F_B(z, m) + b_0 F_C(z, m) \quad (4.85)$$

$$\psi_{a2}(z) = c_2 G_A(z) + c_1 K_A(z) + z + a_0 G_B(z, m) + b_0 G_C(z, m) \quad (4.86)$$

$$\rho_{a2}(z) = f_2 + a_1 H_A(z, m) + b_1 H_B(z, m) + H_1(z, m) \quad (4.87)$$

where

$$F_B(z, m) = \int_0^z \left( \frac{M_A(z, m) Q_{44} - M_B(z, m) Q_{45}}{Q_{44} Q_{55} - Q_{45}^2} - m H_A(z, m) \right) dz \quad (4.88)$$

$$F_C(z, m) = \int_0^z \left( \frac{N_A(z, m) Q_{44} - N_B(z, m) Q_{45}}{Q_{44} Q_{55} - Q_{45}^2} - m H_B(z, m) \right) dz \quad (4.89)$$

$$G_B(z, m) = \int_0^z \left( \frac{M_B(z, m) Q_{55} - M_A(z, m) Q_{45}}{Q_{44} Q_{55} - Q_{45}^2} - H_A(z, m) \right) dz \quad (4.90)$$

$$G_C(z, m) = \int_0^z \left( \frac{N_B(z, m) Q_{55} - N_A(z, m) Q_{45}}{Q_{44} Q_{55} - Q_{45}^2} - H_B(z, m) \right) dz \quad (4.91)$$

$$H_1(z, m) = \int_0^z \frac{(m^2 Q_{13} + 2 m Q_{36} + Q_{23})}{Q_{33}} z dz \quad (4.92)$$

and

$$\begin{aligned} M_A(z, m) = & \int_0^z \left[ \left( Q_{11} + 2 m Q_{16} + m^2 Q_{66} - (m Q_{13} + Q_{36}) \frac{m Q_{13} + Q_{36}}{Q_{33}} \right) F_A(z) \right. \\ & + \left( Q_{26} + m(Q_{12} + Q_{66}) + m^2 Q_{16} - (Q_{23} + m Q_{36}) \frac{m Q_{13} + Q_{36}}{Q_{33}} \right) K_A(z) \\ & \left. - \frac{m Q_{13} + Q_{36}}{Q_{33}} m z \right] dz \end{aligned} \quad (4.93)$$

$$\begin{aligned} M_B(z, m) = & \int_0^z \left[ \left( Q_{26} + m(Q_{12} + Q_{66}) + m^2 Q_{16} - (m Q_{13} + Q_{36}) \frac{Q_{23} + m Q_{36}}{Q_{33}} \right) F_A(z) \right. \\ & + \left( Q_{22} + 2 m Q_{26} + m^2 Q_{66} - (Q_{23} + m Q_{36}) \frac{Q_{23} + m Q_{36}}{Q_{33}} \right) K_A(z) \\ & \left. - \frac{Q_{23} + m Q_{36}}{Q_{33}} m z \right] dz \end{aligned} \quad (4.94)$$

$$\begin{aligned} N_A(z, m) = & \int_0^z \left[ \left( Q_{26} + m(Q_{12} + Q_{66}) + m^2 Q_{16} - (m Q_{13} + Q_{36}) \frac{Q_{23} + m Q_{36}}{Q_{33}} \right) G_A(z) \right. \\ & + \left( Q_{11} + 2 m Q_{16} + m^2 Q_{66} - (m Q_{13} + Q_{36}) \frac{m Q_{13} + Q_{36}}{Q_{33}} \right) K_A(z) \\ & \left. - \frac{Q_{13} + m Q_{36}}{Q_{33}} z \right] dz \end{aligned} \quad (4.95)$$



$$\begin{aligned}
N_B(z, m) = \int_0^z & \left[ \left( Q_{22} + 2mQ_{26} + m^2Q_{66} - (Q_{23} + mQ_{36}) \frac{Q_{23} + mQ_{36}}{Q_{33}} \right) G_A(z) \right. \\
& + \left( Q_{26} + m(Q_{12} + Q_{66}) + m^2Q_{16} - (mQ_{13} + Q_{36}) \frac{Q_{23} + mQ_{36}}{Q_{33}} \right) K_A(z) \\
& \left. - \frac{Q_{23} + mQ_{36}}{Q_{33}} z \right] dz
\end{aligned} \tag{4.96}$$

The mode of deformation corresponding to the  $\beta^2$  model can be written in the following form:

$$\begin{aligned}
u_x(x, y, z) = & \hat{u}_1(x, y) F_A(z) + \hat{u}_2(x, y) K_A(z) + \hat{u}_3(x, y) z + \\
& \hat{u}_4(x, y) F_B(z, m) + \hat{u}_5(x, y) F_C(z, m)
\end{aligned} \tag{4.97}$$

$$\begin{aligned}
u_y(x, y, z) = & \hat{u}_6(x, y) G_A(z) + \hat{u}_7(x, y) K_A(z) + \hat{u}_8(x, y) z + \\
& \hat{u}_9(x, y) G_B(z, m) + \hat{u}_{10}(x, y) G_C(z, m)
\end{aligned} \tag{4.98}$$

$$\begin{aligned}
u_z(x, y, z) = & \hat{u}_{11}(x, y) + \hat{u}_{12}(x, y) H_A(z, m) + \hat{u}_{13}(x, y) H_B(z, m) + \\
& \hat{u}_{14} H_1(z, m).
\end{aligned} \tag{4.99}$$

This mode of deformation now contains fourteen fields:  $\hat{u}_1(x, y), \dots, \hat{u}_{14}(x, y)$ . Again, to reduce the number of fields we impose additional constraints as in the cases of the  $\beta^0$  and  $\beta^1$  models:

$$\hat{u}_2(x, y) = n \hat{u}_1(x, y), \quad \hat{u}_6(x, y) = n \hat{u}_7(x, y) \tag{4.100}$$

$$\hat{u}_5(x, y) = t \hat{u}_4(x, y), \quad \hat{u}_{10}(x, y) = t \hat{u}_9(x, y) \tag{4.101}$$

$$\hat{u}_{13}(x, y) = s \hat{u}_{12}(x, y) \tag{4.102}$$

where  $n, s, t$  are arbitrary constants. The displacement field (4.97)-(4.99), can be written in the following way:

$$u_x(x, y, z) = \hat{u}_1(x, y) [F_A(z) + n K_A(z)] + \hat{u}_3(x, y) z +$$

$$\hat{u}_4(x, y) [F_B(z, m) + t F_C(z, m)] \quad (4.103)$$

$$\begin{aligned} u_y(x, y, z) &= \hat{u}_7(x, y) [n G_A(z) + K_A(z)] + \hat{u}_8(x, y) z + \\ &\quad \hat{u}_9(x, y) [G_B(z, m) + t G_C(z, m)] \end{aligned} \quad (4.104)$$

$$\begin{aligned} u_z(x, y, z) &= \hat{u}_{11}(x, y) + \hat{u}_{12}(x, y) [H_A(z, m) + s H_B(z, m)] + \\ &\quad \hat{u}_{14} H_1(z, m) \end{aligned} \quad (4.105)$$

which can be rewritten as:

$$u_x(x, y, z) = u_1(x, y) F_0(z, n) + u_4(x, y) z + u_7(x, y) F_1(z, m, t) \quad (4.106)$$

$$u_y(x, y, z) = u_2(x, y) G_0(z, n) + u_5(x, y) z + u_8(x, y) G_1(z, m, t) \quad (4.107)$$

$$u_z(x, y, z) = u_3(x, y) + u_6(x, y) H_0(z, m, s) + u_9(x, y) H_1(z, m) \quad (4.108)$$

where  $F_0$ ,  $G_0$ ,  $H_0$ ,  $H_1$  have been previously defined, and

$$\begin{aligned} F_1(z, m, t) &= F_B(z, m) + t F_C(z, m) \\ &= \int_0^z \left( \frac{M_0(z, m, t) Q_{44} - N_0(z, m, t) Q_{45}}{Q_{44} Q_{55} - Q_{45}^2} - m H_0(z, m, t) \right) dz \end{aligned} \quad (4.109)$$

$$\begin{aligned} G_1(z, m, t) &= G_B(z, m) + t G_C(z, m) \\ &= \int_0^z \left( \frac{N_0(z, m, t) Q_{55} - M_0(z, m, t) Q_{45}}{Q_{44} Q_{55} - Q_{45}^2} - H_0(z, m, t) \right) dz \end{aligned} \quad (4.110)$$

and

$$\begin{aligned} M_0(z, m, t) &= M_A(z, m) + t N_A(z, m) \\ &= \int_0^z \left[ \left( Q_{11} + 2m Q_{16} + m^2 Q_{66} - (m Q_{13} + Q_{36}) \frac{m Q_{13} + Q_{36}}{Q_{33}} \right) F_0(z, t) \right. \\ &\quad \left. + \left( Q_{26} + m(Q_{12} + Q_{66}) + m^2 Q_{26} - (Q_{23} + m Q_{36}) \frac{m Q_{13} + Q_{36}}{Q_{33}} \right) G_0(z, t) \right. \\ &\quad \left. - (m + t) \frac{m Q_{13} + Q_{36}}{Q_{33}} z \right] dz \end{aligned} \quad (4.111)$$

$$\begin{aligned}
N_0(z, m, t) = & M_B(z, m) + t N_B(z, m) \\
& \int_0^z \left[ \left( Q_{26} + m(Q_{12} + Q_{66}) + m^2 Q_{16} - (m Q_{13} + Q_{36}) \frac{Q_{23} + m Q_{36}}{Q_{33}} \right) F_0(z, t) \right. \\
& + \left( Q_{22} + 2 m Q_{26} + m^2 Q_{66} - (Q_{23} + m Q_{36}) \frac{Q_{23} + m Q_{36}}{Q_{33}} \right) G_0(z, t) \\
& \left. - (m + t) \frac{Q_{23} + m Q_{36}}{Q_{33}} z \right] dz. \tag{4.112}
\end{aligned}$$

This mode of deformation satisfies the equilibrium equations up to the second power of  $\beta$ , and comprises nine fields and four parameters  $m$ ,  $n$ ,  $s$  and  $t$ . By continuing this process, the equilibrium equations can be satisfied to an arbitrary power of  $\beta$ .

## 4.2 The Limiting Case with Respect to $\beta \rightarrow 0$

One of the definitive properties of a hierarchic sequence of models is that each member converges to the same limit as the exact solution of the corresponding three-dimensional problem as  $h \rightarrow 0$ . The exact solution minimizes the potential energy with respect to all functions  $u_i(x, y)$ ,  $i = 1, 2, \dots$  for which the strain energy is finite. The limit for each plate model is obtained in a similar way as done for the laminated strip. The process can be summarized as follows:

1. Start with the expression of the potential energy for the plate:

$$\begin{aligned}
\Pi = & \frac{1}{2} \int_{-\infty}^{+\infty} \int_{-\infty}^{+\infty} \int_{-h/2}^{+h/2} \left( \sigma_x \epsilon_x + \sigma_y \epsilon_y + \sigma_z \epsilon_z + \tau_{xy} \gamma_{xy} + \tau_{xz} \gamma_{xz} \right. \\
& \left. + \tau_{yz} \gamma_{yz} \right) dx dy dz = \int_{-\infty}^{+\infty} \int_{-\infty}^{+\infty} q(x, y) u_z(x, y, h/2) dx dy. \tag{4.113}
\end{aligned}$$

For a given plate model the strain components are computed from the corresponding displacement expressions, the strains and stresses are written in terms of the displacements and its derivatives, and integrated through the thickness ( $z$ -direction) to obtain the material coefficients. These coefficients form the laminate material stiffness matrix  $[E]$ . Rewriting the potential energy in terms of  $[E]$ :

$$\Pi = \frac{1}{2} \iint_{\Omega} ([D]\{u\})^T [E] [D] \{u\} dx dy - \iint_{\Omega} q(x, y) u_z(x, y, h/2) dx dy \quad (4.114)$$

where  $[D]$  is the differential operator matrix relating the strains and displacements, and  $\{u\}$  denotes the displacement vector function. In the case of the  $\beta^0$  model, the potential energy expression is:

$$\begin{aligned} \Pi = & \frac{1}{2} \int_{-\infty}^{+\infty} \int_{-\infty}^{+\infty} \left[ E_1 \left( \frac{\partial u_1}{\partial x} \right)^2 + 2 E_2 \frac{\partial u_1}{\partial x} \frac{\partial u_2}{\partial x} + E_3 \left( \frac{\partial u_2}{\partial x} \right)^2 + E_4 \left( \frac{\partial u_1}{\partial y} \right)^2 + \right. \\ & 2 E_5 \frac{\partial u_1}{\partial y} \frac{\partial u_2}{\partial y} + E_6 \left( \frac{\partial u_2}{\partial y} \right)^2 + E_7 \left( \frac{\partial u_3}{\partial x} \right)^2 + 2 E_8 \frac{\partial u_3}{\partial x} \frac{\partial u_3}{\partial y} + E_9 \left( \frac{\partial u_3}{\partial y} \right)^2 + \\ & E_{10} u_1^2 + 2 E_{11} u_1 u_2 + E_{12} u_2^2 + 2 E_{13} \frac{\partial u_1}{\partial x} \frac{\partial u_1}{\partial y} + 2 E_{14} \frac{\partial u_1}{\partial x} \frac{\partial u_2}{\partial y} + \\ & 2 E_{15} \frac{\partial u_2}{\partial x} \frac{\partial u_1}{\partial y} + 2 E_{16} \frac{\partial u_2}{\partial x} \frac{\partial u_2}{\partial y} + 2 E_{17} u_1 \frac{\partial u_3}{\partial x} + 2 E_{18} u_2 \frac{\partial u_3}{\partial x} + \\ & \left. 2 E_{19} u_1 \frac{\partial u_3}{\partial y} + 2 E_{20} u_2 \frac{\partial u_3}{\partial y} \right] dx dy - \\ & \int_{-\infty}^{+\infty} \int_{-\infty}^{+\infty} q(x, y) u_3(x, y, h/2) dx dy \end{aligned} \quad (4.115)$$

where:

$$E_1 = \int_{-h/2}^{+h/2} Q_{11} F_0^2 dz, \quad E_2 = \int_{-h/2}^{+h/2} Q_{16} F_0 G_0 dz \quad (4.116)$$

$$E_3 = \int_{-h/2}^{+h/2} Q_{66} G_0^2 dz, \quad E_4 = \int_{-h/2}^{+h/2} Q_{66} F_0^2 dz \quad (4.117)$$

$$E_5 = \int_{-h/2}^{+h/2} Q_{26} F_0 G_0 dz, \quad E_6 = \int_{-h/2}^{+h/2} Q_{22} G_0^2 dz \quad (4.118)$$

$$E_7 = \int_{-h/2}^{+h/2} Q_{55} dz, \quad E_8 = \int_{-h/2}^{+h/2} Q_{45} dz \quad (4.119)$$

$$E_9 = \int_{-h/2}^{+h/2} Q_{44} dz, \quad E_{10} = \int_{-h/2}^{+h/2} Q_{55} (F'_0)^2 dz \quad (4.120)$$

$$E_{11} = \int_{-h/2}^{+h/2} Q_{45} F'_0 G'_0 dz, \quad E_{12} = \int_{-h/2}^{+h/2} Q_{44} (G'_0)^2 dz \quad (4.121)$$

$$E_{13} = \int_{-h/2}^{+h/2} Q_{16} F_0^2 dz, \quad E_{14} = \int_{-h/2}^{+h/2} Q_{12} F_0 G_0 dz \quad (4.122)$$

$$E_{15} = \int_{-h/2}^{+h/2} Q_{66} F_0 G_0 dz, \quad E_{16} = \int_{-h/2}^{+h/2} Q_{26} G_0^2 dz \quad (4.123)$$

$$E_{17} = \int_{-h/2}^{+h/2} Q_{55} F'_0 dz, \quad E_{18} = \int_{-h/2}^{+h/2} Q_{45} G'_0 dz \quad (4.124)$$

$$E_{19} = \int_{-h/2}^{+h/2} Q_{45} F'_0 dz, \quad E_{20} = \int_{-h/2}^{+h/2} Q_{44} G'_0 dz. \quad (4.125)$$

For the  $\beta^1$  model, there are 55 nonzero terms in the laminate material stiffness matrix and 138 nonzero terms in the case of the  $\beta^2$  model.

2. The Euler equations are obtained by taking the variation of the potential energy with respect to each of the field functions  $u_i(x, y)$ , ( $i = 1, 2, \dots, n_f$ ),  $n_f$  being the total number of fields in the model.

$$\delta \Pi(u_i) = \frac{\partial \Pi}{\partial u_i} \delta u_i + \frac{\partial \Pi}{\partial u_{i,x}} \delta u_{i,x} + \frac{\partial \Pi}{\partial u_{i,y}} \delta u_{i,y} = 0 \quad (4.126)$$

where

$$u_{i,x} = \frac{\partial u_i}{\partial x}, \quad u_{i,y} = \frac{\partial u_i}{\partial y}. \quad (4.127)$$

Using Fourier transform, the Euler equations are transformed and the system of linear equations in the transformed field variables  $U_i(\xi, \eta)$  is constructed:

$$[A] \{U\} = \{R\}. \quad (4.128)$$

The matrix  $[A]$  depends on the material stiffness matrix  $[E]$ , and on the Fourier variables  $\xi$  and  $\eta$ , and  $\{R\}$  is the load vector obtained from the transformation of the potential of the external forces.

3. The elements of  $[E]$  are computed for different stacking sequences and the system of equations are solved for  $U_3$ . Note that  $u_3(x, y)$  is the equivalent to the displacement component  $u_{y|0}(x)$  in the laminated strip, which was shown to be the dominant function.

$$D(\xi, \eta) U_3 = B(\xi, \eta) Q \quad (4.129)$$

where

$$\begin{aligned} D(\xi, \eta) = & D_1 \xi^2 + D_2 \xi \eta + D_3 \eta^2 + D_4 \xi^4 + D_5 \xi^3 \eta + \\ & D_6 \xi^2 \eta^2 + D_7 \xi \eta^3 + D_8 \eta^4 + \dots \end{aligned} \quad (4.130)$$

is the determinant of  $[A]$ ,

$$B(\xi, \eta) = B_0 + B_1 \xi^2 + B_2 \xi \eta + B_3 \eta^2 + \dots \quad (4.131)$$

is the determinant of  $[A]$  when the third row is replaced by the load vector  $\{R\}$ , and  $Q(\xi, \eta)$  is the Fourier transform of  $q(x, y)$ .

4. The limit analysis with respect to  $h \rightarrow 0$  is performed and the following coefficients are defined:

$$\alpha_j = \frac{D_i}{B_0} \quad \text{for } i = 1 \rightarrow 3, j = 1 \rightarrow 3 \quad (4.132)$$

$$\lambda_j = \frac{D_i}{B_0} \quad \text{for } i = 4 \rightarrow 8, j = 1 \rightarrow 5. \quad (4.133)$$

Note that  $B_0$  is the first non-zero term of  $B(\xi, \eta)$  and does not depend on  $\xi$  and  $\eta$ . Neglecting derivatives of higher than fourth order, we obtain the general equation:

$$(\alpha_1 \xi^2 + \alpha_2 \xi \eta + \alpha_3 \eta^2) U_3 + (\lambda_1 \xi^4 + \lambda_2 \xi^3 \eta + \lambda_3 \xi^2 \eta^2 + \lambda_4 \xi \eta^3 + \lambda_5 \eta^4) U_3 = Q. \quad (4.134)$$

Denoting  $w(x, y) = u_3(x, y)$ , equation (4.134) has the following form after performing the inverse Fourier transform:

$$\left( \alpha_1 \frac{\partial^2 w}{\partial x^2} + \alpha_2 \frac{\partial^2 w}{\partial x \partial y} + \alpha_3 \frac{\partial^2 w}{\partial y^2} \right) + \left( \lambda_1 \frac{\partial^4 w}{\partial x^4} + \lambda_2 \frac{\partial^4 w}{\partial x^3 \partial y} + \lambda_3 \frac{\partial^4 w}{\partial x^2 \partial y^2} + \lambda_4 \frac{\partial^4 w}{\partial x \partial y^3} + \lambda_5 \frac{\partial^4 w}{\partial y^4} \right) = q. \quad (4.135)$$

where  $\alpha_1, \alpha_2, \alpha_3$  and  $\lambda_1, \lambda_2, \dots, \lambda_5$  depend only on the material coefficients  $E_i$  defined before.

If the hierarchic plate model being evaluated converges to the proper limit, then the coefficients  $\alpha_i$  must be zero. This is because all models must converge to the solution of the problem of elasticity as  $h \rightarrow 0$ . It has been shown [1] that the Kirchhoff model is the limiting case for the infinite strip of isotropic material with respect to  $h \rightarrow 0$ . For the laminated strip (Chapter 3), which is a special case of the laminated plate, the limit analysis showed that the governing differential equation contains only fourth order derivatives. Therefore, unless the coefficients  $\alpha_i$  are zero, the governing equation would be a second order partial differential equation.

When  $\alpha_i$  ( $i = 1, 2, 3$ ) are not zero then the material properties have to be adjusted. The coefficients  $\lambda_i$  may require adjustment also, so that they will have

the same values as those models that converge to the same limit as the theory of elasticity with respect to  $h \rightarrow 0$ .

Following this procedure, and using the symbolic manipulation program Mathematica<sup>1</sup>, it was found that the model characterized by  $\beta^0$  is not a member of the hierarchy because  $\alpha_i \neq 0$ . However, making the transverse shear moduli constant through the thickness, as it was done in the case of the strip,  $\alpha_i$  become zero.

In the case of the strip, closed form solutions could be obtained and the governing differential equations determined in terms of the material coefficients. Because of the complexity of the problem in the case of the plates, it was impossible to determine the coefficients  $\alpha_i$  and  $\lambda_i$  for all hierarchic models and for representative stacking sequences, by other than numerical methods. The following approach have been adopted: The results obtained for the laminated plate were tested numerically for the following stacking sequences which are representative of practical problems:

1. Three-ply laminate:  $90/0/90$ ,  $h=1$ ,
2. Three-ply laminate:  $-45/+45/-45$ ,  $h=1$ ,
3. Three-ply laminate:  $-30/+30/-30$ ,  $h=1$ ,
4. Five-ply laminate:  $0/90/0/90/0$ ,  $h=1$ .

For each stacking sequence the values of the  $[E]$  matrix were computed, and the resulting system of equations are solved for  $w(x, y)$ .

---

<sup>1</sup>Mathematica: A system for doing mathematics by computer. Wolfram Research Inc. (Version 1.2, July 1990)



The model characterized by  $\beta^0$  required two modifications of material properties: One to satisfy the requirement that the  $\alpha_i = 0$ , the other to satisfy the requirement of having the same values of  $\lambda_i$  as the other members of the hierarchy. The  $\beta^1$  and  $\beta^2$  models did not require any modification of the material properties to satisfy either requirement.

From experience acquired with the laminated strip, it was expected that by making the transverse shear moduli constant through the thickness, the coefficients  $\alpha_i$  would become zero. As in the case of the strip, the transverse shear moduli  $Q_{44}$  and  $Q_{55}$  of each layer were made equal to the harmonic averages  $\hat{Q}_{44}$  and  $\hat{Q}_{55}$ :

$$\hat{Q}_{44} = \left( \frac{2}{h} \int_0^{h/2} \frac{1}{Q_{44}(z)} dz \right)^{-1} \quad (4.136)$$

$$\hat{Q}_{55} = \left( \frac{2}{h} \int_0^{h/2} \frac{1}{Q_{55}(z)} dz \right)^{-1} \quad (4.137)$$

while  $Q_{45}$  was made equal to the average  $\bar{Q}_{45}$ :

$$\bar{Q}_{45} = \frac{2}{h} \int_0^{h/2} Q_{45}(z) dz. \quad (4.138)$$

The other modification in the material properties needed for adjusting the values of  $\lambda_i$  in (4.135), such that they are the same as the other models, was obtained from the condition that plane stress constitutive relations are used for each layer  $(k)$ . To accomplish that, the following modifications are sufficient:

$$\tilde{Q}_{ij}^{(k)} = Q_{ij}^{(k)} - \frac{Q_{i3}^{(k)} Q_{j3}^{(k)}}{Q_{33}^{(k)}}, \quad i, j = 1, 2, 6 \quad (4.139)$$

where the  $Q_{ij}^{(k)}$  are the material properties of the  $k$ th layer in the laminate coordinate system. These modifications in the material properties are equivalent to those used

for laminated strip models. The modification of the transverse shear moduli is the counterpart of  $E_6$  constant in the laminated strip, while the modification in the in-plane moduli is the counterpart of substituting  $E_1$  by  $E_1 - E_2^2/E_3$  in the  $\beta^0$  model for the laminated strip (see Chapter 2).

The results of the numerical study are shown in Table 4.1 for the three hierarchic models. Two sets of values are presented for the  $\beta^0$  model: One for the case in which the modifications in the material properties discussed above are implemented ( $\beta_m^0$ ); and the other for the case in which the modification in the shear moduli are included but not in the in-plane moduli ( $\beta_s^0$ ).

These results indicate that the  $\beta^0$  model, without modifications to account for the plane stress conditions in the constitutive equations ( $\beta_s^0$ ), would converge to a different limit as  $h \rightarrow 0$ . When the full set of modifications are introduced ( $\beta_m^0$ ), the values of the coefficients  $\lambda_i$  are almost identical to those of the higher order models. The differences observed in the values of  $\lambda_i$  for the  $\beta_m^0$  and  $\beta^1$  models are very small and vary depending on the stacking sequence. The largest difference (0.28%) occurs for the stacking sequence 3, in the coefficient  $\lambda_4$ . For the other stacking sequences, the differences are below 0.01%. The largest difference between the coefficients of the  $\beta^1$  and  $\beta^2$  models (0.01%), occurs in the coefficients  $\lambda_1$  and  $\lambda_4$  for stacking sequence 2, while for the other stacking sequences the difference is below 0.005%.

Table 4.1: Values of the Coefficients  $\lambda_i$  in [in-lb] for Four Stacking Sequences

MODEL	STACKING SEQUENCE	$\lambda_1$	$\lambda_2$	$\lambda_3$	$\lambda_4$	$\lambda_5$
$\beta_s^0$	90/0/90 $h = 1$	163634	0	222595	0	2022943
$\beta_m^0$		157802	0	208438	0	2014295
$\beta^1$		157816	0	208415	0	2014304
$\beta^2$		157810	0	208421	0	2014303
$\beta_s^0$	-45/+45/-45 $h = 1$	602293	1859309	3153926	1852309	602293
$\beta_m^0$		595134	1859309	3153926	1859309	595134
$\beta^1$		595200	1856500	3154000	1856500	595200
$\beta^2$		595139	1856472	3153957	1856472	595139
$\beta_s^0$	-30/+30/-30 $h = 1$	1227055	2397643	2432075	822774	223028
$\beta_m^0$		1219115	2397643	2417554	822774	216609
$\beta^1$		1219140	2395101	2417636	820488	216629
$\beta^2$		1219119	2395059	2417578	820450	216613
$\beta_s^0$	0/90/0/90/0 $h = 1$	1679640	0	222595	0	506937
$\beta_m^0$		1671512	0	208438	0	500585
$\beta^1$		1671564	0	208331	0	500639
$\beta^2$		1671565	0	208332	0	500638

These results demonstrate that for the representative cases investigated, all the models converge to the same limit as  $h \rightarrow 0$ , provided that the material properties of the  $\beta^0$  model are adjusted as discussed herein.

One important observation from this numerical study is concerned with the classical plate model for laminated plates. The differential equation for mid-plane symmetric laminated plates with the assumption of plane stress conditions and that normals to the middle surface of the plate prior to deformation remain straight and normals after deformation (classical plate model assumptions) is given by [35]:

$$D_{11} \frac{\partial^4 w}{\partial x^4} + 4 D_{16} \frac{\partial^4 w}{\partial x^3 \partial y} + (2 D_{12} + 4 D_{66}) \frac{\partial^4 w}{\partial x^2 \partial y^2} + 4 D_{26} \frac{\partial^4 w}{\partial x \partial y^3} + D_{22} \frac{\partial^4 w}{\partial y^4} = q \quad (4.140)$$

where:

$$D_{ij} = \int_{-h/2}^{+h/2} Q_{ij} z^2 dz. \quad (4.141)$$

The coefficients  $D_{ij}$  are equivalent to  $E_i$ . In the case of the  $\beta^0$  model, for instance, the transverse shear moduli are made constant through the thickness and they can be factored out from the expressions of  $E_i$ . In that case the following relations exist:

$$D_{11} \equiv E_1 \equiv \lambda_1, \quad D_{22} \equiv E_6 \equiv \lambda_5 \quad (4.142)$$

$$4 D_{16} \equiv 4 E_2 \equiv \lambda_2, \quad 4 D_{26} \equiv 4 E_5 \equiv \lambda_4 \quad (4.143)$$

$$2 D_{12} + 4 D_{66} \equiv 2 E_{14} + 4 E_4 \equiv \lambda_3 \quad (4.144)$$

Therefore, there is a reasonable expectation that equation (4.140) is the limiting case of the corresponding problem of elasticity provided the plane stress constitutive

equations are used. When the three-dimensional constitutive equations were used, the values of the coefficients  $\lambda_i$  are those given in Table 4.1 for the case  $\beta_3^0$  and the proper limiting case is not obtained.

### 4.3 Sensitivity Study

The influence of the parameters introduced in each member of the hierarchic sequence of models is evaluated numerically in this Section. The unknown displacement components  $u_i(x, y)$ ,  $i = 1, 2, \dots$ , are solved by means of an experimental program developed for the solution of laminated plates, which is based on the p-version of the finite element method.

Using this program, the examples problems described in Chapter 5 were solved for various combinations of the parameters  $m$ ,  $n$ ,  $s$  and  $t$ . The strain energy of simply supported 3-ply rectangular plates with uniform load was used to assess the influence of the parameters, and the results are presented in Figures 4.1 to 4.8. The material for the laminae is the same material used for the laminated strip problems, with two stacking sequences, 90/0/90 (cross-ply laminate) and  $-45/+45/-45$  (angle-ply laminate). The width to thickness ratio was kept at  $a/h = 4$ , and the aspect ratio of the plate ( $b/a$ ) was either 1 or 3.

The parameter  $n$  in the  $\beta^0$  model (see equations (4.58)-(4.60)) has no influence on the solution. This is because  $n$  is absorbed in the unknown functions  $u_1(x, y)$

and  $u_2(x, y)$  computed in the finite element solution when the transverse shear moduli are made constant through the thickness of the plate.

The influence of the parameters  $m$ ,  $n$ ,  $s$  in the solution of a cross-ply laminate corresponding to the  $\beta^1$  model is shown in Figure 4.1 for  $b/a = 1$  and in Figure 4.2 for  $b/a = 3$ . Figure 4.3 summarizes the results for both aspect ratios. In all these figures, the vertical axis shows the strain energy relative to the one obtained solving the same problem with a three-dimensional finite element program (see Chapter 5 for details). The horizontal axis gives the values assigned to the variable parameter of each curve. The results indicate that there is no influence of the parameter  $n$  in the results, while  $m$  and  $s$  have different influence depending on the aspect ratio of the plate. For instance, an increase in  $s$  improves the solution for  $b/a = 1$ , but does the opposite for  $b/a = 3$ . A similar observation applies for the parameter  $m$ , but in the opposite direction. An increase in  $m$  reduces the quality of the solution for  $b/a = 1$ , but improves the solution for  $b/a = 3$ . Figure 4.4 indicates that there is no influence of either one of the parameter in the solution of the cross-ply laminate and for both aspect ratios.

The influence of the parameters  $m$ ,  $n$ ,  $s$ ,  $t$  in the solution of a cross-ply laminate corresponding to the  $\beta^2$  model is shown in Figure 4.5 for  $b/a = 1$  and in Figure 4.6 for  $b/a = 3$ . For  $b/a = 1$  an increase in  $m$  and  $t$  increases the strain energy of the solution, but while varying  $t$  produces a converging situation, the variation of  $m$  conduces to an unbounded increase in the strain energy. For  $b/a = 3$ , increasing

$t$  makes the strain energy to decrease, while increasing the value of  $m$  makes the strain energy of the solution to decrease first (for  $m \leq 4$ ) and to increase after the value of  $m = 4$ . In both cases there is no influence of the parameter  $n$  and almost no influence of  $s$ .

For the angle-ply laminate the results are shown in Figure 4.7. Again, there is no influence of the parameter  $n$  and also no influence of  $s$ . The other two parameters,  $m$  and  $t$ , have different influence depending on the aspect ratio of the plate.

All of the results presented in Figures 4.1 to 4.7 were obtained varying one parameter at the time while the other three remained constant and equal to unity. Figure 4.8 show the sensitivity study performed for the  $\beta^2$  model for twenty seven different combinations of the parameters  $m$ ,  $n$ ,  $s$ ,  $t$  and for a square, cross-ply laminated plate. In this case the strain energy of the solution is presented and a band of  $\pm 3\%$  around the reference solution is indicated. These results are also shown in Table 4.2.

The results consistently indicate that the influence of the parameters included in each model of the hierarchy is relatively small in terms of the strain energy of the solution. Taking all parameters equal unity appears to be the logical choice based on the results of the present sensitivity study.

**Table 4.2:** Sensitivity Study- $\beta^2$  Model. Simply supported 90/0/90 square plate ( $a/h = 4$ ). Influence of  $m, n, s, t$ .

Case No.	$m$	$n$	$s$	$t$	Strain Energy ( $\times 10^5$ )	Case No.	$m$	$n$	$s$	$t$	Strain Energy ( $\times 10^5$ )
1	1	1	1	1	0.7111145	15	5	5	5	5	0.7375296
2	1	5	1	1	0.7111145	16	2	1	1	1	0.7128474
3	5	1	1	1	0.7256553	17	3	1	1	1	0.7158803
4	1	1	5	1	0.7116944	18	4	1	1	1	0.7202610
5	1	1	1	5	0.7207993	19	6	1	1	1	0.7315889
6	5	5	1	1	0.7256553	20	7	1	1	1	0.7376230
7	1	5	5	1	0.7116944	21	8	1	1	1	0.7439399
8	1	5	1	5	0.7207993	22	9	1	1	1	0.7488515
9	1	1	5	5	0.7213676	23	10	1	1	1	0.7537713
10	1	5	1	5	0.7207993	24	1	1	2	1	0.7116491
11	5	1	5	5	0.7375296	25	1	1	7	1	0.7116989
12	5	5	5	1	0.7252634	26	1	1	1	2	0.7165587
13	1	5	5	5	0.7213676	27	1	1	1	7	0.7215842
14	5	5	1	5	0.7379180						



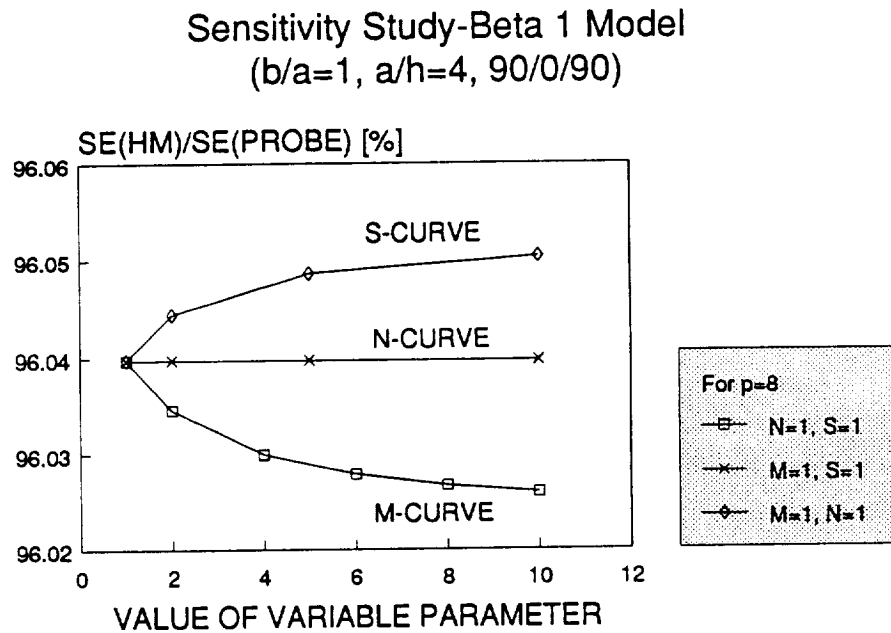


**Figure 4.1:** Cross-ply square plate. Influence of  $m$ ,  $n$ ,  $s$  on the strain energy of the solution.

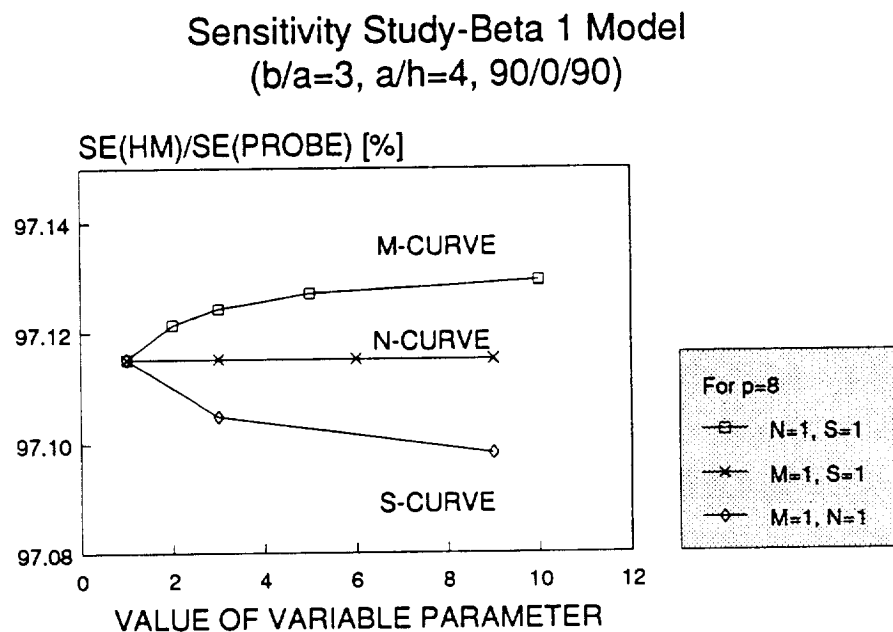


**Figure 4.2:** Cross-ply rectangular plate. Influence of  $m$ ,  $n$ ,  $s$  on the strain energy of the solution.

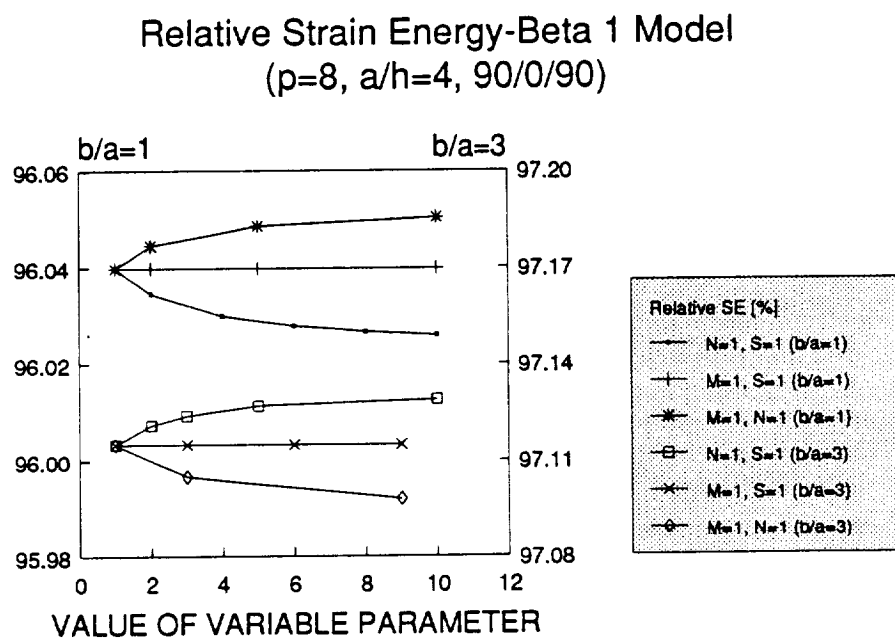


**Figure 4.3:** Cross-ply square and rectangular plate. Influence of  $m$ ,  $n$ ,  $s$  on the strain energy of the solution.

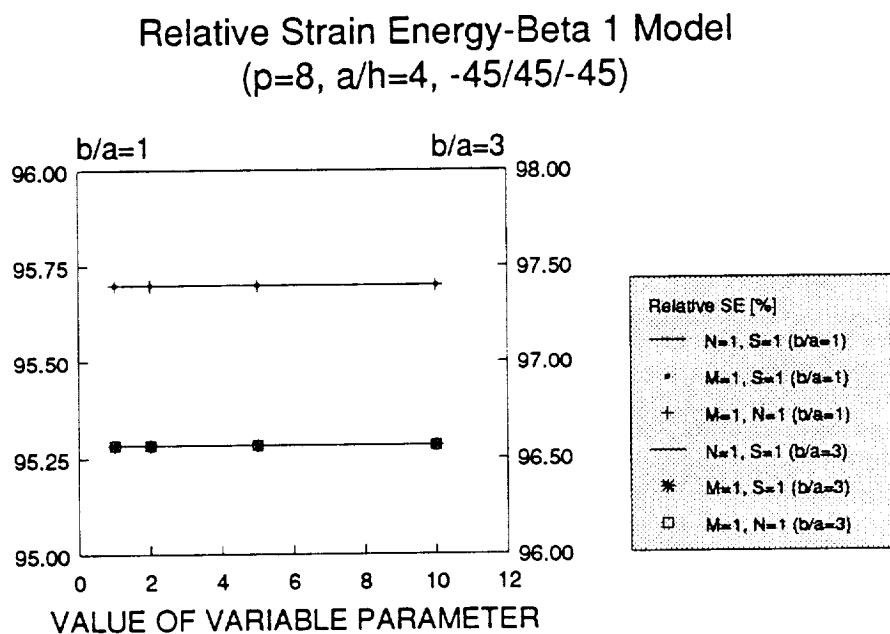


**Figure 4.4:** Angle-ply square and rectangular plate. Influence of  $m$ ,  $n$ ,  $s$  on the strain energy of the solution.

Sensitivity Study-Beta 2 Model  
( $b/a=1$ ,  $a/h=4$ ,  $90/0/90$ )

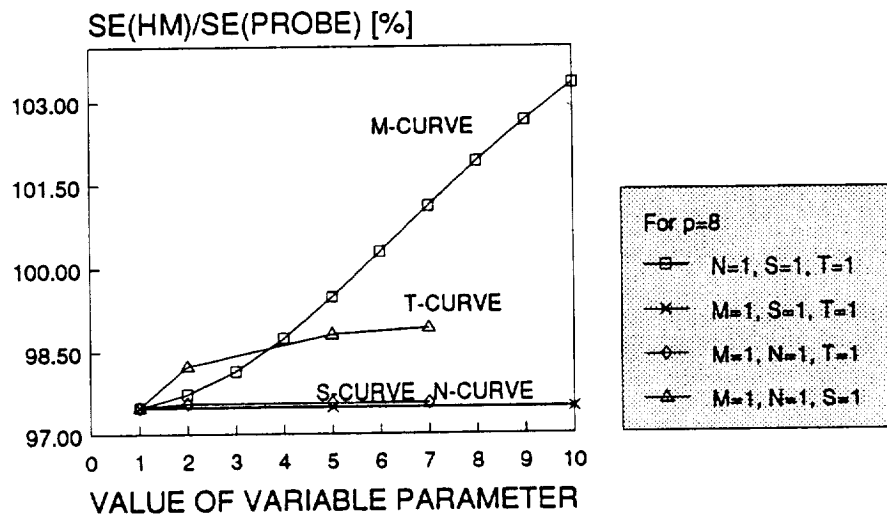


Figure 4.5: Cross-ply square plate. Influence of  $m$ ,  $n$ ,  $s$ ,  $t$  on the strain energy of the solution.

Sensitivity Study-Beta 2 Model  
( $b/a=3$ ,  $a/h=4$ ,  $90/0/90$ )

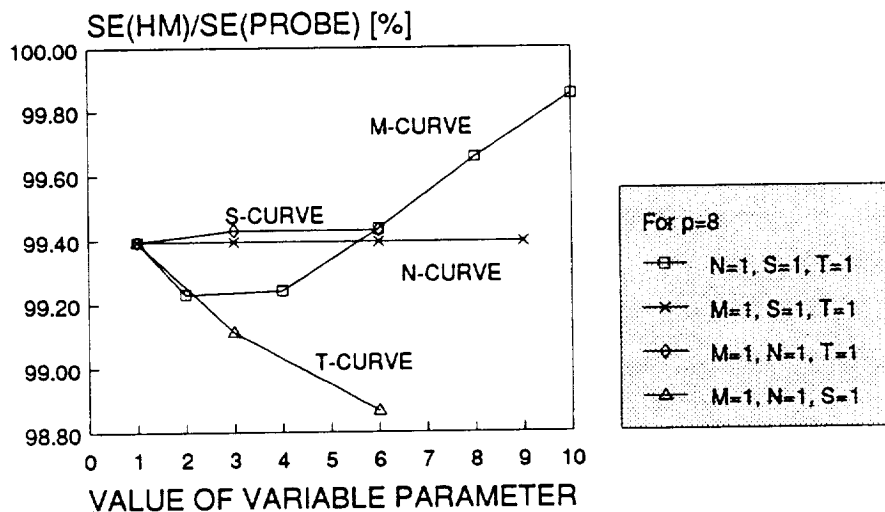
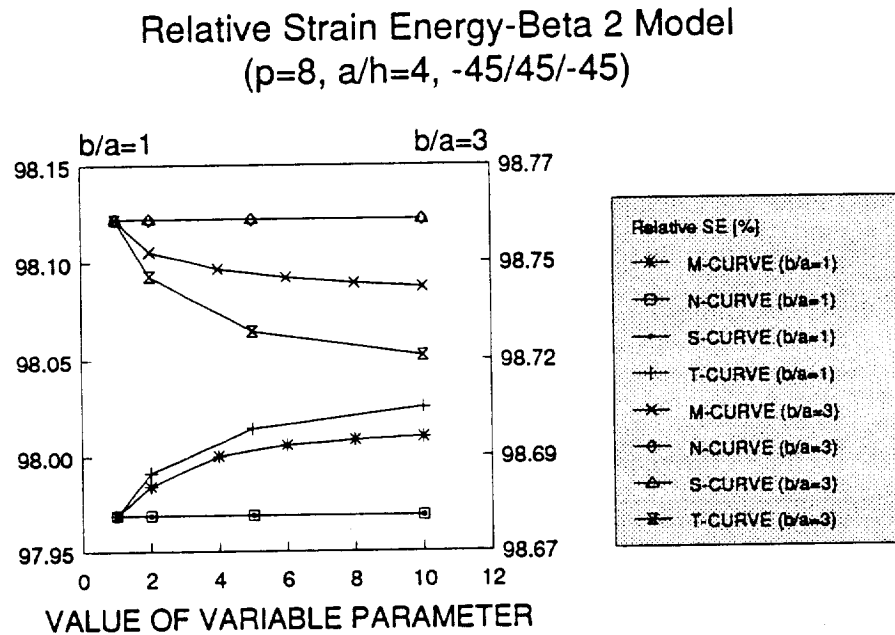
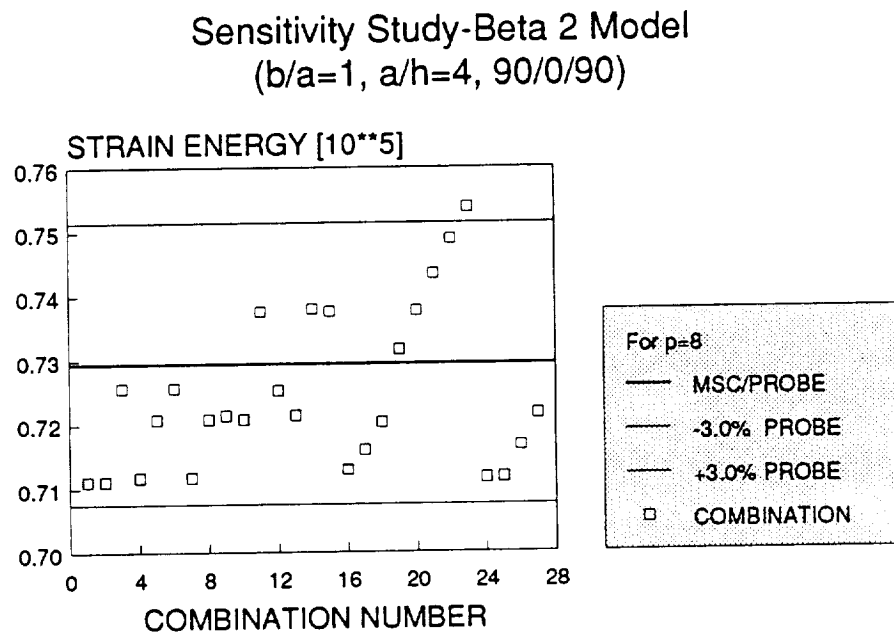


Figure 4.6: Cross-ply rectangular plate. Influence of  $m$ ,  $n$ ,  $s$ ,  $t$  on the strain energy of the solution.



**Figure 4.7:** Angle-ply square and rectangular plate. Influence of  $m$ ,  $n$ ,  $s$ ,  $t$  on the strain energy of the solution.



**Figure 4.8:** Cross-ply square plate. Influence of  $m$ ,  $n$ ,  $s$ ,  $t$  on the strain energy of the solution.

## Chapter 5

### Laminated Plate Examples

Plate models must be evaluated with reference to the corresponding three dimensional problem. Therefore the first task was to establish reliable reference solutions of the model problems, viewed as three-dimensional elasticity problems. The computer code MSC/PROBE was used for this purpose. It is important to remember that we try to assess the errors of modeling, namely to be able to determine how well each member of the hierarchic sequence of models approximates the solution of the three-dimensional elasticity problem.

The quality of each reference solution was controlled by selecting the finite element mesh such that the relative error in energy norm was low; observing the convergence of the functionals of interest and verifying overall equilibrium. In some cases, when the length-to-width ratio of the plate was increased, the estimated error in energy norm also increased. In such cases the reference solution was used only to

compute the transverse displacements. The error in strain energy (and consequently in displacements) is the square of the error in energy norm. If the error in energy norm for a given solution is 10% for instance, the error in the displacements should be about 1%. However, the errors in the derivatives are more sensitive and cannot be used for reference.

Using the finite element method as our solution tool means that we are introducing errors of discretization. If the errors of discretization are large, then it is not possible to assess the errors of modeling.

The cases considered try to cover a wide range of combination of the parameters that have influence on a plate problem. For instance, in a laminated plate it is possible to vary:

- the material properties,
- the number of layers,
- the stacking sequence,
- the thickness of each layer,
- the plate width-to-thickness ratio ( $a/h$ ),
- the plate length-to-width ratio ( $b/a$ ),
- the boundary conditions,
- the type of loading, etc,

which make the number of cases to be analyzed very large, if one wishes to cover all possible combinations. If only three variations of each one of the above parameters were investigated, the total number of combinations would be 512. If for each one of these cases we obtain the reference solution and the solutions for all three members of the hierarchic models described in Chapter 4, the total number of analyses is 2,048. Finally, if for each one of the 2,048 cases, the solution is obtained for p-levels ranging from 1 to 8, the total number of solutions is 16,384.

In the examples analyzed in the following sections several parameters were selected to be constant: The material properties of all layers are the same and only one material is considered; the type of loading is not varied; all layers are of equal thickness and the boundary conditions are homogeneous.

## 5.1 Description of Example Problems

Consider a rectangular plate of uniform thickness  $h$  and planar dimensions  $a$  and  $b$ , composed of perfectly bonded elastic orthotropic layers, symmetrically distributed with respect to the middle plane, (Fig. 5.1). A uniform load  $q(x, y)$  is applied as a normal traction to the top ( $q/2$ ) and bottom ( $q/2$ ) surfaces of the plate, and all layers in the laminate are of equal thickness, and are of a square symmetric unidirectional fibrous composite material possessing the following stiffness properties, which simulate a high-modulus graphite/epoxy composite:

$$E_L = 25.0 \times 10^6 \text{ psi} \quad E_T = 1.0 \times 10^6 \text{ psi}$$

$$G_{LT} = 0.5 \times 10^6 \text{ psi} \quad G_{TT} = 0.2 \times 10^6 \text{ psi}$$

$$\nu_{LT} = \nu_{TT} = 0.25$$

where  $L$  indicates the direction parallel to the fibers,  $T$  is the transverse direction, and  $\nu_{LT}$  is the Poisson ratio (i.e.,  $\nu_{LT} = -\epsilon_{TT}/\epsilon_{LL}$ , where  $\epsilon_{TT}$ ,  $\epsilon_{LL}$  are, respectively, the normal strains in the directions  $T$  and  $L$ ). These material properties were selected from reference [18]. It is important to note, as was pointed out by Pagano in [18], that the highly anisotropic nature of the selected material represent a severe test for any laminated plate model.

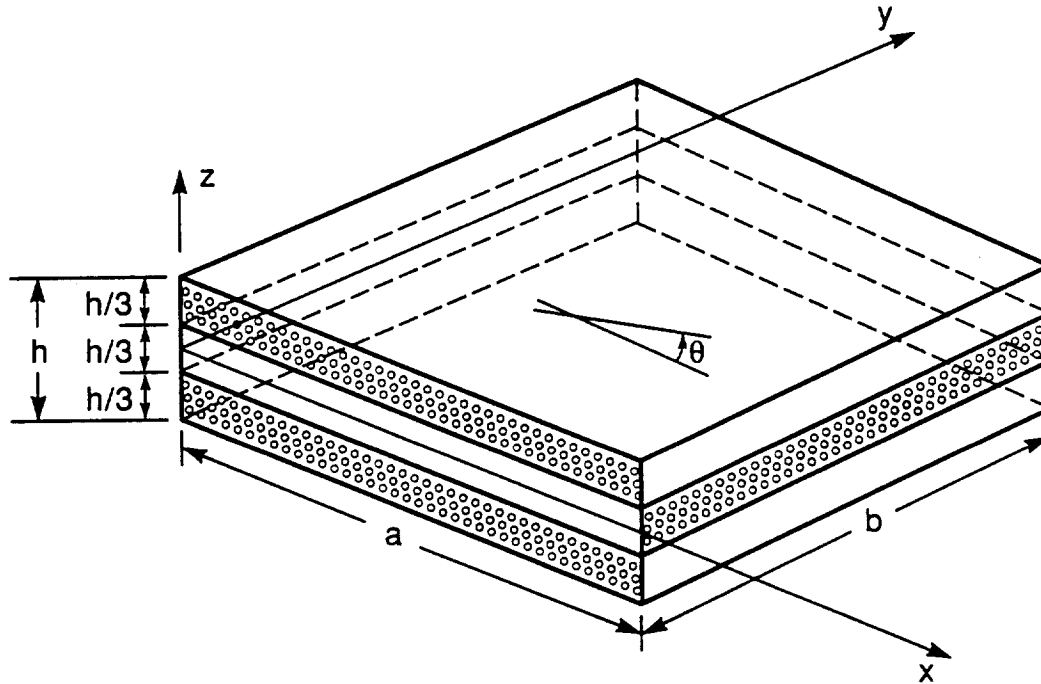


**Figure 5.1:** Model problems: Notation.

When the  $L$  direction coincides with the  $x$  direction, we refer to it as the  $\theta = 0^\circ$  orientation. For a three-ply laminate a designation 90/0/90 means that the central



lamina is oriented with the  $L$  direction parallel to the global  $x$ -axis, and in the two outer layers  $L$  is at  $90^\circ$  with the global  $x$ -axis.

As mentioned earlier, the reference solutions were obtained using the finite element program MSC/PROBE, and the solutions for the plate models were obtained with an experimental program developed during this investigation, in which the algorithm described in Chapter 4 was implemented. In the reference solution obtained with MSC/PROBE each layer was discretized as a three-dimensional element with orthotropic material properties. The solution was obtained for  $p$ -levels ranging from 1 through 8. The solution corresponding to  $p = 8$  will be used as the basis for comparison.

The solutions corresponding to the proposed hierarchic sequence of models were obtained using only one laminated plate element. The polynomial degree was varied from 1 through 8 and the equilibrium equations were satisfied up to the second power of  $\beta$ .

The model that satisfies the equilibrium equations up to the zeroth power of  $\beta$  was modified to satisfy the requirement of converging to the same limit as the problem of elasticity with respect to  $h \rightarrow 0$ , as described in Chapter 4. To accomplish that, the transverse shear moduli  $Q_{44}$  and  $Q_{55}$  of each layer were made equal to the harmonic averages  $\hat{Q}_{44}$  and  $\hat{Q}_{55}$ , while  $Q_{45}$  was made equal to the average  $\bar{Q}_{45}$ . In the case of three layers, for instance, the harmonic averages are:

$$\hat{Q}_{44} = 3 \left( \frac{1}{Q_{44}^{(1)}} + \frac{2}{Q_{44}^{(2)}} \right)^{-1} \quad \hat{Q}_{55} = 3 \left( \frac{1}{Q_{55}^{(1)}} + \frac{2}{Q_{55}^{(2)}} \right)^{-1} \quad (5.1)$$

and the average is:

$$\bar{Q}_{45} = \frac{1}{3} (Q_{45}^{(1)} + 2 Q_{45}^{(2)}) . \quad (5.2)$$

The superscripts (1), (2) refer to the central and outer layer respectively. The following changes were also introduced for each layer ( $k$ ):

$$\tilde{Q}_{ij}^{(k)} = Q_{ij}^{(k)} - \frac{Q_{i3}^{(k)} Q_{j3}^{(k)}}{Q_{33}^{(k)}}, \quad i, j = 1, 2, 6. \quad (5.3)$$

These modifications in the material properties are equivalent to the ones introduced for the laminated strip models. The modification of the transverse shear moduli (5.1), (5.2) is the counterpart of  $E_6$  constant in the laminated strip, while the modification of the in-plane moduli (5.3) is the counterpart of substituting  $E_1$  by  $E_1 - E_2^2/E_3$  in the  $\beta^0$  model for the laminated strip (see Chapter 2).

We will denote the modified model characterized by  $\beta^0$  with  $\beta_m^0$ . No modifications are necessary for the other members of the hierarchy as discussed in Section 4.2. The following normalized quantities are defined to present the results at a given location ( $x_n, y_n, z_n$ ):

$$(\bar{\sigma}_x, \bar{\sigma}_y, \bar{\tau}_{xy}) = \frac{1}{q} (\sigma_x, \sigma_y, \tau_{xy}) \quad (5.4)$$

$$(\bar{\tau}_{zx}, \bar{\tau}_{yz}) = \frac{1}{q} (\tau_{zx}, \tau_{yz}) \quad (5.5)$$

$$(\bar{u}_x, \bar{u}_y) = \frac{E_T h^2}{q a^3} (u_x, u_y) \quad (5.6)$$

$$U_z = \frac{100 E_T h^3 u_z(x_n, y_n, 0)}{q a^4} \quad (5.7)$$

where  $q$  is the applied traction,  $h$  is the thickness of the plate and  $u_z(x_n, y_n, 0)$  is the vertical displacement of the middle plane of the plate at  $x = x_n, y = y_n$ .

Two groups of problems are evaluated in the following Sections:

1. Cross-ply laminate with all four edges simply supported (only the transverse displacement  $u_z$  is set to zero: *soft simple support*) and two aspect ratios ( $b/a = 1$  and  $b/a = 3$ ). The influence of the number of layers and other boundary conditions in the central deflection of square plates were also investigated.
2. Angle-ply laminate with all four edges simply supported, two aspect ratios ( $b/a = 1$  and  $b/a = 3$ ) and two ply orientations ( $-45/+45/-45$  and  $-30/+30/-30$ ). Other ply orientations and boundary conditions were also considered.

For those problems in which the estimated error in energy norm was larger than 5%, only the values of the displacements are reported. In those cases the error of discretization become too large to allow proper assessment of modeling errors in terms of stresses. Table 5.1 shows the estimated errors in energy norm at  $p = 8$  for all cases considered in the following sections. Even though the errors of discretization can be controlled by meshing and by p-extension, limitations of the experimental computer program imposed certain restrictions. The reported values of the estimated error in energy norm are the best that could be obtained with the experimental code. For those cases in which the error in energy norm of the plate models was larger than 5%, and the error of the solution obtained with MSC/PROBE was also large, only the displacements were compared.

Table 5.1: Estimated Relative Error in Energy Norm (%) at  $p = 8$ 

MODEL	a/h	b/a=1	b/a=3	b/a=1	b/a=1	b/a=3
		90/0/90	90/0/90	-45/45/-45	-30/30/-30	-45/45/-45
$\beta^0$	4	0.15	0.34	0.35	0.29	4.73
$\beta^1$		0.58	0.50	2.29	2.30	3.91
$\beta^2$		0.67	0.50	2.57	2.56	3.44
MSC/PROBE		0.40	0.44	3.27	2.84	1.73
$\beta^0$	10	0.35	1.82	2.36	2.77	5.66
$\beta^1$		0.57	2.14	2.28	3.49	5.12
$\beta^2$		0.60	1.94	2.20	3.76	5.15
MSC/PROBE		0.19	1.01	1.94	1.55	3.70
$\beta^0$	20	1.38	3.39	6.80	6.17	6.61
$\beta^1$		1.24	3.32	8.44	7.51	5.50
$\beta^2$		1.16	3.32	8.39	7.49	5.53
MSC/PROBE		0.28	0.67	3.12	2.88	4.59
$\beta^0$	100	1.89	1.49	13.20	14.09	9.15
$\beta^1$		1.97	1.63	10.30	11.39	9.00
$\beta^2$		2.01	1.65	10.15	11.17	8.99
MSC/PROBE		0.08	0.07	15.61	14.03	11.26

## 5.2 Cross-ply Laminate

In this Section the results for cross-ply laminated plates are presented. Two cases were analyzed in detail: A three-ply square ( $b/a = 1$ ) simply supported plate, and a three-ply rectangular ( $b/a = 3$ ) simply supported plate. For these cases the results include deflections, normal and shear stress distributions, and estimated relative error in energy norm for the three hierarchic models and for the reference solution.

Also included is the influence of the number of layers in the end deflection of a square plate with one edge clamped and the other three edges free. Finally, the central deflection of a three- and a five-ply plate with two opposite sides simply supported (soft simple support) are included.

### 5.2.1 Square Plate

The results for a three-ply orthotropic (or cross-ply, 90/0/90) simply supported square plate are shown in Fig. 5.2 to Fig. 5.15 and summarized in Table 5.2. In all cases the results are those corresponding to  $p = 8$ . The load consisted of a uniform normal load  $q(x, y)$  half of which was applied on the top surface, half on the bottom surface of the plate. The support conditions on all edges of the plate are those of a soft simple support, i.e. only the transverse displacement is set to zero on each edge ( $u_z = 0$ ).

Figure 5.16 shows the mesh used for the reference solution of the cross-ply laminate obtained with MSC/PROBE for the length-to-thickness ratio of 10. Due to

symmetry, only one fourth of the plate was considered in the analysis. Small elements were used near the edges of the plate to limit the influence of the singularities coming from the boundaries. The same mesh configuration was used for all  $a/h$  ratios. Figure 5.17 shows the deformed configuration.

Fig. 5.2 shows the central transverse displacement of the plate as a function of the  $a/h$  ratio. For large  $a/h$  ratios all models yield similar results. As  $a/h$  decreases, the  $\beta^0$  model underestimates the deflection while the  $\beta^1$  and  $\beta^2$  models remain very close to the MSC/PROBE solution. A very small difference between the  $\beta^1$  and  $\beta^2$  models is also observed in this case. See also Table 5.2, column  $U_z(a/2, a/2, 0)$ .

The in-plane displacements  $\bar{u}_x(0, a/2, z)$ ,  $\bar{u}_y(a/2, 0, z)$  for two  $a/h$  ratios are shown in Figures 5.3 to 5.6. The solution of the  $\beta^0$  model can only produce linear variation for the in-plane displacements. For  $a/h = 10$  this approximation is close enough, but for  $a/h = 4$  the approximation is very different from the reference solution and the other members of the hierarchy. Note that the  $\beta^1$  model is in excellent agreement with the reference solution, but can only produce piecewise linear approximation. The  $\beta^2$  model on the other hand, gives results that are almost indistinguishable from those of the reference solution.

The normal stress distributions  $\bar{\sigma}_x(a/2, a/2, z)$ ,  $\bar{\sigma}_y(a/2, a/2, z)$  for  $a/h = 4$  and  $a/h = 10$  are shown in Figures 5.7 to 5.10. The  $\beta^0$  model underestimates the maximum normal stress  $\bar{\sigma}_y$  by 40% for  $a/h = 4$  (Fig. 5.9) and 10% for  $a/h = 10$

**Table 5.2:** Normalized Stresses and Displacements for a Simply Supported 90/0/90 Square Plate ( $b/a = 1$ )

MODEL	a/h	$U_z$ (a/2, a/2, 0)	$\bar{\sigma}_x$ (a/2, a/2, h/2)	$\bar{\sigma}_y$ (a/2, a/2, h/2)	$\bar{\tau}_{zx}$ (0, a/2, 0)	$\bar{\tau}_{yz}$ (a/2, 0, 0)
$\beta^0$	4	2.720	1.53	11.05	2.47	2.65
$\beta^1$		3.019	1.87	15.71	2.31	1.88
$\beta^2$		3.051	1.88	17.55	2.26	1.87
MSC/PROBE		3.122	1.90	18.30	2.01	1.87
$\beta^0$	10	1.037	4.98	79.04	4.80	7.24
$\beta^1$		1.149	5.21	86.02	4.60	6.44
$\beta^2$		1.156	5.24	87.67	4.63	6.41
MSC/PROBE		1.172	5.24	88.30	4.31	6.51
$\beta^0$	20	0.764	15.59	324.3	8.93	14.69
$\beta^1$		0.796	14.66	330.3	8.70	14.18
$\beta^2$		0.798	14.67	332.0	8.72	14.13
MSC/PROBE		0.802	14.68	332.8	8.63	14.13
$\beta^0$	100	0.670	351.2	8142	43.29	74.27
$\beta^1$		0.672	309.4	8098	42.77	73.83
$\beta^2$		0.672	309.3	8100	42.28	73.82
MSC/PROBE		0.673	310.4	8105	45.13	74.09

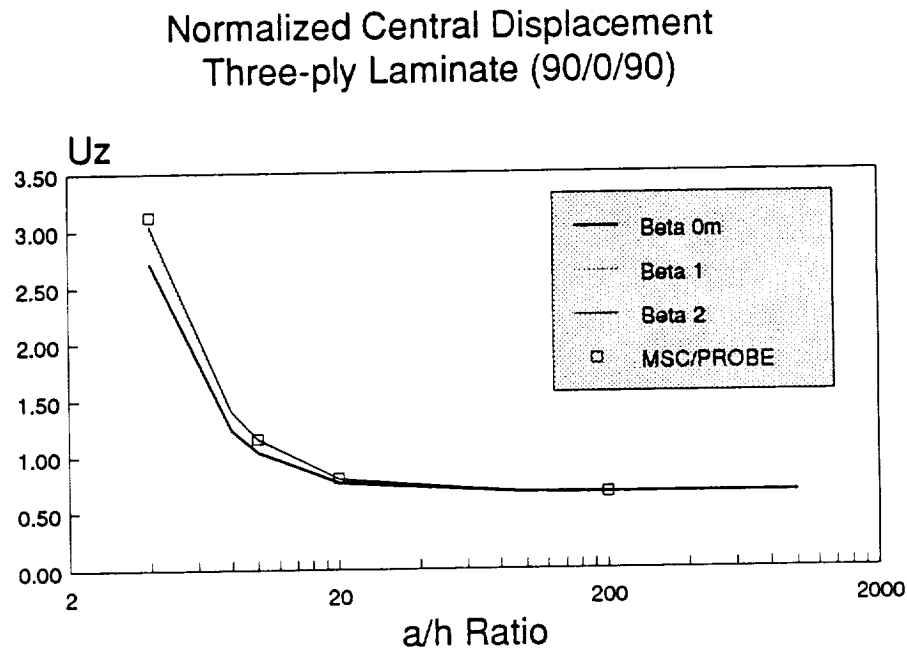


**Figure 5.2:** Simply supported orthotropic (90/0/90) square plate: The function  $U_z(a/2, a/2, 0)$ .

(Fig. 5.10). Those figures for the  $\beta^1$  and  $\beta^2$  models are (14%, 2.6%) and (4%, 0.7%), respectively. For low  $a/h$  ratios, there is a big improvement over the  $\beta^0$  model due to the presence of the piecewise linear terms in the displacement field in the  $\beta^1$  model and from the piecewise quadratic terms of the  $\beta^2$  model. For large  $a/h$  ratios, the quality of the  $\beta^0$  solution greatly improves. As mentioned earlier, low order models provide adequate response for large  $a/h$  ratios, but behave poorly for low  $a/h$  ratios. The  $\bar{\sigma}_x$  stress distribution is very closely represented by all the models for both  $a/h$  ratios (Figures 5.7 and 5.8).



The transverse shear and normal stresses were computed by integration of the equilibrium equations. The in-plane stresses were computed from the finite element solution directly, that is by computing the first derivatives of the displacement components, but equations (4.21), (4.22) and (4.23) were used for computing the transverse shear and normal stresses:

$$\tau_{zx} = - \int_0^z \left( \frac{\partial \sigma_x}{\partial x} + \frac{\partial \tau_{xy}}{\partial y} \right) dz + C_1 \quad (5.8)$$

$$\tau_{yz} = - \int_0^z \left( \frac{\partial \tau_{xy}}{\partial x} + \frac{\partial \sigma_y}{\partial y} \right) dz + C_2 \quad (5.9)$$

$$\sigma_z = - \int_0^z \left( \frac{\partial \tau_{xz}}{\partial x} + \frac{\partial \tau_{yz}}{\partial y} \right) dz + C_3 \quad (5.10)$$

where  $C_1$ ,  $C_2$  and  $C_3$  are integration constants determined from the stress condition at the surface of the plate. For zero shear stress at  $z = \pm h/2$  and zero normal stress at  $z = 0$ , we have:

$$\tau_{zx} = \int_0^{h/2} \left( \frac{\partial \sigma_x}{\partial x} + \frac{\partial \tau_{xy}}{\partial y} \right) dz - \int_0^z \left( \frac{\partial \sigma_x}{\partial x} + \frac{\partial \tau_{xy}}{\partial y} \right) dz \quad (5.11)$$

$$\tau_{yz} = \int_0^{h/2} \left( \frac{\partial \tau_{xy}}{\partial x} + \frac{\partial \sigma_y}{\partial y} \right) dz - \int_0^z \left( \frac{\partial \tau_{xy}}{\partial x} + \frac{\partial \sigma_y}{\partial y} \right) dz \quad (5.12)$$

$$\sigma_z = - \int_0^z \left( \frac{\partial \tau_{xz}}{\partial x} + \frac{\partial \tau_{yz}}{\partial y} \right) dz \quad (5.13)$$

The transverse shear stress distributions at the mid-section of two adjacent sides of the plate are shown in Figures 5.11 to 5.14. Observe that there is only a very small difference between the  $\beta^1$  and the  $\beta^2$  models. The similarity of shear stresses for the  $\beta^1$  and  $\beta^2$  models was observed in the case of the laminated strip also. To fully reproduce the shear stress profile, a higher order model is required. It was shown in the case of the strip that the  $\beta^3$  model is sufficient for producing excellent results.

Nevertheless, the results given by the  $\beta^1$  and  $\beta^2$  models are very satisfactory. The transverse normal stress at the middle of the plate is shown in Figure 5.15.

Figures 5.18 and 5.19 show the estimated relative error in energy norm as a function of the number of degrees of freedom for p-levels ranging from 1 to 8. Similar convergence is observed for all models and for the reference solution. Note that in all cases the estimated relative error in energy norm is below 1% for  $p = 8$ . The convergence rate is algebraic (i.e., the relationship between the energy norm and the number of degrees of freedom is very nearly a straight line on a log-log scale). This rate of convergence is governed by the singularities associated with the four corners and the edges.

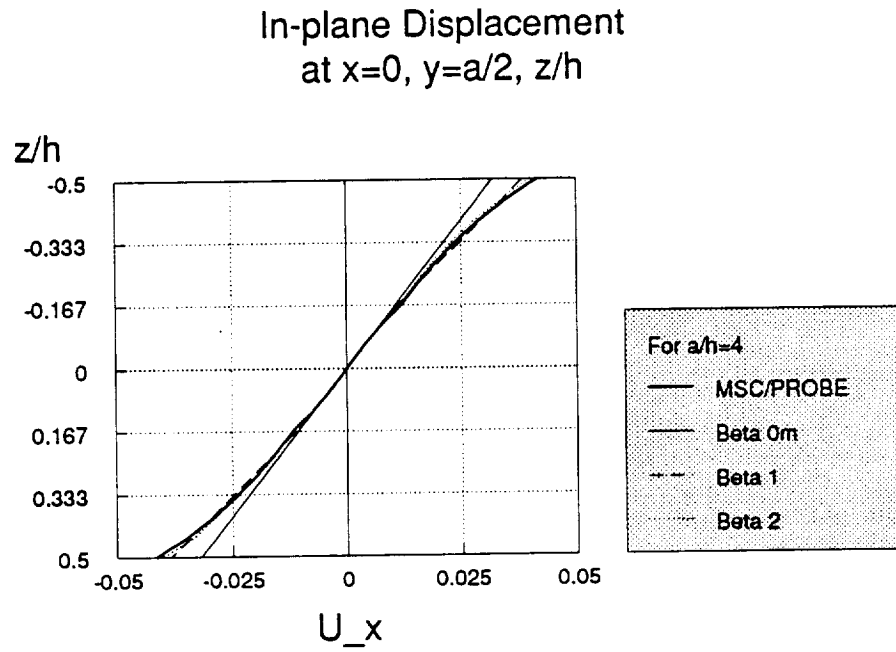


**Figure 5.3:** Simply supported orthotropic (90/0/90) square plate: The function  $\bar{u}_x(0, a/2, z)$  for  $a/h = 4$ .

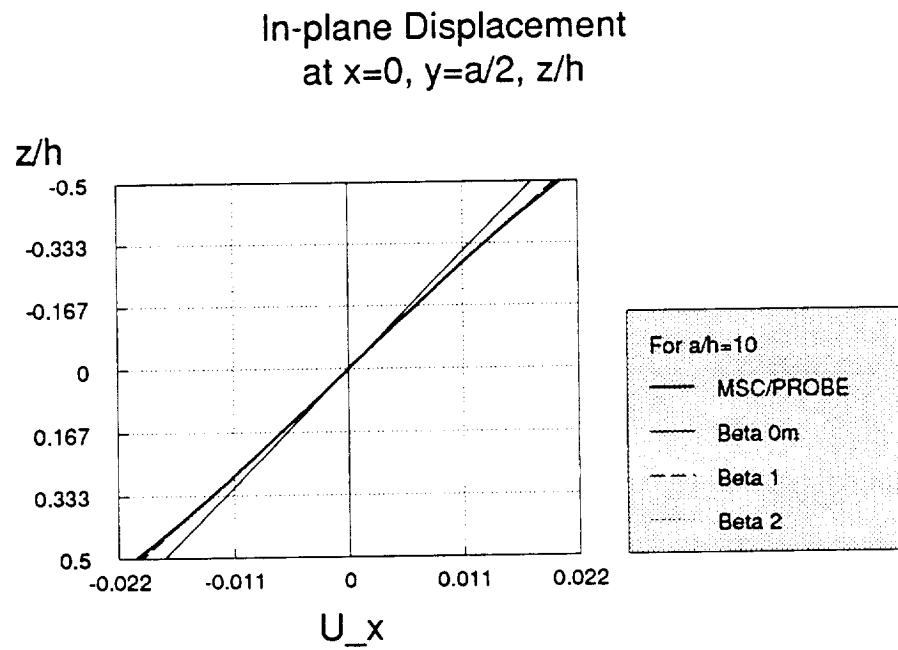


**Figure 5.4:** Simply supported orthotropic (90/0/90) square plate: The function  $\bar{u}_x(0, a/2, z)$  for  $a/h = 10$ .

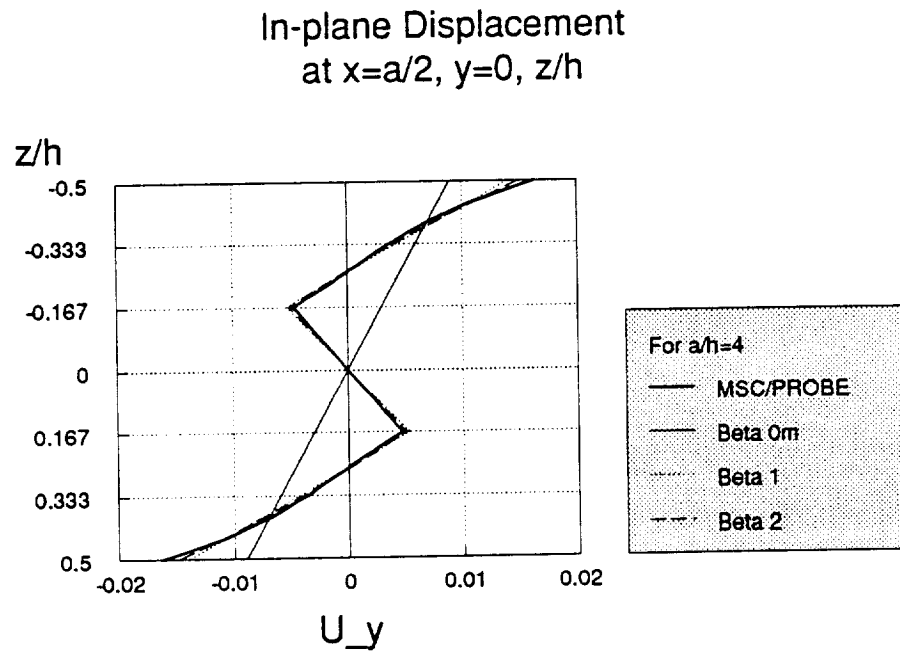


**Figure 5.5:** Simply supported orthotropic (90/0/90) square plate: The function  $\bar{u}_y(a/2, 0, z)$  for  $a/h = 4$ .

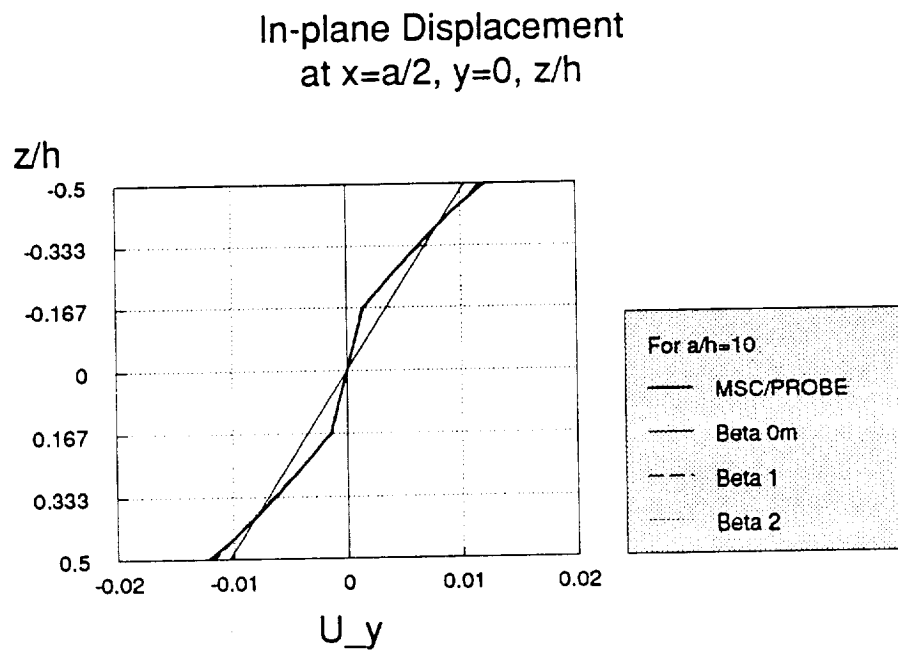


**Figure 5.6:** Simply supported orthotropic (90/0/90) square plate: The function  $\bar{u}_y(a/2, 0, z)$  for  $a/h = 10$ .

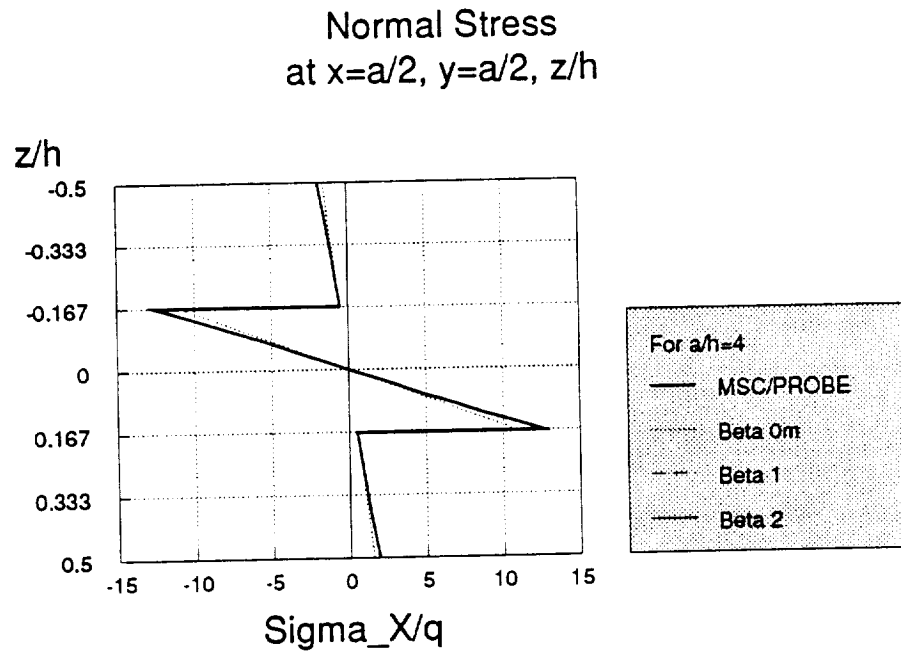


**Figure 5.7:** Simply supported orthotropic (90/0/90) square plate: The function  $\bar{\sigma}_x(a/2, a/2, z)$  for  $a/h = 4$ .

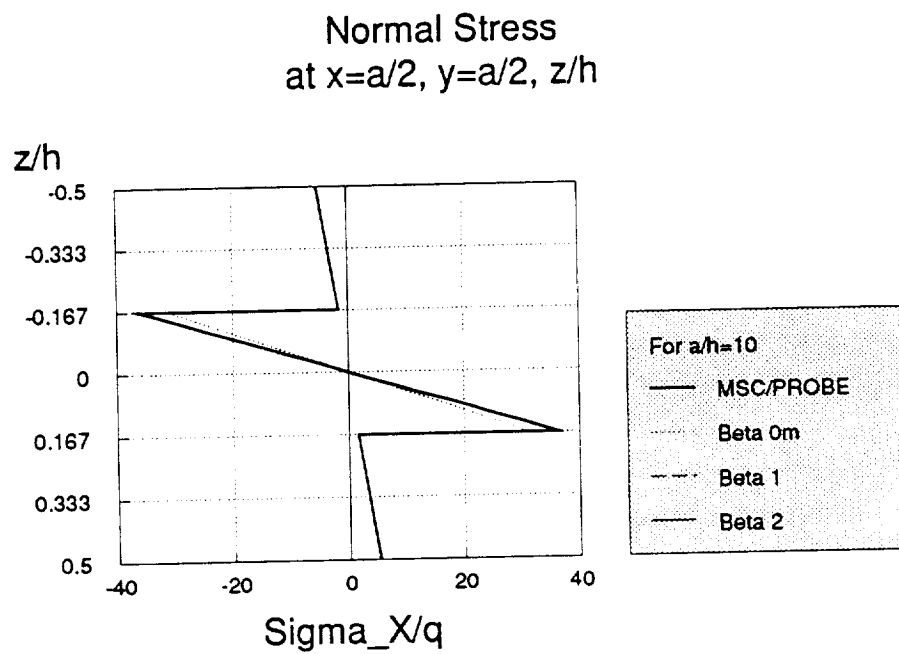


**Figure 5.8:** Simply supported orthotropic (90/0/90) square plate: The function  $\bar{\sigma}_x(a/2, a/2, z)$  for  $a/h = 10$ .

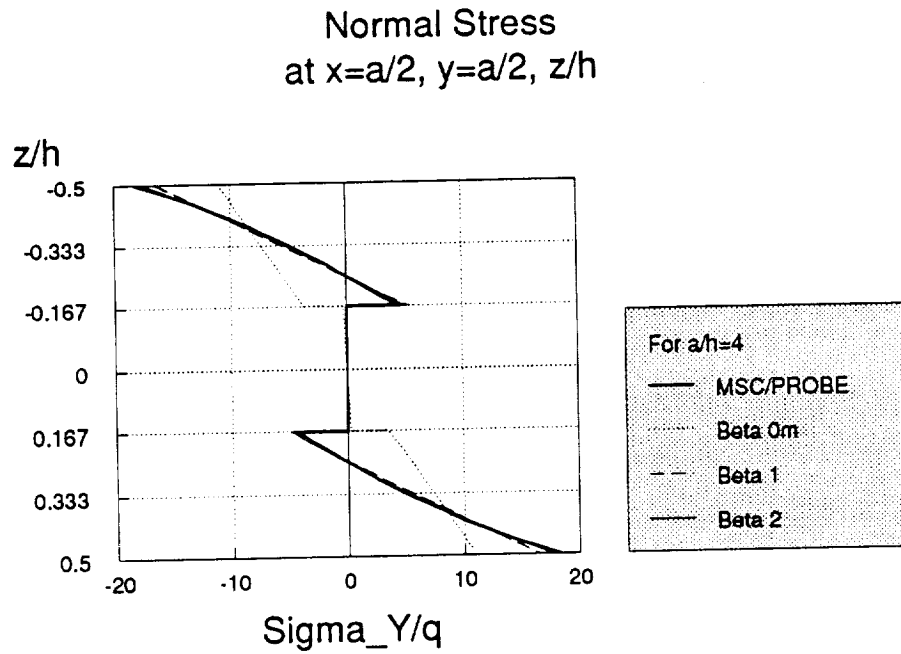


**Figure 5.9:** Simply supported orthotropic (90/0/90) square plate: The function  $\bar{\sigma}_y(a/2, a/2, z)$  for  $a/h = 4$ .

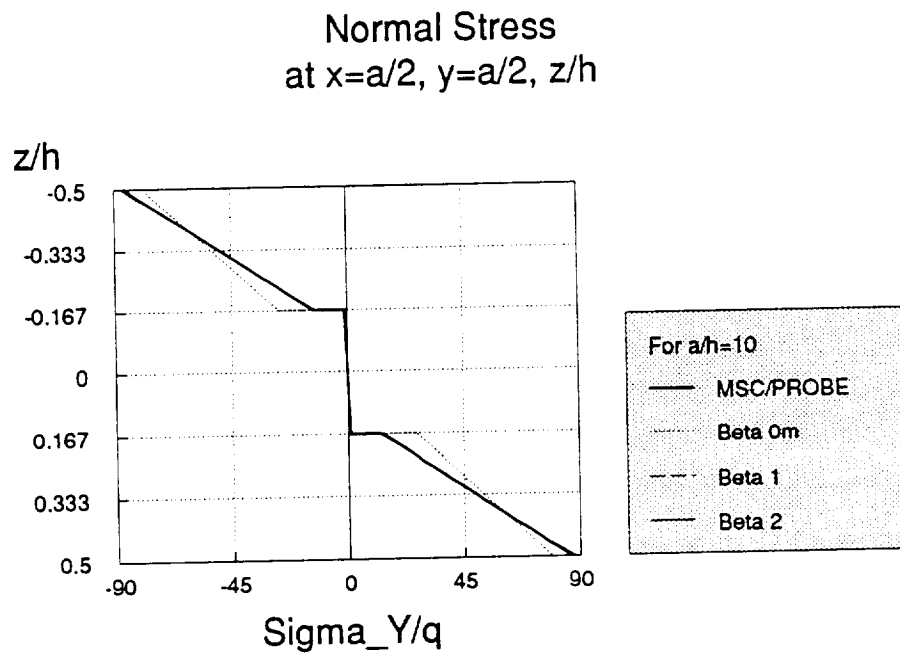


**Figure 5.10:** Simply supported orthotropic (90/0/90) square plate: The function  $\bar{\sigma}_y(a/2, a/2, z)$  for  $a/h = 10$ .

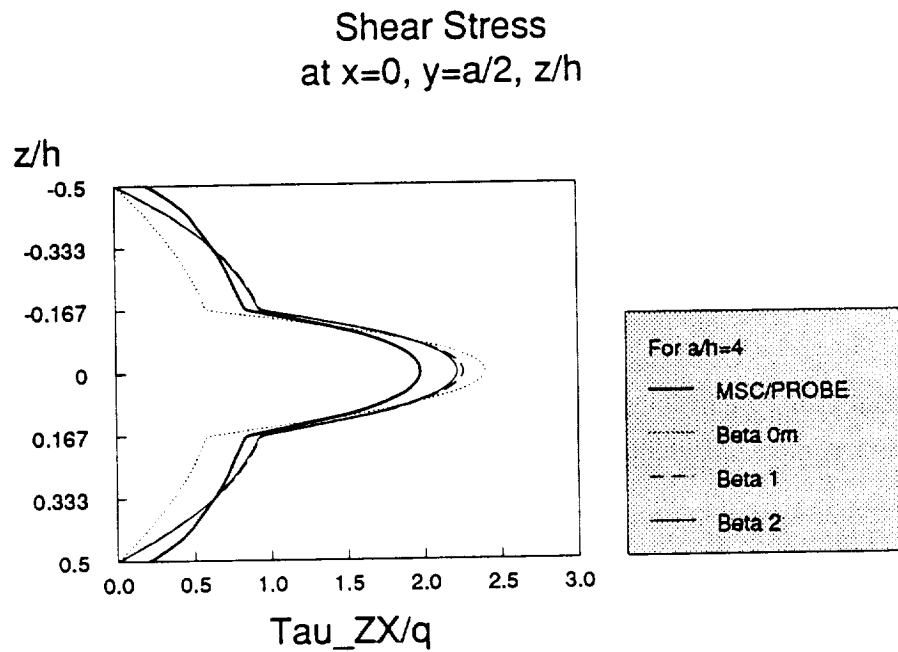


**Figure 5.11:** Simply supported orthotropic (90/0/90) square plate: The function  $\bar{\tau}_{zx}(0, a/2, z)$  for  $a/h = 4$ .

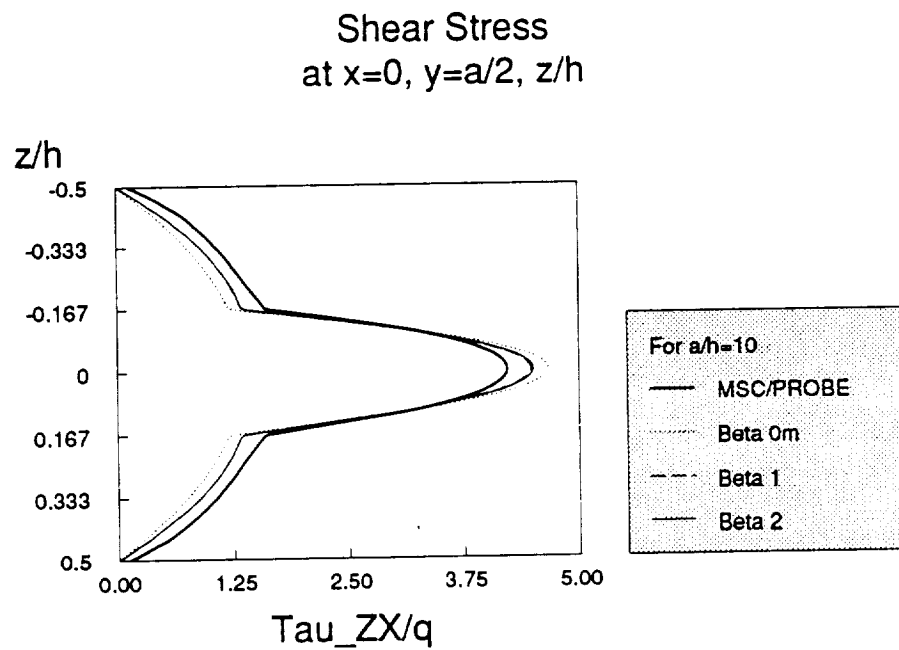


**Figure 5.12:** Simply supported orthotropic (90/0/90) square plate: The function  $\bar{\tau}_{zx}(0, a/2, z)$  for  $a/h = 10$ .

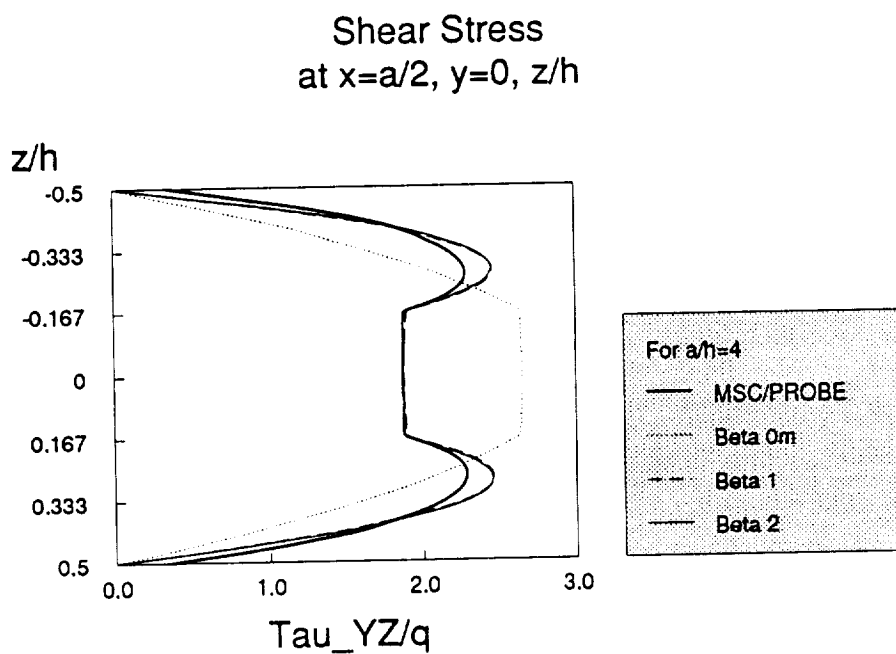


**Figure 5.13:** Simply supported orthotropic (90/0/90) square plate: The function  $\bar{\tau}_{yz}(a/2, 0, z)$  for  $a/h = 4$ .

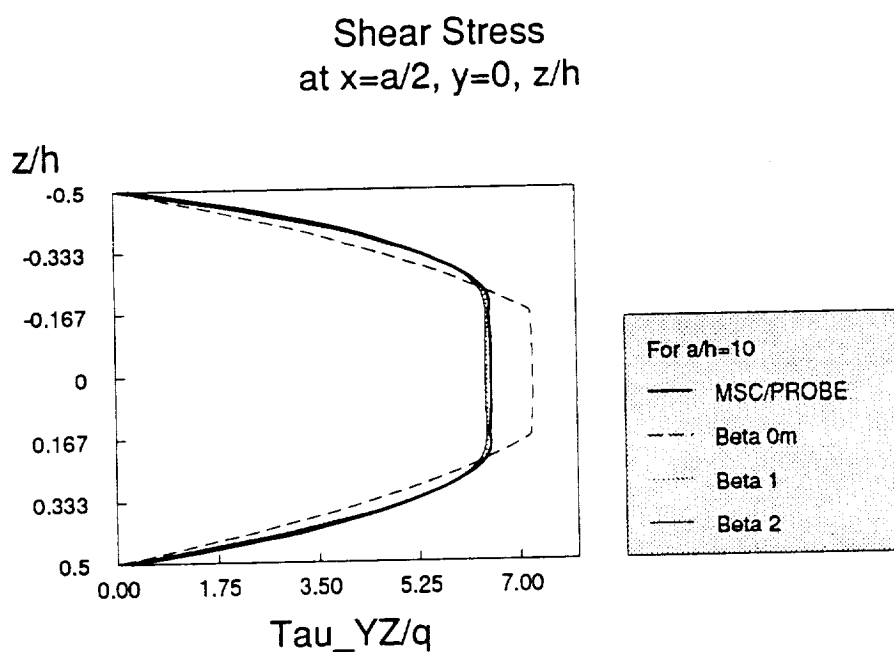


**Figure 5.14:** Simply supported orthotropic (90/0/90) square plate: The function  $\bar{\tau}_{yz}(a/2, 0, z)$  for  $a/h = 10$ .



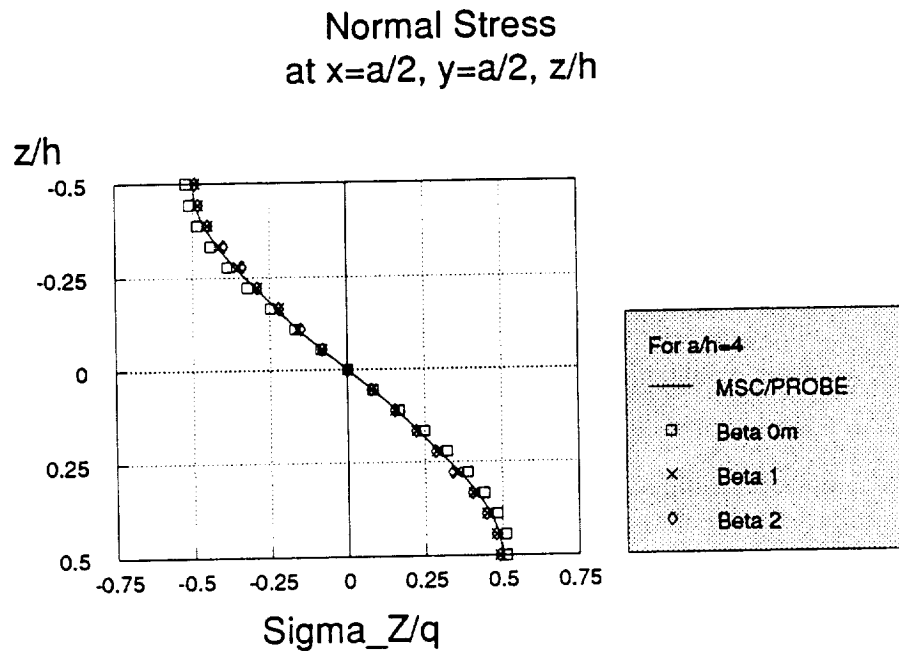


**Figure 5.15:** Simply supported orthotropic (90/0/90) square plate: The function  $\bar{\sigma}_z(a/2, a/2, z)$  for  $a/h = 4$ .

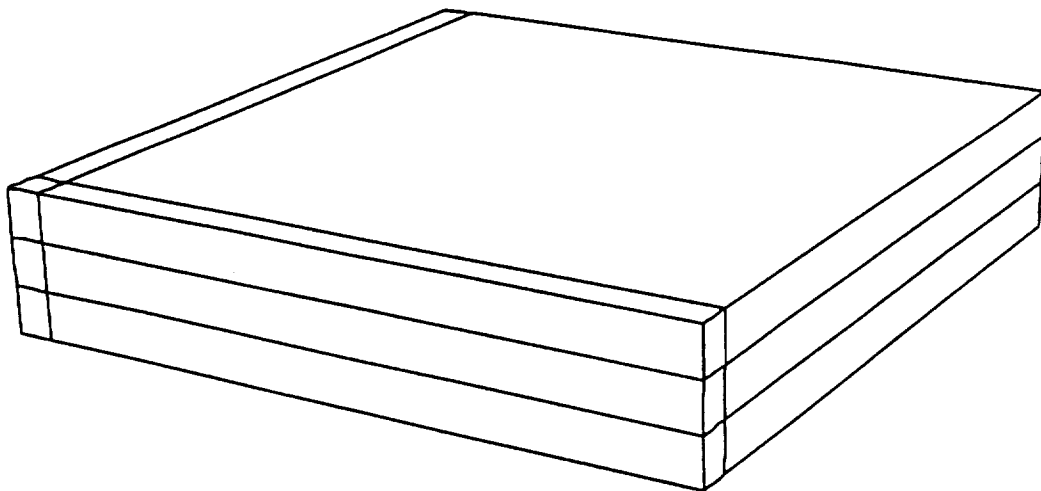


**Figure 5.16:** Simply supported orthotropic (90/0/90) square plate: Finite element mesh for the reference solution ( $a/h = 10$ ).

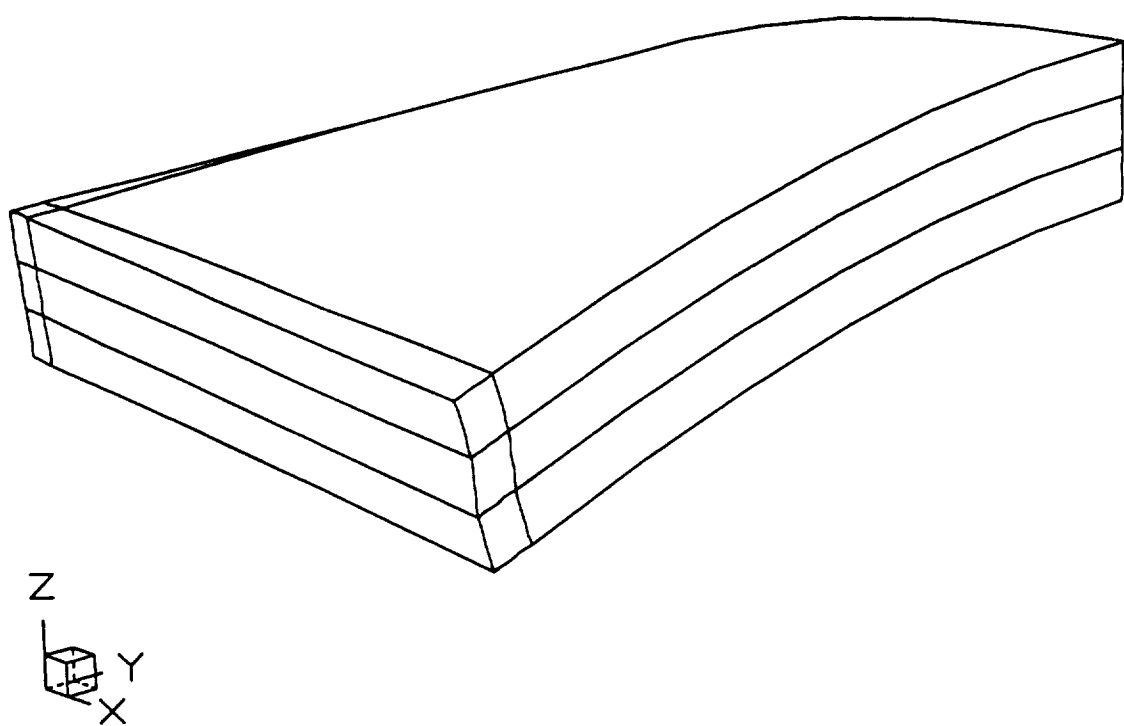


**Figure 5.17:** Simply supported orthotropic (90/0/90) square plate: Deformed configuration ( $a/h = 10$ ).

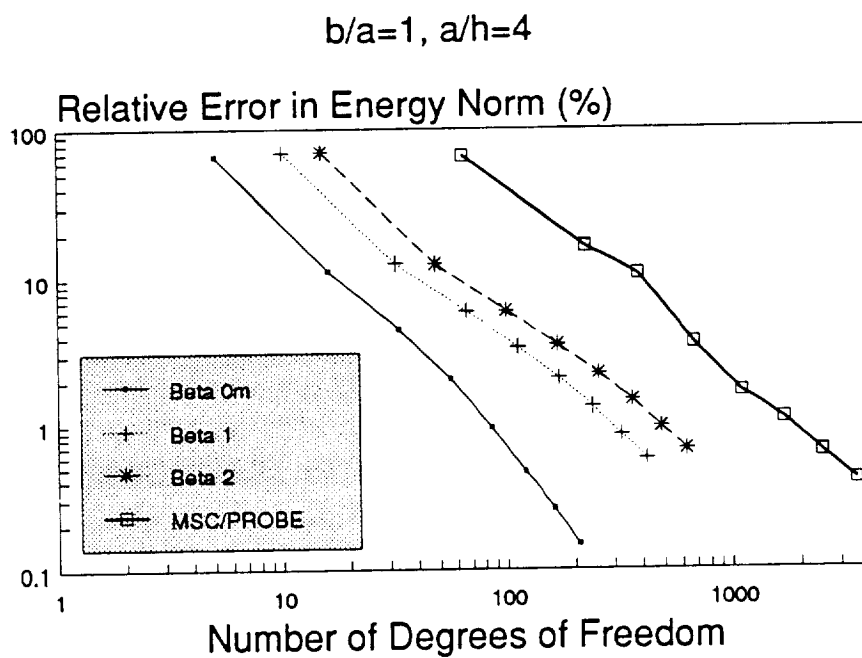


**Figure 5.18:** Simply supported orthotropic (90/0/90) square plate: Estimated relative error in energy norm for  $a/h = 4$ .

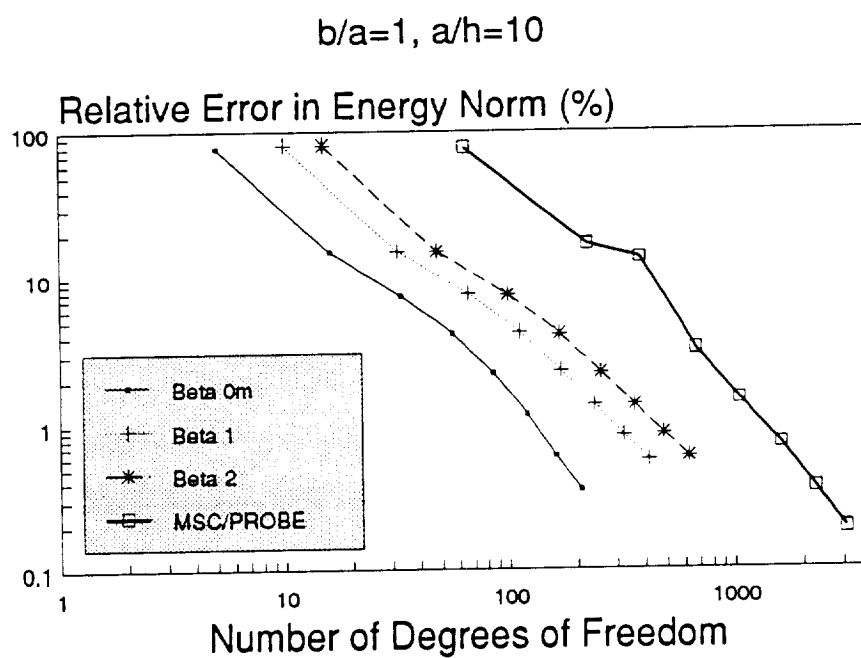


**Figure 5.19:** Simply supported orthotropic (90/0/90) square plate: Estimated relative error in energy norm for  $a/h = 10$ .

### 5.2.2 Rectangular Plate

The stress distribution at representative locations in a three-ply orthotropic (or cross-ply, 90/0/90) simply supported rectangular plate ( $b/a = 3$ ) are shown in Figures 5.20 to 5.23. In all cases the results are those corresponding to  $p = 8$  and  $a/h = 4$ . The loading and support conditions are the same as for the square plate.

The results are also summarized in Table 5.3 for several width-to-thickness ratios. The quality of approximation is similar to that obtained for the square plate. Note that the approximation of the in-plane stress components is always better than the approximation in the transverse shear stresses. Higher order models are required to obtain a more precise shear stress distribution, as was shown in Chapter 3 for the laminated strip problem.

### 5.2.3 Other Cases of Cross-ply Laminates

The influence of the number of layers on the end deflection of a cross-ply square plate with one side clamped and the other three free is shown in Fig. 5.24 for three different  $a/h$  ratios. In all cases the fibers in the outer layers were kept normal to the clamped edge of the plate. Also included in the figure are the results of the deflection computed using a simplified beam formula, which is valid for the case  $a/h \rightarrow \infty$ . According to reference [36], the end deflection of a cantilever beam of length  $a$  and thickness  $h$  with uniform load  $q$  is:

$$u_z = \frac{q a^4}{8 D_{11}} \quad (5.14)$$

**Table 5.3:** Normalized Stresses and Displacements for a Simply Supported 90/0/90 Rectangular Plate ( $b/a = 3$ )

MODEL	a/h	$U_z$ (a/2, b/2, 0)	$\bar{\sigma}_x$ (a/2, b/2, h/2)	$\bar{\sigma}_y$ (a/2, b/2, h/2)	$\bar{\tau}_{zx}$ (0, b/2, 0)	$\bar{\tau}_{yz}$ (a/2, 0, 0)
$\beta^0$	4	11.00	6.65	15.32	5.93	2.81
$\beta^1$		10.76	6.72	13.28	5.46	2.18
$\beta^2$		11.00	6.88	13.64	5.42	2.18
MSC/PROBE		11.04	6.87	13.40	5.09	2.31
$\beta^0$	10	8.421	41.75	100.4	14.92	7.89
$\beta^1$		8.391	39.42	94.40	14.34	7.54
$\beta^2$		8.431	39.52	94.70	14.37	7.49
MSC/PROBE		8.441	39.59	94.09	14.04	7.70
$\beta^0$	20	8.014	166.7	403.4	29.63	16.33
$\beta^1$		8.010	155.7	386.6	28.94	16.12
$\beta^2$		8.021	155.6	386.8	28.96	16.09
MSC/PROBE		8.028	156.0	386.2	28.53	16.52
$\beta^0$	100	7.849	4144	10070	147.0	81.38
$\beta^1$		7.849	3857	9709	144.1	80.27
$\beta^2$		7.850	3851	9703	144.1	80.27
MSC/PROBE		7.858	3867	9735	149.4	81.32

where

$$D_{11} = \int_{-h/2}^{+h/2} Q_{11} z^2 dz. \quad (5.15)$$

The deflection computed by the use of (5.14) is identified as 'Beam ( $a/h \rightarrow \infty$ )'.

The results indicate that when the number of layers increases then the bending stiffness of the plate decreases to a limiting value. The property of the laminate will be square symmetric but not isotropic [37]. When the longitudinal and transverse properties are equal, a material is called square symmetric. For the laminate this means:

$$D_{11} = \int_{-h/2}^{+h/2} Q_{11} z^2 dz = D_{22} = \int_{-h/2}^{+h/2} Q_{22} z^2 dz. \quad (5.16)$$

The influence of different boundary conditions in the central deflection of a square plate is shown in Figures 5.25 and 5.26. Two opposite sides simply supported and the other two sides free are considered in this case. The results are for a three- and a five-ply laminate, and include the values of the deflection computed with the plate models as well as with the previously evaluated strip models. As can be observed both the plate and strip model yield similar results.

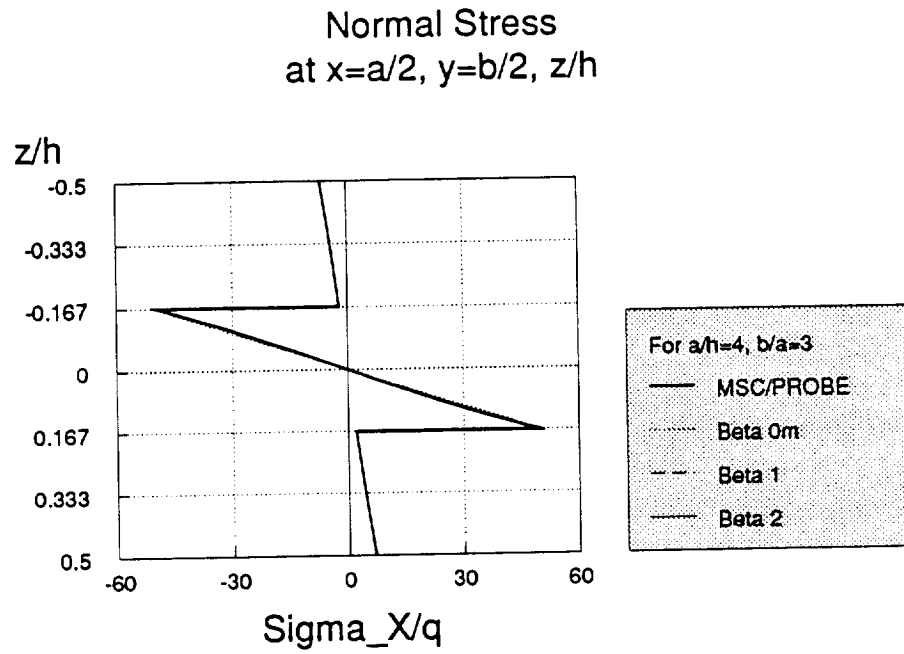


**Figure 5.20:** Simply supported orthotropic (90/0/90) rectangular plate: The function  $\bar{\sigma}_x(a/2, b/2, z)$  for  $a/h = 4$ .

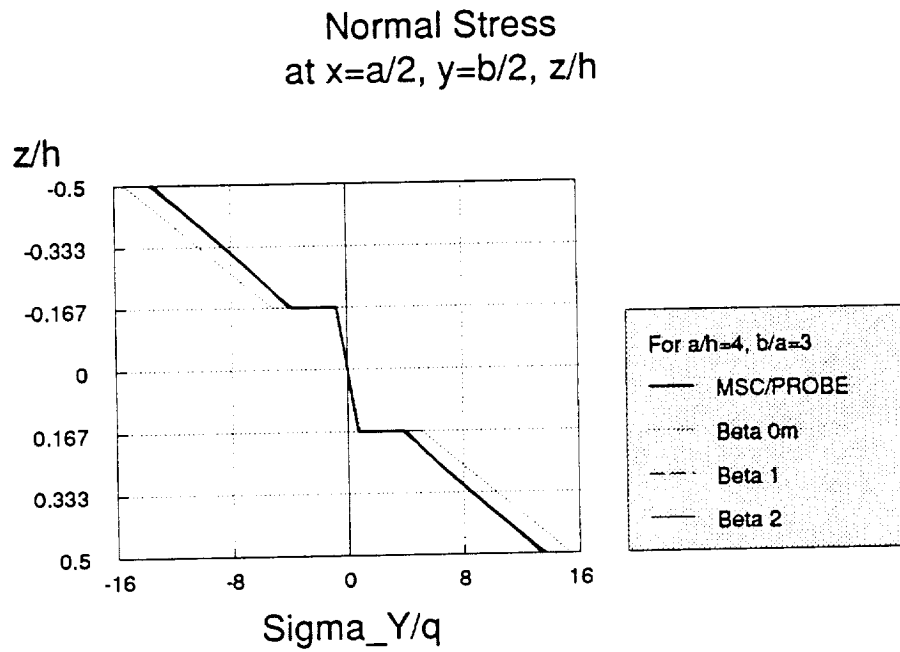


**Figure 5.21:** Simply supported orthotropic (90/0/90) rectangular plate: The function  $\bar{\sigma}_y(a/2, b/2, z)$  for  $a/h = 4$ .

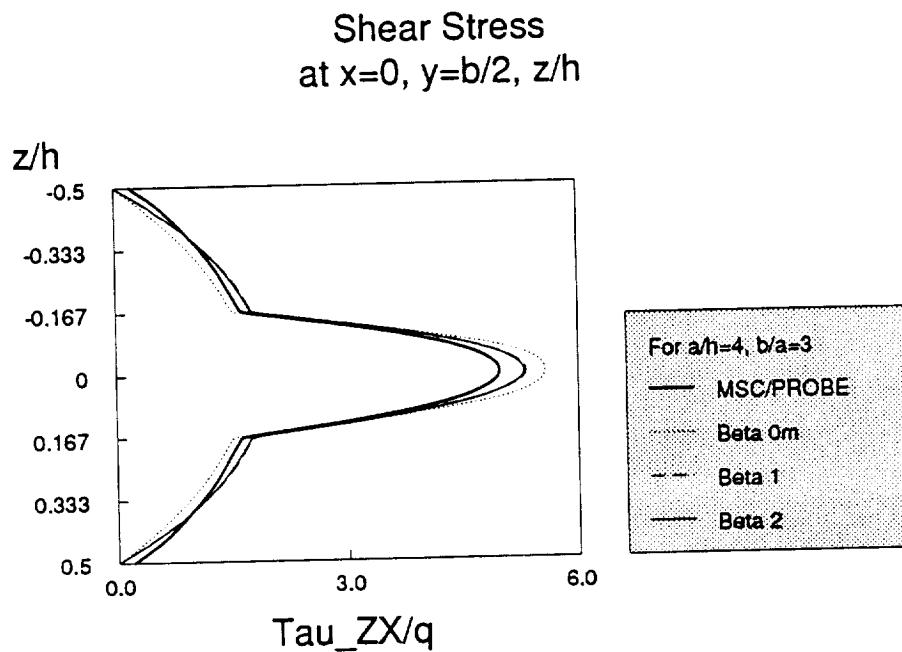


**Figure 5.22:** Simply supported orthotropic (90/0/90) rectangular plate: The function  $\bar{\tau}_{zx}(0, b/2, z)$  for  $a/h = 4$ .

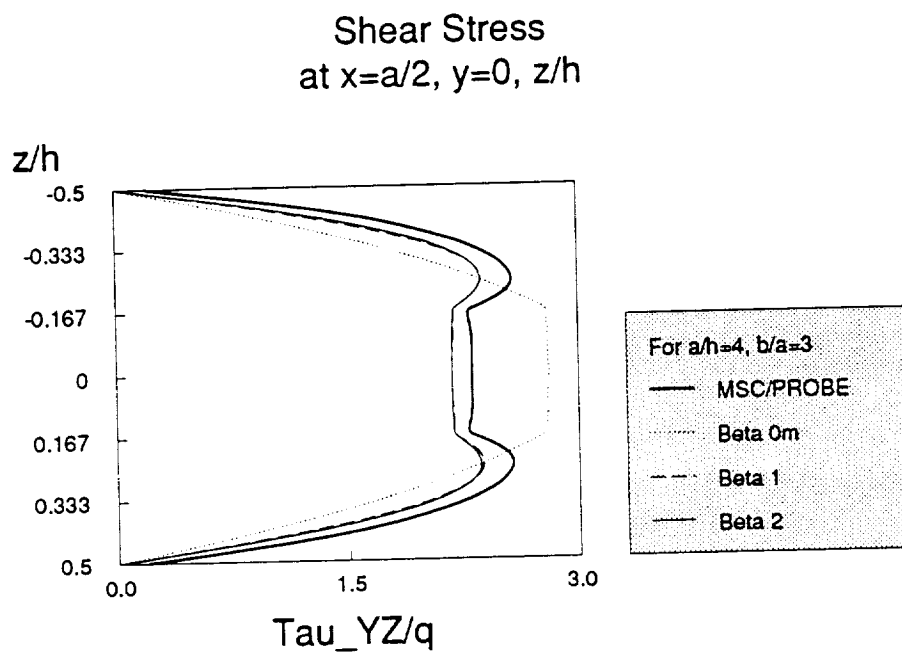


**Figure 5.23:** Simply supported orthotropic (90/0/90) rectangular plate: The function  $\bar{\tau}_{yz}(a/2, 0, z)$  for  $a/h = 4$ .



### Normalized End Displacement Influence of Number of Layers

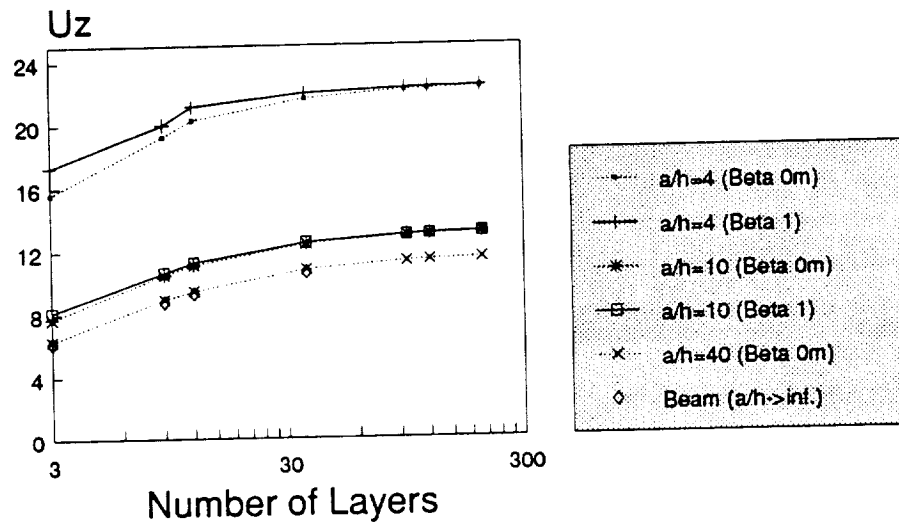


Figure 5.24: Orthotropic (90/0/90) square plate, one side clamped. Influence of number of layers in  $U_z(a/2, a, 0)$ .

### Normalized Central Displacement Three-ply Laminate (90/0/90)

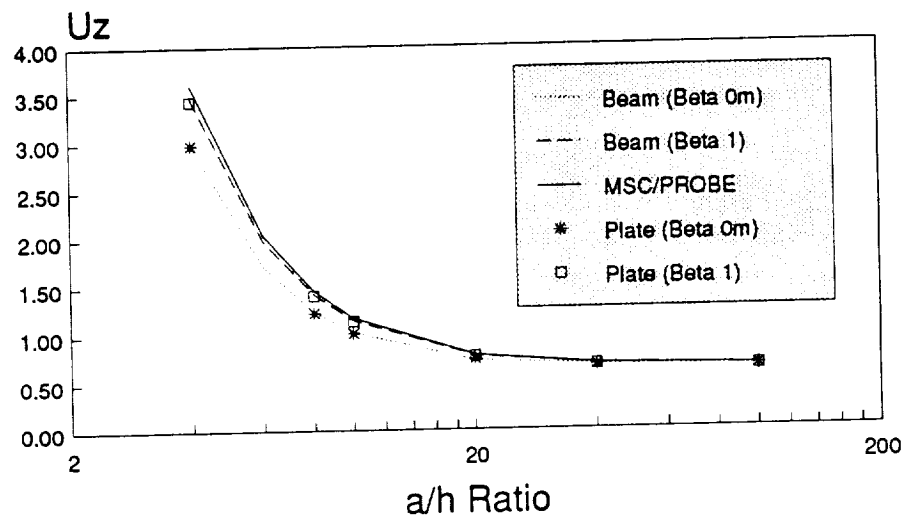


Figure 5.25: Three-ply square plate. Two sides simply supported: The function  $U_z(a/2, a/2, 0)$ .

### 5.3 Angle-ply Laminate

In this Section we present the results for angle-ply laminated plates. There are three cases which are analyzed in detail: A three-ply square ( $b/a = 1$ ) simply supported plate with a stacking sequence  $-45/+45/-45$ , a three-ply square simply supported plate with a stacking sequence  $-30/+30/-30$ , and a three-ply rectangular ( $b/a = 3$ ) simply supported plate with a stacking sequence  $-45/+45/-45$ . As before, the results include deflections, normal and shear stress distributions and estimated relative error in energy norm for all three models and for the reference solution.

Also included is the case of a three-ply laminated square plate in which the angle of the fibers in each layer was varied between  $0$  and  $90^\circ$ .

#### 5.3.1 Square $-45/+45/-45$ Plate

The results for a three-ply simply supported square angle-ply laminated plate are shown in Fig. 5.27 to Fig. 5.33 for the stacking sequence  $-45/+45/-45$ . The results are also shown in Table 5.4 for several  $a/h$  ratios. In this case the transverse deflection computed for each hierarchic model shows a similar behavior as in the case of the cross-ply laminate (Figure 5.27). Note however, that the difference between the  $\beta^0$  model on one hand and the  $\beta^1$ ,  $\beta^2$  models on the other is larger than before. Also, the in-plane displacements (Figures 5.28, 5.29) and stresses (Figures 5.30-5.32) for  $a/h = 4$  show the same trend as in the cross-ply laminate.

The  $\beta^0$  model always underestimates displacements and normal stresses, while the  $\beta^1$  and  $\beta^2$  models give much closer approximations.

Higher order models are required to obtain more precise shear stress distributions. The same situation holds for the transverse normal stress  $\sigma_z$  (Fig. 5.33) which was computed directly from the finite element solution. The transverse normal stress can also be computed by integration of the equilibrium equations as described for the cross-ply laminate, and better results are obtained.

Comparing Figures 5.34, 5.35 with Figures 5.18, 5.19, the rate of convergence for the angle-ply laminate is not as high as in the case of cross-ply laminate. The relative error in energy norm at  $p = 8$  is now larger for the same number of degrees of freedom. The simply supported angle-ply laminate represents a less smooth problem than the cross-ply laminate.

### 5.3.2 Square $-30/+30/-30$ Plate

The results for a three-ply simply supported square angle-ply laminated plate are shown in Figures 5.36 to 5.43 for the orientation  $-30/+30/-30$ . In this case the transverse deflection computed for each hierarchic model shows a similar behavior as in the case of the  $-45/+45/-45$  laminate (Figure 5.36). Note however, that the difference between the  $\beta^0$  and the  $\beta^1$  model is larger than before, and that the solution corresponding to the  $\beta^2$  model is farther apart from the  $\beta^1$  model. The results are also summarized in Table 5.5 for several width-to-thickness ratios.

**Table 5.4:** Normalized Stresses and Displacements for a Simply Supported  $-45/+45/-45$  Square Plate ( $b/a = 1$ )

MODEL	a/h	$U_z$ (a/2, a/2, 0)	$\bar{\sigma}_x$ (a/2, a/2, h/2)	$\bar{\tau}_{xy}$ (a/2, a/2, h/2)	$\bar{\tau}_{zx}$ (0, a/2, 0)
$\beta^0$	4	2.410	5.69	4.28	2.18
$\beta^1$		2.894	7.45	5.66	1.95
$\beta^2$		2.952	8.06	6.23	1.93
MSC/PROBE		3.007	7.94	6.05	2.02
$\beta^0$	10	0.994	32.59	26.25	4.11
$\beta^1$		1.130	35.26	28.77	3.81
$\beta^2$		1.147	36.12	29.59	3.77
MSC/PROBE		1.155	35.24	28.70	4.97
$\beta^0$	20 (*)	0.741	-	-	-
$\beta^1$		0.783	-	-	-
$\beta^2$		0.789	-	-	-
MSC/PROBE		0.793	-	-	-
$\beta^0$	100 (*)	0.609	-	-	-
$\beta^1$		0.613	-	-	-
$\beta^2$		0.613	-	-	-
MSC/PROBE		0.615	-	-	-

(\*) Estimated relative error in energy norm larger than 5% for all models

The in-plane displacements (Figure 5.37), normal stresses (Figures 5.38, 5.39 and 5.40), and shear stresses (Figures 5.41-5.43) for  $a/h = 4$  show the same trend as before. Note, however, that in this case the approximation in the transverse shear stresses (Fig. 5.41) is not as close to the reference solution as in the previous cases. The characteristics of the exact solution near the boundaries requires the use of higher order models if the shear stress distribution is of primary interest.

### 5.3.3 Rectangular $-45/+45/-45$ Plate

The results for a rectangular plate ( $b/a = 3$ ) with ply orientation  $-45/+45/-45$  are shown in Figures 5.44 to 5.48. Even though the relative error in energy norm for this problem is larger for the same  $a/h$  ratio than for the equivalent square plate (see Table 5.1) the approximation for each hierarchic model is very similar to the one obtained for the square plate with the same stacking sequence and for the case  $a/h = 4$ .

The numerical results included in Table 5.6 for different width-to-thickness ratios, combined with the information provided in Table 5.1, are indicating that the characteristic of the exact solution is less smooth than for the square plate. In this case for  $a/h = 10$  the estimated error in energy norm was already larger than 5% and no shear stress values are included. However, in-plane normal stresses are less sensitive than the transverse shear, and good convergence to the reference solution can be realized.

**Table 5.5:** Normalized Stresses and Displacements for a Simply Supported  $-30/+30/-30$  Square Plate ( $b/a = 1$ )

MODEL	a/h	$U_z$ (a/2, a/2, 0)	$\bar{\sigma}_x$ (a/2, a/2, h/2)	$\bar{\sigma}_y$ (a/2, a/2, h/2)	$\bar{\tau}_{zx}$ (0, a/2, 0)	$\bar{\tau}_{yz}$ (a/2, 0, 0)
$\beta^0$	4	2.374	8.47	3.54	3.05	1.91
$\beta^1$		2.806	11.11	4.61	2.71	1.88
$\beta^2$		2.897	12.29	5.04	2.69	1.84
MSC/PROBE		2.917	12.0	4.98	2.38	1.49
$\beta^0$	10	0.986	52.37	20.33	6.28	4.57
$\beta^1$		1.098	55.40	21.40	5.97	4.22
$\beta^2$		1.120	56.78	21.90	5.95	4.20
MSC/PROBE		1.123	55.90	21.57	6.01	3.64
$\beta^0$	20 (*)	0.750	-	-	-	-
$\beta^1$		0.783	-	-	-	-
$\beta^2$		0.790	-	-	-	-
MSC/PROBE		0.792	-	-	-	-
$\beta^0$	100 (*)	0.636	-	-	-	-
$\beta^1$		0.638	-	-	-	-
$\beta^2$		0.639	-	-	-	-
MSC/PROBE		0.640	-	-	-	-

(\*) Estimated relative error in energy norm larger than 5% for all models

**Table 5.6:** Normalized Stresses and Displacements for a Simply Supported  $-45/+45/-45$  Rectangular Plate ( $b/a = 3$ )

MODEL	a/h	$U_z$ (a/2, b/2, 0)	$\bar{\sigma}_x$ (a/2, b/2, h/2)	$\bar{\sigma}_y$ (a/2, b/2, h/2)	$\bar{\tau}_{zx}$ (0, b/2, 0)	$\bar{\tau}_{yz}$ (a/2, 0, 0)
$\beta^0$	4	5.002	11.47	9.33	3.33	2.71
$\beta^1$		6.204	14.41	11.73	3.05	2.40
$\beta^2$		6.333	15.37	12.58	3.04	2.38
MSC/PROBE		6.388	15.40	12.50	2.74	2.33
$\beta^0$	10	2.572	72.48	62.09	-	-
$\beta^1$		2.843	75.08	63.98	-	-
$\beta^2$		(*)	76.20	64.96	-	-
MSC/PROBE		2.852	76.94	65.27	-	-
$\beta^0$	20	2.189	-	-	-	-
$\beta^1$		2.261	-	-	-	-
$\beta^2$		(*)	-	-	-	-
MSC/PROBE		2.278	-	-	-	-
$\beta^0$	100	2.041	-	-	-	-
$\beta^1$		2.044	-	-	-	-
$\beta^2$		(*)	-	-	-	-
MSC/PROBE		2.050	-	-	-	-

(\*) Estimated relative error in energy norm larger than 5% for all models

### 5.3.4 Other Cases of Angle-ply Laminate

The influence of fiber orientation in the central deflection of a three-ply square plate with two opposite sides simply supported (2-sides SS) and four sides simply supported (4-sides SS) is shown in Fig. 5.49. In this case the  $a/h$  ratio was kept constant at  $a/h = 10$  and the orientation of the fibers in the central layer was varied between  $0^\circ$  and  $90^\circ$ . The fibers in the outer layers were always at  $90^\circ$  with the fibers in the central layer. The results for the  $\beta^0$  and  $\beta^1$  models are included for each boundary condition.

When all sides are simply supported, the central deflection of the plate  $U_z$  is maximum when the central layer is either  $0^\circ$  or  $90^\circ$ . As may be anticipated the minimum deflection occurs for  $\theta = 45^\circ$ . When two sides are simply supported and the fibers in the central layer run parallel to the supported edges ( $\theta = 0^\circ$ ), the deflection is minimum. As  $\theta$  increases so does the deflection, and the maximum takes place for  $\theta$  between  $60^\circ$  and  $70^\circ$ .



Normalized Central Displacement  
Five-ply Laminate (90/0/90/0/90)

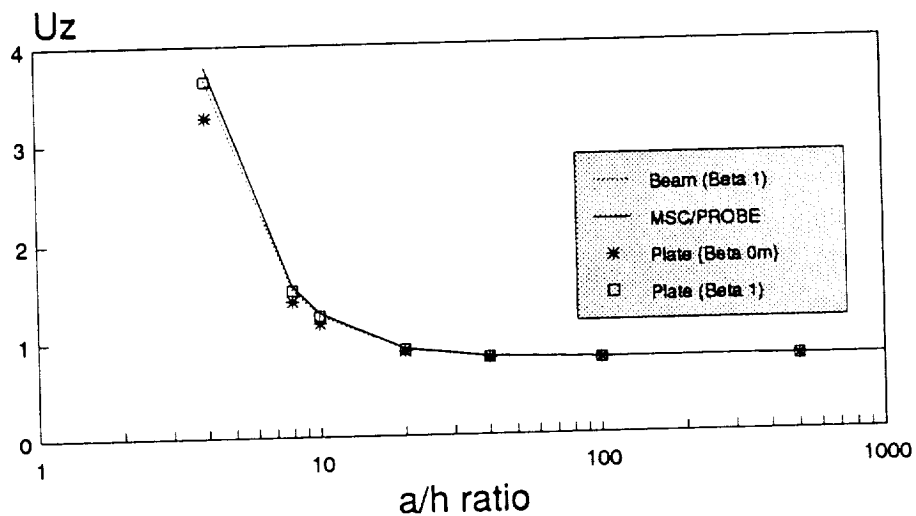


**Figure 5.26:** Five-ply square plate. Two sides simply supported: The function  $U_z(a/2, a/2, 0)$ .

Normalized Central Displacement  
Three-ply Laminate (-45/45/-45)

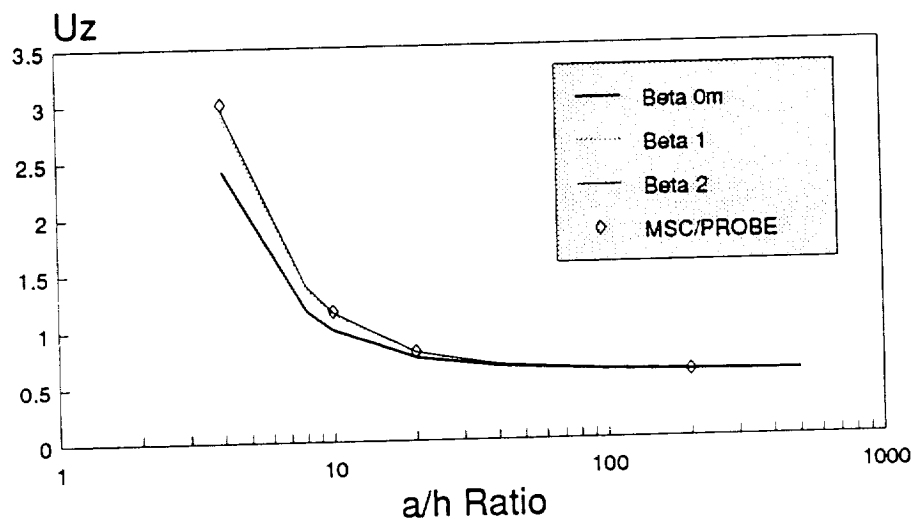


**Figure 5.27:** Simply supported angle-ply (-45/ + 45/ - 45) square plate: The function  $U_z(a/2, a/2, 0)$ .

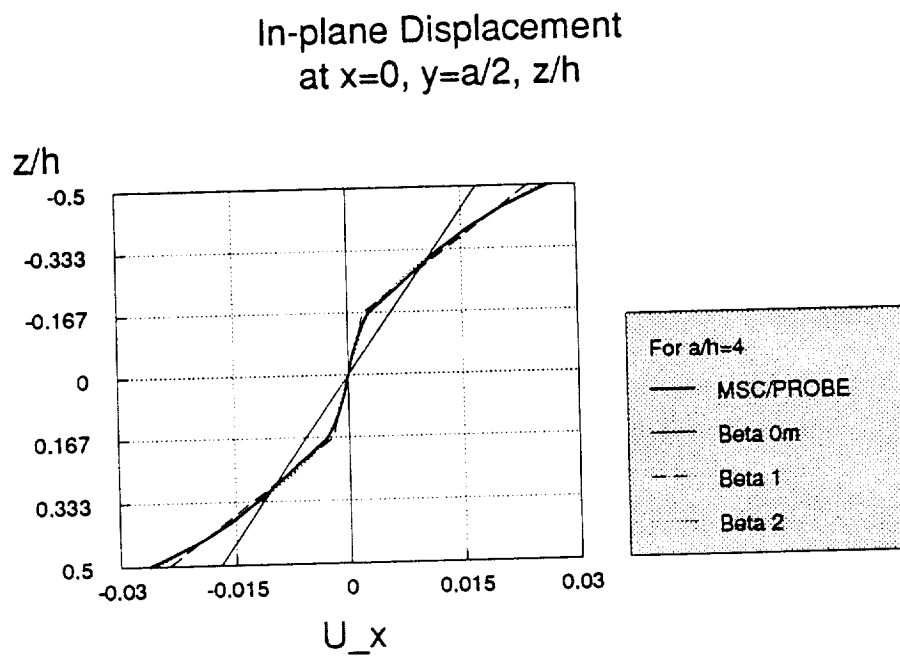


**Figure 5.28:** Simply supported angle-ply ( $-45^\circ / +45^\circ - 45^\circ$ ) square plate: The function  $\bar{u}_x(0, a/2, z)$  for  $a/h = 4$ .

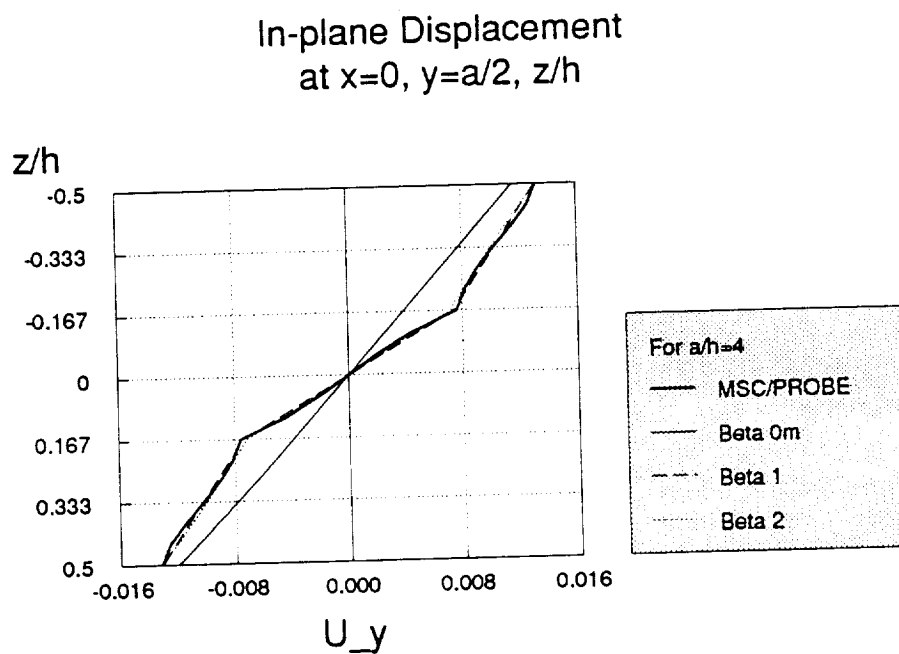


**Figure 5.29:** Simply supported angle-ply ( $-45^\circ / +45^\circ - 45^\circ$ ) square plate: The function  $\bar{u}_y(0, a/2, z)$  for  $a/h = 4$ .

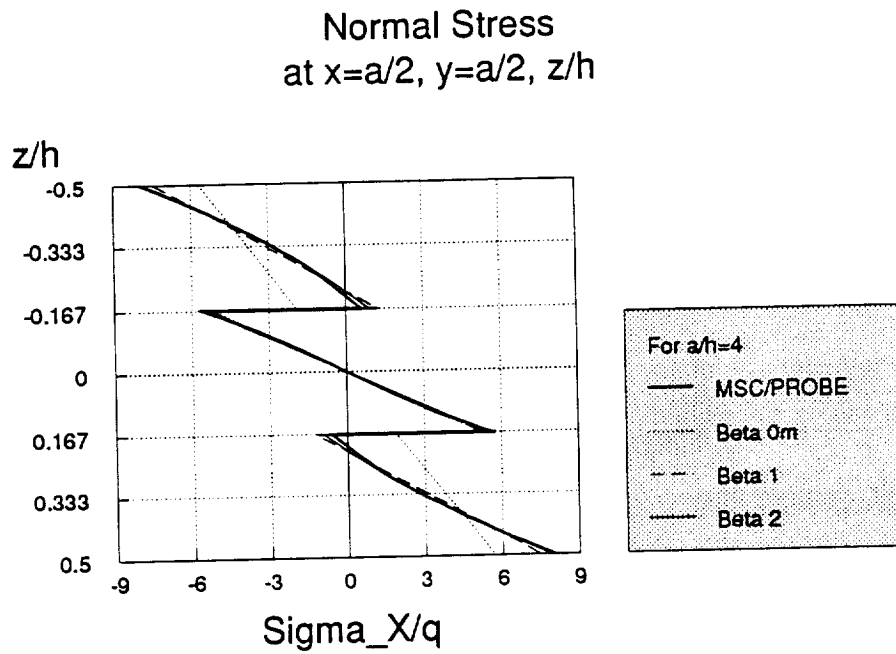


**Figure 5.30:** Simply supported angle-ply  $(-45^\circ / +45^\circ - 45^\circ)$  square plate: The function  $\bar{\sigma}_x(a/2, a/2, z)$  for  $a/h = 4$ .

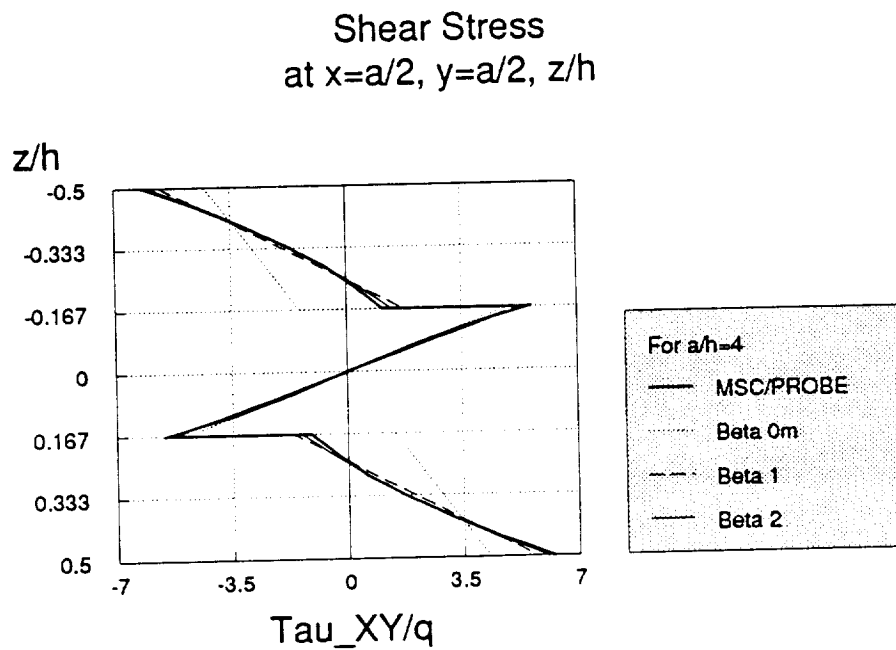


**Figure 5.31:** Simply supported angle-ply  $(-45^\circ / +45^\circ - 45^\circ)$  square plate: The function  $\bar{\tau}_{xy}(a/2, a/2, z)$  for  $a/h = 4$ .

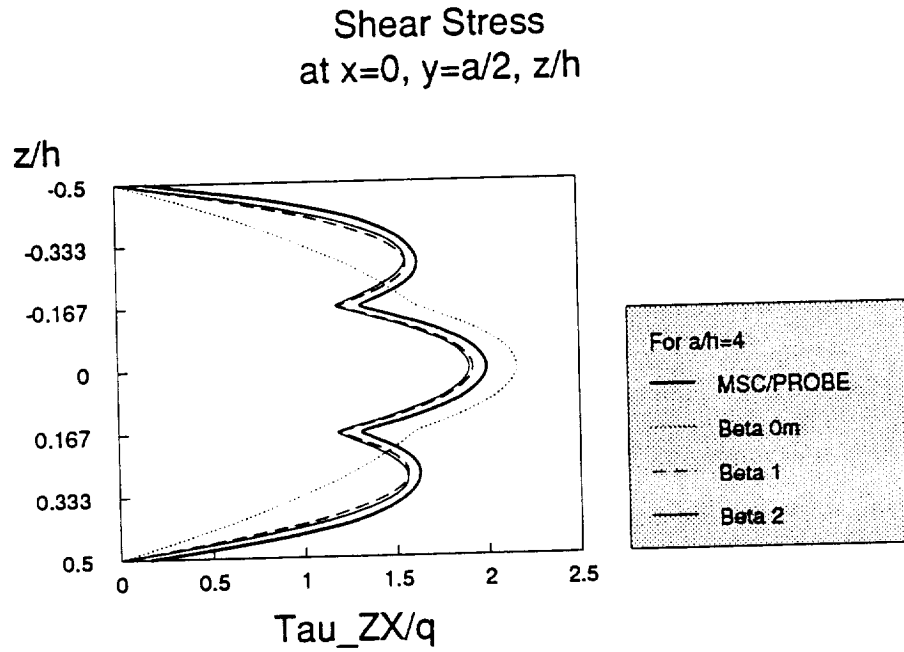


**Figure 5.32:** Simply supported angle-ply ( $-45^\circ / +45^\circ - 45^\circ$ ) square plate: The function  $\bar{\tau}_{zx}(0, a/2, z)$  for  $a/h = 4$ .

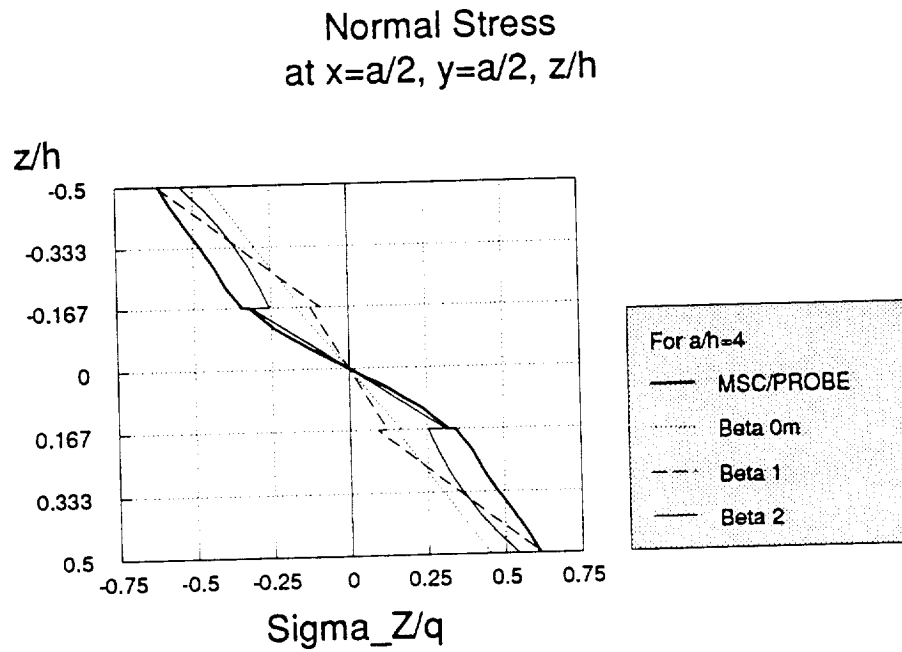


**Figure 5.33:** Simply supported angle-ply ( $-45^\circ / +45^\circ - 45^\circ$ ) square plate: The function  $\bar{\sigma}_z(a/2, a/2, z)$  for  $a/h = 4$ .

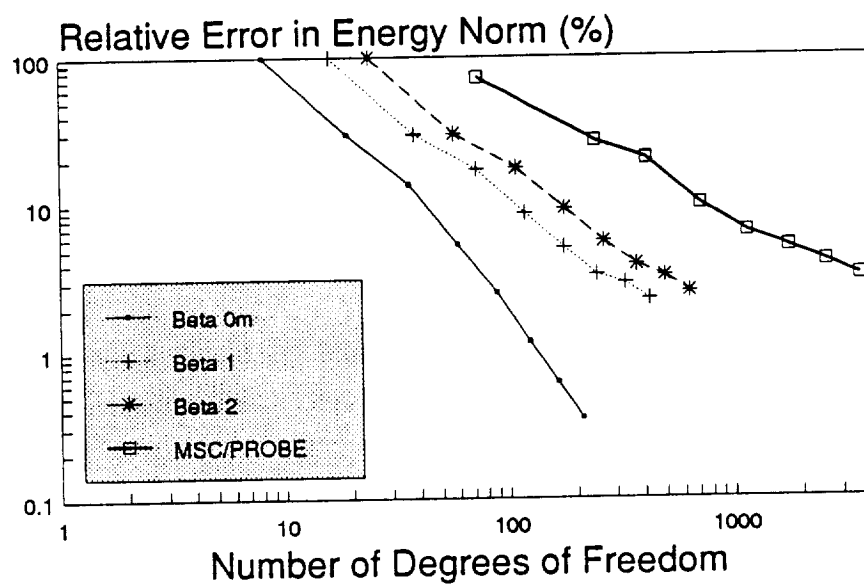


Figure 5.34: Simply supported angle-ply ( $-45^\circ / +45^\circ / -45^\circ$ ) square plate. Estimated relative error in energy norm for  $a/h = 4$ .

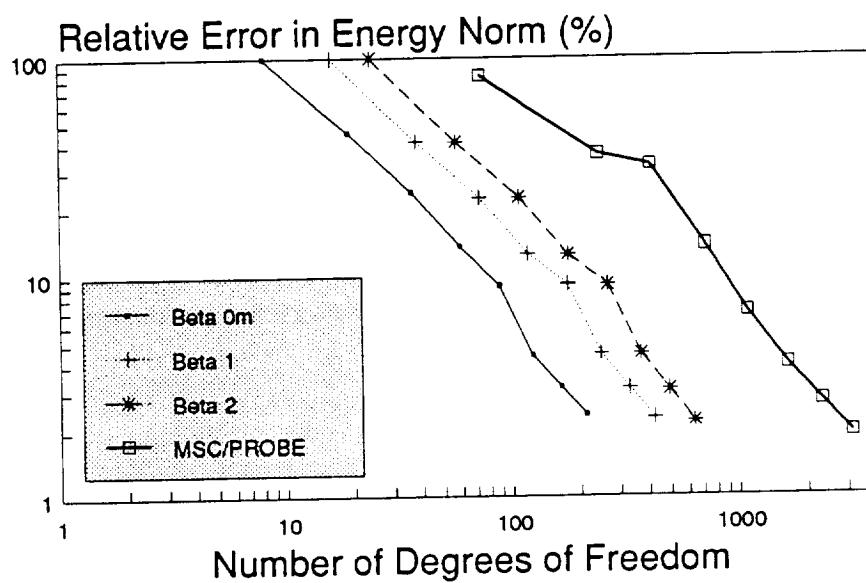


Figure 5.35: Simply supported angle-ply ( $-45^\circ / +45^\circ / -45^\circ$ ) square plate. Estimated relative error in energy norm for  $a/h = 10$ .

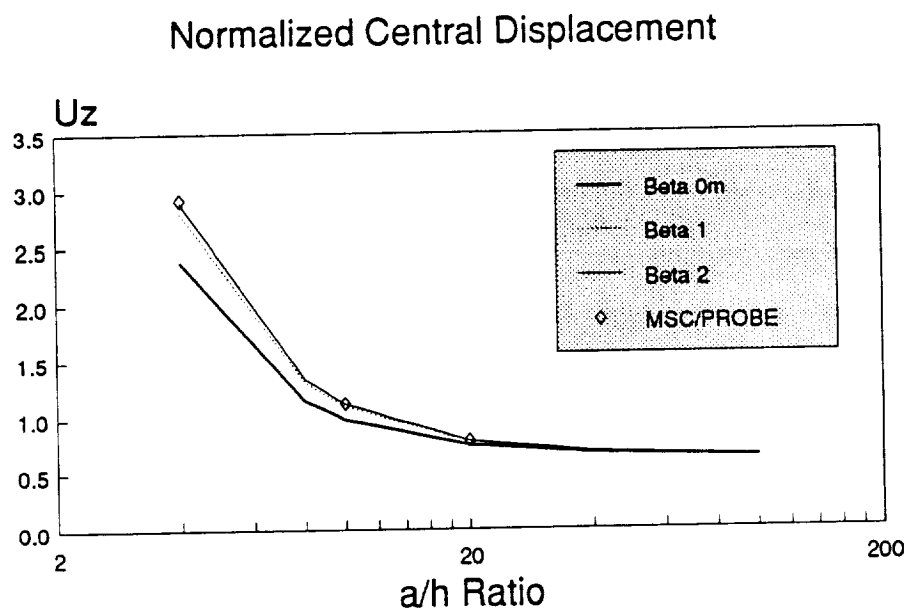


Figure 5.36: Simply supported angle-ply  $(-30/+30/-30)$  square plate: The function  $U_z(a/2, a/2, 0)$ .

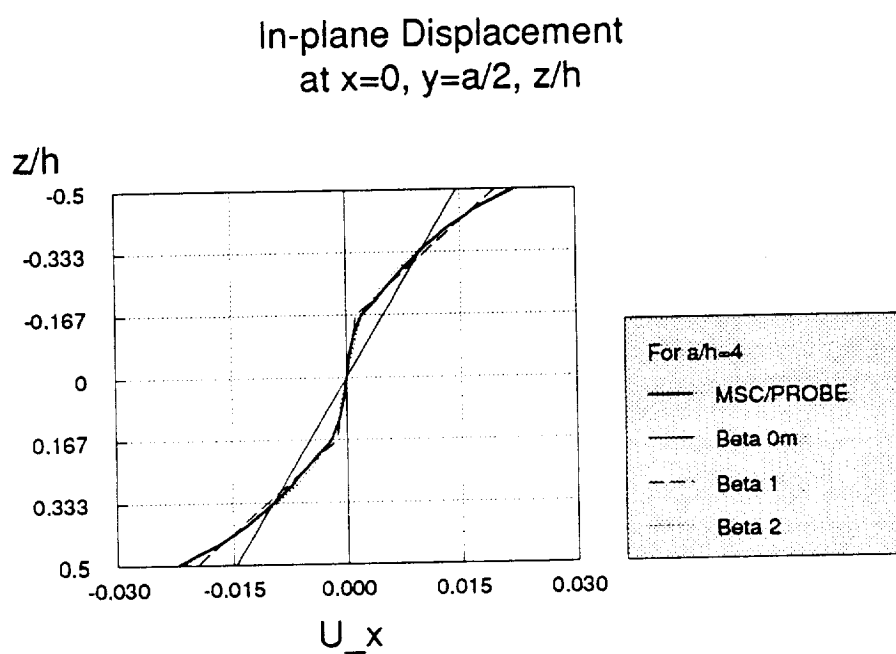


Figure 5.37: Simply supported angle-ply  $(-30/+30/-30)$  square plate: The function  $\bar{u}_x(0, a/2, z)$  for  $a/h = 4$ .

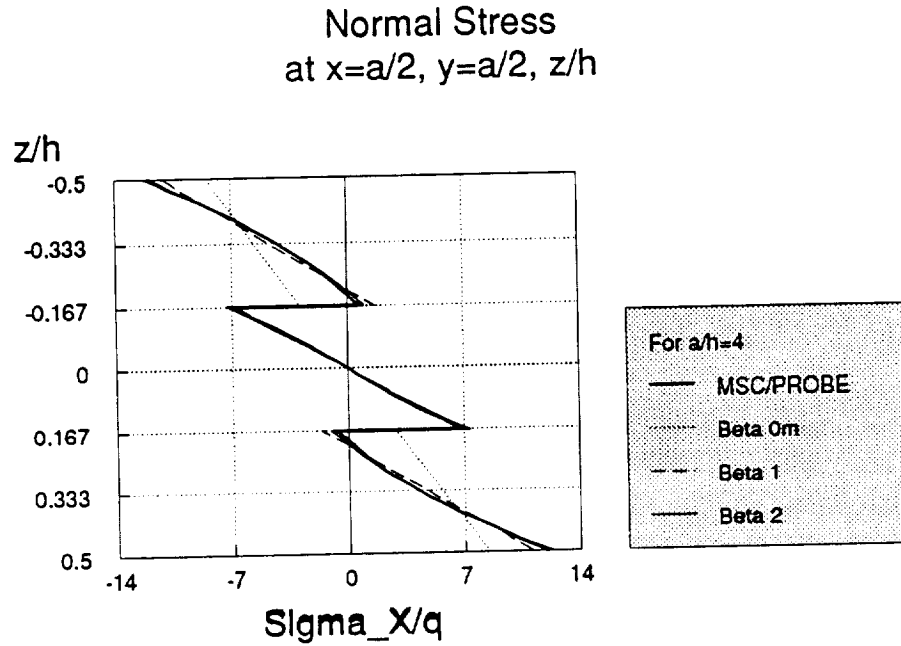


Figure 5.38: Simply supported angle-ply  $(-30/+30/-30)$  square plate: The function  $\bar{\sigma}_x(a/2, a/2, z)$  for  $a/h = 4$ .

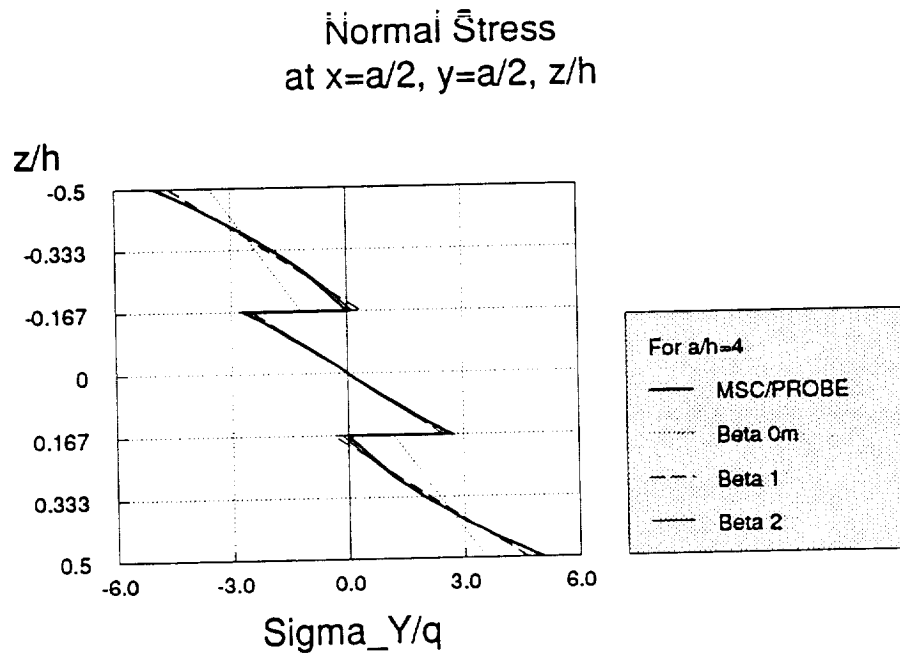


Figure 5.39: Simply supported angle-ply  $(-30/+30/-30)$  square plate: The function  $\bar{\sigma}_y(a/2, a/2, z)$  for  $a/h = 4$ .

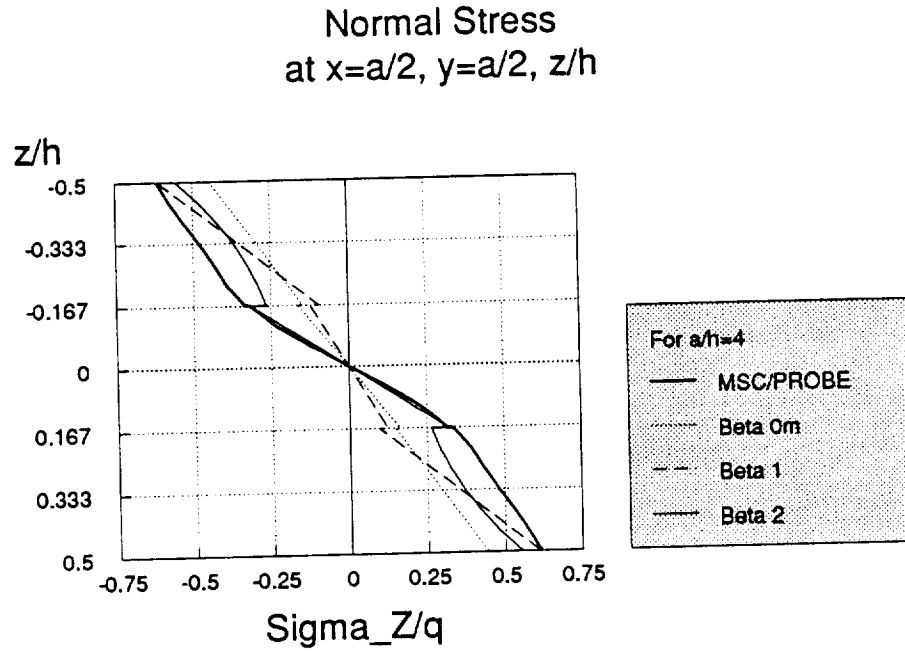


Figure 5.40: Simply supported angle-ply ( $-30^\circ/+30^\circ/-30^\circ$ ) square plate: The function  $\bar{\sigma}_z(a/2, a/2, z)$  for  $a/h = 4$ .

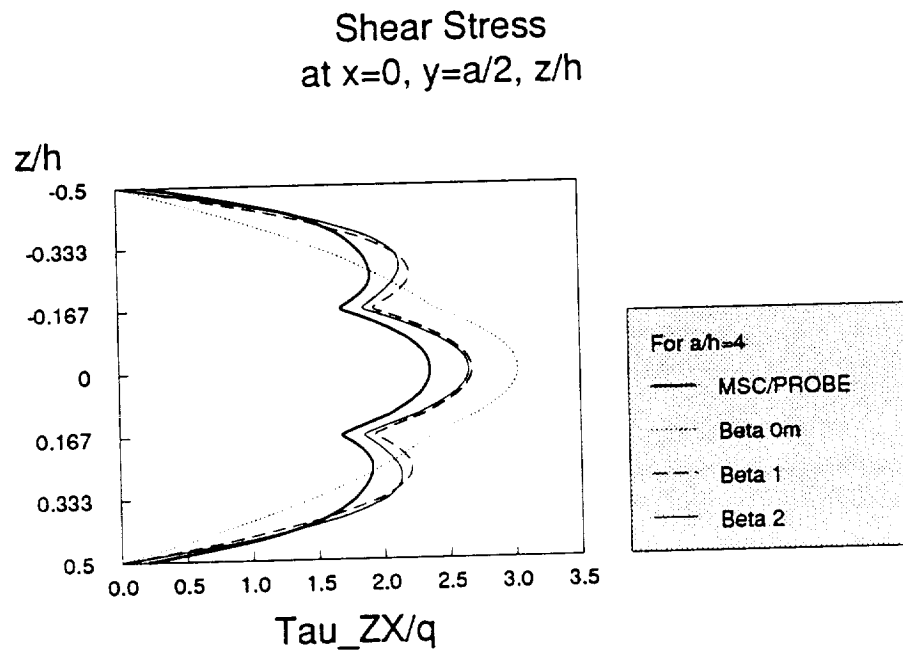
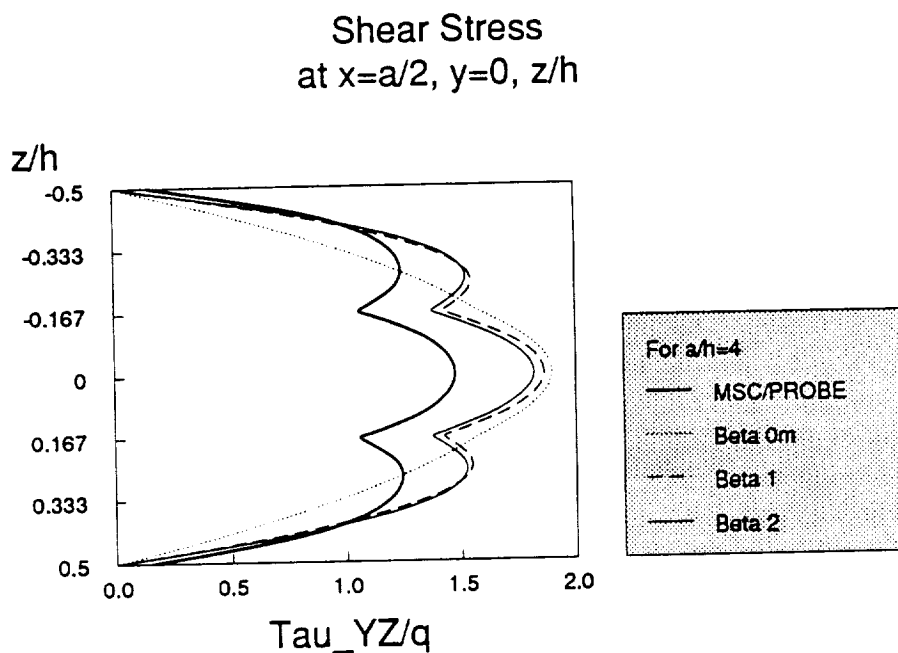
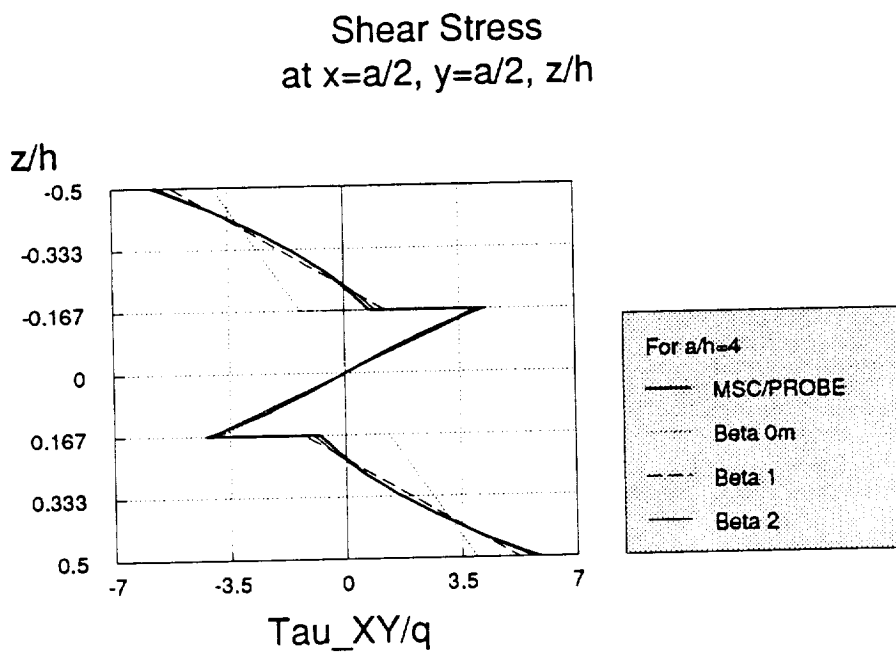


Figure 5.41: Simply supported angle-ply ( $-30^\circ/+30^\circ/-30^\circ$ ) square plate: The function  $\bar{\tau}_{zx}(0, a/2, z)$  for  $a/h = 4$ .





**Figure 5.42:** Simply supported angle-ply  $(-30/+30/-30)$  square plate: The function  $\bar{\tau}_{yz}(a/2, 0, z)$  for  $a/h = 4$ .



**Figure 5.43:** Simply supported angle-ply  $(-30/+30/-30)$  square plate: The function  $\bar{\tau}_{xy}(a/2, 0, z)$  for  $a/h = 4$ .

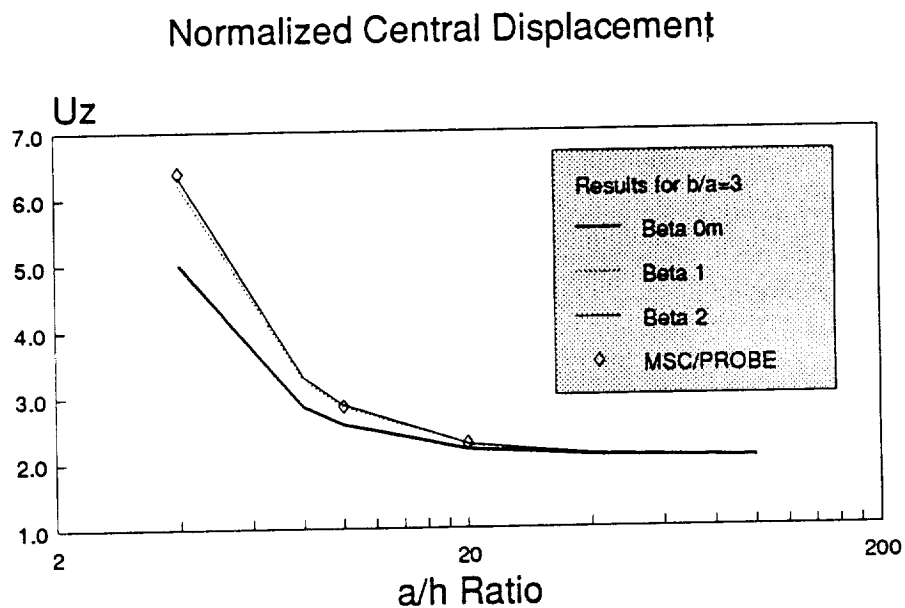


Figure 5.44: Simply supported angle-ply  $(-45^\circ / +45^\circ - 45^\circ)$  rectangular plate:  
The function  $U_z(a/2, a/2, 0)$ .

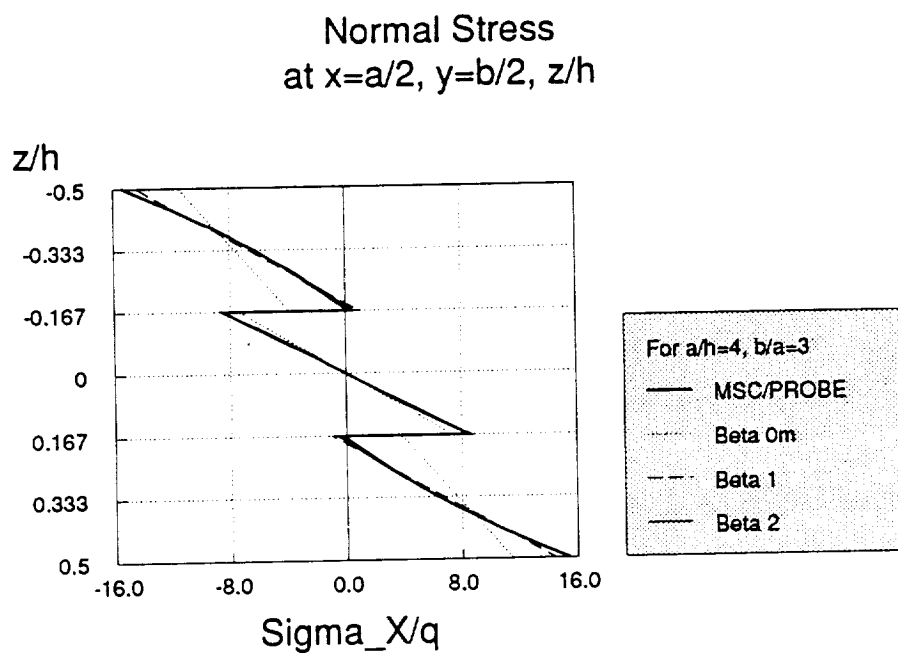
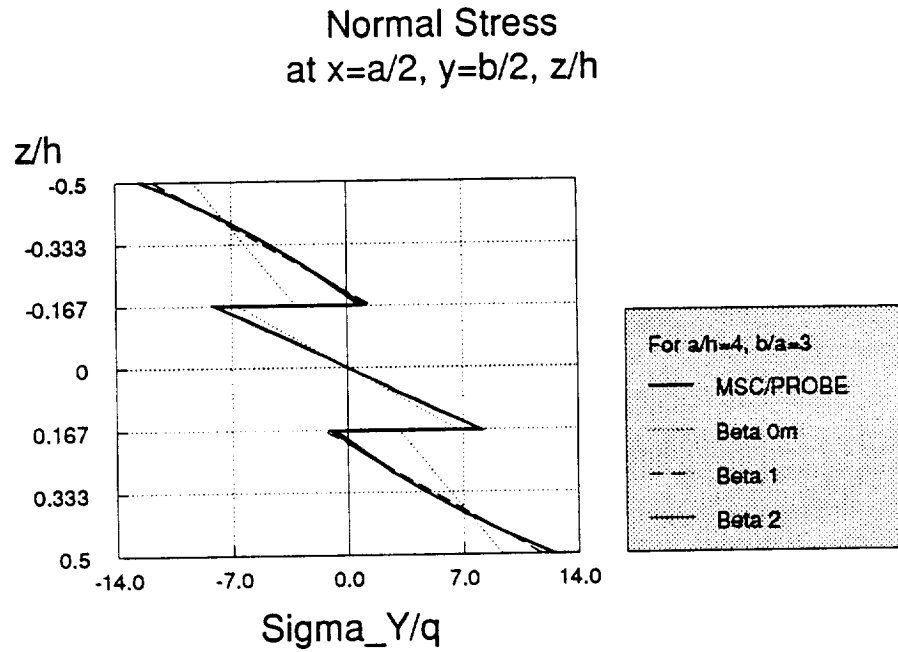
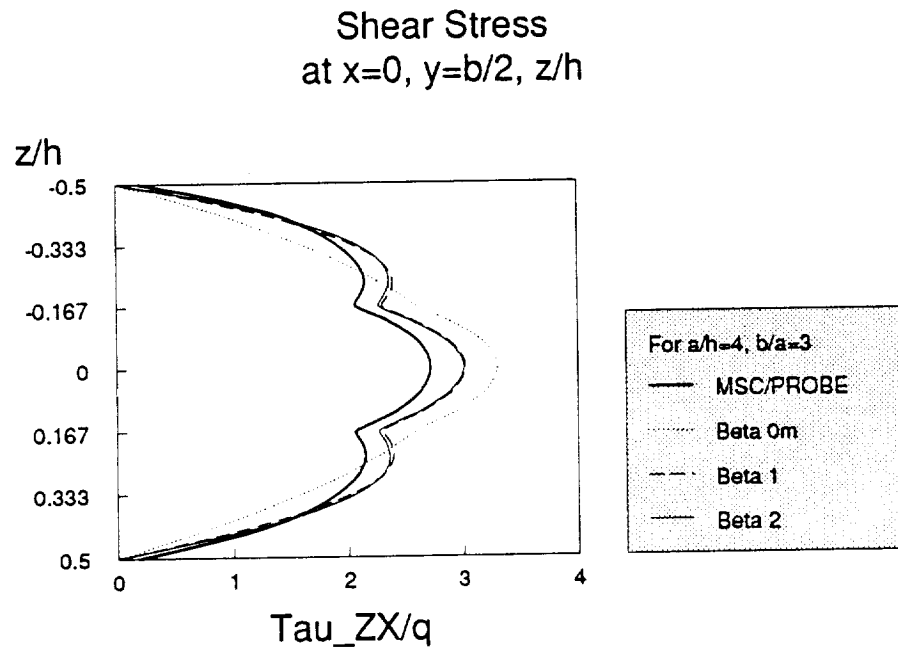


Figure 5.45: Simply supported angle-ply  $(-45^\circ / +45^\circ - 45^\circ)$  rectangular plate:  
The function  $\bar{\sigma}_x(a/2, b/2, z)$  for  $a/h = 4$ .



**Figure 5.46:** Simply supported angle-ply  $(-45^\circ / +45^\circ - 45^\circ)$  rectangular plate:

The function  $\bar{\sigma}_y(a/2, b/2, z)$  for  $a/h = 4$ .



**Figure 5.47:** Simply supported angle-ply  $(-45^\circ / +45^\circ - 45^\circ)$  rectangular plate:

The function  $\bar{\tau}_{zx}(0, b/2, z)$  for  $a/h = 4$ .

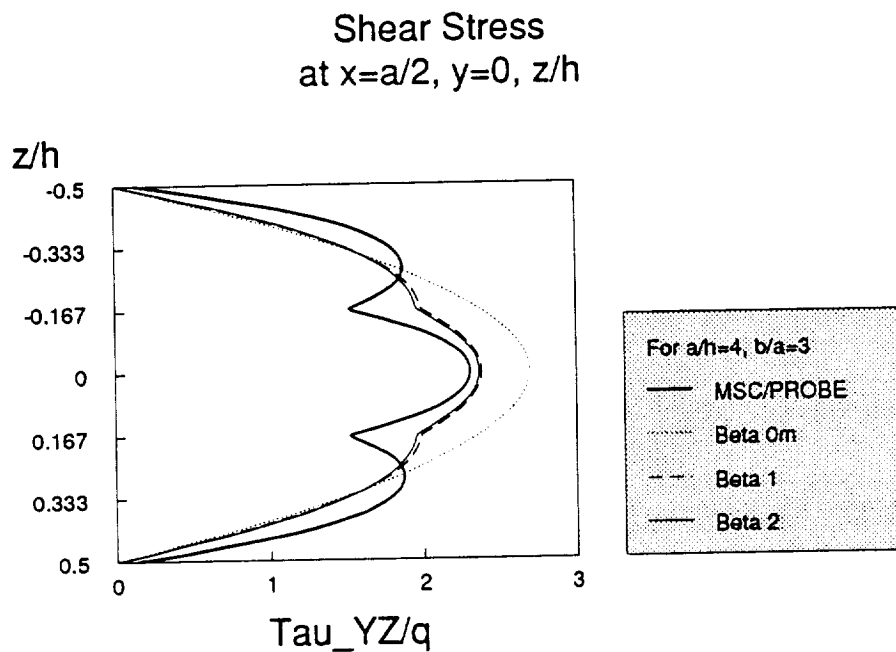


**Figure 5.48:** Simply supported  $-45^\circ / +45^\circ / -45^\circ$  rectangular plate: The function  $\bar{\tau}_{yz}(a/2, 0, z)$  for  $a/h = 4$ .

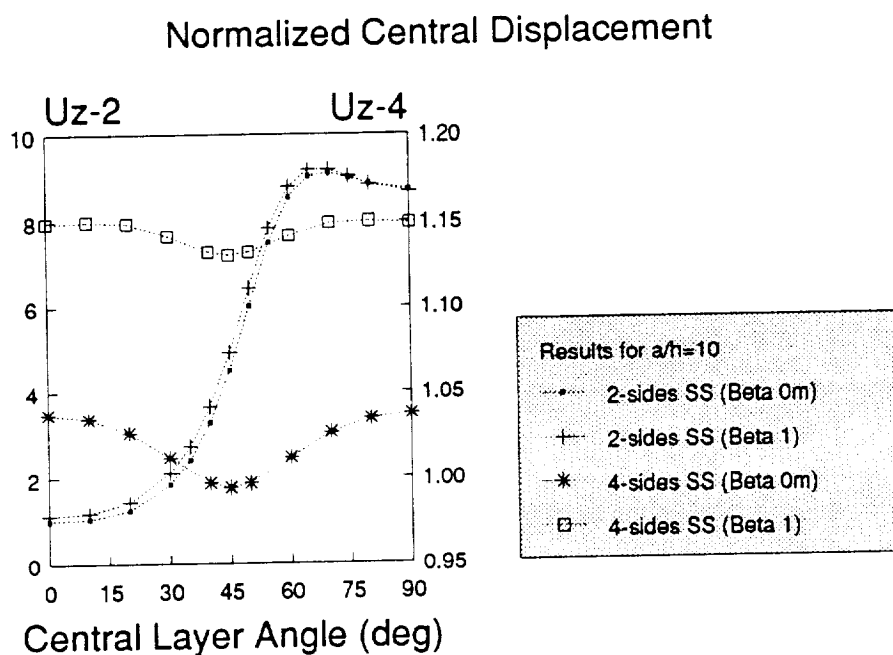


**Figure 5.49:** Square plate. Influence of fiber orientation on a three-ply laminate: The function  $U_z(a/2, a/2, 0)$ .

## 5.4 Conclusions

1. The hierarchic models for mid-plane symmetric laminated plates developed in Chapter 4 have been tested by solving benchmark problems. Good correlation between the proposed hierarchic sequence of models and a three-dimensional reference solution has been found for a wide range of problems investigated.
2. All models converge to the same limit as the problem of three-dimensional elasticity with respect to  $h \rightarrow 0$ . Adjustment of the materials properties of the model characterized by  $\beta^0$  was required to satisfy this requirement. The model characterized by  $\beta^0$  is the Reissner-Mindlin model, generalized for laminated composites, when the modified material properties are used (also known as *first order shear deformation model*).
3. For a fixed plate thickness, as more members were added to the hierarchy the solution was closer to the reference solution. Better approximation is realized for the displacements and for the in-plane stress components even for low order members of the hierarchy than for the transverse shear stresses. At the boundaries, higher order models are required, in general. In some cases models higher than  $\beta^2$  may be necessary to approximate the shear stress distribution as was demonstrated by the examples in connection with the laminated strip in Chapter 3.

4. The class of problems investigated clearly demonstrated the capability of the proposed hierarchic sequence of models in approximating the solution of the problem of three-dimensional elasticity to the desired degree of accuracy. Thus, these models are suitable for obtaining both the structural and the detailed response of laminated plates.

## Chapter 6

### Summary and Conclusions

The objective of this research has been to develop mathematical models for the analysis of laminated plates. The choice of the proper model for a particular application is problem dependent, that is, depends on the exact solution of the corresponding fully three-dimensional problem, which in this investigation was the problem of three-dimensional elasticity; the goals of computation; the degree of precision required, and the method by which the data of interest are computed.

In general, the solution of the problem of three-dimensional elasticity in the smooth interior regions is very close to the solution corresponding to the low order model, whereas the solution near the boundaries is more complicated and thus requires the use of higher models. Typically, investigation of structural response can be performed with low order models but the investigation of strength response requires high order models.

For these reasons models have to be chosen adaptively. If the models are simple (*classical plate model, first-order shear-deformation model*) they are economical and provide reasonable approximation to the structural response, but fail to provide accurate representation of the strength response. If the model is more elaborate (*high-order shear-deformation models, discrete-layer models*), they provide better strength response at the expense of greater computational complexity, even for those cases in which structural response was the only goal of the computation.

Hierarchic sequence of models make it possible to select the model best suited for a particular analysis. In this investigation the question of how models should be selected from a particular hierarchic sequence was not addressed. The main idea is relatively simple. The transverse variation of the displacement functions should be selected such that they are orthogonal or very nearly orthogonal in the energy space. In that case the size of the field functions  $u_{x|i}$ ,  $u_{y|i}$ ,  $u_{z|i}$ , measured in the energy norm, will give an indication of the importance of the  $i$ th term in the hierarchy. One can expect that as  $i$  increases the size of  $u_{x|i}$ ,  $u_{y|i}$ ,  $u_{z|i}$  will decrease.

The derivation of a hierarchic sequence of models for laminated plates was first outlined for the particular case of cylindrical bending (the strip problem) and their performance was demonstrated on the basis of the degree to which the equilibrium equations of the two-dimensional elasticity are satisfied. The powers of the parameter  $\beta$ , representing the degree to which the equilibrium equations of are satisfied, have been used to identify members of the hierarchic sequence.



The numerical implementation of this hierarchic sequence of models proved their capability of approaching the solution of the problem of two-dimensional elasticity to the required degree of accuracy.

Hierarchic models for mid-plane symmetric laminated plates were also developed based on a single parameter  $\beta$ . The powers of the parameter  $\beta$ , representing the degree to which the equilibrium equations of three-dimensional elasticity are satisfied, have been used for identifying members of the hierarchic sequence. The selection of a displacement field based on a single parameter, combined with the proper selection of the constants in the transverse shape functions, resulted in a sequence of models in which the number of fields added for each increment in the power of  $\beta$  is three. In this way the increase in complexity, as more members are added to the hierarchy, was minimized.

In the interest of computational efficiency, the hierarchic sequence of models has been extended downward to include the models characterized by  $\beta^0$  and  $\beta^1$ . This required a modification of material properties, which is analogous to the generally accepted modification of material properties used in the Reissner-Mindlin model for homogeneous isotropic plates. In fact, the model characterized by  $\beta^0$  is the Reissner-Mindlin model, generalized for laminated plates, when the modified material properties are used. In the special case, when the shear modulus is independent of  $z$ , the hierarchic model is the Reissner-Mindlin model. The shear

correction factor can be assigned arbitrarily since the requirements set for hierarchic models are satisfied independently of the shear correction factor.

Good correlation between the proposed hierarchic sequence of models and a three-dimensional reference solution (MSC/PROBE) has been found for a wide range of problems investigated. The class of problems investigated clearly demonstrated the capability of the proposed hierarchic sequence of models in approximating the solution of the problem of three-dimensional elasticity to the desired degree of accuracy. Thus the hierarchic framework described in this work allows the development of reliable predictive capabilities for the structural and strength responses of structural components made of laminated composites.

## Chapter 7

### Acknowledgements

I wish to thank Dr. Barna Szabó for his assistance, guidance and encouragement. Also for his readiness to share his knowledge and for his enthusiasm and support.

Special gratitude is extended to Professor Ivo Babuška for his insights and guidance. His seminal contributions have made this work possible.

I also wish to thank Dr. Christopher Schwab from the University of Maryland for his suggestions and ideas during the development of the formulation of the plate models.

To the best secretary of Washington University, Mrs. Ann Lacy, who was always ready to help, I give much thanks for her assistance in preparing both my proposal and this dissertation.

Finally, I want to thank my wife Liliana and my children Lisa and Luis for their encouragement and support while I was carrying out this work.

## Appendix A

### Laminated Strip: Expansion of the Equilibrium Equations up to the Third Power of $\beta$

Differentiating equations (2.31) to (2.33) with respect to  $\beta$  three times and letting  $\beta = 0$ , the following equations are obtained for the real parts:

$$(E_6\phi'_{a3})' - (E_6\psi_{b2})' - E_2\psi'_{b2} - E_1\phi_{a1} = 0 \quad (\text{A.1})$$

$$(E_3\psi'_{a3})' - E_6\phi'_{b2} - (E_2\phi_{b2})' - E_6\psi_{a1} = 0. \quad (\text{A.2})$$

Start with (A.1) and from (2.54) and (2.74):

$$\begin{aligned} (E_6\phi'_{a3})' &= (E_6\psi_{b2})' + E_2\psi'_{b2} + E_1\phi_{a1} \\ (E_6\phi'_{a3})' &= (E_6\psi_{b2})' - E_2 \left\{ a_1 \left[ \frac{y}{E_3} + \frac{E_2}{E_3} F_0 \right] + d_0 \frac{E_2}{E_3} y \right\} + E_1 \{ a_1 F_0 + d_0 y \} \\ (E_6\phi'_{a3})' &= (E_6\psi_{b2})' + a_1 \left\{ F_0 \left( E_1 - \frac{E_2^2}{E_3} \right) - \frac{E_2}{E_3} y \right\} + d_0 \left\{ \left( E_1 - \frac{E_2^2}{E_3} \right) y \right\}. \end{aligned}$$

Integrating once:

$$E_6\phi'_{a3} = E_6(d_2 - a_1 F_1 - d_0 F_3) + a_1 \int_0^y \left[ F_0 \left( E_1 - \frac{E_2^2}{E_3} \right) - \frac{E_2}{E_3} y \right] dy$$

$$\begin{aligned}
& +d_0 \int_0^y \left( E_1 - \frac{E_2^2}{E_3} \right) y \, dy + a_3 \\
\phi'_{a3} &= d_2 + a_1 \left\{ -F_1 + \frac{1}{E_6} \int_0^y \left[ F_0 \left( E_1 - \frac{E_2^2}{E_3} \right) - \frac{E_2}{E_3} y \right] dy \right\} \\
& +d_0 \left\{ -F_3 + \frac{1}{E_6} \int_0^y \left( E_1 - \frac{E_2^2}{E_3} \right) y \, dy \right\} + \frac{a_3}{E_6}
\end{aligned}$$

then, integrating again:

$$\phi_{a3} = d_2 y + a_3 F_0(y) + a_1 F_2(y) + d_0 F_4(y) \quad (\text{A.3})$$

where:

$$F_4(y) = \int_0^y \left\{ \frac{1}{E_6(t)} \int_0^t \left( E_1(t) - \frac{E_2^2(t)}{E_3(t)} \right) t \, dt - F_3(t) \right\} dt. \quad (\text{A.4})$$

From (A.2), and using (2.62) and (2.72):

$$\begin{aligned}
(E_3 \psi'_{a3})' &= E_6 \phi'_{b2} + (E_2 \phi_{b2})' + E_6 \psi_{a1} \\
(E_3 \psi'_{a3})' &= b_0 \int_0^y \left[ \left( E_1 - \frac{E_2^2}{E_3} \right) F_0 - \frac{E_2}{E_3} y \right] dy - E_6 (c_1 + b_0 F_1) + b_2 \\
& + (E_2 \phi_{b2})' + E_6 (b_0 F_1 + c_1)
\end{aligned}$$

integrating once:

$$\begin{aligned}
E_3 \psi'_{a3} &= b_0 \int_0^y \left\{ \int_0^y \left[ \left( E_1 - \frac{E_2^2}{E_3} \right) F_0 - \frac{E_2}{E_3} y \right] dy \right\} dy + b_2 y + E_2 \phi_{b2} + d \\
\psi'_{a3} &= b_0 \frac{1}{E_3} \int_0^y \left\{ \int_0^y \left[ \left( E_1 - \frac{E_2^2}{E_3} \right) F_0 - \frac{E_2}{E_3} y \right] dy \right\} dy + b_2 \frac{y}{E_3} \\
& + b_0 \frac{E_2}{E_3} F_2 - c_1 \frac{E_2}{E_3} y + b_2 \frac{E_2}{E_3} F_0 + \frac{d}{E_3}
\end{aligned}$$

$$\begin{aligned}\psi'_{a3} = & b_0 \left\{ \frac{1}{E_3} \int_0^y \left\{ \int_0^y \left[ \left( E_1 - \frac{E_2^2}{E_3} F_0 \right) - \frac{E_2}{E_3} y \right] dy \right\} dy + \frac{E_2}{E_3} F_2 \right\} \\ & + b_2 \left\{ \frac{y}{E_3} + \frac{E_2}{E_3} F_0 \right\} - c_1 \frac{E_2}{E_3} y + \frac{d}{E_3}\end{aligned}$$

integrating again:

$$\begin{aligned}\psi_{a3} = & b_0 \int_0^y \left\{ \frac{1}{E_3} \int_0^y \left\{ \int_0^y \left[ \left( E_1 - \frac{E_2^2}{E_3} \right) F_0 - \frac{E_2}{E_3} y \right] dy \right\} dy + \frac{E_2}{E_3} F_2 \right\} dy \\ & + b_2 \underbrace{\int_0^y \left( \frac{E_2}{E_3} F_0 + \frac{y}{E_3} \right) dy}_{F_1} - c_1 \underbrace{\int_0^y \frac{E_2}{E_3} y dy}_{F_3} + d \int_0^y \frac{dy}{E_3} + f.\end{aligned}$$

Because of symmetry  $d = 0$ , and calling  $b_3 = f$ , we finally have:

$$\psi_{a3}(y) = b_0 F_5(y) + b_2 F_1(y) - c_1 F_3(y) + b_3 \quad (\text{A.5})$$

where:

$$\begin{aligned}F_5(y) = & \int_0^y \left\{ \frac{1}{E_3(t)} \int_0^y \left( \int_0^y \left[ \left( E_1(t) - \frac{E_2^2(t)}{E_3(t)} \right) F_0(t) - \frac{E_2(t)}{E_3(t)} t \right] dt \right) dt \right. \\ & \left. + \frac{E_2}{E_3} F_2(t) \right\} dt.\end{aligned} \quad (\text{A.6})$$

Additional transverse functions, to satisfy the equilibrium equations up to higher power of  $\beta$ , are found following the same procedure described herein.

## Appendix B

### Laminated strips: Computation of the Transverse Functions for a 3-ply Laminate

The transverse functions  $F_0(y)$ ,  $F_1(y)$ ,  $F_2(y)$  and  $F_3(y)$  are integrated for the 3-ply laminate problem indicated in Figure B.1. The material properties are assumed to be constant within each lamina.

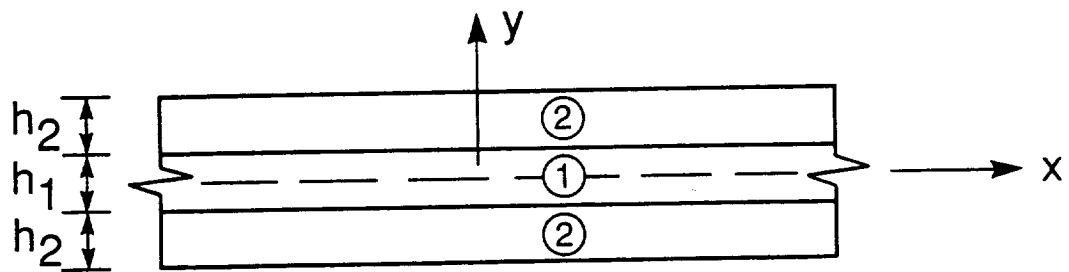


Figure B.1: Three-ply laminate. Notation.

a)  $F_0(y)$ : from (2.39)

$$F_0(y) = \int_0^y \frac{dt}{E_6(t)}. \quad (\text{B.1})$$

For lamina 1, we have

$$F_0(y) = \frac{y}{E_{61}}.$$

It is convenient to factor out a coefficient to avoid working with very small numbers, so we will use the largest value of the material stiffness matrix on any lamina in the laminate. Calling this quantity  $E_c$ , the new  $F_0(y)$  will be:

$$\bar{F}_0(y) = E_c F_0(y) = \frac{E_c}{E_{61}} y.$$

Furthermore the overbar can be dropped since the  $E_c$  multiplying  $F_0(y)$  can be absorbed in the constant  $a_0$  that multiplies  $F_0(y)$  in the expression for  $\phi_0(y)$ .

For lamina 2, we have:

$$F_0(y) = \int_0^{h_1/2} \frac{E_c}{E_{61}} dt + \int_{h_1/2}^y \frac{E_c}{E_{62}} dt = \frac{E_c}{E_{61}} \frac{h_1}{2} + \frac{E_c}{E_{62}} \left( y - \frac{h_1}{2} \right)$$

or

$$F_0(y) = \frac{E_c}{E_{62}} y + \frac{h_1}{2} \left( \frac{E_c}{E_{61}} - \frac{E_c}{E_{62}} \right).$$

The expressions of  $F_0(y)$  for layers 1 and 2 can be summarized as follows:

$$F_0(y) = \begin{cases} p_0 y \\ p_1 + p_2 y \end{cases} \quad (\text{B.2})$$

where:

$$p_0 = \frac{E_c}{E_{61}} \quad (\text{B.3})$$



$$p_1 = \frac{h_1}{2} \left( \frac{E_c}{E_{61}} - \frac{E_c}{E_{62}} \right) \quad (\text{B.4})$$

$$p_2 = \frac{E_c}{E_{62}}. \quad (\text{B.5})$$

b)  $F_1(y)$ : from (2.64) we have

$$F_1(y) = \int_0^y \left( \frac{E_2(t)}{E_3(t)} F_0(t) + \frac{t}{E_3(t)} \right) dt. \quad (\text{B.6})$$

Using the same factor as before, we can write:

$$F_1(y) = \int_0^y \left( \frac{E_2(t)}{E_3(t)} F_0(t) + \frac{E_c}{E_3(t)} t \right) dt. \quad (\text{B.7})$$

For lamina 1:

$$F_1(y) = \int_0^y \left( \frac{E_{21}}{E_{31}} \frac{E_c}{E_{61}} + \frac{E_c}{E_{31}} \right) t dt = \left( \frac{E_{21}}{E_{31}} \frac{E_c}{E_{61}} + \frac{E_c}{E_{31}} \right) \frac{y^2}{2} = q_0 y^2.$$

For lamina 2:

$$F_1(y) = \int_0^{h_1/2} \left( \frac{E_{21}}{E_{31}} \frac{E_c}{E_{61}} + \frac{E_c}{E_{31}} \right) t dt + \int_{h_1/2}^y \left[ \frac{E_{22}}{E_{32}} (p_1 + p_2 t) + \frac{E_c}{E_{32}} t \right] dt$$

or

$$F_1(y) = q_0 \frac{h_1^2}{4} + \left[ \left( \frac{E_{22}}{E_{32}} p_2 + \frac{E_c}{E_{32}} \right) \frac{t^2}{2} + \frac{E_{22}}{E_{32}} p_1 t \right]_{h_1/2}^y$$

Finally:

$$F_1(y) = \begin{cases} q_0 y^2 \\ q_1 + q_2 y + q_3 y^2 \end{cases} \quad (\text{B.8})$$

where

$$q_0 = \frac{1}{2} \frac{E_c}{E_{31}} \left( \frac{E_{21}}{E_{61}} + 1 \right) \quad (\text{B.9})$$

$$q_1 = \frac{q_0 h_1^2}{4} - \left( \frac{E_{22}}{E_{32}} p_2 + \frac{E_c}{E_{32}} \right) \frac{h_1^2}{8} - \frac{E_{22}}{E_{32}} p_1 \frac{h_1}{2} \quad (\text{B.10})$$

$$q_2 = \frac{E_{22}}{E_{32}} p_1 \quad (\text{B.11})$$

$$q_3 = \frac{1}{2} \left( \frac{E_{22}}{E_{32}} p_2 + \frac{E_c}{E_{32}} \right). \quad (\text{B.12})$$

c)  $F_2(y)$ : from (2.75), and using (B.2) and (B.8)

$$F_2(y) = \int_0^y \left\{ \frac{1}{E_6(t)} \int_0^y \left[ \left( E_1(t) - \frac{E_2^2(t)}{E_3(t)} \right) F_0(t) - \frac{E_2(t)}{E_2(t)} t \right] dt - F_1(t) \right\} dt. \quad (\text{B.13})$$

For lamina 1:

$$\begin{aligned} F_{2(y)} &= \int_0^y \left\{ \frac{1}{E_{61}} \int_0^y \left[ \left( E_{11} - \frac{E_{21}^2}{E_{31}} \right) p_0 - \frac{E_{21}}{E_{31}} \right] t dt - q_0 t^2 \right\} dt \\ &= \int_0^y \left\{ \frac{1}{E_{61}} \left[ \left( E_{11} - \frac{E_{21}^2}{E_{31}} \right) p_0 - \frac{E_{21}}{E_{31}} \right] \frac{t^2}{2} - q_0 t^2 \right\} dt \\ &= \left\{ \frac{1}{2E_{61}} \left[ \left( E_{11} - \frac{E_{21}^2}{E_{31}} \right) p_0 - \frac{E_{21}}{E_{31}} \right] - q_0 \right\} \frac{y^3}{3} = t_0 y^3. \end{aligned}$$

The integration across lamina 2 is performed in a similar way as before, and we finally get:

$$F_2(y) = \begin{cases} t_0 y^3 \\ t_1 + t_2 y + t_3 y^2 + t_4 y^3 \end{cases} \quad (\text{B.14})$$

where:

$$t_0 = \frac{1}{3} \left( \frac{r_0}{E_{61}} - q_0 \right) \quad (\text{B.15})$$

$$t_1 = t_0 \frac{h_1^3}{8} - \left( \frac{r_1}{E_{62}} - q_1 \right) \frac{h_1}{2} - \left( \frac{r_2}{E_{62}} - q_2 \right) \frac{h_1^2}{8} - \left( \frac{r_3}{E_{62}} - q_3 \right) \frac{h_1^3}{24} \quad (\text{B.16})$$

$$t_2 = \frac{r_1}{E_{62}} - q_1 \quad (\text{B.17})$$

$$t_3 = \frac{1}{2} \left( \frac{r_2}{E_{62}} - q_2 \right) \quad (\text{B.18})$$

$$t_4 = \frac{1}{3} \left( \frac{r_3}{E_{62}} - q_3 \right) \quad (\text{B.19})$$

$$r_0 = \frac{1}{2} \left[ \left( E_{11} - \frac{E_{21}^2}{E_{31}} \right) p_0 - \frac{E_{21}}{E_{31}} \right] \quad (\text{B.20})$$

$$r_1 = r_0 \frac{h_1^2}{4} - \left[ \left( E_{12} - \frac{E_{22}^2}{E_{32}} \right) p_2 - \frac{E_{22}}{E_{32}} \right] \frac{h_1^2}{8} - \left( E_{12} - \frac{E_{22}^2}{E_{32}} \right) p_1 \frac{h_1}{2} \quad (\text{B.21})$$

$$r_2 = \left( E_{12} - \frac{E_{22}^2}{E_{32}} \right) p_1 \quad (\text{B.22})$$

$$r_3 = \frac{1}{2} \left[ \left( E_{12} - \frac{E_{22}^2}{E_{32}} \right) p_2 - \frac{E_{22}}{E_{32}} \right] \quad (\text{B.23})$$

d)  $F_3(y)$ : from (2.76)

$$F_3(y) = \int_0^y \frac{E_2(t)}{E_3(t)} t dt. \quad (\text{B.24})$$

Performing the integration across lamina 1 and 2 we get:

$$F_3(y) = \begin{cases} z_0 y^2 \\ z_1 + z_2 y^2 \end{cases} \quad (\text{B.25})$$

where:

$$z_0 = \frac{1}{2} \frac{E_{21}}{E_{31}} \quad (\text{B.26})$$

$$z_1 = \left[ \frac{z_0}{4} - \frac{1}{8} \frac{E_{22}}{E_{32}} \right] h_1^2 \quad (\text{B.27})$$

$$z_2 = \frac{1}{2} \frac{E_{22}}{E_{32}}. \quad (\text{B.28})$$

The integration of these and all other transverse functions can be performed numerically, and for any number of layers. The direct integration for a 3-ply symmetric laminate was performed to show the polynomial degree of some of the functions, and to solve the example problems described in Chapter 3.

## Appendix C

### Laminated Strip: Lamina Stiffness Submatrices

Consider the two dimensional model of a laminated strip shown in Figure C.1.

From equation (3.10) and (3.11), the stiffness matrix of lamina  $k$  is given by:

$$[K]^{(k)} = \int_0^\ell \int_{y_k}^{y_{k+1}} [Q]^T [E]^{(k)} [Q] dy dx \quad (C.1)$$

where  $[Q]$  is given in (3.8) and  $[E]^{(k)}$  by (3.12). When the equilibrium equations are satisfied up the second power of  $\beta$ , a total of 36 submatrices (only 21 are different) are contained in (C.1). Each submatrix of (C.1) is obtained in the following way:

$$[K_{11}] = \int_0^\ell \int_{y_k}^{y_{k+1}} [Q_{11}^T \ Q_{11}^T \ Q_{31}^T] [E]^{(k)} \begin{Bmatrix} Q_{11} \\ Q_{21} \\ Q_{31} \end{Bmatrix} dy dx. \quad (C.2)$$

Using the mapping (3.6), from (3.7):  $dx = \frac{\ell}{2} d\xi$  so we can write:

$$[K_{11}] = \frac{\ell}{2} \int_{-1}^{+1} \int_{y_k}^{y_{k+1}} \left[ Q_{11}^T (E_1^{(k)} Q_{11} + E_4^{(k)} Q_{31}) + Q_{31}^T (E_4^{(k)} Q_{11} + E_6^{(k)} Q_{31}) \right] dy d\xi$$

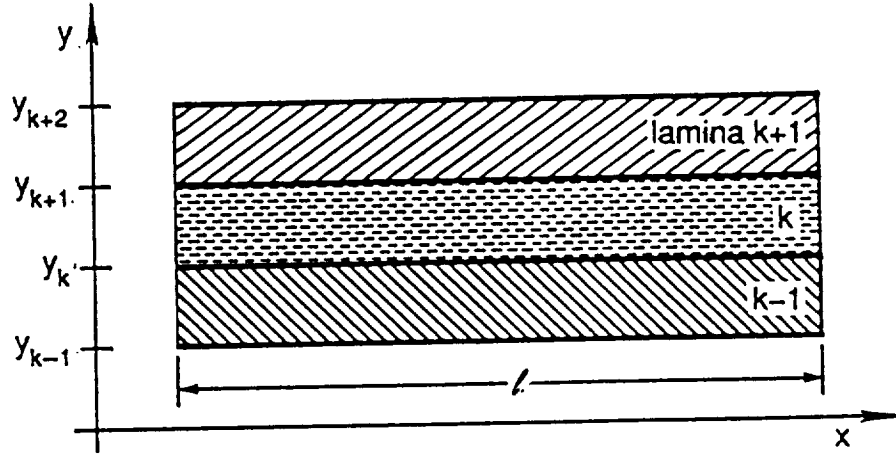


Figure C.1: Laminated Strip. Notation

$$\begin{aligned}
 = & E_1^{(k)} \frac{\ell}{2} \int_{-1}^{+1} \int_{y_k}^{y_{k+1}} \left( \frac{2y}{\ell} \right)^2 \{N'\} [N'] dy d\xi + E_4^{(k)} \frac{\ell}{2} \int_{-1}^{+1} \int_{y_k}^{y_{k+1}} \frac{2y}{\ell} \{N'\} [N] dy d\xi \\
 & + E_4^{(k)} \frac{\ell}{2} \int_{-1}^{+1} \int_{y_k}^{y_{k+1}} \frac{2y}{\ell} \{N\} [N'] dy d\xi + E_6^{(k)} \frac{\ell}{2} \int_{-1}^{+1} \int_{y_k}^{y_{k+1}} \{N\} [N] dy d\xi.
 \end{aligned}$$

Evaluating the integrals across lamina  $k$ , and using the definitions of  $[K_{st}]$ ,  $[M_{st}]$  and  $[L_{st}]$  given in Section 3.1, we finally have for  $[K_{11}]$ :

$$\begin{aligned}
 [K_{11}] = & \frac{2}{3\ell} (y_{k+1}^3 - y_k^3) E_1^{(k)} [K_{st}] + \frac{E_4^{(k)}}{2} (y_{k+1}^2 - y_k^2) ([L_{st}] + [L_{st}]^T) \\
 & + \frac{E_6^{(k)}}{2} h_k \ell [M_{st}].
 \end{aligned} \tag{C.3}$$

Similarly, the other submatrices of (C.1) are:

First row:

$$[K_{12}] = \frac{E_4^{(k)}}{\ell} (y_{k+1}^2 - y_k^2) [K_{st}] + E_6^{(k)} h_k [L_{st}]^T \tag{C.4}$$

$$[K_{13}] = \frac{2}{\ell} E_1^{(k)} H_1 [K_{st}] + E_4^{(k)} (H_2 [L_{st}] + H_3 [L_{st}]^T) + \frac{\ell}{2} E_6^{(k)} H_4 [M_{st}] \tag{C.5}$$

$$[K_{14}] = E_2^{(k)} H_8 [L_{st}] + \frac{2}{\ell} E_4^{(k)} H_9 [K_{st}] + \frac{\ell}{2} E_5^{(k)} H_{10} [M_{st}] + E_6^{(k)} H_{11} [L_{st}]^T \tag{C.6}$$

$$[K_{15}] = \frac{2}{\ell} E_1^{(k)} H_{34} [K_{st}] + E_4^{(k)} (H_{35} [L_{st}] + H_{36} [L_{st}]^T) + \frac{\ell}{2} E_6^{(k)} H_{37} [M_{st}] \tag{C.7}$$

$$[K_{16}] = \frac{2}{\ell} E_4^{(k)} H_{24}[L_{st}] + E_2^{(k)} H_{25}[L_{st}] + E_6^{(k)} H_{26}[L_{st}]^T + \frac{\ell}{2} E_5^{(k)} H_{15}[M_{st}]. \quad (C.8)$$

Second row:

$$[K_{22}] = \frac{2}{\ell} h_k E_6^{(k)} [K_{st}] \quad (C.9)$$

$$[K_{23}] = \frac{2}{\ell} E_4^{(k)} H_3[K_{st}] + E_6^{(k)} H_4[L_{st}] \quad (C.10)$$

$$[K_{24}] = E_5^{(k)} H_{10}[L_{st}] + \frac{2}{\ell} E_6^{(k)} H_{11}[K_{st}] \quad (C.11)$$

$$[K_{25}] = \frac{2}{\ell} E_4^{(k)} H_{36}[K_{st}] + E_6^{(k)} H_{37}[L_{st}] \quad (C.12)$$

$$[K_{26}] = \frac{2}{\ell} E_6^{(k)} H_{26}[K_{st}] + E_5^{(k)} H_{15}[L_{st}]. \quad (C.13)$$

Third row:

$$[K_{33}] = \frac{2}{\ell} E_1^{(k)} H_5[K_{st}] + E_4^{(k)} H_6 ([L_{st}] + [L_{st}]^T) + \frac{\ell}{2} E_6^{(k)} H_7[M_{st}] \quad (C.14)$$

$$[K_{34}] = \frac{2}{\ell} E_4^{(k)} H_{16}[K_{st}] + E_6^{(k)} H_{17}[L_{st}]^T + E_2^{(k)} H_{18}[L_{st}] + \frac{\ell}{2} E_5^{(k)} H_{19}[M_{st}] \quad (C.15)$$

$$[K_{35}] = \frac{2}{\ell} E_1^{(k)} H_{38}[K_{st}] + (H_{39}[L_{st}] + H_{40}[L_{st}]^T) + \frac{\ell}{2} E_6^{(k)} H_{41}[M_{st}] \quad (C.16)$$

$$[K_{36}] = \frac{2}{\ell} E_4^{(k)} H_{27}[K_{st}] + E_2^{(k)} H_{28}[L_{st}] + E_6^{(k)} H_{29}[L_{st}]^T + \frac{\ell}{2} E_5^{(k)} H_{30}[M_{st}]. \quad (C.17)$$

Fourth row:

$$[K_{44}] = \frac{\ell}{2} E_3^{(k)} H_{12}[M_{st}] + E_5^{(k)} H_{13} ([L_{st}] + [L_{st}]^T) + \frac{2}{\ell} H_{14} E_6^{(k)} [K_{st}] \quad (C.18)$$

$$[K_{45}] = \frac{2}{\ell} E_4^{(k)} H_{42}[K_{st}] + E_6^{(k)} H_{43}[L_{st}] + E_2^{(k)} H_{44}[L_{st}]^T + \frac{\ell}{2} E_5^{(k)} H_{45}[M_{st}] \quad (C.19)$$

$$[K_{46}] = \frac{2}{\ell} E_6^{(k)} H_{20}[K_{st}] + E_5^{(k)} (H_{21}[L_{st}] + H_{22}[L_{st}]^T) + \frac{\ell}{2} E_3^{(k)} H_{23}[M_{st}]. \quad (C.20)$$

Fifth row:

$$[K_{55}] = \frac{2}{\ell} E_1^{(k)} H_{46}[K_{st}] + E_4^{(k)} H_{47} ([L_{st}] + [L_{st}]^T) + \frac{\ell}{2} E_6^{(k)} H_{48}[M_{st}] \quad (C.21)$$

$$[K_{56}] = \frac{2}{\ell} E_4^{(k)} H_{49}[K_{st}] + E_2^{(k)} H_{50}[L_{st}] + E_6^{(k)} H_{51}[L_{st}]^T + \frac{\ell}{2} E_5^{(k)} H_{52}[M_{st}]. \quad (C.22)$$

Sixth row:

$$[K_{66}] = \frac{2}{\ell} E_6^{(k)} H_{31}[K_{st}] + E_5^{(k)} H_{32} ([L_{st}] + [L_{st}]^T) + \frac{\ell}{2} E_3^{(k)} H_{33}[M_{st}] \quad (C.23)$$

where:

$$\begin{aligned} H_1 &= \int_{y_k}^{y_{k+1}} y F_0 dy & H_2 &= \int_{y_k}^{y_{k+1}} y F_0' dy \\ H_3 &= \int_{y_k}^{y_{k+1}} F_0 dy & H_4 &= \int_{y_k}^{y_{k+1}} F_0' dy \\ H_5 &= \int_{y_k}^{y_{k+1}} (F_0)^2 dy & H_6 &= \int_{y_k}^{y_{k+1}} F_0 F_0' dy \\ H_7 &= \int_{y_k}^{y_{k+1}} F_0' F_0' dy & H_8 &= \int_{y_k}^{y_{k+1}} y F_1' dy \\ H_9 &= \int_{y_k}^{y_{k+1}} y F_1 dy & H_{10} &= \int_{y_k}^{y_{k+1}} F_1' dy \\ H_{11} &= \int_{y_k}^{y_{k+1}} F_1 dy & H_{12} &= \int_{y_k}^{y_{k+1}} (F_1')^2 dy \\ H_{13} &= \int_{y_k}^{y_{k+1}} F_1 F_1' dy & H_{14} &= \int_{y_k}^{y_{k+1}} (F_1)^2 dy \\ H_{15} &= \int_{y_k}^{y_{k+1}} F_3' dy & H_{16} &= \int_{y_k}^{y_{k+1}} F_1 F_0 dy \\ H_{17} &= \int_{y_k}^{y_{k+1}} F_1 F_0' dy & H_{18} &= \int_{y_k}^{y_{k+1}} F_1' F_0 dy \\ H_{19} &= \int_{y_k}^{y_{k+1}} F_1' F_0' dy & H_{20} &= \int_{y_k}^{y_{k+1}} F_1 F_3 dy \\ H_{21} &= \int_{y_k}^{y_{k+1}} F_1 F_3' dy & H_{22} &= \int_{y_k}^{y_{k+1}} F_1' F_3 dy \\ H_{23} &= \int_{y_k}^{y_{k+1}} F_1' F_3' dy & H_{24} &= \int_{y_k}^{y_{k+1}} y F_3 dy \\ H_{25} &= \int_{y_k}^{y_{k+1}} y F_3' dy & H_{26} &= \int_{y_k}^{y_{k+1}} F_3 dy \\ H_{27} &= \int_{y_k}^{y_{k+1}} F_0 F_3 dy & H_{28} &= \int_{y_k}^{y_{k+1}} F_0 F_3' dy \end{aligned}$$

$$\begin{aligned}
H_{29} &= \int_{y_k}^{y_{k+1}} F_0' F_3 dy & H_{30} &= \int_{y_k}^{y_{k+1}} F_0' F_3' dy \\
H_{31} &= \int_{y_k}^{y_{k+1}} (F_3)^2 dy & H_{32} &= \int_{y_k}^{y_{k+1}} F_3 F_3' dy \\
H_{33} &= \int_{y_k}^{y_{k+1}} (F_3')^2 dy & H_{34} &= \int_{y_k}^{y_{k+1}} y F_2 dy \\
H_{35} &= \int_{y_k}^{y_{k+1}} y F_2' dy & H_{36} &= \int_{y_k}^{y_{k+1}} F_2 dy \\
H_{37} &= \int_{y_k}^{y_{k+1}} F_2' dy & H_{38} &= \int_{y_k}^{y_{k+1}} F_0 F_2 dy \\
H_{39} &= \int_{y_k}^{y_{k+1}} F_0 F_2' dy & H_{40} &= \int_{y_k}^{y_{k+1}} F_0' F_2 dy \\
\\ 
H_{41} &= \int_{y_k}^{y_{k+1}} F_0' F_2' dy & H_{42} &= \int_{y_k}^{y_{k+1}} F_1 F_2 dy \\
H_{43} &= \int_{y_k}^{y_{k+1}} F_1 F_2' dy & H_{44} &= \int_{y_k}^{y_{k+1}} F_1' F_2 dy \\
H_{45} &= \int_{y_k}^{y_{k+1}} F_1' F_2' dy & H_{46} &= \int_{y_k}^{y_{k+1}} (F_2)^2 dy \\
H_{47} &= \int_{y_k}^{y_{k+1}} F_2 F_2' dy & H_{48} &= \int_{y_k}^{y_{k+1}} (F_2')^2 dy \\
H_{49} &= \int_{y_k}^{y_{k+1}} F_2 F_3 dy & H_{50} &= \int_{y_k}^{y_{k+1}} F_2 F_3' dy \\
H_{51} &= \int_{y_k}^{y_{k+1}} F_2' F_3 dy & H_{52} &= \int_{y_k}^{y_{k+1}} F_2' F_3' dy.
\end{aligned}$$

These 52 coefficients have to be evaluated for each lamina of the strip. For the 3-ply laminate indicated in Figure B.1, the following values are computed.

1. For lamina 1, using (B.2), (B.14) and (B.25):

$$\begin{aligned}
H_1 &= \int_{-h_1/2}^{+h_1/2} p_0 y^2 dy = p_0 \frac{h_1^3}{12} & H_2 &= \int_{-h_1/2}^{+h_1/2} p_0 y dy = 0 \\
H_3 &= \int_{-h_1/2}^{+h_1/2} p_0 y dy = 0 & H_4 &= \int_{-h_1/2}^{+h_1/2} p_0 dy = p_0 h_1
\end{aligned}$$



$$H_5 = \int_{-h_1/2}^{+h_1/2} p_0^2 y^2 dy = p_0^2 \frac{h_1^3}{12}$$

$$H_7 = \int_{-h_1/2}^{+h_1/2} p_0^2 dy = p_0^2 h_1$$

$$H_9 = \int_{-h_1/2}^{+h_1/2} q_0 y^3 dy = 0$$

$$H_6 = \int_{-h_1/2}^{+h_1/2} p_0^2 y dy = 0$$

$$H_8 = \int_{-h_1/2}^{+h_1/2} 2 q_0 y^2 dy = q_0 \frac{h_1^3}{6}$$

$$H_{10} = \int_{-h_1/2}^{+h_1/2} 2 q_0 y dy = 0$$

$$H_{11} = \int_{-h_1/2}^{+h_1/2} q_0 y^2 dy = q_0 \frac{h_1^3}{12} = \frac{H_8}{2}$$

$$H_{13} = \int_{-h_1/2}^{+h_1/2} 2 q_0^2 y^3 dy = 0$$

$$H_{15} = \int_{-h_1/2}^{+h_1/2} 2 z_0 y dy = 0$$

$$H_{17} = \int_{-h_1/2}^{+h_1/2} q_0 p_0 y^2 dy = q_0 p_0 \frac{h_1^3}{12}$$

$$H_{19} = \int_{-h_1/2}^{+h_1/2} 2 p_0 q_0 y dy = 0$$

$$H_{12} = \int_{-h_1/2}^{+h_1/2} (2 q_0 y)^2 dy = q_0^2 \frac{h_1^3}{3}$$

$$H_{14} = \int_{-h_1/2}^{+h_1/2} q_0^2 y^4 dy = q_0^2 \frac{h_1^5}{80}$$

$$H_{16} = \int_{-h_1/2}^{+h_1/2} p_0 q_0 y^3 dy = 0$$

$$H_{18} = \int_{-h_1/2}^{+h_1/2} 2 q_0 p_0 y^2 dy = 2 H_{17}$$

$$H_{20} = \int_{-h_1/2}^{+h_1/2} q_0 z_0 y^4 dy = q_0 z_0 \frac{h_1^5}{80}$$

$$H_{21} = \int_{-h_1/2}^{+h_1/2} 2 q_0 z_0 y^3 dy = 0$$

$$H_{23} = \int_{-h_1/2}^{+h_1/2} 4 q_0 z_0 y^2 dy = q_0 z_0 \frac{h_1^3}{3}$$

$$H_{25} = \int_{-h_1/2}^{+h_1/2} 2 z_0 y^2 dy = z_0 \frac{h_1^3}{6}$$

$$H_{22} = \int_{-h_1/2}^{+h_1/2} 2 q_0 z_0 y^3 dy = 0$$

$$H_{24} = \int_{-h_1/2}^{+h_1/2} z_0 y^3 dy = 0$$

$$H_{26} = \int_{-h_1/2}^{+h_1/2} z_0 y^2 dy = z_0 \frac{h_1^3}{12} = \frac{H_{25}}{2}$$

$$H_{27} = \int_{-h_1/2}^{+h_1/2} p_0 z_0 y^3 dy = 0$$

$$H_{29} = \int_{-h_1/2}^{+h_1/2} p_0 z_0 y^2 dy = p_0 z_0 \frac{h_1^3}{12}$$

$$H_{28} = \int_{-h_1/2}^{+h_1/2} 2 p_0 z_0 y^2 dy = p_0 z_0 \frac{h_1^3}{6}$$

$$H_{30} = \int_{-h_1/2}^{+h_1/2} 2 p_0 z_0 y dy = 0$$

$$H_{31} = \int_{-h_1/2}^{+h_1/2} z_0^2 y^4 dy = z_0^2 \frac{h_1^5}{80}$$

$$H_{33} = \int_{-h_1/2}^{+h_1/2} (2 z_0 y)^2 dy = z_0^2 \frac{h_1^3}{3}$$

$$H_{35} = \int_{-h_1/2}^{+h_1/2} 3 t_0 y^3 dy = 0$$

$$H_{32} = \int_{-h_1/2}^{+h_1/2} 2 z_0^2 y^3 dy = 0$$

$$H_{34} = \int_{-h_1/2}^{+h_1/2} t_0 y^4 dy = t_0 \frac{h_1^5}{80}$$

$$H_{36} = \int_{-h_1/2}^{+h_1/2} t_0 y^3 dy = 0$$

$$\begin{aligned}
H_{37} &= \int_{-h_1/2}^{+h_1/2} 3 t_0 y^2 dy = t_0 \frac{h_1^3}{4} & H_{38} &= \int_{-h_1/2}^{+h_1/2} p_0 t_0 y^4 dy = p_0 t_0 \frac{h_1^5}{80} \\
H_{39} &= \int_{-h_1/2}^{+h_1/2} 3 p_0 t_0 y^3 dy = 0 & H_{40} &= \int_{-h_1/2}^{+h_1/2} p_0 t_0 y^3 dy = 0 \\
H_{41} &= \int_{-h_1/2}^{+h_1/2} 3 p_0 t_0 y^2 dy = p_0 t_0 \frac{h_1^3}{4} & H_{42} &= \int_{-h_1/2}^{+h_1/2} q_0 t_0 y^5 dy = 0 \\
H_{43} &= \int_{-h_1/2}^{+h_1/2} 3 q_0 t_0 y^4 dy = 3 q_0 t_0 \frac{h_1^5}{80} & H_{44} &= \int_{-h_1/2}^{+h_1/2} 2 q_0 t_0 y^4 dy = 2 q_0 t_0 \frac{h_1^5}{80} \\
H_{45} &= \int_{-h_1/2}^{+h_1/2} 6 q_0 t_0 y^3 dy = 0 & H_{46} &= \int_{-h_1/2}^{+h_1/2} t_0^2 y^6 dy = t_0^2 \frac{h_1^7}{448} \\
H_{47} &= \int_{-h_1/2}^{+h_1/2} 3 t_0^2 y^5 dy = 0 & H_{48} &= \int_{-h_1/2}^{+h_1/2} (3 t_0 y^2)^2 dy = 9 t_0^2 \frac{h_1^5}{80} \\
H_{49} &= \int_{-h_1/2}^{+h_1/2} t_0 z_0 y^5 dy = 0 & H_{50} &= \int_{-h_1/2}^{+h_1/2} 2 t_0 z_0 y^4 dy = t_0 z_0 \frac{h_1^5}{40} \\
H_{51} &= \int_{-h_1/2}^{+h_1/2} 3 t_0 z_0 y^4 dy = 3 t_0 z_0 \frac{h_1^5}{80} & H_{52} &= \int_{-h_1/2}^{+h_1/2} 6 t_0 z_0 y^3 dy = 0.
\end{aligned}$$

2. For lamina 2, using (B.2), (B.8), (B.14) and (B.25):

$$H_1 = \int_{h_1/2}^{h_1/2+h_2} (p_1 y + p_2 y^2) dy = p_1 \frac{A_2}{2} + p_2 \frac{A_1}{3}$$

$$\text{where: } A_2 = \left( \frac{h_1}{2} + h_2 \right)^2 - \left( \frac{h_1}{2} \right)^2, \quad A_1 = \left( \frac{h_1}{2} + h_2 \right)^3 - \left( \frac{h_1}{2} \right)^3$$

$$H_2 = \int_{h_1/2}^{h_1/2+h_2} p_2 y dy = p_2 \frac{A_2}{2}$$

$$H_3 = \int_{h_1/2}^{h_1/2+h_2} (p_1 + p_2 y) dy = p_1 h_2 + p_2 \frac{A_2}{2}$$

$$H_4 = \int_{h_1/2}^{h_1/2+h_2} p_2 dy = p_2 h_2$$

$$H_5 = \int_{h_1/2}^{h_1/2+h_2} (p_1 + p_2 y)^2 dy = p_1^2 h_2 + p_1 p_2 A_2 + \frac{p_2^2 A_1}{3}$$

$$H_6 = \int_{h_1/2}^{h_1/2+h_2} (p_1 + p_2 y) p_2 dy = p_1 p_2 h_2 + p_2^2 \frac{A_2}{2}$$

$$H_7 = \int_{h_1/2}^{h_1/2+h_2} p_2^2 dy = p_2^2 h_2$$

$$H_8 = \int_{h_1/2}^{h_1/2+h_2} (q_2 + 2q_3 y) y dy = q_2 \frac{A_2}{2} + \frac{2}{3} q_3 \frac{A_3}{4}$$

$$H_9 = \int_{h_1/2}^{h_1/2+h_2} (q_1 + q_2 y + q_3 y^2) y dy = \frac{q_1 A_2}{2} + \frac{q_2 A_1}{3} + q_3 \frac{A_3}{4}$$

$$\text{with: } A_3 = \left(\frac{h_1}{2} + h_2\right)^4 - \left(\frac{h_1}{2}\right)^4, \quad A_4 = \left(\frac{h_1}{2} + h_2\right)^5 - \left(\frac{h_1}{2}\right)^5$$

$$H_{10} = \int_{h_1/2}^{h_1/2+h_2} (q_2 + 2q_3 y) dy = q_2 h_2 + q_3 A_2$$

$$H_{11} = \int_{h_1/2}^{h_1/2+h_2} (q_1 + q_2 y + q_3 y^2) dy = q_1 h_2 + q_2 \frac{A_2}{2} + q_3 \frac{A_1}{3}$$

$$H_{12} = \int_{h_1/2}^{h_1/2+h_2} (q_2 + 2q_3 y)^2 dy = q_2^2 h_2 + 2q_2 q_3 A_2 + \frac{4}{3} q_3^2 A_1$$

$$\begin{aligned} H_{13} &= \int_{h_1/2}^{h_1/2+h_2} (q_1 + q_2 y + q_3 y^2) (q_2 + 2q_3 y) dy \\ &= q_1 q_2 h_2 + (2q_1 q_3 + q_2^2) \frac{A_2}{2} + q_2 q_3 A_1 + q_3^2 \frac{A_3}{2} \end{aligned}$$

$$\begin{aligned} H_{14} &= \int_{h_1/2}^{h_1/2+h_2} (q_1 + q_2 y + q_3 y^2)^2 dy \\ &= q_1^2 h_2 + q_1 q_2 A_1 + (2q_1 q_3 + q_2^2) \frac{A_1}{3} + q_2 q_3 \frac{A_3}{2} + q_3^2 \frac{A_4}{5} \end{aligned}$$

$$H_{15} = \int_{h_1/2}^{h_1/2+h_2} 2z_2 y dy = z_2 A_2$$

$$\begin{aligned} H_{16} &= \int_{h_1/2}^{h_1/2+h_2} (q_1 + q_2 y + q_3 y^2) (p_1 + p_2 y) dy \\ &= p_1 q_1 h_2 + (p_1 q_2 + q_1 p_2) \frac{A_2}{2} + (p_1 q_3 + p_2 q_2) \frac{A_1}{3} + p_2 q_3 \frac{A_3}{4} \end{aligned}$$

$$H_{17} = \int_{h_1/2}^{h_1/2+h_2} (q_1 + q_2 y + q_3 y^2) p_2 dy = p_2 q_1 h_2 + p_2 q_2 \frac{A_2}{2} + p_2 q_3 \frac{A_1}{3}$$

$$H_{18} = \int_{h_1/2}^{h_1/2+h_2} (p_1 + p_2 y) (q_2 + 2q_3 y) dy = p_1 q_2 h_2 + (p_2 q_2 + 2p_1 q_3) \frac{A_2}{2} + 2p_2 q_3 \frac{A_1}{3}$$

$$H_{19} = \int_{h_1/2}^{h_1/2+h_2} p_2 (q_2 + 2q_3 y) dy = p_2 q_2 h_2 + p_2 q_3 A_2$$

$$\begin{aligned}
H_{20} &= \int_{h_1/2}^{h_1/2+h_2} (q_1 + q_2 y + q_3 y^2)(z_1 + z_2 y^2) dy \\
&= q_1 z_1 h_2 + q_2 z_1 \frac{A_2}{2} + (q_1 z_2 + q_3 z_1) \frac{A_1}{3} + q_2 z_2 \frac{A_3}{4} + q_3 z_2 \frac{A_4}{5}
\end{aligned}$$

$$H_{21} = \int_{h_1/2}^{h_1/2+h_2} (q_1 + q_2 y + q_3 y^2)(2z_2 y) dy = q_1 z_2 A_2 + \frac{2}{3} q_2 z_2 A_1 + \frac{1}{2} q_3 z_2 A_3$$

$$H_{22} = \int_{h_1/2}^{h_1/2+h_2} (q_2 + 2q_3 y)(z_1 + z_2 y^2) dy = q_2 z_1 h_2 + q_3 z_1 A_2 + q_2 z_2 \frac{A_1}{3} + q_3 z_2 \frac{A_3}{2}$$

$$H_{23} = \int_{h_1/2}^{h_1/2+h_2} (q_2 + 2q_3 y)(2z_2 y) dy = q_2 z_2 A_2 + \frac{4}{3} q_3 z_2 A_1$$

$$H_{24} = \int_{h_1/2}^{h_1/2+h_2} (z_1 y + z_2 y^3) dy = z_1 \frac{A_2}{2} + z_2 \frac{A_3}{4}$$

$$H_{25} = \int_{h_1/2}^{h_1/2+h_2} (2z_2 y^2) dy = \frac{2}{3} z_2 A_1$$

$$H_{26} = \int_{h_1/2}^{h_1/2+h_2} (z_1 + z_2 y^2) dy = z_1 h_2 + z_2 \frac{A_1}{3}$$

$$H_{27} = \int_{h_1/2}^{h_1/2+h_2} (p_1 + p_2 y)(z_1 + z_2 y^2) dy = p_1 z_1 h_2 + p_2 z_1 \frac{A_2}{2} + p_1 z_2 \frac{A_1}{3} + p_2 z_2 \frac{A_3}{4}$$

$$H_{28} = \int_{h_1/2}^{h_1/2+h_2} (p_1 + p_2 y) 2z_2 y dy = p_1 z_2 A_2 + \frac{2}{3} p_2 z_2 A_1$$

$$H_{29} = \int_{h_1/2}^{h_1/2+h_2} p_2 (z_1 + z_2 y^2) dy = p_2 z_1 h_2 + p_2 z_2 \frac{A_1}{3}$$

$$H_{30} = \int_{h_1/2}^{h_1/2+h_2} 2 p_2 z_2 y dy = p_2 z_2 A_2$$

$$H_{31} = \int_{h_1/2}^{h_1/2+h_2} (z_1 + z_2 y^2)^2 dy = z_1^2 h_2 + \frac{2}{3} z_1 z_2 A_1 + z_2^2 \frac{A_4}{5}$$

$$H_{32} = \int_{h_1/2}^{h_1/2+h_2} (z_1 + z_2 y^2)(2z_2 y) dy = z_1 z_2 A_2 + z_2^2 \frac{A_3}{2}$$

$$H_{33} = \int_{h_1/2}^{h_1/2+h_2} (2z_2 y)^2 dy = \frac{4}{3} z_2^2 A_1$$

$$H_{34} = \int_{h_1/2}^{h_1/2+h_2} (t_1 y + t_2 y^2 t_3 y^3 + t_4 y^4) dy = t_1 \frac{A_2}{3} + t_2 \frac{A_1}{3} + t_3 \frac{A_3}{4} + t_4 \frac{A_4}{5}$$

$$H_{35} = \int_{h_1/2}^{h_1/2+h_2} (t_2 y + 2t_3 y^2 + 3t_4 y^3) dy = t_2 \frac{A_2}{2} + \frac{2}{3} t_3 A_1 + \frac{3}{4} t_4 A_3$$

$$H_{36} = \int_{h_1/2}^{h_1/2+h_2} (t_1 + t_2 y + t_3 y^2 + t_4 y^3) dy = t_1 h_2 + t_2 \frac{A_2}{2} + t_3 \frac{A_1}{3} + t_4 \frac{A_3}{4}$$

$$H_{37} = \int_{h_1/2}^{h_1/2+h_2} (t_2 + 2t_3y + 3t_4y^2)dy = t_2h_2 + t_3A_2 + t_4A_1$$

$$\begin{aligned} H_{38} &= \int_{h_1/2}^{h_1/2+h_2} (p_1 + p_2y)(t_1 + t_2y + t_3y^2 + t_4y^3)dy \\ &= p_1t_1h_2 + (p_1t_2 + p_2t_1)\frac{A_2}{2} + (p_1t_3 + p_2t_2)\frac{A_1}{3} \\ &\quad + (p_1t_4 + p_2t_3)\frac{A_3}{4} + p_2t_4\frac{A_4}{5} \end{aligned}$$

$$\begin{aligned} H_{39} &= \int_{h_1/2}^{h_1/2+h_2} (p_1 + p_2y)(t_2 + 2t_3y + 3t_4y^2)dy \\ &= p_1t_2h_2 + (2p_1t_3 + p_2t_2)\frac{A_2}{2} + (3p_1t_4 + 2p_2t_3)\frac{A_1}{3} + \frac{3}{4}p_2t_4A_3 \end{aligned}$$

$$\begin{aligned} H_{40} &= \int_{h_1/2}^{h_1/2+h_2} (t_1 + t_2y + t_3y^2 + t_4y^3)p_2dy \\ &= t_1p_2h_2 + p_2t_2\frac{A_2}{2} + p_2t_3\frac{A_1}{3} + p_2t_4\frac{A_3}{4} \end{aligned}$$

$$H_{41} = \int_{h_1/2}^{h_1/2+h_2} p_2(t_2 + 2t_3y + 3t_4y^2)dy = p_2t_2h_2 + p_2t_3A_2 + p_2t_4A_1$$

$$\begin{aligned} H_{42} &= \int_{h_1/2}^{h_1/2+h_2} (q_1 + q_2y + q_3y^2)(t_1 + t_2y + t_3y^2 + t_4y^3)dy \\ &= q_1t_1h_2 + (q_1t_2 + q_2t_1)\frac{A_2}{2} + (q_1t_3 + q_2t_2 + q_3t_1)\frac{A_1}{3} \\ &\quad + (q_1t_4 + q_2t_3 + q_3t_2)\frac{A_3}{4} + (q_2t_4 + q_3t_3)\frac{A_4}{5} + q_3t_4\frac{A_5}{6} \end{aligned}$$

with:  $A_5 = \left(\frac{h_1}{2} + h_2\right)^6 - \left(\frac{h_1}{2}\right)^6$ ,  $A_6 = \left(\frac{h_1}{2} + h_2\right)^7 - \left(\frac{h_1}{2}\right)^7$

$$\begin{aligned} H_{43} &= \int_{h_1/2}^{h_1/2+h_2} (q_1q_2y + q_3y^2)(t_2 + 2t_3y + 3t_4y^2)dy \\ &= q_1t_2h_2 + (2q_1t_3 + q_2t_2)\frac{A_2}{2} + (3q_1t_4 + 2q_2t_3 + q_3t_2)\frac{A_1}{3} \\ &\quad + (3q_2t_4 + 2q_3t_3)\frac{A_3}{4} + 3q_3t_4\frac{A_4}{5} \end{aligned}$$

$$\begin{aligned}
H_{44} &= \int_{h_1/2}^{h_1/2+h_2} (q_2 + 2q_3y)(t_1 + t_2y + t_3y^2 + t_4y^3)dy \\
&= q_2t_1h_2 + (q_2t_2 + 2q_3t_1)\frac{A_2}{2} + (q_2t_3 + 2q_3t_2) \\
&\quad + (q_2t_4 + 2q_3t_3)\frac{A_3}{4} + 2q_3t_4\frac{A_4}{5}
\end{aligned}$$

$$\begin{aligned}
H_{45} &= \int_{h_1/2}^{h_1/2+h_2} (q_2 + 2q_3y)(t_2 + 2t_3y + 3t_4y^2)dy \\
&= q_2t_2h_2 + (2q_2t_3 + 2q_3t_2)\frac{A_2}{2} + (3q_2t_4 + 4q_3t_3)\frac{A_1}{3} + 6q_3t_4\frac{A_3}{4}
\end{aligned}$$

$$\begin{aligned}
H_{46} &= \int_{h_1/2}^{h_1/2+h_2} (t_1 + t_2y + t_3y^2t_4y^3)^2dy \\
&= t_1^2h_2 + t_1t_2A_2 + (2t_1t_3 + t_2^2)\frac{A_1}{3} + (t_1t_4 + t_2t_3)\frac{A_3}{2} \\
&\quad + (2t_2t_4 + t_3^2)\frac{A_4}{5} + t_3t_4\frac{A_5}{3} + t_4^2\frac{A_6}{7}
\end{aligned}$$

$$\begin{aligned}
H_{47} &= \int_{h_1/2}^{h_1/2+h_2} (t_1 + t_2y + t_3y^2 + t_4y^3)(t_2 + 2t_3y + 3t_4y^2)dy \\
&= t_1t_2h_2 + (2t_1t_3 + t_2^2)\frac{A_2}{2} + (t_1t_4 + t_2t_3)A_1 \\
&\quad + (2t_2t_4 + t_3^2)\frac{A_3}{2} + t_3t_4A_4 + t_4^2\frac{A_5}{2}
\end{aligned}$$

$$\begin{aligned}
H_{48} &= \int_{h_1/2}^{h_1/2+h_2} (t_2 + 2t_3y + 3t_4y^2)(t_2 + 2t_3y + 3t_4y^2)dy \\
&= t_2^2h_2 + 2t_2t_3A_2 + (6t_2t_4 + 4t_3^2)\frac{A_1}{3} + 3t_3t_4A_3 + 9t_4^2\frac{A_4}{5}
\end{aligned}$$

$$\begin{aligned}
H_{49} &= \int_{h_1/2}^{h_1/2+h_2} (t_1 + t_2y + t_3y^2 + t_4y^3)(z_1 + z_2y^2)dy \\
&= t_1z_1h_2 + t_2z_1\frac{A_2}{2} + (t_1z_2 + t_3z_1)\frac{A_1}{3} + (t_2z_2 + t_4z_1)\frac{A_3}{4} \\
&\quad + t_3z_2\frac{A_4}{5} + t_4z_2\frac{A_5}{6}
\end{aligned}$$

$$\begin{aligned}
H_{50} &= \int_{h_1/2}^{h_1/2+h_2} (t_1 + t_2 y + t_3 y^2 + t_4 y^3)(2z_2 y) dy \\
&= t_1 z_2 A_2 + 2t_2 z_2 \frac{A_1}{3} + t_3 z_2 \frac{A_3}{2} + 2t_4 z_2 \frac{A_4}{5}
\end{aligned}$$

$$\begin{aligned}
H_{51} &= \int_{h_1/2}^{h_1/2+h_2} (t_2 + 2t_3 y + 3t_4 y^2)(z_1 + z_2 y^2) dy \\
&= t_2 z_1 h_2 + t_3 z_1 A_2 + (t_2 z_2 + 3t_4 z_1) \frac{A_1}{3} + t_3 z_2 \frac{A_3}{2} + 3t_4 z_2 \frac{A_4}{5}
\end{aligned}$$

$$H_{52} = \int_{h_1/2}^{h_1/2+h_2} (t_2 + 2t_3 y + 3t_4 y^2)(2z_2 y) dy = t_2 z_2 A_2 + \frac{4}{3} t_3 z_2 A_1 + \frac{3}{2} t_4 z_2 A_3.$$

The integration of these and all other coefficients necessary to compute the stiffness submatrices can be performed numerically, and for any number of layers. The direct integration was performed to solve the model problems described in Chapter 3.

## Appendix D

### Laminated Strip: The Load Vector

The load vector will be computed for the three-ply laminate indicated in Figure D.1, and for the case of the  $\beta^2$  expansion of the displacement functions as given in (2.77), (2.78).

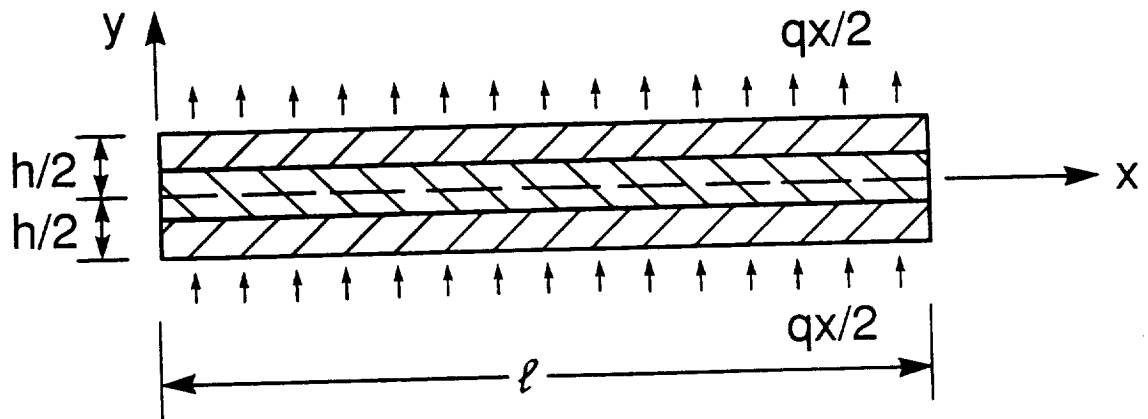


Figure D.1: Three-ply problem. Notation.



The potential of the external forces was determined in Chapter 3, and is given by (3.25):

$$\mathcal{F}(u) = \frac{\ell}{2} \int_{-1}^{+1} \frac{q_x(\xi)}{2} u_y(\xi, h/2) d\xi + \frac{\ell}{2} \int_{-1}^{+1} \frac{q_x(\xi)}{2} u_y(\xi, -h/2) d\xi$$

but  $u_y(\xi, h/2) = u_y(\xi, -h/2)$  because of symmetry, then

$$\mathcal{F}(u) = \frac{\ell}{2} \int_{-1}^{+1} q_x(\xi) u_y(\xi, h/2) d\xi \quad (\text{D.1})$$

also from (2.78) and (3.3):

$$u_y(\xi, h/2) = \sum_{j=1}^{p+1} b_j^{(1)} N_j(\xi) + F_1(h/2) \sum_{j=1}^{p+1} b_j^{(2)} N_j(\xi) + F_3(h/2) \sum_{j=1}^{p+1} b_j^{(3)} N_j(\xi). \quad (\text{D.2})$$

For the case of  $q_x(\xi) = \text{constant} = q$ , using (D.2) into (D.1):

$$\begin{aligned} \mathcal{F}(u) = \frac{q\ell}{2} \left( \int_{-1}^{+1} \sum_{j=1}^{p+1} b_j^{(1)} N_j(\xi) d\xi + F_1(h/2) \int_{-1}^{+1} \sum_{j=1}^{p+1} b_j^{(2)} N_j(\xi) d\xi \right. \\ \left. + F_3(h/2) \int_{-1}^{+1} \sum_{j=1}^{p+1} b_j^{(3)} N_j(\xi) d\xi \right) \end{aligned} \quad (\text{D.3})$$

but

$$\int_{-1}^{+1} N_1(\xi) d\xi = 1, \quad \int_{-1}^{+1} N_2(\xi) d\xi = 1$$

$$\int_{-1}^{+1} N_3(\xi) d\xi = -\frac{1}{\sqrt{6}}, \quad \int_{-1}^{+1} N_j(\xi) d\xi = 0, \quad j = 4, 5, \dots, p+1.$$

then:

$$\begin{aligned} \mathcal{F}(u) = \frac{q\ell}{2} \left( (b_1^{(1)} + b_2^{(1)} - \frac{2}{\sqrt{6}} b_3^{(1)}) + F_1(h/2)(b_1^{(2)} + b_2^{(2)} - \frac{2}{\sqrt{6}} b_3^{(2)}) \right. \\ \left. + F_3(h/2)(b_1^{(3)} + b_2^{(3)} - \frac{2}{\sqrt{6}} b_3^{(3)}) \right) \end{aligned} \quad (\text{D.4})$$

or

$$\mathcal{F}(u) = [b^{(1)}] \{r^{(1)}\} + [b^{(2)}] \{r^{(2)}\} + [b^{(3)}] \{r^{(3)}\} \quad (\text{D.5})$$

where:

$$[b^{(1)}] = [b_1^{(1)} \quad b_2^{(1)} \quad b_3^{(1)} \dots b_{p+1}^{(1)}]$$

$$[b^{(2)}] = [b_1^{(2)} \quad b_2^{(2)} \quad b_3^{(2)} \dots b_{p+1}^{(2)}]$$

$$[b^{(3)}] = [b_1^{(3)} \quad b_2^{(3)} \quad b_3^{(3)} \dots b_{p+1}^{(3)}]$$

are the vectors of the unknown coefficients of the functions  $u_{y|i}(x)$ ; and

$$[r^{(1)}] = \frac{q\ell}{2} [1 \quad 1 \quad -2/\sqrt{6} \quad 0 \dots 0]$$

$$[r^{(2)}] = F_1(h/2) \frac{q\ell}{2} [1 \quad 1 \quad -2/\sqrt{6} \quad 0 \dots 0]$$

$$[r^{(3)}] = F_3(h/2) \frac{q\ell}{2} [1 \quad 1 \quad -2/\sqrt{6} \quad 0 \dots 0]$$

are the load sub-vectors associated with the above unknown vectors.

Using expressions (B.8) and (B.25):

$$F_1(h/2) = q_1 + q_2 \frac{h}{2} + q_3 \left(\frac{h}{2}\right)^2 \quad (\text{D.6})$$

$$F_3(h/2) = z_1 + z_2 \left(\frac{h}{2}\right)^2 \quad (\text{D.7})$$

where  $q_1$ ,  $q_2$ ,  $q_3$ ,  $z_1$  and  $z_2$  depend on the material properties and thickness of each layer of the laminate, and are given in Appendix B. The global load vector is obtained assembling the load sub-vectors computed above. For the  $\beta^2$  model there are six sub-vectors:

$$\{R\} = \left\{ [0] \quad [r^{(1)}] \quad [0] \quad [r^{(2)}] \quad [0] \quad [r^{(3)}] \right\}^T$$

This is the expression of the load vector for a 3-ply laminated strip with uniform loading on top and bottom surfaces to be used in (3.28).

## Appendix E

### Laminated Strip: Computation of Engineering Quantities

a) Horizontal displacements. After the finite element solution is obtained, the  $u_x$  displacement component for the  $\beta^2$  model at any given point across the laminated is given by:

$$u_x(\xi, y) = ([a^{(1)}]y + [a^{(2)}]F_0(y) + [a^{(3)}]F_2(y)) \{N(\xi)\}.$$

For the simply supported case, the horizontal displacement at the support location ( $x = 0$ , or  $\xi = -1$ ) will be:

$$u_x(-1, y) = a_1^{(1)}y + a_1^{(2)}F_0(y) + a_1^{(3)}F_2(y). \quad (\text{E.1})$$

Note that  $N_1(-1) = 1$ , and  $N_i(-1) = 0$ ,  $i = 2, 3, \dots, p+1$ , and only the coefficient  $a_1$  is included in (E.1) for each term of the expansion.

For lamina 1 of the model problems, using the results obtained in Appendix B for the integration of the transverse functions, we have:

$$u_x(-1, y) = a_1^{(1)} y + a_1^{(2)} p_0 y + a_1^{(3)} t_0 y^3. \quad (\text{E.2})$$

For lamina 2:

$$u_x(-1, y) = a_1^{(1)} y + a_1^{(2)} (p_1 + p_2 y) + a_1^{(3)} (t_1 + t_2 y + t_3 y^2 + t_4 y^3). \quad (\text{E.3})$$

b) Longitudinal stress  $\sigma_x$ . To determine the longitudinal stress  $\sigma_x$  we use equation (2.6) and (3.8) as follows:

$$\begin{aligned} \epsilon_x &= \frac{\partial u_x}{\partial x} = \frac{2}{\ell} [N'] \{a^{(1)}\} y + \frac{2}{\ell} [N'] \{a^{(2)}\} F_0(y) + \frac{2}{\ell} [N'] \{a^{(3)}\} F_2(y) \\ \epsilon_y &= \frac{\partial u_y}{\partial y} = [N] \{b^{(2)}\} F_1'(y) + [N] \{b^{(3)}\} F_3'(y). \end{aligned}$$

For the case  $E_4 = E_5 = 0$ :

$$\sigma_x = E_1 \epsilon_x + E_2 \epsilon_y$$

$$\begin{aligned} \sigma_x(\xi, y) &= \frac{2}{\ell} E_1 [N'] \left( \{a_1^{(1)}\} y + \{a^{(2)}\} F_0(y) + \{a^{(3)}\} F_2(y) \right) \\ &\quad + E_2 [N] \left( \{b^{(2)}\} F_1'(y) + \{b^{(3)}\} F_3'(y) \right). \end{aligned} \quad (\text{E.4})$$

For the problem of the infinite strip described in Chapter 3, the longitudinal stress at the symmetry section ( $\xi = 1$ ) are:

$$\begin{aligned} \sigma_x(1, y) &= \frac{2}{\ell} E_1 \sum_{i=1}^{p+1} N_i'(\xi = 1) \left( a_i^{(1)} y + a_i^{(2)} F_0(y) + a_i^{(3)} F_2(y) \right) \\ &\quad + E_2 \left( b_2^{(2)} F_1'(y) + b_2^{(3)} F_3'(y) \right) \end{aligned} \quad (\text{E.5})$$

For lamina 1:

$$\begin{aligned}\sigma_x(1, y) = & \frac{2}{\ell} E_{11} \sum_{i=1}^{p+1} N'_i(\xi=1) (a_i^{(1)} y + a_i^{(2)} p_0 y + a_i^{(3)} t_0 y^3) \\ & + 2 E_{21} (E_{21} b_2^{(2)} q_0 y + b_2^{(3)} z_0 y). \end{aligned} \quad (\text{E.6})$$

For lamina 2:

$$\begin{aligned}\sigma_x(1, y) = & \frac{2}{\ell} E_{12} \sum_{i=1}^{p+1} N'_i(\xi=1) \left[ a_i^{(1)} y + a_i^{(2)} (p_1 + p_2 y) + a_i^{(3)} (t_1 + t_2 y + t_3 y^2 \right. \\ & \left. + t_4 y^3) \right] + E_{22} \left[ b_2^{(2)} (q_2 + 2 q_3 y) + 2 b_2^{(3)} z_2 y \right]. \end{aligned} \quad (\text{E.7})$$

c) Transverse shear stress  $\tau_{xy}$ . Let us consider the equilibrium equation (2.2):

$$\frac{\partial \tau_{xy}}{\partial y} = -\frac{\partial \sigma_x}{\partial x} \quad (\text{E.8})$$

integrating across the thickness

$$\tau_{xy} = \int_0^y -\frac{\partial \sigma_x}{\partial x} dy + g(x). \quad (\text{E.9})$$

From (E.4), we have

$$\begin{aligned}\frac{\partial \sigma_x}{\partial x} = & \frac{4}{\ell^2} E_1 [N''] \left( \{a^{(1)}\} y + \{a^{(2)}\} F_0(y) + \{a^{(3)}\} F_2(y) \right) \\ & + \frac{2}{\ell} E_2 [N'] \left( \{b^{(2)}\} F'_1(y) + \{b^{(3)}\} F'_3(y) \right)\end{aligned}$$

then:

$$\begin{aligned}\tau_{xy}(\xi, y) = & -\frac{4}{\ell^2} [N''] \left( \{a^{(1)}\} \int_0^y E_1 y dy + \{a^{(2)}\} \int_0^y E_1 F_0(y) dy \right. \\ & \left. + \{a^{(3)}\} \int_0^y E_1 F_2(y) dy \right) - \frac{2}{\ell} [N'] \left( \{b^{(2)}\} \int_0^y E_2 F'_1 dy \right. \\ & \left. + \{b^{(3)}\} \int_0^y E_2 F'_3 dy \right) + g(x). \end{aligned} \quad (\text{E.10})$$

For the problem of the infinite laminated strip described in Chapter 3, the shear stress  $\tau_{xy}$  at the antisymmetry section ( $\xi = -1$ ) is obtained from (E.10).

For lamina 1:

$$\begin{aligned} \tau_{xy}(-1, y) = & -\frac{4}{\ell^2} [N''] \left( \{a^{(1)}\} E_{11} \frac{y^2}{2} + \{a^{(2)}\} p_0 E_{11} \frac{y^2}{2} + \{a^{(3)}\} E_{11} t_0 \frac{y^4}{4} \right) \\ & - \frac{2}{\ell} [N'] \left( \{b^{(2)}\} q_0 E_{21} y^2 + \{b^{(3)}\} E_{21} z_0 y^2 \right) + g(x) \end{aligned}$$

or

$$\begin{aligned} \tau_{xy}(-1, y) = & -\frac{4}{\ell^2} [N''] E_{11} \left( \{a^{(1)}\} + \{a^{(2)}\} p_0 + \{a^{(3)}\} t_0 \frac{y^2}{2} \right) \frac{y^2}{2} \\ & - \frac{2}{\ell} [N'] E_{21} \left( \{b^{(2)}\} q_0 + \{b^{(3)}\} z_0 \right) y^2 + g(x). \end{aligned}$$

For lamina 2:

$$\begin{aligned} \tau_{xy}(-1, y) = & -\frac{4}{\ell^2} [N''] \left( \{a^{(1)}\} \left[ E_{11} \frac{h_1^2}{8} + \frac{E_{12}}{2} (y^2 - \frac{h_1^2}{4}) \right] + \{a^{(2)}\} \left[ E_{11} p_0 \frac{h_1^2}{8} \right. \right. \\ & + E_{12} p_1 (y - \frac{h_1}{2}) + \frac{E_{12}}{2} p_2 (y^2 - \frac{h_1^2}{4}) \left. \right] + \{a^{(3)}\} \left[ E_{11} t_0 \frac{h_1^4}{64} \right. \\ & + E_{12} t_1 (y - \frac{h_1}{2}) + E_{12} \frac{t_2}{2} (y^2 - \frac{h_1^2}{4}) + E_{12} \frac{t_3}{3} (y^3 - \frac{h_1^3}{8}) \\ & + E_{12} \frac{t_4}{4} (y^4 - \frac{h_1^4}{16}) \left. \right] - \frac{2}{\ell} [N'] \left( \{b^{(2)}\} \left[ E_{21} q_0 \frac{h_1^2}{4} \right. \right. \\ & + E_{22} q_2 (y - \frac{h_1}{2}) + E_{22} q_3 (y^2 - \frac{h_1^2}{4}) \left. \right] + \{b^{(3)}\} \left[ E_{21} z_0 \frac{h_1^2}{4} \right. \\ & + E_{22} z_2 (y^2 - \frac{h_1^2}{4}) \left. \right] \left. \right) + g(x) \end{aligned}$$

where  $g(x)$  is determined with the condition of zero shear of the free surface:

$$\tau_{xy}(-1, h/2) = 0$$

then:

$$g(x) = \frac{4}{\ell^2} [N''] \left[ \{a^{(1)}\} \left( E_{11} \frac{h_1^2}{8} + E_{12} \frac{A_2}{2} \right) + \{a^{(2)}\} \left( E_{11} p_0 \frac{h_1^2}{8} \right. \right.$$

$$\begin{aligned}
& + E_{12} p_1 h_2 + E_{12} p_2 \frac{A_2}{2} \Big) + \{a^{(3)}\} \left( E_{11} t_0 \frac{h_1^4}{64} + E_{12} (t_1 h_2 + t_2 \frac{A_2}{2} \right. \\
& \left. + t_3 \frac{A_1}{3} + t_4 \frac{A_3}{4}) \right) \Big] + \frac{2}{\ell} [N'] \left[ \{b^{(2)}\} \left( E_{21} q_0 \frac{h_1^2}{4} + E_{22} (q_2 h_2 + q_3 A_2) \right) \right. \\
& \left. + \{b^{(3)}\} \left( E_{21} z_0 \frac{h_1^2}{4} + E_{22} z_2 A_2 \right) \right].
\end{aligned}$$

These are the expressions that have been used to compute the displacements and stresses reported for the first model problem described in Chapter 3.



## Vita

Ricardo Luis Actis

Date of Birth: 6/3/52

Place of Birth: Avellaneda, Argentina

Undergraduate Study: University of La Plata, Argentina, 5-year degree in  
Aeronautical Engineering, 1975

Graduate Study: Washington University, Saint Louis, Missouri  
M.Sc. in Mechanical Engineering, 1985  
Washington University, Saint-Louis, Missouri  
D.Sc. expected December, 1991

Professional Experience: Structural designer, Luisoni and Associates,  
Argentina, 1974-1975  
Division Manager, National Institute of Industrial  
Technology, Argentina, 1976-1983  
Staff Engineer, FACTS, Inc., St. Louis, Missouri,  
1985

Structural and Stress Analysis Engineer,

Weld-Met International, Inc.,

St. Louis, Missouri, 1990-

Teaching Experience: Teaching Assistant, University of La Plata,

Argentina, 1976-1983

Assistant Professor of Aeronautical Engineering,

University of La Plata, Argentina,

1985-1987.

Teaching Assistant, Washington University,

1988-

#### Publications:

1. R. L. Actis, "Effect of Geometry and Boundary Conditions in the Stability of Circumferential Cracks in Pressurized Pipes", *National Institute of Industrial Technology, Argentina*, May 1981. (in spanish).
2. R. L. Actis and O. Zannoni, "Residual Stress Measurements in Welded Plates", *II Scientific Latinoamerican Congress*, May 1984. (in spanish).
3. R. L. Actis, "The Use of Fracture Mechanic in Design", *A Course Book published by the University of La Plata*, April 1987. (in spanish).

4. R. L. Actis and A. D. Dimarogonas, "Non-linear Effects due to Closing Cracks in Vibrating Beams", *12th Biennial ASME Conference on Mechanical Vibration and Noise*, Montreal, Canada, September 17-20, 1989.
5. I. Babuška, B. A. Szabó and R. L. Actis, "Hierarchic Models for Laminated Composites", *Center for Computational Mechanics, Washington University, Report: WU/CCM-90/4*, December 1990. Accepted for publication in the *International Journal for Numerical Methods in Engineering*.
6. R. L. Actis, "Hierarchic Models for Laminated Plates", *D.Sc Dissertation*, Washington University, 1991.

December 1991

## Bibliography

- [1] B. Szabó and I. Babuška. *Finite Element Analysis*. John Wiley and Sons, Inc., New York, 1991.
- [2] R. K. Kapania and S. Raciti. Recent advances in analysis of laminated beams and plates, part 1: Shear effects and buckling. *A.I.A.A. Journal*, 27, No. 7:923–934, 1989.
- [3] E. Reissner. On the theory of bending of elastic plates. *Journal of Mathematics and Physics*, 23:184–191, 1944.
- [4] R. D. Mindlin. Influence of rotary inertia and shear on flexural motion of isotropic elastic plates. *Journal of Applied Mechanics*, 18:31–38, 1951.
- [5] Y. Stavsky. *On the Theory of Heterogeneous Anisotropic Plates*. PhD thesis, M. I. T., Cambridge, Massachusetts, 1959.
- [6] J. M. Whitney and J. N. Pagano. Shear deformation in heterogeneous anisotropic plates. *Journal of Applied Mechanics*, 37:1031–1036, 1970.

- [7] E. Reissner. On bending of elastic plates. *Quarterly of Applied Mathematics*, 5:55–69, 1947.
- [8] J. M. Whitney. Shear correction factors for orthotropic laminates under static load. *Journal of Applied Mechanics*, 40:302–304, 1973.
- [9] A. K. Noor. A posteriori estimates for shear correction factors in multilayered composite cylinders. *Journal of Engineering Mechanics, ASCE*, 115, No. 6:1225–1244, 1989.
- [10] A. K. Noor, W. S. Burton, and J. M. Peters. Assessment of computational models for multilayered composite cylinders. *Analytical and Computational Models of Shells*, 3:419–441, 1989.
- [11] A. K. Noor and W. S. Burton. Assessment of computational models for multilayered composite shells. *Applied mechanics Review*, 43:67–97, 1990.
- [12] J. M. Whitney and C. T. Sun. A higher order theory for extensional motion of laminated composites. *Journal of Sound and Vibration*, 30:85–97, 1973.
- [13] K. H. Lo, R. M. Christensen, and E. M. A high-order theory of plate deformation. part 1: Homogeneous plates; part 2: Laminated plates. *Journal of Applied Mechanics, ASME*, 44:663–676, 1977.
- [14] V. Chomkwah and X. J. R. Avula. A high-order theory for laminated composite plates using lagrange multiplier technique. *Computers and Structures*, 37, No. 5:845–861, 1990.

- [15] J. N. Reddy. A simple higher-order theory for laminated composite plates. *Journal of Applied Mechanics*, 51:745–752, 1984.
- [16] J. N. Reddy and C. F. Liu. A higher-order shear deformation theory of laminated elastic shells. *International Journal of Engng. Sci.*, 23, No. 3:319–330, 1985.
- [17] W. Gilewski and M. Radwandska. A survey of finite elements models for the analysis of moderately thick shells. *Finite elements in analysis and design*, 9:1–21, 1991.
- [18] N. J. Pagano. Exact solutions for rectangular bidirectional composites and sandwich plates. *Journal of Composite Materials*, 4:20–34, 1970.
- [19] J. N. Reddy and W. C. Chao. A comparison of closed-form and finite-element solutions of thick laminated anisotropic rectangular plates. *Nuclear Engineering Designs*, 64:153–167, 1981.
- [20] S. Srinivas. A refined analysis of composite laminates. *Journal of Sound and Vibration*, 30, No. 4:495–507, 1973.
- [21] M. Di Sciuva. An improved shear-deformation theory for moderately thick multilayered anisotropic shells and plates. *Journal of Applied Mechanics*, 54:589–596, 1987.
- [22] M. Di Sciuva. Development of an anisotropic, multilayered, shear-deformable rectangular plate element. *Computers and Structures*, 21, No. 4:789–796, 1985.

- [23] A. Toledano and H. Murakami. A composite plate theory for arbitrary laminate configurations. *Journal of Applied Mechanics*, 54:181–189, 1987.
- [24] E. Reissner. On a certain mixed variational principle and a proposed application. *International Journal for Numerical Methods in Engineering*, 20:1366–1368, 1984.
- [25] K. Bhaskar and T. K. Varadan. Refinement of higher-order laminated plate theories. *A.I.A.A. Journal*, 27, No. 12:1830–1831, 1989.
- [26] E. J. Barbero and J. N. Reddy. An accurate determination of stresses in thick laminates using a generalized plate theory. *International Journal for Numerical Methods in Engineering*, 29:1–14, 1990.
- [27] D. Morgenstern. Herleitung der plattentheorie aus der dreidimensionalen elastizitätstheorie. *Arch. Rational Mech.*, 42:145–152, 1959.
- [28] B. A. Szabó and G. J. Sahrman. Hierarchic plate and shell models based on p-extension. *International Journal for Numerical Methods in Engineering*, 26:1855–1881, 1988.
- [29] B. A. Szabó. Hierarchic plate and shell models based on p-extension. *Analytical and Computational Models of Shells*, 3:317–331, 1989.
- [30] I. Babuška and L. Li. The problem of plate modeling. theoretical and computational results. Technical Report BN-1116, Institute for Physical Science and Technology, University of Maryland, December 1990.

- [31] I. Babuška and L. Li. Hierarchic modeling of plates. *Computers and Structures*, 40, No. 2:419–430, 1991.
- [32] C. Schwab. *Dimensional Reduction for elliptic boundary value problems*. PhD thesis, University of Maryland, Department of Mathematics, College Park, 1989.
- [33] D. N. Arnold and R. S. Falk. Edge effects in the reissner-mindlin plate theory. In A. K. Noor, T. Belytschko, and The American Society of Mechanical Engineers J. C. Simo, editors, *Analytical and Computational Models of Shells*, pages 71–89, 1989.
- [34] F. B. Hildebrand. *Methods in Applied Mathematics*. Prentice-Hall, Inc., Second Edition, 1965.
- [35] J. E. Ashton and J. M. Whitney. *Theory of Laminated Plates*. *Progress in Material Science Series, Volume IV*. Technomic Publishing Co., Inc., 1970.
- [36] J. R. Vinson and R. L. Sierakowski. *The Behavior of Structures Composed of Composite Materials*. Martinus Nijhoff Publishers, 1986.
- [37] S. W. Tsai and H. T. Hahn. *Introduction to Composite Materials*. Technomic Publishing Co., Inc., 1980.



Short Title: Hierarchic Laminated Plate Models   Actis, D.Sc. 1991

